MECHANICAL PROPERTIES AND FRACTURE PARAMETERS OF SUSTAINABLE CONCRETE PRODUCED WITH RECYCLED AGGREGATES

by

Hasan Yıldırım

B.S., Civil Engineering, Yıldız Technical University, 2009

M.S., Civil Engineering, Boğaziçi University, 2012

Submitted to the Institute for Graduate Studies in
Science and Engineering in partial fulfillment of
the requirements for the degree of
Doctor of Philosophy

Graduate Program in Civil Engineering

Boğaziçi University

2023

ACKNOWLEDGEMENTS

First and foremost, I would like to express my deepest gratitude and appreciation to my thesis supervisor Prof. Nilüfer Özyurt Zihnioğlu and co-supervisor Prof. Turan Özturan for their guidance, continuous advice, and encouragement throughout the whole research, their support and valuable remarks were greatly useful and helpful to achieve effective and beneficial results. This dissertation would not have been possible without their invaluable support and guidance.

I would like to thank my thesis committee members Prof. Özkan Şengül and Assist. Prof. İrem Zeynep Yıldırım for their useful suggestions and comments throughout my study, and I would also like to thank Prof. Özgür Çakır and Assist. Prof. Esat Selim Kocaman for their interest and spending time in examining my thesis and being part of my thesis jury.

I am very grateful to TÜBİTAK, the Scientific and Technological Research Council of Turkey, for their financial support during my Ph.D. education. I am also grateful to Boğaziçi University BAP - Scientific Research Projects for their financial support (Project ID: 15A04D2).

I would like to acknowledge Akçansa Cement Industry and Trade Inc., Bolu Cement Industry Inc., Boğaziçi Concrete Industry and Trade Inc., ISTAC Inc., and BASF-YKS Construction Chemicals for material supply.

A special thanks to my colleagues and friends Assist. Prof. Abdullah Huzeyfe Akca, Assoc. Prof. Ahmet Onur Pehlivan, Assoc. Prof. Anıl Niş, Dr. Onur Öztürk and Olcay Gürabi Aydoğan for their support and encouragement throughout my project.

I would like to express my deepest thanks to Ümit Melep for his technical assistance and labor during the experiments. I appreciate his presence, otherwise laboratory work would be so difficult.

My warm and sincere thanks to my dear parents and to my twin brother Hüseyin for their endless support and constant encouragement throughout my life.

Finally, I would like to express my deepest gratitude to my beloved wife, Ebru, for her infinite love, trust, and understanding. Without her support, patience, and encouragement, the completion of this research would not have been possible for me. Therefore, I am grateful for the opportunity to dedicate this thesis to her.

ABSTRACT

MECHANICAL PROPERTIES AND FRACTURE PARAMETERS OF SUSTAINABLE CONCRETE PRODUCED WITH RECYCLED AGGREGATES

In this study, the mechanical properties and fracture parameters of sustainable concrete mixtures produced with different recycled aggregates at a w/c of 0.50 were investigated. To produce sustainable concrete mixtures, recycled concrete aggregates (RCA), recycled brick aggregates (RBA), and recycled fly ash aggregates (FAA) were used in total replacement, by volume, of natural crushed stone coarse aggregates (CSt). The recycled aggregates were utilized in six different sustainable concrete mixtures as plain (RCA, RBA, FAA) and surface treated (TRCA, TRBA, TFAA) by employing ground granulated blast furnace slag (GGBFS) slurry during concrete production as a multi-step concrete mixing method. Microstructural investigations were also carried out on samples taken from recycled aggregates and hardened concrete specimens to examine the effect of recycled aggregate treatment during the concrete mixing procedure with slag slurry on the mechanical properties and fracture parameters of the recycled aggregate concrete. The results of the experiments conducted in this study revealed that complete replacement of the crushed stone coarse aggregate with recycled aggregates reduced the unit weight of fresh concrete by up to 17%, while the compressive strength values were in line with the limitations for structural use. Besides, the treatment of recycled aggregates with GGBFS slurry improved the mechanical properties and fracture parameters of recycled aggregate concrete mixtures with increased statistical reliability. For example, treating recycled aggregates with slag slurry not only increased the bond strength between the reinforcement bars and the concrete mixtures, but also decreased the minimum required anchorage length for the reinforcement to carry the load. The findings of the microstructural investigations confirmed the formation of secondary hydration products as a result of the pozzolanic activity of fine slag grains, which penetrated and filled the voids and cracks on the surface of the treated recycled aggregates and in the interfaces between these aggregates and the concrete matrix, improving the mechanical properties and fracture parameters of the recycled concrete mixtures.

ÖZET

GERİ KAZANILMIŞ AGREGALARDAN ÜRETİLEN SÜRDÜRÜLEBİLİR BETONLARIN MEKANİK ÖZELLİKLERİ VE KIRILMA PARAMETRELERİ

Bu çalışma kapsamında, birbirinden farklı geri kazanışmış agregalar kullanılarak 0.50 su/çimento oranı ile üretilmiş sürdürülebilir betonların mekanik özellikleri ve kırılma parametreleri incelenmiştir. Sürdürülebilir beton karışımlarının üretilmesinde doğal iri kırma taş yerine geri kazanışmış beton (RCA), tuğla (RBA) ve uçucu kül agregaları (FAA) hacimsel olarak tamamen ikame edilmiştir. Geri kazanılmış agregalar altı farklı sürdürülebilir beton karışımında direkt (RCA, RBA, FAA) ve çok aşamalı bir beton karışım metodu olarak öğütülmüş yüksek fırın cürufu (GGBFS) bulamacı uygulaması ile iyileştirilerek (TRCA, TRBA, TFAA) değerlendirilmiştir. Cüruf bulamacıyla beton karışımı sırasında geri kazanılmış agregalara yapılan iyileştirmenin bu agregalarla üretilen betonların mekanik özelliklerine ve kırılma parametrelerine etkilerini incelemek amacıyla, geri kazanılmış agregalardan ve sertleşmiş beton numunelerinden alınan örnekler üzerinde mikroyapı incelemeleri de gerçekleştirilmiştir. Yapılan deneyler sonucunda, kırma taş yerine geri kazanılmış agregaların kullanılmasının taze betonun birim ağırlığını %17'ye kadar düşürürken, basınç dayanımı açısından üretilen betonların yapısal amaçla kullanıma uygun olduğu görülmüştür. Ayrıca, geri kazanılmış agregaların öğütülmüş yüksek fırın cürufu bulamacı ile iyileştirilmesi, sürdürülebilir betonların mekanik özelliklerini ve kırılma parametrelerini olumlu yönde etkilemiş ve sonuçların istatistiksel güvenilirliğini arttırmıştır. Örneğin, geri kazanılmış agregaların cüruf bulamacıyla iyileştirilmesi, yalnızca donatı çubukları ile beton karışımları arasındaki aderans dayanımını artırmakla kalmamış, aynı zamanda donatının yük taşıyabilmsi için gereken minimum ankraj boyu uzunluğunu da azaltmıştır. Mikroyapı incelemelerinin bulguları, geri kazanılmış agregaların yüzeyindeki boşluklara ve çatlaklara ve bu agregalar ile beton matrisi arasındaki arayüzlere nüfuz eden ve onları dolduran ince cüruf tanelerinin puzolanik aktivitesinin bir sonucu olarak, beton üretimi sırasında geri kazanılmış agregaların cüruf bulamacıyla direkt buluşturulmasına bağlı olarak betonun mekanik özelliklerini ve kırılma parametrelerini iyileştirdiği düşünülen ikincil hidratasyon ürünlerinin oluşumunu doğrulamıştır.

TABLE OF CONTENTS

LIST OF FIGURES

LIST OF TABLES

LIST OF SYMBOLS

A	Area under the load-displacement curve of the beam specimen
a_0	Initial notch depth
a_0	Notch depth
A_b	Area of the deformed bar
a_c	Effective critical crack length
b	Width of beam
C_i	Initial compliance
D	Diameter of the spherical particles
D	Diameter of the disc
d	Depth of beam
d	Diameter of deformed steel bars
d_b	Nominal bar diameter
e	Percentage error in average
E_b	Modulus of elasticity
E_c	Modulus of elasticity
F_c	Compressive strength
f_c	Compressive strength
F_{net}	Flexural strength
F_t	Splitting tensile strength
f_t	Splitting tensile strength
f_y	Specified yield strength of the bar
g	Gravitational acceleration
G_F	Fracture energy
h	Depth/thickness of the beam specimen
H	Height to fall
h_0	Thickness of the knife-edge
K_{IC}^{S}	Critical stress intensity factor or fracture toughness
L	Length of the beam specimen
L	Support span

l_b	Bond length
l_{ch}	Characteristic length
l_d	Development length
m	Mass of a single pellet
m	Mass of the beam specimen
m	Mass of the hammer
n_{cr}	Critical revolution per minute
n	Minimum number of tests
P	Maximum load
P	Capillary force
P_c	Cohesive force
P_{max}	Maximum pull-out load
P_{max}	Peak load
R	Radius of the disc
R^2	Coefficient of determination
S	Span length of the beam specimen
t	Value of the Student's t-distribution
t	Time taken by the hammer to fall
U	Impact energy per blow of the hammer
v	Coefficient of variation
V	Velocity of the hammer at impact moment
w	Centrifugal acceleration
W	Weight of the hammer
W_0	Self-weight of the beam specimen
α	Inclination angle of pelletizer disc
α	Reinforcement location factor
β	Angle of the disc to horizontal plane
β	Meniscus angle between particle and the liquid binder
β	Reinforcement coating factor
ε	Porosity of a pellet
μ	Coefficient of friction between pellet and the disc
γ	Reinforcement size factor
δ_{max}	Maximum deflection

λ	Concrete factor
σ	Surface tension of liquid
σ	Standard deviation
τ_{ACI}	Minimum bond strength required according to ACI
τ_b	Bond strength between rebar and concrete
τ_{bot}	Bond strength of the bottom bar
τ_{cube}	Bond strength of the bar in cubic specimen
τ_{exp}	Experimental bond strength
τ_{nz}	Normalized bond strength
τ_{top}	Bond strength of the top bar
τ_u	Ultimate bond strength

LIST OF ACRONYMS/ABBREVIATIONS

ACI	American Concrete Institute
ACV	Aggregate Crushing Value
AIV	Aggregate Impact Value
ASTM	American Society for Testing and Materials
BS	British Standard
CDW	Construction and Demolition Waste
CMOD	Crack Mouth Opening Displacement
$CMOD_c$	Critical Crack Mouth Opening Displacement
CoV	Coefficient of Variation
CSA	Canadian Standards Association
C-S-H	Calcium Silicate Hydrate
CSt	Natural Crushed Stone Coarse Aggregates
CStC	Control Concrete Produced with Crushed Stone Coarse Aggregate
$CTOD_c$	Critical Crack-Tip Opening Displacement
EDAX	Energy Dispersive X-ray Analysis
EN	European Standard
ESEM	Environmental Scanning Electron Microscope
FA	Fly Ash
FAA	Recycled Fly Ash Aggregates
FAAC	Recycled Fly Ash Aggregate Concrete
FC	First Crack
FI	Flakiness Index
GGBFS	Ground Granulated Blast Furnace Slag
ITZs	Aggregate-Matrix Interfaces
JCI-S	Japan Concrete Institute Standard
LVDTs	Linear Variable Differential Transformers
NZS	New Zealand Standard
RBA	Recycled Brick Aggregates
RBAC	Recycled Brick Aggregate Concrete

RCA	Recycled Concrete Aggregates
RCAC	Recycled Concrete Aggregate Concrete
RH	Relative Humidity
rpm	Rotation Per Minute
SD	Standard Deviation
SE	Standard Error
SEM	Scanning Electron Microscopy
MAUD	Material Analysis Using Diffraction
SP	Superplasticizer
SSD	Saturated Surface Dry
TFAA	Treated Recycled Fly Ash Aggregates
TFAAC	Treated Recycled Fly Ash Aggregate Concrete
TRBA	Treated Recycled Brick Aggregates
TRBAC	Treated Recycled Brick Aggregate Concrete
TRCA	Treated Recycled Concrete Aggregates
TRCAC	Treated Recycled Concrete Aggregate Concrete
TS	Turkish Standard
UR	Ultimate Resistance
XRD	X-Ray Diffraction

1. INTRODUCTION

In recent years, with rapid industrialization and urbanization, huge amounts of construction and demolition waste (CDW) have been generated, especially in developing countries. The disposal of these wastes causes environmental and landfill problems [1]–[5]. Therefore, the recycling and reuse of construction and demolition waste is of crucial importance for the protection of the environment and the effective use of natural resources [6]–[9]. From this point of view, the high potential of recycled aggregates obtained from CDW to be utilized as an alternative source to reduce the dependence of the construction industry on natural aggregates explains the focus on recycled aggregate concrete in recent decades [10]–[25]. Although the reuse of CDW as recycled aggregate is environmentally beneficial, cement mortar adhered to recycled aggregate particles leads to some serious problems of increased porosity and water absorption with a decreased strength capacity in recycled aggregate concrete [26], [27]. Therefore, in the literature, to improve the quality of recycled aggregates and the performance of recycled aggregate concrete, the three principal technical methods are highlighted: (i) removal of residual cement mortar [28]–[42], (ii) coating of recycled aggregates [29], [36], [40], [41], [43]–[55], and (iii) multi-step concrete mixing methods with pozzolanic admixtures [41], [42], [52], [56]–[68]. It has been reported that treating the recycled aggregates by multi-step concrete mixing methods with pozzolanic admixtures is an efficient and practical way rather than the removal of old adhered mortar or the coating of recycled aggregates, which are cost-intensive and/or time-consuming methods with secondary environmental impacts [5], [49], [59], [69]–[73].

In order to build sustainable and environment-friendly structures and infrastructures, which has been one of the most important challenges in the construction industry for many years, researchers have also tried to find valuable applications of industrial by-products such as fly ash (FA) and ground granulated blast furnace slag (GGBFS) in the construction industry. It has been shown that the construction industry has the ability to consume FA and GGBFS, which are by-products of coal-fired thermal power plants and the iron manufacturing industry, respectively, in various applications such as sub-base and pavement base practices for subgrade stabilization, construction of backfills and embankments, manufacturing of ceramics, production of pozzolanic cement, cement replacement in concrete production, brick and block manufacturing, production of alkali-activated

geopolymer concrete and artificial aggregate production [74]–[107]. The large-scale utilization of fly ash, for instance, to produce fly ash aggregates, which has been practiced in many countries, may reduce the rapid use of natural aggregates in the construction industry and prevent the depletion of natural resources [75], [108]–[110]. It also prevents rural areas, seasides, and river beds from being damaged and provides a remarkable reduction in greenhouse gas emissions by reducing aggregate mining activities and subsequent operations that contribute to CO_2 emission [75], [109], [111]. Additionally, the recycling of fly ash through aggregate production reduces the need for landfills or storage lagoons for the disposal of fly ash and prevents air and underground water pollution [112]–[114]. Cold bonding and sintering are the most frequently used methods to produce fly ash aggregate [97], [108], [115]–[124]. Cold bonding, which depends on the pozzolanic activity of fly ash, is more economical than the energy-intensive sintering process, but usually results in lower strength aggregates [125]–[127]. Various studies in the literature investigated the mechanical properties of concrete produced with cold-bonded fly ash aggregates [112], [117], [125], [128]–[130]. The use of cold-bonded fly ash aggregates in place of normal weight aggregates in concrete resulted in lower mechanical properties. However, concrete produced with surface treated cold-bonded fly ash aggregates by means of water glass or cement-silica fume slurry impregnation for surface coating before concrete production had higher mechanical properties than concrete produced with untreated cold-bonded fly ash aggregates [117], [128], [131]. Similarly, the mechanical properties of concrete produced with plain cold-bonded fly ash aggregates increased when fly ash aggregates were treated by adding polypropylene fibers and tire chips into fly ash pellets for reinforcing them during agglomeration process [132].

In this study, the mechanical properties and fracture parameters of sustainable concrete mixtures produced with different recycled aggregates were investigated. To produce sustainable concrete mixtures, recycled concrete aggregates (RCA), recycled brick aggregates (RBA), and cold-bonded recycled fly ash aggregates (FAA) were used as coarse aggregates in total replacement, by volume, of natural crushed stone coarse aggregates (CSt). The recycled aggregates were utilized in six different sustainable concrete mixtures as plain (RCA, RBA, FAA) with a conventional concrete production method and surface treated (TRCA, TRBA, TFAA) with the “Direct Slurry Method” by employing GGBFS slurry during concrete production as a multi-step concrete mixing approach.

Within the scope of the "Direct Slurry Method", it was preferred to produce sustainable concrete mixtures by first mixing the aforementioned recycled aggregates with slag slurry during concrete production to fill the voids and cracks on the surface of the recycled aggregates with fine slag grains and to enhance the interface between these aggregates and cement paste in concrete due to the formation of hydration products as a result of the pozzolanic activity of the slag, both of which increase the microstructural density. The reason for choosing slag as a pozzolanic admixture is because there are very limited studies in the literature that examine the improvement in the mechanical properties and fracture parameters of concrete produced with recycled aggregates treated with slag slurry by a multi-step concrete mixing method. In addition, the mechanical properties and fracture parameters of concrete mixtures produced with different recycled coarse aggregates (RCA, RBA, and FAA) treated with slag slurry by a multi-step concrete mixing method have not been comparatively examined in the same study before.

In summary, this study gives the opportunity to show the effects of originally different recycled coarse aggregates on the mechanical properties and fracture parameters of recycled aggregate concrete and the potential of the most favorable recycled aggregate treatment method, which has been reported as an efficient and practical way regarding cost and time constraints for the construction industry with no secondary environmental impacts compared to the other treatment methods mentioned above, in terms of sustainable concrete production.

2. LITERATURE REVIEW

2.1. Production of Recycled Aggregates from CDW

Construction and Demolition Waste (CDW) refers to damaged and surplus materials generated during the construction, renovation, or demolition of buildings and structures [133], [134]. Recycling of CDW is of paramount importance to achieve the goals of sustainable development. The recycling of CDW in the construction industry helps to reduce landfill waste, conserve natural resources, and decrease energy consumption and greenhouse gas emissions associated with the production of traditional construction materials [134]–[136]. One of the most common ways to recycle CDW is through the production of recycled aggregate. Recycled aggregate obtained from CDW is a sustainable alternative to natural aggregate in concrete production. However, CDW is a heterogeneous material, with varying characteristics and composition, which affects its recycling and reuse as recycled aggregates in concrete production. The composition of CDW is highly variable and can include materials such as concrete, bricks, tiles, ceramics, wood, metal, plastics, paper, glass, and other materials [1], [137]–[140]. The presence of contaminants or impurities in CDW can affect the quality of the recycled aggregate produced. Therefore, it is important to carefully select and sort CDW materials before recycling. The CDW recycling process aims to convert bulk materials into smaller sizes to obtain desirable grading through the use of stationary or mobile recycling plants with different types of crushers, such as jaw crushers, impact crushers, and cone crushers [141]–[143]. It involves several steps, including collection, transportation, sorting, crushing, screening, and washing [144], [145]. The screening of recycled aggregates is necessary to remove any impurities or contaminants. The removal of these contaminants helps to ensure that the recycled aggregates produced from CDW meet the required quality standards.

2.2. Evaluation of Adhered Mortar in Recycled Aggregates Obtained from CDW

In addition to the contaminants existing in CDW, the presence of old adhered mortar in the recycled aggregates produced should also be managed as much as possible because it affects the quality of the recycled aggregates.

Although recycling CDW as aggregate is an eco-friendly practice as it is used in concrete production to reduce the environmental impact of the construction industry, the presence of residual cement mortar on recycled aggregate particles can cause significant issues such as increased porosity and water absorption with decreased strength in recycled aggregate and so in resulting concrete [26]–[28]. To overcome these challenges and enhance the quality of recycled aggregates, as well as the performance of recycled aggregate concrete, various technical methods have been suggested in the literature. These methods include the removal of residual cement mortar [28]–[42], [133] (e.g., mechanical grinding, ball milling, pre-soaking in acid solution, thermal expansion method, freeze–thaw method, thermal & mechanical treatment together, ultrasonic cleaning), coating of recycled aggregates [29], [36], [40], [41], [43]–[55], [133] (e.g., polymer impregnation, carbonation treatment, sodium silicate impregnation, pre-coating with puzzolanic slurry), and multi-step concrete mixing procedures with pozzolanic admixtures [41], [42], [52], [56]–[68] (e.g., two-stage mixing approach, double and triple mixing methods). It has been reported that, the most efficient and practical way of treating recycled aggregates is through multi-step concrete mixing methods with pozzolanic admixtures. This method is preferred over the removal of old adhered mortar or the coating of recycled aggregates, which can be expensive, time-consuming, and have secondary environmental impacts [5], [49], [59], [69]–[73].

2.3. Production of Recycled Aggregates from Fly Ash

There are two primary methods for producing fly ash aggregate, namely cold bonding and sintering [93], [97], [108], [115]–[124], [146]–[151]. Cold bonding is generally considered a more cost-effective approach to fly ash aggregate production compared to sintering, as it is a matrix bonding process that saves energy. On the other hand, sintering is an energy-intensive process that requires high temperature. However, the effectiveness of cold bonding depends on the ability of the pozzolanic reactivity of fly ash to form pellets with calcium hydroxide at room temperature. In addition, the fly ash aggregate produced through cold bonding has a lower strength than that produced through sintering [125]–[127].

In the current study, the cold bonding technique was utilized for the production of fly ash aggregate.

2.3.1. Cold Bonding

Cold bonding is a method of producing aggregates by mixing fly ash with cementitious materials, such as lime, cement, clay, or shale. The process starts with a mixture of fly ash and the chosen cementitious material, which is then transported to a pelletizer disc. Water is sprayed onto the mixture while the disc rotates at a predetermined inclination angle and speed, forming circular-shaped pellets. The bonding between the cementitious materials and fly ash particles occurs through chemical reactions, facilitated by the pozzolanic reaction of fly ash. This reaction produces calcium silicate hydrates, which are the primary elements responsible for strengthening the matrix [116]–[118], [121], [122], [124]–[127], [147], [151].

2.3.2. Sintering Method

The process of sintering is used to harden fly ash pellets by causing the particles to come together at their points of contact. This process is carried out in two stages. Initially, the mixture of cementitious material and fly ash is formed into pellets using a pelletizer disc through a cold bonding process, which is followed by a thermal treatment in which the fly ash pellets produced, along with coal, move on a sintering strand and undergo sintering by burning the coal with specialized units of a kiln, such as a furnace hood, which acts as a heat source. The temperature during the burning process should be maintained between 1050 and 1250˚C [93], [108], [119], [120], [123]–[125], [127], [147], [149]–[151]. The entire process is depicted in Figure 2.1.

The items illustrated in Figure 2.1, which outlines the production process for sintered fly ash aggregates, are as follows: (1) Pan mill, (2) Vibrating screen, (3) Bucket elevator, (4) Silo for coal, (5) Silo for clay, (6) Silo for fly ash, (7) Belt conveyor, (8) Pneumatic conveyor, (9) Ribbon mixer, (10) Bucket elevator, (11) Water sprayer, (12) Pelletizer, (13) Furnace hood, (14) Sinter strand/sintering belt, (15) Strand draught fan, (16) Chimney, (17) Belt conveyor, (18) Jaw crusher, (19) Size grader, (20) Finished product.

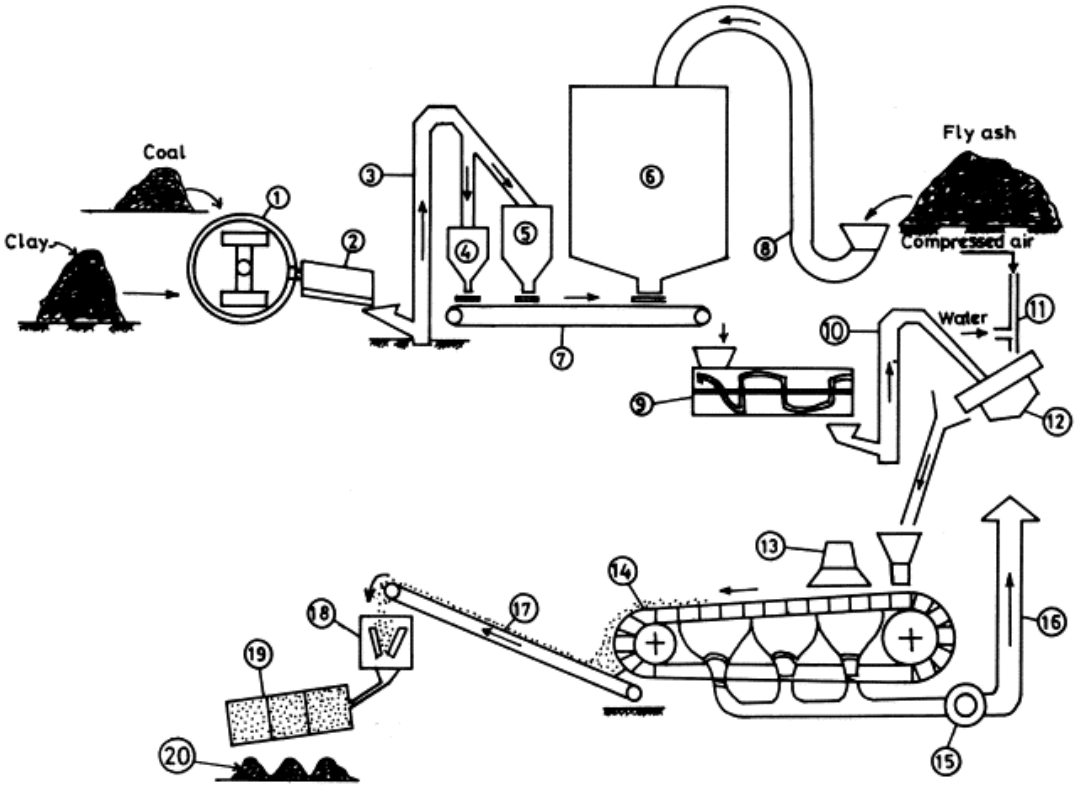

Figure 2.1. Diagrammatic illustration of the sintering process to produce fly ash aggregates [108].

2.3.3. Definition and Theory of Pelletization

The process of pelletization involves the consolidation of fine and moisturized particles, such as dust or powders, into larger and solid materials without the need for external force, which are then transformed into pellets through the use of a rotating pelletizer disc or drum. The resulting pellets acquire strength through the mechanical forces generated during the process, as they collide with one another and with the walls of the pelletizer disc [97], [108]. The shape of the pellets is usually spherical or slightly angular, and their color may vary based on the properties of the materials used in the dry mixes. The size distribution of the pellets can be adjusted by manipulating the position of the scrapping blades within the inner and outer paths of the pelletizer pan [117].

Various factors can impact both the pelletization process and the strength of the resulting pellets. Such factors include the characteristics of the raw materials, including their particle size distribution and wettability, as well as the moisture content in the medium and

the amount of binder used in the process. Additionally, the duration of the pelletization process, as well as the rotation speed and angle of the pelletizer disc or drum relative to the normal, can play a crucial role [97], [115], [116].

Through the examination and analysis of these parameters in accordance with the principles of mechanics and kinetics, a theory on the process of pelletization has been developed. The fundamental aspects of this theory can be summarized as follows [97]:

Moisturizing a fine-grained material results in the formation of a thin liquid film on the surface of the grains, creating a meniscus between them that takes on bridge-like structures (Figure 2.2 a). When these particles are subjected to rotation within a pelletizer disc or drum, they develop spherical shapes that exhibit increased bonding forces between grains as a result of both centrifugal and gravitational forces (Figure 2.2 b and c) [97].

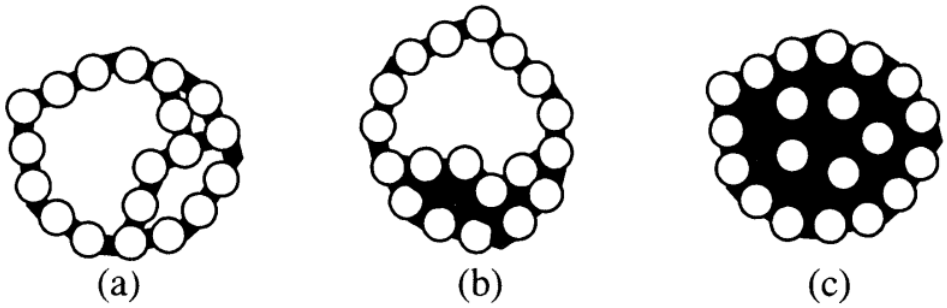

Figure 2.2. Mechanism of pellet formation [97].

The strength of the pellets is determined by various parameters of the pelletization process, including the pressure exerted on the pellets due to the capillary and cohesive forces. Capillary forces (P), which are associated with the surface tension generated by the height of the liquid column, have a significant impact on the coherence of the pellets. The magnitude of the capillary force is affected by the diameter of the particles (D) and the angle of the meniscus (β) formed between the particle and the liquid binder [97]. The coherence of the moisturized particles is directly proportional to the capillary forces acting on the pellets, as shown in Figure 2.3.

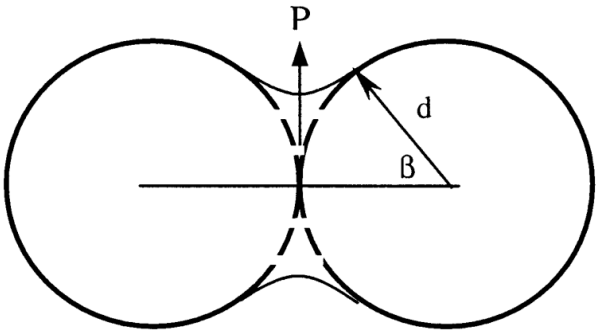

Figure 2.3. Schematic representation of the surface tension force generated by a water bridge formed between two grains [97].

The pelletization process comprises of three stages, which are characterized by the degree of water filling the intergranular spaces. In the pendular state, water exists only at the contact points of the grains. The funicular state, in addition to the conditions of the pendular state, has some pores completely filled with water. The capillary state occurs when all the intergranular spaces are saturated with water, and no water film is present on the pellet surface. The capillary state is the ideal state for pellet formation as it facilitates the application of the highest tension force by the binder between the particles [97].

The capillary and cohesive forces exerted on fine material particles can be formulated by making some assumptions and simplifications [97]. Firstly, all particles are assumed to be spherical and have uniform diameters. Secondly, the bonding pattern throughout the ball section is assumed to be uniform. Thirdly, the particles are assumed to be evenly distributed within the ball. Finally, it is assumed that the effective bonding forces fluctuate around the average value. Based on these assumptions, following equation can be derived to calculate cohesive forces in the capillary state:

$$P_c = 8\frac{(1-\varepsilon)\sigma}{\varepsilon D} \tag{2.1}$$

where P_c represents the cohesive force applied to the structure in the capillary state, ε is the ball porosity, σ refers to the surface tension of the liquid and D is the diameter of the spherical particle [97].

The strength of a fresh pellet is determined by two key factors: the cohesive force that is applied to the particles during the pelletization process and the interlocking effects. The strength of the pellet is the result of the combination of these two factors. The magnitude of the cohesive force depends on the void ratio of the structure, while the strength gained through interlocking is affected by the surface texture of the particles. Nevertheless, the cohesion that forms during the pelletization process can be considered as equal to the strength of the fresh pellet [97].

The rate of size growth of pellets can be managed during the pelletization process by adjusting the feeding rate of the binder. To ensure process efficiency, the amount of binder used should be predetermined based on the desired or minimum void ratio of the final product. This represents the optimized condition, which is also known as the ‘capillary state’. Any deviation from this optimal binder amount can lead to the destruction of the capillary force, resulting in a significant variation in the size and engineering properties of the produced pellets. Therefore, it is crucial to maintain the moisture content of the mixture below or equal to the optimum level to achieve the desired performance of the final product [97].

It is also necessary to determine the changes in the movement of pellets in the pelletization disc according to the revolution speed of the disc as shown in Figure 2.4. When the revolution speed of the disc is low, the gravitational force governs the movement of pellets. Conversely, when the speed is high, the movement is regulated by the centrifugal force. If one of these forces becomes dominant, it results in the formation of loosely structured pellets or cessation of pelletization, particularly in the case of the centrifugal force where moisture-induced adhesion leads to particle sticking on the side walls of the disc [97].

There are other factors that play a crucial role in determining the optimal pelletization process. These factors include the disc pelletizer’s revolution speed to avoid the prevalence of either gravitational or centrifugal forces, the angle between the pelletization disc’s plane and the normal, and the disc’s diameter. Figure 2.5 illustrates the forces that affect an individual pellet during the pelletization process in a pelletization disc with a radius of ‘R’[97].

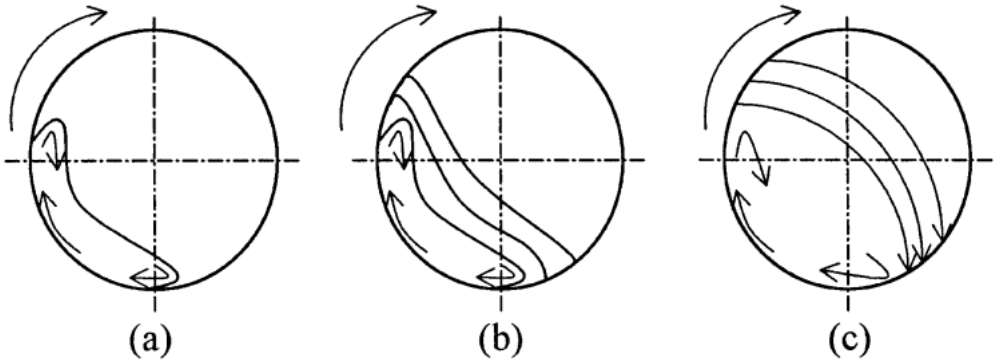

Figure 2.4. Motion of material rotating at various speeds in disc pelletizer [97].

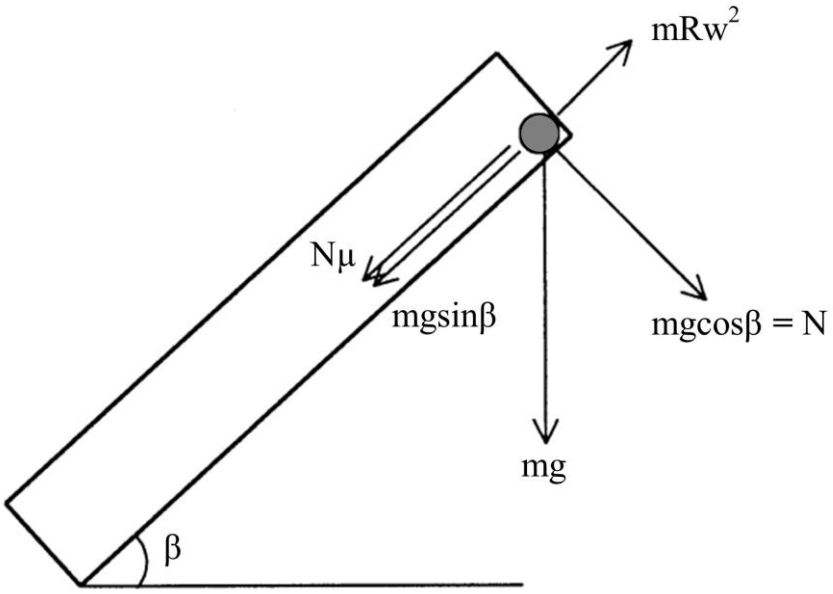

Figure 2.5. The forces exerted on a single pellet throughout the pelletization process [97].

The parameters affecting the pelletization process and the strength of an individual pellet have been theoretically examined and have resulted in the following equation expressed in terms of 'critical revolutions per minute'. The critical state is defined as the equilibrium point between gravitational and centrifugal forces on the pelletization disc's plane [97]. The equation is given as:

$$mg(\sin\beta) + \mu mg(\cos\beta) = mRw^2 \qquad (2.2)$$

where m represents the individual pellet's mass, g refers to the gravitational acceleration, β is the angle between the disc's plane and the normal in degrees, μ represents the coefficient of friction between the pellet and the disc, R is the radius of the disc, and w refers to the centrifugal acceleration in radians per square second [97].

Nevertheless, in the case of equilibrium between centrifugal acceleration and gravitational forces, the normal force that the pellet exerts approaches zero, leading to the simplification of Equation 2.2 to:

$$mg(\sin\beta) = mRw^2 \tag{2.3}$$

At this point, the 'critical revolutions per min' can be calculated using the following formula [97]:

$$n_{cr} = \frac{42.3}{\sqrt{D}}\sqrt{sin\alpha} \tag{2.4}$$

where n_{cr} represents the critical revolutions per minute (rpm), D is the disc diameter in meters, and α is the disc inclination angle in degrees.

2.4. Physical Properties of recycled aggregates

2.4.1. Density of recycled aggregates

The density of recycled aggregates obtained from construction and demolition waste (CDW) has been extensively investigated in recent academic studies. It has been widely reported that the density of recycled aggregates is generally lower than that of natural aggregates due to the porosity of the old adhered mortar in recycled aggregates [30], [37], [38], [46], [51], [55], [152]–[154].

For instance, recent research by Kisku et al. [64] examined the density of recycled aggregates obtained from CDW and found that the average density of recycled aggregates was significantly lower than that of natural aggregates. Similarly, studies by Pawluczuk et

al. [31] and Poon and Chan [155] also reported that the density of recycled aggregates was generally lower than that of natural aggregates due to the presence of adhered mortar on the surface of the recycled aggregates. Topçu and Şengel [156] also showed that the density of recycled aggregates decreased as the amount of adhered mortar increased. Similarly, studies by Çakır and Dilbas [39] and Etxeberria et al. [157] found that the density of recycled aggregates decreased with an increase in the amount of adhered mortar.

The density of recycled aggregates has also been observed to increase with an increase in particle size. This phenomenon can be explained by the fact that larger particles tend to contain less porous residual mortar compared to finer recycled aggregates [41], [158], [159].

2.4.2. Water Absorption of recycled aggregates

The use of recycled aggregates obtained from CDW in concrete production has been investigated extensively in recent years. One of the important properties of these recycled aggregates is their water absorption capacity, which is typically higher than that of natural aggregates due to the porosity of old adhered mortar present in recycled aggregates [41], [159]–[165].

Several studies have examined the water absorption capacities of recycled aggregates, and varying water absorption capacities have been reported due to the variation of the content of old adhered mortar in recycled aggregates [152], [154], [155]. Furthermore, an increase in particle size was found to decrease the water absorption capacity of the recycled aggregates, which was attributed to a reduced amount of porous residual mortar in the coarser recycled aggregates [41], [158], [159], [165].

In the literature, in order to decrease the water absorption capacity and increase the density of recycled aggregates, which are basically due to the porosity of residual cement mortar adhered to recycled aggregates, various technical methods have been suggested. These methods can be categorized into three groups: (i) removal of residual cement mortar [28]–[42], (ii) coating of recycled aggregates [29], [36], [40], [41], [43]–[55], and (iii) multi-step concrete mixing methods with pozzolanic admixtures [41], [42], [52], [56]–[68]. To improve the quality of recycled aggregates and so the resulting concrete, the methods in the

former category are focused directly on removing the residual cement mortar, which is the most porous and least dense part of the recycled aggregates. However, methods for coating of recycled aggregates and multi-step concrete mixing methods with pozzolanic admixtures are generally based on the mechanism of filling the open pores and cracks on the surface of recycled aggregates and strengthening the interface between these aggregates and cement paste in concrete, both of which increase the microstructural density.

In the case of recycled fly ash aggregates, it can be concluded that their density is lower than that of natural aggregates whereas the water absorption capacity of them is higher with regard to the studies investigating the properties of recycled fly ash aggregates [112], [117], [125], [128]–[132].

Chi et al. [166] conducted a study to investigate the density, and water absorption of cold-bonded fly ash aggregates with different ratios of cement to fly ash. The results revealed that as the content of cement with a higher specific gravity than fly ash increased, there was a corresponding increase in the specific gravity and bulk density of the fly ash pellets. Furthermore, a decrease in porosity was observed, which led to a reduction in water absorption.

Baykal and Döven [97] conducted a study on the effects of different binders (8% cement and lime by weight of fly ash) on the physical properties of cold-bonded fly ash pellets. It was found that the unit weight of the pellets increased by 2-8% when binders were added to fly ash. In addition, the specific gravity values of the fly ash aggregates increased, while the porosity and water absorption decreased with the addition of binders. On average, the specific gravity increased by 3-4% and water absorption decreased by 4-9% with the addition of lime and cement to fly ash pellets, compared to those of fly ash pellets produced without additives.

In a research study carried out by Gesoglu et al. [128], various types of fly ash with different physical and chemical properties were treated with water-glass and cement-silica fume slurry, resulting in specific gravity values of cold-bonded fly ash aggregates ranging from 1.72 to 1.80. For a specific group of fly ash aggregates, while the water absorption rate decreased from 27% to 3.0% and 18% by weight, the specific gravity increased from 1.78

to 1.79 and 1.80 following the water-glass and cement-silica fume slurry treatment, respectively.

2.5. Mechanical Properties of Recycled Aggregates

Recycling construction and demolition waste (CDW) and fly ash, which is a by-product of coal-fired thermal power plants, into recycled aggregates is an efficient way to reduce the amount of waste sent to landfills and to decrease the demand for natural aggregates. However, the quality of recycled aggregates is a significant concern as it may affect the durability and mechanical properties of the resulting concrete. Two important properties to assess the mechanical quality of recycled aggregates are the aggregate crushing value (ACV, %) and the aggregate impact value (AIV, %).

2.5.1. Aggregate Crushing Value

The aggregate crushing value (ACV, %) is an important mechanical property of the recycled aggregates. Several studies have shown that recycled aggregates have a higher ACV compared to natural aggregates due to the porosity of the old adhered mortar in recycled aggregates obtained from CDW [141], [160], [167], [168]. The porosity in recycled aggregates can cause a reduction in the strength of aggregates. In addition, the ACV of recycled aggregates has been found to be negatively correlated with their unit weight. This negative correlation can be attributed to the fact that recycled aggregates, which have a higher porosity, are less dense and more prone to crushing.

A study by Babu et al. [33] investigated the ACV of recycled aggregates obtained and found that the ACV of recycled aggregates was higher than that of natural aggregates. Another study by Kisku et al. [64] examined the properties of recycled aggregates and concluded that the ACV of recycled aggregates was higher compared to natural aggregates. The authors attributed this to the presence of adhered mortar in the recycled aggregates.

It is important to note that a higher ACV indicates a higher degree of mechanical flaws in the material. The higher the ACV, the more prone the material is to crushing. Therefore, recycled aggregates with higher ACV may be less suitable for certain applications that

require high strength. In this respect, it is important to carefully consider ACV when selecting recycled aggregates for different applications.

2.5.2. Aggregate Impact Value

The aggregate impact value (AIV, %) is another important characteristic of recycled aggregates. Studies have shown that recycled aggregates obtained from CDW have higher AIV values compared to natural aggregates due to the presence of old adhered mortar, which is the most porous and least dense part of recycled aggregates, and other contaminants [33], [56], [66], [169], [170]. This porosity of old adhered mortar in recycled aggregates can increase the AIV value, making the material more susceptible to fragmentation under impact loads. In addition, several studies have reported a negative correlation between AIV values and the unit weight of aggregates. This could be due to the fact that a higher unit weight indicates a denser material with fewer voids, which would provide more resistance to fragmentation under impact loads [32], [50], [64].

Furthermore, it is worth noting that the higher the AIV value of a material, the more mechanically flawed it is likely to be. A higher AIV value indicates that the material is more susceptible to cracking and breaking under impact loads, which could impact its overall durability and strength. Thus, it is essential to consider the quality of recycled aggregate carefully before using it as a replacement for natural aggregate in concrete production.

Recycled fly ash aggregates have also been reported to be less favourable than natural aggregates in terms of crushing strength and impact resistance since their ACV and AIV values are significantly higher compared to those of natural aggregates [130], [171], [172].

2.6. Fresh Concrete Properties

Fresh concrete is generally defined as concrete that has not yet set and hardened. The characteristics of recycled aggregates vary from those of conventional aggregates, and the incorporation of recycled aggregates in concrete causes notable alterations in the properties of fresh concrete, including density, workability, and air content.

The density of fresh concrete is a fundamental property that describes the weight of the concrete per unit volume. It is affected by various factors, including the types of aggregates and cement, the amount of water and other ingredients used in the production of concrete, and the air content present in the concrete mixture.

Studies have shown that the density of recycled aggregate concrete is generally lower than that of natural aggregate concrete [157], [164]. This is due to the presence of porosity in the old adhered mortar of the recycled aggregates, which can reduce the overall density of the concrete. For example, Younis and Pilakoutas [164] found that increasing the amount of recycled aggregates in the mix led to a decrease in the density of the resulting concrete.

Another significant property of fresh concrete is workability which refers to the ease and homogeneity of concrete mixture and its ability to be placed, compacted, and finished without segregation and bleeding. Cohesiveness, which is the ability of particles to stick together, and homogeneity, which is the uniformity of the mixture, are important factors affecting workability. Several factors affecting the workability of fresh concrete have been investigated in the literature. These include the water-to-cement ratio, types of aggregates, particle size distribution, angularity, and surface texture of aggregates, amount of fine materials, presence of puzzolanic additives, and amount of superplasticizer in the concrete mixture.

The workability of fresh concrete is also associated with other important properties, such as density and air content. In the literature, there are numerous studies that have focused on the workability of recycled aggregate concrete. It has generally been observed that the fresh concrete properties of recycled aggregate concrete are inferior to those of natural concrete.

Recycled aggregate concrete is known to be less workable than natural aggregate concrete due to the presence of old adhered mortar in the recycled aggregate, as well as the angularity and surface roughness of the recycled aggregates [64], [160], [161], [165], [169], [173]. Moreover, the water absorption capacity of recycled aggregates is higher compared to natural aggregates, leading to a higher water demand in the mixture. However, it has been

reported that the use of high-range water reducers and viscosity-modifying admixtures can significantly improve the workability of recycled aggregate concrete.

Topçu and Şengel [156] conducted experiments to assess the workability of fresh concrete specimens with waste concrete aggregates. Their findings revealed that workability decreased with an increase in the proportion of waste concrete aggregates, and the decrease was about 15-20% when compared to natural concrete. The decline in workability was due to the high water absorption capacity of waste concrete aggregates.

Various techniques have been proposed to mitigate the workability issues of concrete with recycle aggregate [136]. These methods involve: (1) increasing the water content of the concrete mixes in proportion to the water requirement of dry recycled aggregates; (2) pre-saturating the recycled aggregate in water for a certain period of time (e.g., 10-20 minutes or 24 hours prior to utilization); (3) increasing the moisture level of recycled aggregate up to 70-80% of its complete water absorption capacity; (4) increasing the dosage of super-plasticizer; and (5) increasing the cement content in the concrete mixture.

According to Kou et al. [174], the inclusion of ground granulated blast furnace slag and fly ash in the concrete mixture was also found to be beneficial in enhancing the workability of recycled aggregate concrete.

In the study conducted by Li et al. [68], it was observed that concrete mixes containing coarse recycled aggregate coated with pozzolanic powder exhibited greater slump compared to mixes containing coarse recycled aggregate prepared through conventional methods. The improved workability was due to the coating of recycled aggregate surface by pozzolanic powder which reduced the amount of water absorbed by the recycled aggregate and also addressed the problem of poor workability caused by the presence of attached mortar in recycled aggregates.

Güneyisi et al. [41] conducted a study to examine the impact of various surface treatment methods on the characteristics of self-compacting concrete incorporating recycled aggregates. Their findings revealed that different treatment techniques applied to the aggregates, including pre-soaking in acid solution, water glass and cement-silica fume slurry

impregnation, as well as a two-stage mixing approach, led to enhanced workability of the recycled aggregate concrete.

2.7. Hardened Concrete Properties

2.7.1. Compressive Strength and Modulus of Elasticity

Compressive strength is a crucial factor in the design and quality control of concrete mixtures [175], [176]. It is widely considered due to its simplicity and cost-effectiveness, making it a key parameter addressed by reinforced concrete structural design codes [177], [178]. Therefore, many studies have focused on evaluating and reporting the compressive strength of concrete [179]–[181].

Numerous previous research studies have investigated the influence of utilizing recycled aggregates on the compressive strength of concrete mixtures. While most of these studies reported varying degrees of strength reduction [161], [182], some studies also showed increased strength values [3], [183], [184], indicating the obtained results depend on the type of recycled aggregate used and the implementation method.

Regarding the study conducted by Topçu and Şengel [156], two different concrete mixtures made entirely with recycled aggregates exhibited a reduction of 33% and 23.5% in compressive strength compared to control concrete.

Previous studies have reported that decreasing the ratio of aggregate to cement can improve the compressive strength of recycled aggregate concrete [185], [186], attributing the reduction in strength to the low crushing strength of the recycled aggregates and a weak interfacial transition zone.

Poon et al. [2] stated that the compressive strength of concrete produced with recycled aggregate from a source of high-strength concrete is superior to that of concrete made with recycled aggregate from a source of normal-strength concrete.

The reduction in compressive strength was primarily attributed to factors such as a weak interfacial transition zone, low quality of recycled aggregates, and the presence of impurities [187], [188]. To improve the performance of recycled aggregate concrete, researchers have proposed various approaches, such as using recycled aggregates from superior sources [189], [190], employing a two-stage mixing approach [173], [191], coating recycled aggregates using carbonation treatment method [168], and removal of residual mortar in recycled aggregates with different techniques such as ball milling [192] and presoaking in an acid solution [36], and considering partial replacement of natural aggregates with recycled aggregates in concrete mixtures [184], among others.

The modulus of elasticity is another crucial mechanical property that is considered in concrete mixtures. Similar to compressive strength, concrete mixtures with recycled aggregates usually show lower values of modulus of elasticity than those with natural aggregates [190], [193]. With respect to Etxeberria et al. [194], for instance, the modulus of elasticity showed a reduction of almost 20% when natural coarse aggregates were completely replaced with recycled coarse aggregates. The lower modulus of elasticity of concrete with recycled aggregates was attributed to a weaker bonding between the aggregate and cement paste and the porosity of the resulting concrete. On the other hand, Kou et al. [195] found that the addition of fly ash for a 25% replacement of ordinary Portland cement improved the modulus of elasticity of concrete containing recycled aggregate by 20%, 50%, and 100% replacement of natural coarse aggregate.

2.7.2. Splitting Tensile Strength

Several studies have investigated the splitting tensile strength of recycled aggregate concrete mixtures. In most cases, these mixtures show lower performance compared to those with natural aggregates [60], [64], [152]. The decreased strength is mostly attributed to factors such as those mentioned above for compressive strength, including the porosity of recycled aggregates, a weak interfacial transition zone between the recycled aggregate and the concrete matrix, and the presence of impurities in the source of recycled aggregate.

Additionally, the literature provides insights into the effects of different techniques for improving the performance of recycled aggregate concrete on splitting tensile strength.

Researchers have explored strategies such as using cement replacement materials in concrete mixture [195], [196], applying surface treatments to improve the bond between recycled aggregates and the cementitious matrix, presoaking in acid solution for removal of residual mortar in recycled aggregates [197], optimizing mix proportions [195], using proper mixing approach [198], and using fibers to compensate for the reduced performance [197], [199].

2.7.3. Flexural Strength

Flexural strength evaluation is another common technique for assessing the performance of concrete mixtures under tensile stresses. Several studies have examined the flexural performance of recycled aggregate concrete mixtures, mostly reporting reduced strength values [170], [200].

The literature investigates various techniques to enhance the performance of recycled aggregate concrete on flexural strength. These techniques include the use of chopped fibers [197], [199], a two-stage mixing approach [60], supplementary cementitious materials [196], [200], and pre-soaking in an acid solution [170]. However, it should be noted that most of the implemented approaches only partially compensate for the reduction in flexural performance resulting from the use of recycled aggregates instead of natural ones.

Aside from the investigations on the mechanical properties of concrete made with recycled aggregate obtained from CDW, a number of studies have also examined the mechanical properties of concrete produced with cold-bonded fly ash aggregates [112], [117], [125], [128]–[132]. The utilization of cold-bonded fly ash aggregates as a replacement for normal weight aggregates in concrete led to a reduction in mechanical properties such as compressive strength, modulus of elasticity, splitting tensile strength, and flexural strength. However, the application of water glass or cement-silica fume slurry impregnation to cold-bonded fly ash aggregates for surface coating as a treatment method before the production of concrete improved the mechanical properties compared to untreated cold-bonded fly ash aggregates [117], [128], [131]. Similarly, incorporating polypropylene fibers and tire chips into fly ash pellets during the agglomeration process improved the mechanical properties of concrete produced with plain cold-bonded fly ash aggregates [132].

2.7.4. Impact Resistance

Concrete is a widely used construction material due to its durability and strength. However, it can still be vulnerable to sudden loads or impacts, which can lead to cracks, fractures, or even collapse. Some examples of sudden loads that concrete can be subjected to include:

- Earthquakes: Seismic activity can subject concrete structures to sudden and intense forces, leading to structural damage or collapse.
- Vehicle collisions: Concrete barriers, pillars, and walls can be subjected to sudden loads during vehicle collisions, potentially leading to structural damage or failure.
- Blasts and explosions: Concrete structures may be subjected to sudden loads during blasts or explosions, which can cause structural damage or collapse.
- Impacts of heavy machinery or equipment: Concrete slabs or pavements may be subjected to sudden loads during heavy machinery or equipment impacts, potentially leading to cracking or structural damage.

Therefore, it is important to design concrete to withstand sudden loads and impacts, and to conduct regular inspections and maintenance to identify any signs of damage or deterioration. Impact tests are an important method used to measure the performance of concrete against sudden loads and impacts. One commonly used impact test method is the drop weight impact test, as recommended by ACI 544.2R-89 [201]. This test involves dropping a 4.5 kg steel hammer from a height of 1000 mm onto the central surface of cylindrical concrete specimens. The impact test measures the resistance of the concrete to sudden and intense forces and can help identify any potential weaknesses or vulnerabilities in the material. In general, impact tests are an important tool in evaluating the performance of concrete and ensuring the safety and reliability of structures in a variety of applications.

Impact tests are important not only for conventional concrete but also for recycled aggregate concrete (RAC). While much attention has been paid to the quasi-static behavior of RAC, it is equally important to study the dynamic behavior of this material under high strain rate loadings induced by events such as earthquakes, explosions, and accidental impacts. Such events are likely to occur on various civilian and military infrastructures, and

understanding the behavior of RAC under these conditions is essential for its safe and effective use in such applications. By studying the dynamic behavior of RAC, engineers and researchers can develop more durable and resilient structures that can withstand extreme loading conditions, while also promoting sustainability by using recycled materials [202].

Xia et al. [203] used the impact test method as recommended by ACI 544.2R-89 [201] to evaluate the impact resistance of fiber reinforced recycled aggregate concrete and they also measured the effect of maximum recycled aggregate size at the same time. According to their results shown in Table 2.1, there is no significant difference in the impact resistance of concrete samples with different sizes of recycled aggregate.

Table 2.1. Impact resistance of recycled aggregate concrete [203].

Maximum recycled aggregate size (mm)	**The average number of blows for first crack**	**The average number of blows for failure**	**The impact energy after first cracking (J)**
9.5	3.75	3.75	0
19	4.25	4.25	0
31.5	3.50	3.50	0

Xiao et al. [202] applied another impact test method by using Split Hopkinson Pressure Bar (SHPB) test. In this test strain rates vary between 10/s and 100/s while that of quasi-static loading is around 0.00001/s. They evaluated the cracking behavior of the cylindrical concrete specimens and monitored prominent differences between normal aggregate concrete and recycled aggregate concrete, Figure 2.6.

In quasi-static loading, the cracked area in recycled aggregate concrete (RAC) was larger than the damage in natural aggregate concrete. Considering Lemaitre's strain equivalence principle [204] the larger damage zone resulted in a lower strength of the RAC. But when the strain rate increased, the crack propagation in RAC changed, and instead of cracking both old ITZ and new ITZ the crack occurred at the weakest zone. In the very limited time of impact loading, the micro cracks might not have enough time to develop in

the other ITZ. This situation caused a lower number of cracks in the RAC at a high strain rate than the quasi-static state. Therefore, RAC at higher strain rates had higher strength values.

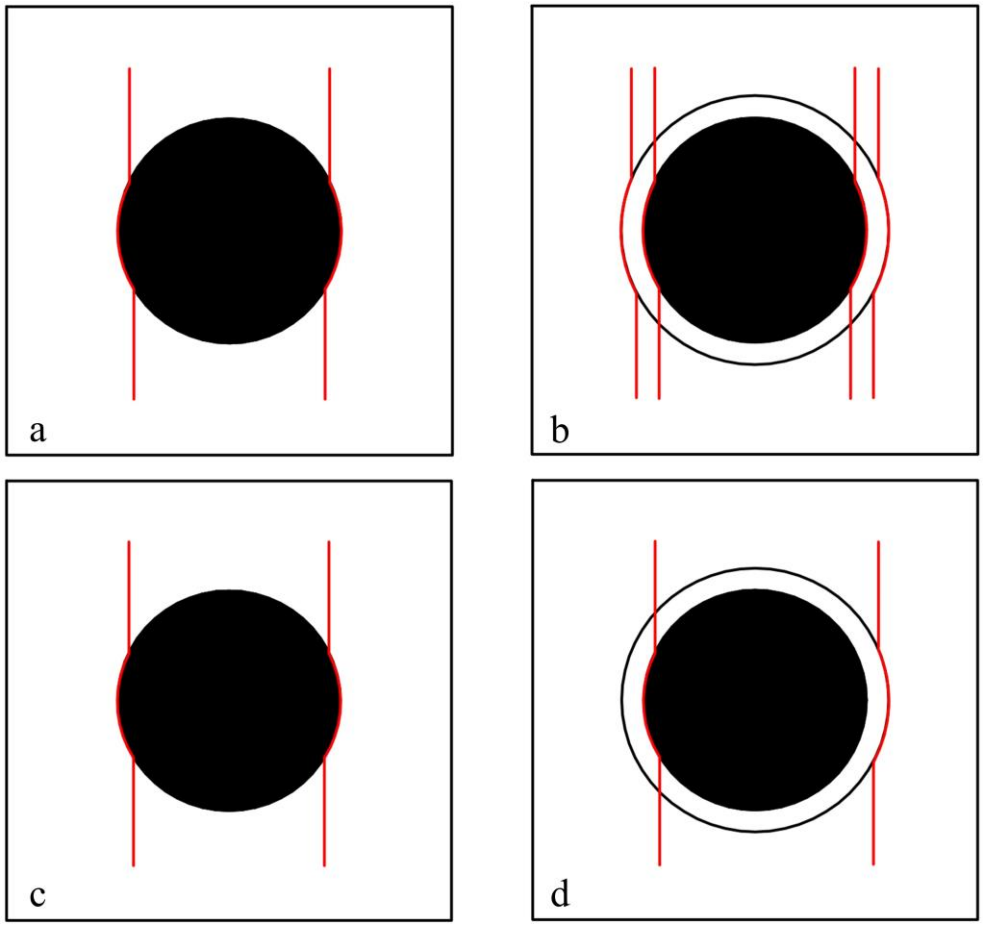

Figure 2.6. Simplified features of crack patterns of a) NAC and b) RAC under static loading, c) NAC and d) RAC under impact loading [202].

In the study by Rao et al. [169], an examination was carried out to assess the response of recycled aggregate concrete when subjected to a drop weight impact loading. The findings indicated a decrease in the impact resistance of recycled aggregate concrete as the proportion of recycled aggregate in the concrete increased. This result was attributed to the presence of micro-cracks in the recycled coarse aggregate, as well as weaker interfaces between the aggregate and the old and new mortar.

2.7.5. Fracture Parameters

Fracture parameters and impact resistance are both important aspects of the mechanical behavior of concrete, and they are closely related. Fracture parameters, such as fracture toughness and critical crack tip opening displacement, describe the ability of concrete to resist the propagation of existing cracks or the initiation of new cracks under different loading conditions. By understanding the fracture parameters and impact resistance of concrete, engineers and researchers can develop more durable and resilient structures that can withstand various loading conditions while maintaining their structural integrity and safety.

There are several fracture parameters that provide a different perspective on the behavior of concrete under different loading conditions, and are often used in combination to develop a comprehensive understanding of the properties and performance. Fracture toughness, energy absorption capacity, characteristic length, crack resistance, crack tip deformation, J integral, crack resistance curve, etc. are commonly used to describe the mechanical behavior of concrete and its resistance to cracking and failure.

Fracture toughness is a measure of the ability of concrete to resist the propagation of an existing crack, and it is defined as the amount of energy required to propagate a crack through a unit area of concrete, and it is typically measured using test methods such as the three-point bending test or the compact tension test. Higher fracture toughness indicates that the material is more resistant to cracking and can absorb more energy before failure. The cracking behavior of recycled aggregate concrete (RAC) depends on the quality of both old ITZ and new ITZ, and therefore, fracture parameters of RAC generally differ from natural aggregate concrete (NAC). The pre-existing cracks in RA constitute a key role in crack propagation under any kind of loading conditions. Chakraborty and Subramaniam [205] inferred that RAC requires less fracture energy for wider crack mouth opening. When RAC was subjected to a stress field generated by flexure, the material required less fracture energy as the crack mouth opening increased during crack penetration. In other words, the energy required to propagate a crack through the RAC decreases as the size of the crack increases. This can be attributed to the heterogeneity of the RAC and the presence of weaker interfaces between the recycled aggregates and the cement paste.

Li et al. [206] conducted a similar experiment on RAC and NAC and obtained consisted results with Chakraborty and Subramaniam [205] in terms of fracture energy. On the other hand, they observed that RAC had very similar fracture toughness values with NAC if RAC had a similar compressive strength level with NAC. Moreover, when the replacement ratio of the recycled aggregate was less than 70%, the fracture toughness of the RAC remained unchanged. If the replacement ratio of recycled aggregate exceeded 70%, the fracture toughness of RAC decreased by 10% at maximum.

Treating recycled aggregates could have several potential benefits for the fracture properties of concrete made with recycled aggregates because the treatment material could fill in the pores and micro cracks on the surface of the aggregates, leading to an improved interfacial bonding between the aggregates and the cement paste. Kazemian et al. [38] conducted a research to evaluate the performance of treated recycled aggregate concrete so they treated recycled aggregates by using calcium metasilicate slurry. According to the results, they observed an improvement in the fracture energy of treated recycled aggregate concrete.

In a study conducted by Gesoglu et al. [207], an investigation was carried out to examine the fracture parameters of self-compacting concretes incorporating recycled aggregates using a three-point bending test. The researchers employed recycled aggregates as a partial or complete substitute for natural aggregates in the concrete mixtures. The findings revealed a decrease in the fracture energy or capacity for energy absorption, as well as the characteristic length of the concrete mixtures, when recycled aggregates were used instead of natural aggregates. It is important to highlight that there exists an inverse correlation between the characteristic length and the brittleness of concrete. Specifically, as the characteristic length decreases in magnitude, the brittleness of the concrete increases.

2.7.6. Bond Strength between Rebar and Concrete

Although recycled aggregate concrete (RAC) has been a subject of study since the 1970s, its use in structural applications is relatively new. Due to a growing awareness of the importance of sustainable development and the preservation of the natural environment, many countries in Europe, as well as Japan and the United States, have already allowed the

use of RAC for construction. The bond between the concrete and the steel reinforcement is critical to the strength and stability of a reinforced concrete structure, and the use of recycled aggregates in the concrete may affect this bond. Therefore, Breccolotti and Materazzi [208] tried to determine if a modified design approach was necessary to ensure the adequate bond strength of the steel reinforcement in recycled aggregate concrete. They conducted pull-out tests on 200x200 mm concrete prisms with 14mm diameter reinforcing steel, as it is shown in Figure 2.7 and found that the use of RAC slightly affected the normalised bond strength compared to the use of natural aggregate concrete (NAC).

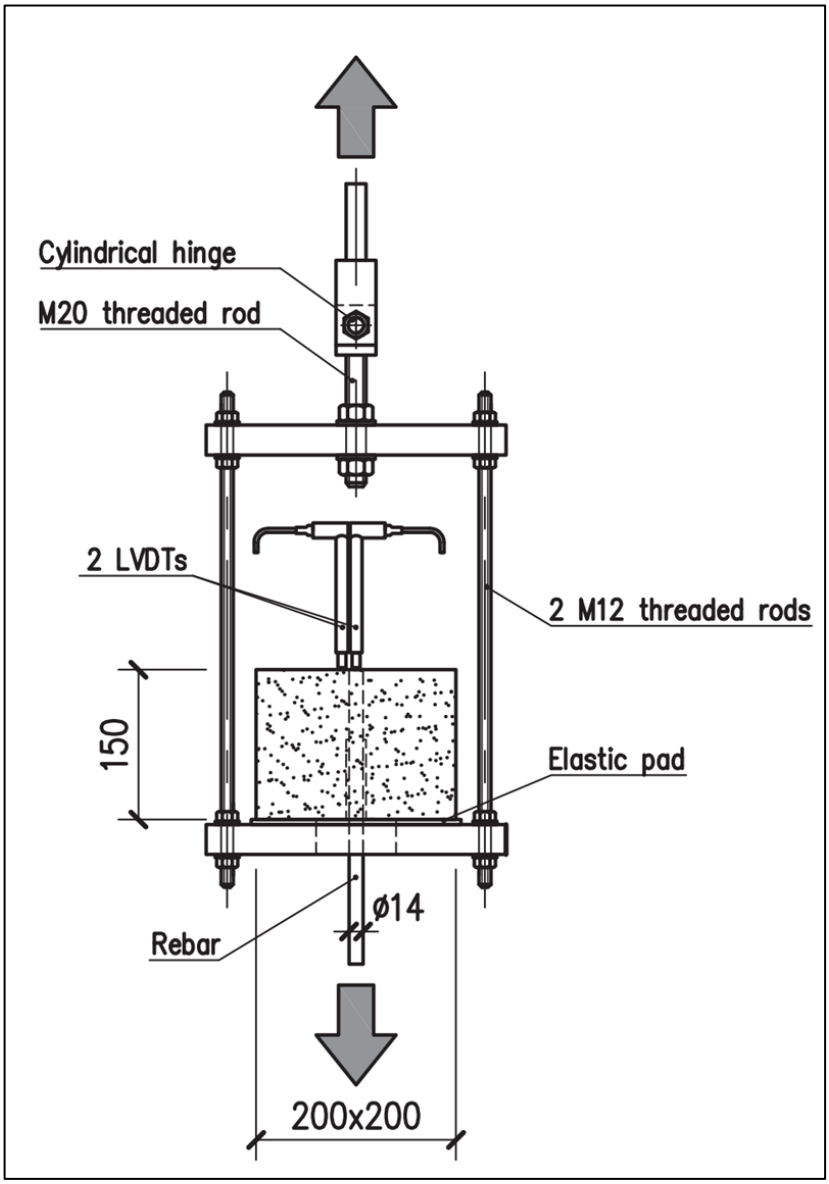

Figure 2.7. Pull-out test setup [208].

In their study, Namarak et al. [209] examined the bond strength between the reinforcement bar and the concrete containing recycled aggregate. They conducted experiments using recycled coarse aggregates (RCA) as a complete substitute for natural coarse aggregates (NCA) in concrete mixtures. The findings indicated a reduction in the bond strength between the reinforcement bar and the concrete when recycled aggregate was used. This can be attributed to the higher porosity of RCA compared to NCA, resulting in a weaker interface between recycled aggregate and cement paste, as opposed to the interface in conventional concrete.

Pandurangan et al. [35] investigated the impact of various treatment methods on the bond strength of concrete made with recycled aggregate. They produced concrete specimens by incorporating different types of coarse aggregate: natural coarse aggregate, untreated recycled coarse aggregate, and recycled coarse aggregate subjected to acid, mechanical, and thermal treatments. The incorporation of recycled coarse aggregates, either partially or completely replacing natural coarse aggregates in the concrete mixtures, resulted in a decrease in the bond strength between the reinforcement bar and the concrete. However, when recycled aggregates were pre-soaked in an acid solution or subjected to mechanical or thermal treatment, the bond strength improved compared to that of using untreated recycled aggregates in concrete mixtures. These treatment methods reduced the amount of residual mortar adhered to the recycled aggregates and enhanced the strength performance of the resulting concrete.

3. EXPERIMENTAL STUDY

In this study, the mechanical properties of concrete mixtures produced with different recycled aggregates were investigated. To produce sustainable concrete mixtures, three different recycled aggregates were used as coarse aggregates in total replacement, by volume, of crushed limestone. The recycled aggregates were used as plain and surface treated by the direct slurry method with ground granulated blast furnace slag. Microstructural investigations were also carried out on aggregate particles and aggregate-matrix interfaces (ITZs) of untreated and treated concrete mixtures to analyze the effect of recycled aggregate treatment on the mechanical properties of concrete.

3.1. Materials

CEM I type Portland cement and ground granulated blast furnace slag (GGBFS) were used in concrete mixtures as cementitious materials. Crushed stone (CSt), crushed sand, and river sand were used as natural aggregates. An F-type fly ash was utilized in order to produce recycled fly ash aggregates (FAA). Recycled brick aggregates (RBA) and recycled concrete aggregates (RCA) from a demolished building rubble were also used to produce recycled concrete mixtures. A naphthalene sulfonated formaldehyde superplasticizer was used to provide the required workability of fresh concrete. Deformed steel bars were used to produce pull-out test specimens.

3.1.1. Cement

CEM I 42.5 R Portland cement supplied by Akçansa Cement Industry and Trade Inc. was used in concrete production as binding material. The physical, chemical and mechanical properties of cement used in this study are illustrated in Tables 3.1, 3.2 and 3.3, respectively.

3.1.2. Ground Granulated Blast Furnace Slag

The ground granulated blast furnace slag (GGBFS) used as cement replacement material in concrete production and as filler material for the treatment of recycled aggregate

was provided by Bolu Cement Industry Inc. The physical and chemical properties of GGBFS are shown in Tables 3.4 and 3.5, respectively.

Table 3.1. Physical properties of cement.

Physical Properties		**Test Results**
Density	(g/cm^3)	3.14
Initial Setting Time	(min.)	103
Final Setting Time	(min.)	173
Le Chatelier	(mm)	1
Specific Surface	(cm^2/g)	3490
Residue on 45µm sieve	(%)	4.5
Residue on 90µm sieve	(%)	0.3

Table 3.2. Chemical composition of cement.

Chemical Composition		**Test Results**
SiO_2	(%)	19.80
Insoluble Residue	(%)	0.29
Al_2O_3	(%)	5.58
Fe_2O_3	(%)	3.42
CaO	(%)	63.70
MgO	(%)	1.22
SO_3	(%)	3.34
Loss on Ignition	(%)	1.85
Cl^-	(%)	0.04
Na_2O/K_2O	(%)	0.24 - 0.66
Unknown	(%)	0.15
S.CaO - Free Lime	(%)	2.20
Mineralogical Composition	C_3S	47.92
	C_2S	20.70
	C_3A	9.01
	C_4AF	10.41
LSF		0.96

Table 3.3. Mechanical properties of cement.

Strength characteristics/day	**Standards**	**Test results**
Early Strength (2 day)	≥20 MPa	27.0
Early Strength (7 day)	-	42.0
Standard Strength (28 day)	≥42.5 MPa	55.0
	≤62.5 MPa	

Table 3.4. Physical properties of GGBFS.

Physical Properties		**Test Results**
Density	(g/cm^3)	2.95
Specific Surface	(cm^2/g)	5253
Pozzolanic Activity Index 7 day	(%)	53.3
Pozzolanic Activity Index 28 day	(%)	75.0
Initial Setting Time	(min.)	260
Residue on 45μm sieve	(%)	1.4
Residue on 90μm sieve	(%)	0.0

Table 3.5. Chemical composition of GGBFS.

Chemical Composition		**Test Results**
SiO_2	(%)	40.95
Al_2O_3	(%)	12.10
Fe_2O_3	(%)	1.28
CaO	(%)	36.63
MgO	(%)	5.48
SO_3	(%)	0.16
Na_2O	(%)	0.56
K_2O	(%)	0.36
Loss on Ignition	(%)	0.11
Cl^-	(%)	0.018

3.1.3. Fly Ash

An F-type fly ash from Çatalağzı Thermal Power Plant, Zonguldak, Turkey, with a density of 2.13 g/cm^3 was used in the production of recycled fly ash aggregates. The chemical composition of the fly ash and the specification requirements are shown in Table 3.6. The physical properties of the fly ash are also given in Table 3.7.

Table 3.6. Chemical composition of fly ash and specification requirements.

Composition (%)	**Fly ash**	**ASTM C618 (Class-F)**
$SiO_2+Al_2O_3+Fe_2O_3$	86.30	70 (min)
MgO	2.08	5 (max)
CaO	2.10	<10
SO_3	0.20	5 (max)
Loss on Ignition	3.30	6 (max)

Fly ash complies with the requirements of Class F as limited by ASTM C618 [210].

Table 3.7. Physical properties of fly ash.

Physical Properties		**Test Results**
Density	(g/cm^3)	2.13
Pozzolanic Activity Index 28 day	(%)	83.0
Pozzolanic Activity Index 90 day	(%)	97.0
Residue on 45µm sieve	(%)	29.4

3.1.4. Aggregates

Natural sand and crushed sand (0-4 mm) with specific gravities of 2.65 and 2.70, respectively, were used as fine aggregates as well as crushed stone (CSt) as coarse aggregates (4-16mm) in concrete production. Recycled brick aggregates (RBA), recycled concrete aggregates (RCA), and recycled fly ash aggregates (FAA) were also used as a total replacement of crushed stone coarse aggregates for the production of recycled concrete mixtures. The crushed RBA and RCA were obtained from an aggregate recycling plant of

İSTAÇ (The İstanbul Environmental Protection and Waste Processing Corporation). The aggregate recycling process in this plant is generally as follows. First, construction and demolition waste taken from the site was crushed into relatively small parts with the help of an excavator with a hydraulic impact hammer. Then the concrete or masonry parts were transported to a jaw crusher using a track loader. After the crushing operation, steel bars (if any) were separated from the obtained product using a magnetic separator. In the end, the crushed aggregates were sieved to the desired sizes and the final products were transported to the plant storage area using dump trucks. Recycled fly ash aggregates, FAA, on the other hand, were produced through the cold-bonding agglomeration process under laboratory conditions.

3.1.4.1. Preparation of Fly Ash Aggregates. Fly ash aggregates were produced through the cold-bonding agglomeration process by a pelletizing disc shown in Figure 3.1. The pelletizer disc has a diameter of 80 cm and a height of 40 cm. To produce fly ash pellets, dry fly ash-cement mixtures were fed into the disc with an inclination angle of 43˚ and rotated at 45 rpm according to the results of Baykal and Döven [97]. In the next step, water was sprayed onto the powder mixtures during the first 10 minutes of the agglomeration process at an amount of 23-27% of the total weight of material to obtain the spherical pellets. An extra 10 minutes was allocated to further compaction of the fresh pellets to increase their strength. Fly ash aggregates were produced with a cement-to-fly ash ratio of 0.1 by weight. The fresh pellets were preserved in plastic bags and left for final hardening inside a curing room at a temperature of 20±2 ˚C and 90±5% RH for 28 days.

Figure 3.1. General view of the pelletizing disc and the production of fly ash aggregate.

3.1.4.2. Tests and Measurements on Coarse Aggregates. RBA, RCA and FAA were sieved into 4-8mm and 8-16mm size fractions to be used for replacing the CSt coarse aggregates No-I and No-II, respectively, as seen in Figure 3.2. Unit weight (ASTM C29 [211]), specific gravity and water absorption (ASTM C127 [212]) values of aggregates were determined according to the specified standards as well as the flakiness index (FI, %) of the coarse aggregates with reference to BS EN 933-3 [213]. Since the recycled aggregates used in this study were obtained and reproduced under special conditions, it is important to determine the flakiness index, which is a geometric property, for each one. Because, as the flakiness index of the aggregates increases, the workability of the concrete decreases, the water requirement and the amount of entrapped air increase, and consequently the strength of the concrete is adversely affected. In this respect, it is recommended that the flakiness index shall not exceed 40% for crushed rock or crushed gravel so that any aggregate can be used in concrete production [214]. Aggregate crushing values (ACV,%) and aggregate impact values (AIV,%) of CSt, RCA, RBA and FAA were also identified in compliance with BS 812-110 [215] and BS 812-112 [216], respectively, to investigate the correlation of these values with the compressive strength and impact resistance of the concrete mixtures produced with the related aggregates. For a cohesive and homogeneous concrete production, the optimal grain size distribution of the aggregates was designated with respect to TS 802 [217].

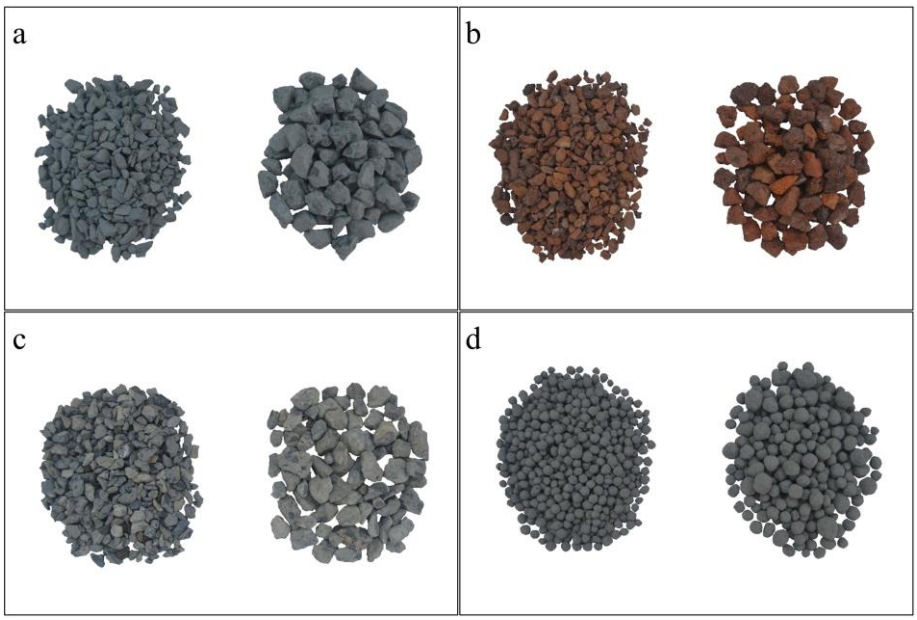

Figure 3.2. Separated aggregates into two groups: (a) CSt, (b) RBA, (c) RCA, (d) FAA.

3.1.5. Superplasticizer

As a chemical admixture, Rheobuild-1000, which is an ASTM C494 [218] Type F high range water-reducing superplasticizer, was used in concrete mixtures so as to get the slump of 18±2 cm. Rheobuild-1000 was procured by BASF-YKS Construction Chemicals.

Table 3.8. Properties of superplasticizer.

Properties	Test Results
Color	Dark Brown
Physical State	Liquid
Odor	Musty
Specific Gravity	1.21
pH	Approx. 7.0
Chloride Content	≤ 0.1% (BS EN 480-10 [219])
Alkali Content	≤ 5% (BS EN 480-12 [220])
Boiling Point	212 ˚F (100 ˚C)
Freeze Point	28 ˚F (-2 ˚C)
Water Solubility	Completely Soluble

3.1.6. Reinforcing Steel

Ribbed steel bars (S420), which had a diameter of 14 mm, were used to determine the bond strength through pull-out test.

3.2. Concrete Mix Design and Concrete Casting

3.2.1. Aggregate Grading

The experiments of sieve analysis conducted on crushed stone (CSt), crushed sand and natural sand according to TS 802. The maximum grain size of the aggregates preferred to be used in this study was 16 mm. The outcomes of the sieve analysis are shown in Table 3.9.

With reference to the results of the sieve analysis, it was determined to mix crushed stone, crushed sand, and natural sand in proportions of 55, 40 and 5% of the total aggregate volume, respectively, in concrete production. Crushed stone coarse aggregate No-I and No-II, on the other hand, were considered to be used equally by volume for optimum grain size distribution. The grading curve constructed to be utilized in the ultimate concrete mixture concerning the limitations recommended by TS 802 can be seen in Figure 3.3.

Table 3.9. Sieve analysis of the aggregates.

Sieve Size (mm)	Percent Passing (%)			
	Crushed Stone		Crushed Sand	Natural Sand
	No-I	No-II		
16.00	100	100	100	100
8.00	100	0	100	100
4.00	0	0	97.86	100
2.00	0	0	67.94	100
1.00	0	0	43.29	99.48
0.50	0	0	25.42	93.05
0.25	0	0	14.57	8.38

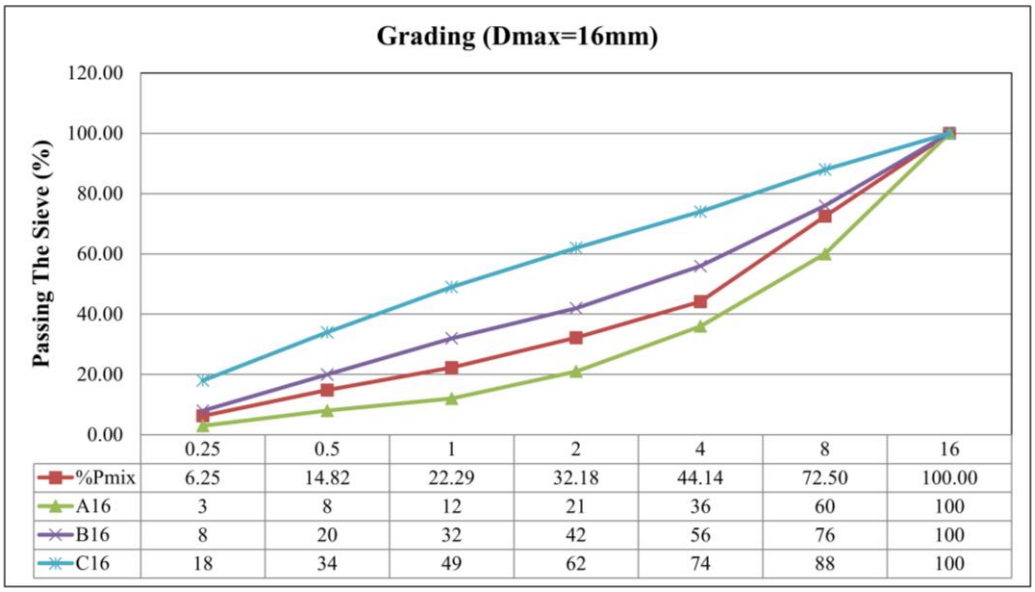

Figure 3.3. Aggregate grading.

3.2.2. Concrete Mix Design

The control concrete mixture (CStC) was produced using 321.4 kg/m^3 Portland cement, 128.6 kg/m^3 GGBFS, 85.05 kg/m^3 and 693.25 kg/m^3 natural and crushed sand, respectively, 476.61 kg/m^3 crushed stone No-I and No-II, each, and 212.14 kg/m^3 water at a w/c of 0.50. The total cementitious material used in the concrete mixture was 450 kg/m^3. The cement replacement ratio of GGBFS was determined to be 40% by weight, because it was recommended as the optimum replacement ratio in the literature [221]. The water content in the concrete mixture was calculated regarding the cement equivalence factor of 0.8 for GGBFS with respect to TS 13515 [222] and TS EN 206-1 [223]. The control concrete was designed to have a compressive strength of 40-50 MPa. Six recycled aggregate concrete mixtures were produced by replacing both the No-I and No-II crushed stone coarse aggregates in the control concrete with recycled aggregates, which were utilized as plain (RBA, RCA, FAA) and surface treated (TRBA, TRCA, TFAA) by GGBFS slurry, on volume basis, as given in Table 3.10. Thus, changes in the amount of ingredients were eliminated to investigate the performance of the recycled aggregates regarding the mechanical properties of the concrete. RBA, RCA and FAA were used as a total replacement of CSt coarse aggregates in recycled aggregate concrete mixtures to reveal the most disadvantageous situation for each recycled aggregate.

A sufficient amount of superplasticizer (SP) was added into the concrete mixtures to get a slump of 18 ± 2 cm.

Table 3.10. The mix proportions of concrete mixtures (kg/m^3).

Concrete Mixtures	**Coarse Aggregates (kg/m^3)**								**SP**	
	CSt		**RCA**		**RBA**		**FAA**		**(%)**	**(kg/m^3)**
	No-I	**No-II**	**No-I**	**No-II**	**No-I**	**No-II**	**No-I**	**No-II**		
CStC	476.61	476.61	-	-	-	-	-	-	0.85	3.825
RCAC	-	-	423.65	428.95	-	-	-	-	0.75	3.375
TRCAC	-	-	423.65	428.95	-	-	-	-	0.75	3.375
RBAC	-	-	-	-	367.17	370.70	-	-	0.65	2.925
TRBAC	-	-	-	-	367.17	370.70	-	-	0.65	2.925
FAAC	-	-	-	-	-	-	291.26	294.79	0.55	2.475
TFAAC	-	-	-	-	-	-	291.26	294.79	0.55	2.475

Concrete mixtures were designated considering the coarse aggregates with which concrete mixtures were produced. For instance, the one produced with the crushed stone (CSt) coarse aggregate represented by the notation of CStC. Similarly, TFAAC represents the concrete mixture produced with the treated recycled fly ash aggregate (TFAA). Here, the letter "C" at the end of the notation stands for the word "Concrete". The former letters, on the other hand, symbolize the abbreviation of the plain or treated coarse aggregate used to produce the relevant concrete mixtures.

3.2.3. Concrete Casting

A special procedure was applied for the concrete casting to minimize the slump loss due to the high water absorption of the recycled aggregates. For this purpose, recycled aggregates were first submerged in water for 24 hours to be saturated and then kept on large scale sieves for 1 hour to be surface dried before mixing. The concrete mixtures of CStC, RCAC, RBAC and FAAC were cast in reference to ASTM C192 [224], however, a specific procedure was performed for casting TRCAC, TRBAC and TFAAC as illustrated in Figure 3.4 with reference to the previous studies [60], [61], [68], [225].

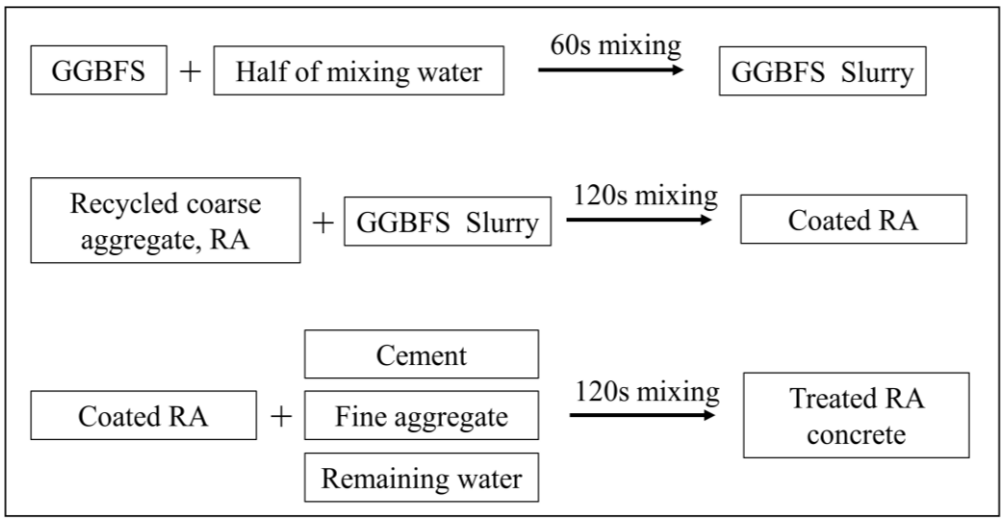

Figure 3.4. Direct slurry method for the production of treated recycled aggregate concrete.

The GGBFS was mixed with half of the mixing water for sixty seconds in a bucket to obtain the GGBFS slurry by means of a stirrer motor before having the treated recycled aggregate concrete mixtures, as shown in Figure 3.5. Then, recycled coarse aggregates were

coated with GGBFS slurry in a concrete mixer for two minutes. The slurry-coated recycled aggregates can be viewed in Figure 3.6.

The slump and unit weight of fresh concrete were measured immediately after concrete production with regard to ASTM C143 [226] and ASTM C138 [227], respectively.

Figure 3.5. Preparation of GGBFS slurry with a stirrer motor.

Figure 3.6. GGBFS slurry coated recycled aggregates: (a) TRCA, (b) TRBA, (c) TFAA.

3.2.4. Concrete Test Specimens and Curing Conditions

After concrete casting, all specimens were finished with a steel trowel and the specimens were covered with nylon sheets to prevent loss of water. The specimens were then left in the laboratory environment for 24 hours. Following that, specimens were demolded

and labeled before they were stored to meet curing conditions. Cylinder and beam specimens were stored in a curing pool at a temperature of 20±2˚C for 28 days until testing, while pull-out specimens were preserved inside a curing room at a temperature of 20±2 ˚C and 90±5% RH for 28 days.

The dimensions and number of concrete specimens produced to test certain mechanical properties and fracture parameters in the scope of this study are shown in Table 3.11.

Table 3.11. Concrete specimens tested for certain mechanical properties in this study.

Concrete Mixtures	**Cylinder Specimens (100x200 mm)**		**Cylinder Specimens (150x300 mm)**	**Beam Specimens (100x100x350 mm)**	**Pull-Out Specimens**		**Total**
					Cubic Specimens (200x200x200 mm)	**Column Specimens (200x200x600 mm)**	
	F_c & E_c	**F_t**	**Impact Resistance**	**F_{net}, E_b, G_F, l_{ch}, K_{IC}^S, $CTOD_c$**	**τ_b**		
CStC	12	12	6 (x4)	12	3	3	48
RCAC	13	13	6 (x4)	12	3	3	50
TRCAC	14	13	6 (x4)	12	3	3	51
RBAC	14	13	6 (x4)	12	3	3	51
TRBAC	13	12	6 (x4)	12	3	3	49
FAAC	13	13	6 (x4)	12	3	3	50
TFAAC	13	13	6 (x4)	12	3	3	50
Total	92	89	42	84	21	21	349

The symbols given in the table for certain mechanical properties and fracture parameters are explained in the 'List of Symbols'.

3.3. Tests on Hardened Concrete

3.3.1. Determination of Mechanical Properties

3.3.1.1. Compressive Strength. The compressive strength test was performed on 100x200mm cylinder specimens using a 500 kN capacity testing machine in accordance with ASTM C39 [228]. For the sake of simplicity, the cylinder specimens were grinded before testing with a grinding machine in regards to ASTM C42 [229] instead of capping the ends of the cylinder specimens with sulfur mortar according to ASTM C617 [230] to have the loading plates parallel to each other during loading for a uniform stress distribution. Cylinder specimens were loaded axially as demonstrated in Figure 3.7 at a constant rate of 4.8 kN/sec until failure occurred.

3.3.1.2. Static Modulus of Elasticity. A test to measure the modulus of elasticity was performed on the cylinder specimens, which were tested for compressive strength, with respect to ASTM C 469 [231]. The longitudinal deformations of the concrete specimens under uniaxial loading were measured using two LVDTs that were placed on the specimens and connected to a data acquisition system, as shown in Figure 3.7. Then, the longitudinal strain, which is defined as the total longitudinal deformation divided by the effective gage length, was calculated to construct a stress-strain curve for each specimen. The slope of such curves gives the static elastic modulus of concrete.

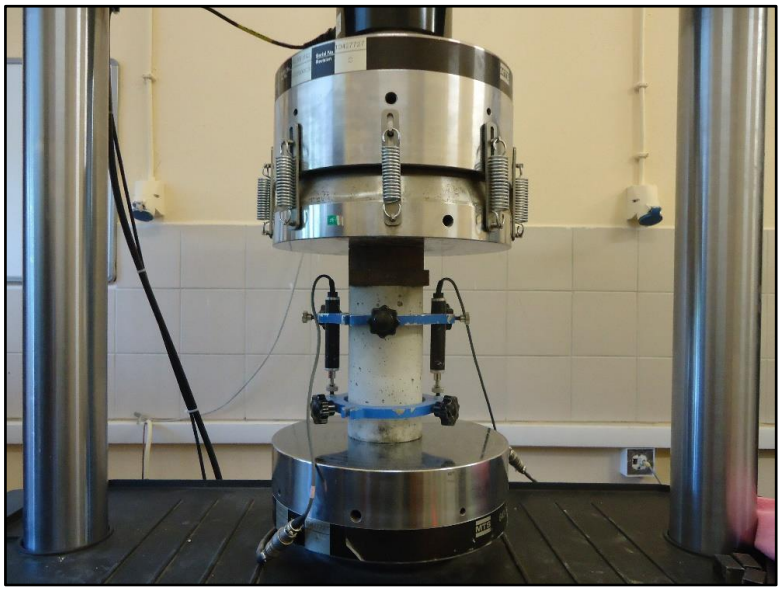

Figure 3.7. Test setup for compressive strength and modulus of elasticity.

3.3.1.3. Splitting Tensile Strength. The splitting tensile strength test was performed on 100x200mm cylinder specimens in reference to ASTM C 496 [232]. The load was applied in a diametrically opposite direction to a cylinder specimen laid on its side as presented in Figure 3.8 by the help of a testing machine with 3000 kN capacity at a constant rate of 0.5 kN/s.

3.3.1.4. Flexural Strength. Twelve 100x100x350mm beam specimens with a 30 mm notch at mid-span for each concrete mixture were prepared and tested to determine the flexural strength according to JCI-S-001 [233]. Beam specimens with a clear span of 300 mm were statically loaded under a three-point bending test using a 100 kN capacity MTS Landmark

Closed-Loop Displacement Controlled Dynamic Testing Machine at a constant CMOD (crack mouth opening displacement) rate of 0.05 mm/min. The deflection of the beam specimens was measured with the help of LVDTs that were placed at mid-span parallel to loading direction. The test setup can be seen in Figure 3.9. The net flexural strength of the beam specimens was calculated with the formula recommended by ASTM D 7264 [234] as follows:

$$F_{net} = \frac{3PL}{2b(h - a_0)^2} \tag{3.1}$$

where P is the maximum load, N, L is the support span, mm, b refers to the width of the beam specimen, mm, h refers to the depth/thickness of the beam specimen, mm, and a_0 is the notch depth, mm.

Figure 3.8. Test setup for splitting tensile strength.

3.3.1.5. Impact Resistance. The impact resistance of the concrete specimens was measured using the methodology of the "modified ACI drop-weight impact test" proposed by Badr and Ashour [235]. The test was performed on 50mm-thick notched disks sliced from 150x300mm notched cylinder specimens with a drop-weight impact test setup, as illustrated in Figure 3.10. This test was conducted with equipment that consists of a standard, manually operated compaction hammer (4.54 kg) with a drop of 457 mm (ASTM D 1557 [236]), an

impact piston, and a flat base plate with two steel notches to fix the disk specimens during repeated impact loading. The impact piston was produced with a hardened steel bar (13 mm in diameter by 50 mm in length), which was utilized for providing a 50 mm line of impact, attached to a 50 mm hardened steel cylinder with a height of 50 mm, as seen in Figure 3.11. The hammer was repeatedly dropped on the impact piston to apply impact load through the line of two 25 mm triangular notches located at the ends of the the diameter of disk specimens until failure occurred. The disk specimens failed by cracking through the line of impact and two notches (Figure 3.12) were accepted in order to determine the average drop-weight impact energy of the concrete mixtures. However, any other cracking pattern was rejected.

The formulas for the calculation of the impact energy per blow of the hammer as reported by Gopalaratnam and Shah [237] and Mohammadi *et al.* [238] are given as follows:

$$H = \frac{gt^2}{2} \tag{3.2}$$

$$V = gt \tag{3.3}$$

$$m = \frac{W}{g} \tag{3.4}$$

$$U = \frac{mV^2}{2} \tag{3.5}$$

where H is the height of the fall, t is the time taken by the hammer to fall a height of 457 mm, g is the acceleration due to gravity, V is the velocity of the hammer at impact moment, W is the weight of the hammer, m is mass of the hammer and U is the impact energy per blow of the hammer. Substituting the relevant values into the equations above, impact energy per blow of the hammer can be found as below:

$$457 = \frac{9810 \times t^2}{2} \rightarrow t \cong 0.305\ sec \tag{3.6}$$

$$V = 9810 \times 0.305 = 2992.05\ mm/sec \tag{3.7}$$

$$4.54 = \frac{W}{9.81} \rightarrow W \cong 44.54\ N \tag{3.8}$$

$$U = \frac{44.54(2992.05)^2}{2 \times 9810} \cong 20323\ \ Nmm \tag{3.9}$$

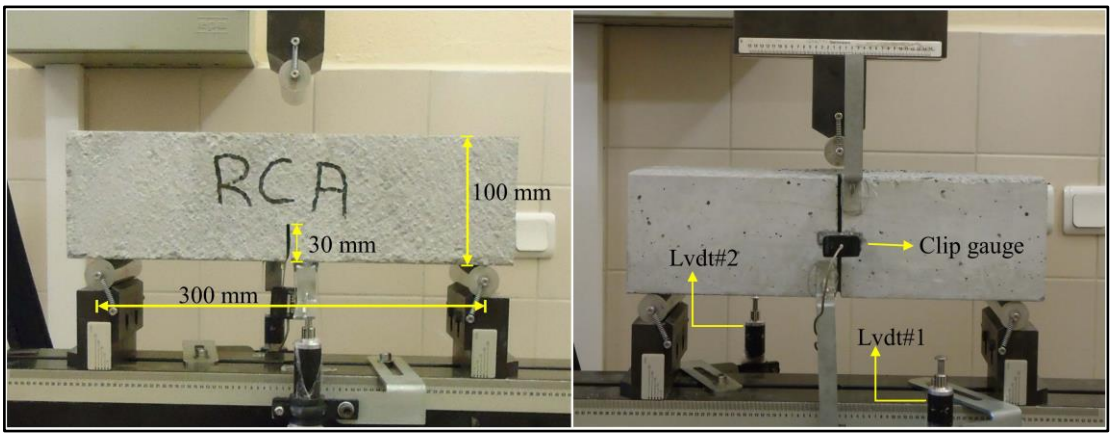

Figure 3.9. Test setup for flexural strength.

Figure 3.10. Test setup for drop weight impact resistance.

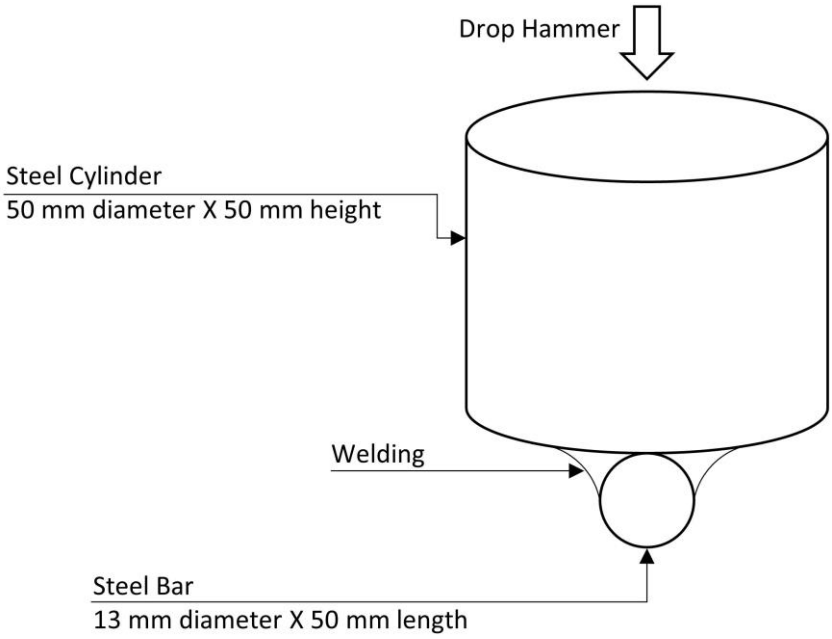

Figure 3.11. The schematic view of the impact piston.

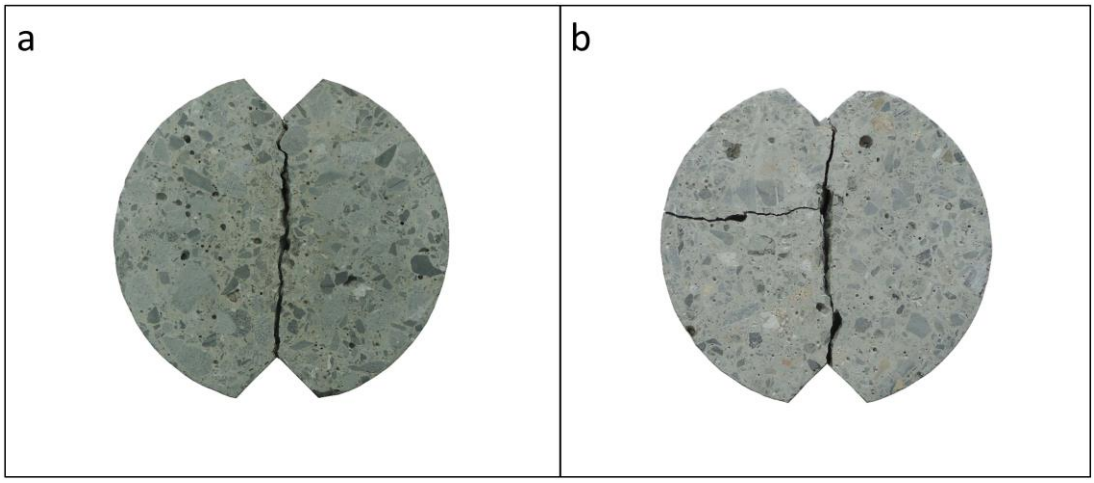

Figure 3.12. Notched specimens: (a) Accepted failure, (b) Rejected failure.

3.3.2. Fracture Properties of Concrete under Three Point Bending

The critical stress intensity factor known as the fracture toughness (K_{IC}^{S}) and the corresponding critical crack-tip opening displacement ($CTOD_c$) of the beam specimens with a notch at mid-span were determined under three point bending test for all the concrete mixtures according to the two-parameter fracture model proposed by Jenq and Shah [239]–[241]. The critical crack tip opening displacement occurs at the initial notch tip when the

applied load reaches its peak value, indicating the limit beyond which crack starts to propagate in an unstable manner. Here, the unstable crack growth implies that the crack instinctively propagates even if the load remains constant or decreases [242]. The stress intensity factor is another significant fracture parameter of the concrete for measuring fracture performance, which refers to the ability of concrete to withstand crack extension or the capacity of concrete to resist the brittle fracture [243].

The critical stress intensity factor for the concrete mixtures produced in this study was determined using the expressions below [240], [244]:

$$K_{IC}^{S} = 3(P_{max} + 0.5W)\frac{S\sqrt{\pi a_c}}{2d^2 b}F(a_c/d) \tag{3.10}$$

where P_{max} is the peak load, $W = W_0 S/L$, W_0 is the self-weight of the beam specimen, S is the span length, L is the beam length, d is the beam depth, b is the beam width, and

$$F(a_c/d) = \frac{1.99 - (a_c/d)(1 - a_c/d)[2.15 - 3.93(a_c/d) + 2.70(a_c/d)^2]}{\sqrt{\pi}(1 + 2\,a_c/d\,)(1 - a_c/d)^{3/2}} \tag{3.11}$$

where a_c is the effective critical crack length that was calculated by the formula defined as below [242], [243], [245]–[247]:

$$a_c = \frac{2}{\pi}\ (d + h_0)arctan\sqrt{\frac{bE_b(CMOD_c)}{32.6P_{max}} - 0.1135} - h_0 \tag{3.12}$$

where h_0 is the thickness of the knife-edge on which the clip gauge is attached to measure the crack mouth opening displacement (CMOD), $CMOD_c$ is the critical crack mouth opening displacement at peak load, and E_b is the modulus of elasticity that was determined by the following formula [240], [244]:

$$E_b = \frac{6Sa_0V(\alpha_0)}{C_i d^2 b} \tag{3.13}$$

where C_i is the initial compliance obtained from the Load-CMOD curve as the inverse of the slope of the initial loading cycle from 10% to 40% of the peak load, a_0 is the initial notch depth, and $V(\alpha_0)$ is the geometric function that was computed as below [240], [244]:

$$V(\alpha_0) = 0.76 - 2.28\alpha_0 + 3.87(\alpha_0)^2 - 2.04(\alpha_0)^3 + \frac{0.66}{(1-\alpha_0)^2} \quad (3.14)$$

where $\alpha_0 = (a_0 + h_0)/(d + h_0)$.

The critical crack tip opening displacement ($CTOD_c$) of the concrete mixtures was determined by the following equations [240], [244]:

$$CTOD_c = \frac{6(P_{max} + 0.5W)Sa_cV(a_c/d)}{E_b d^2 b}\,\beta(a_0/a_c) \quad (3.15)$$

$$V(a_c/d) = 0.76 - 2.28(a_c/d) + 3.87(a_c/d)^2 - 2.04(a_c/d)^3 + \frac{0.66}{(1-a_c/d)^2} \quad (3.16)$$

$$\beta(a_0/a_c) = [(1 - a_0/a_c)^2 + (1.081 - 1.149\frac{a_c}{d})(a_0/a_c - (a_0/a_c)^2]^{1/2} \quad (3.17)$$

In addition to (K_{IC}^S) and $CTOD_c$, the fracture energy or energy absorption capacity of the concrete, G_F, under three point bending test conducted on the beam specimens was also calculated for all the concrete mixtures produced in this study by the formula as defined below [248]:

$$G_F(N/m) = \frac{A + mg\frac{S}{L}\delta_{max}}{b(d - a_0)} \quad (3.18)$$

where A is the area (N m) under the load-displacement curve of the beam specimen, b, d, S, L, a_0, m, δ_{max} and g are the width (m), depth (m), support span (m), length (m), notch depth (m), mass (kg), maximum deflection (m) and gravitational acceleration, respectively.

Moreover, as a measure of brittleness, the characteristic length of the concrete mixtures was determined by the following expression [249]:

$$l_{ch} = \frac{E_b G_F}{f_t^2} \tag{3.19}$$

where l_{ch} is the characteristic length (mm), E_b is the modulus of elasticity (N/mm^2), G_F is the fracture energy (N/m) and f_t is the direct tensile strength that was replaced by the splitting tensile strength (N/mm^2) in this study. Here, it should be noted that as the magnitude of the characteristic length decreases, the brittleness of the concrete increases.

3.3.3. Bond Developed with Reinforcing Bar

In order to determine the bond strength developed between the reinforcing bar and the concrete, the pull-out test was applied to 200x200x200mm cubic specimens with a single ribbed bar embedded vertically along a central axis perpendicular to the concrete casting direction as detailed in Figure 3.13 in compliance with BS EN 10080 [250].

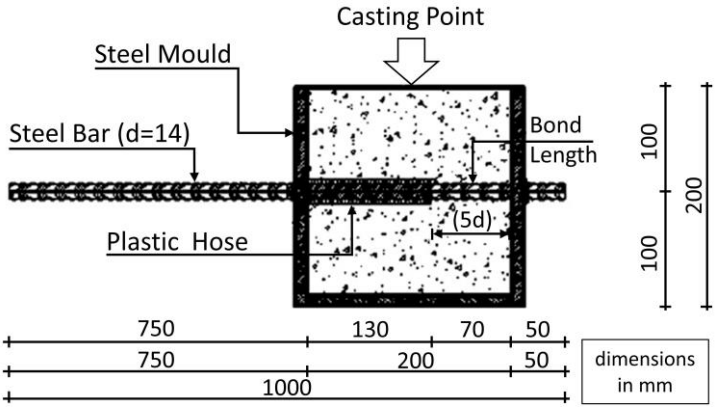

Figure 3.13. Section view of a cubic specimen for bond strength.

The top-bar effect (bond variation over height) was also investigated by comparing the bond strength values of the deformed reinforcing bars located at the top, middle, and bottom perpendicular to the long axis and equidistant from the vertical sides of the prism for all concrete mixtures by means of a pull-out test on 200x200x600 mm column specimens as seen in Figure 3.14.

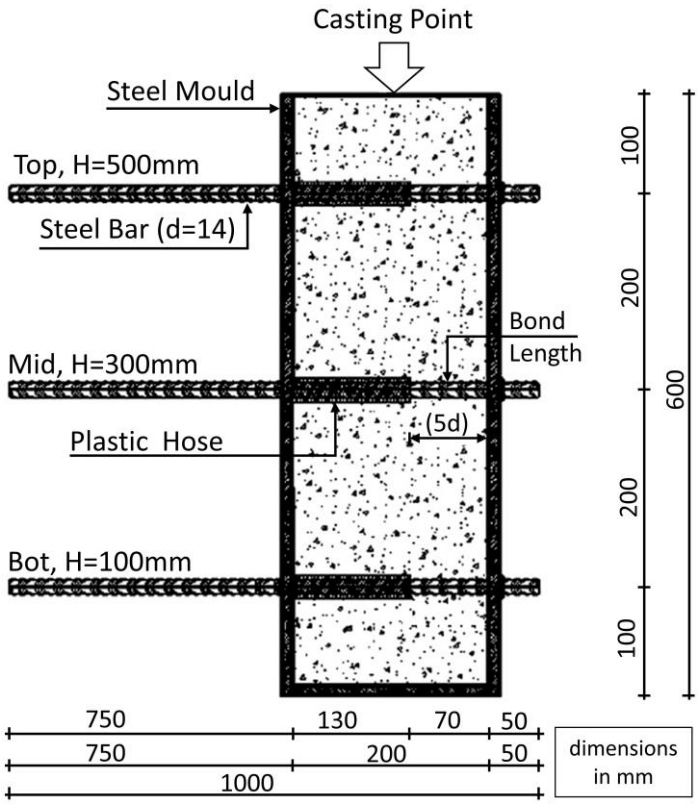

Figure 3.14. Section view of a column specimen for top-bar effect.

On the other hand, the effect of the overlying and underlying concrete layers was examined by comparing the bond strength values of the reinforcing bars in cubic specimens with the bond strength values of the bottom and the top rebars in column specimens, τ_{bot} and τ_{top}, respectively.

The column top rebars and the rebars in cubic specimens have the same overlying concrete layer thickness of 100 mm; however, different underlying layer thicknesses of 500 and 100 mm, respectively. Similarly, the column bottom rebars and the rebars in cubic specimens have the same underlying layer thickness of 100 mm, while they have different overlying concrete layer thicknesses of 500 and 100 mm, respectively. For this reason, the ratios τ_{bot}/τ_{cube} and τ_{top}/τ_{cube} were evaluated so as to examine the impact of the overlying and underlying concrete layers on the bond strength developed between the reinforcing bar and the concrete, respectively. Herein, it should be pointed out that the ratio τ/τ_{cube} lower than 1.0 indicates a negative effect on the bond strength of the corresponding overlying and underlying concrete layer for $\tau = \tau_{bot}$ and $\tau = \tau_{top}$, respectively. As opposed to that, ratio

values bigger than 1.0 refer to higher homogeneity and better compaction of the material [251].

The pull-out test was conducted on the cubic and column specimens by applying an axial tensile load on the reinforcing bars embedded in the concrete. The reinforcing bars gripped in jaws installed on the moving head of the testing machine were pulled while the concrete specimens were placed and fixed on the stationary head. The slip of the reinforcing bars was measured using two LVDTs that were attached to the steel bar at the loaded end above the stationary head. The readings obtained via those two LVDTs with the help of a data acquisition system were averaged to eliminate any accidental eccentricity. Another LVDT was also mounted at the free end of the reinforcing bar in order to measure the free-end slip. The free end of the steel bar remained unstressed during the test. The anchorage length of the deformed steel bars (S420), which had a diameter (d) of 14 mm, was 70 mm (5d) for all concrete mixtures tested over cubic and column specimens. The test was performed by using a 200 kN capacity universal testing machine at a constant displacement rate of 0.02 mm/sec. The test setup for cubic and column specimens can be seen in Figures 3.15 and 3.16, respectively.

The ultimate bond strength values of deformed reinforcing bars embedded in concrete were calculated by the formula given below [252]:

$$\tau_u = \frac{P_{max}}{\pi d_b l_b} \ (MPa) \tag{3.20}$$

where P_{max} is the maximum pull-out load, N, d_b is the nominal bar diameter, mm, and l_b refers to the bond length, mm. At this point, in order to make a fair comparison between different concrete mixtures, the ultimate bond strength values were normalized by taking the variation of compressive strength of the concrete mixtures into account as follows [209], [253], [254]:

$$\tau_{nz} = \frac{\tau_u}{\sqrt{f_c}} \ (MPa^{0.5}) \tag{3.21}$$

where τ_{nz} is the normalized bond strength and f_c is the compressive strength of the related concrete mixtures.

On the other hand, the ultimate bond strength values obtained as a result of the experiments conducted in this study were compared with the minimum required bond strength values predicted using the following design equation suggested by ACI 318-02 [255]:

$$\tau_{ACI} = \frac{A_b f_y}{\pi d_b l_d} \ (MPa) \tag{3.22}$$

where A_b is the area of the deformed bar, mm^2, f_y is the specified yield strength of the bar, N/mm^2, d_b is the nominal bar diameter, mm, and l_d is the development length, mm, of the bar that can be calculated by the equation below [255]:

$$l_d = \left(0.03 \frac{f_y(\alpha\beta\gamma\lambda)}{\sqrt{f_c}}\right) d_b \tag{3.23}$$

where f_y is the specified yield strength of the bar, psi, α is the reinforcement location factor that can be set to 1.3 when the horizontal reinforcing bar is placed in such a position where more than 304.8 mm (12 in.) of fresh concrete is cast below the bar and 1.0 for other cases, β is the reinforcement coating factor that should be taken as 1.0 for uncoated bars, γ is the reinforcement size factor that should be set to 0.8 for No.6 and smaller bars (No.6 bar has a diameter of 19.1 mm according to ASTM A615 [256]), λ is the concrete factor that can be taken as 1.3 when lightweight concrete is utilized or 1.0 when normal weight concrete is preferred, and f_c is the compressive strength of the concrete, psi.

Development length (l_d) is defined as "*the length of bar required to develop f_s, the stress in the reinforcement resulting from the loads applied to the structure*" by ACI 408R-03 [257].

Figure 3.15. Test setup for pull-out test on cube specimens.

Figure 3.16. Test setup for pull-out test on column specimens.

3.4. Microstructural Analysis

In this part of the study, microstructural investigations were conducted on both individual aggregates and concrete samples obtained from the concrete specimens to analyze the effect of recycled aggregate treatment on the mechanical properties of recycled aggregate concrete mixtures by using the equipment in Boğaziçi University Advanced Technologies Research and Development Center.

An environmental scanning electron microscope equipped with a unit for energy-dispersive X-ray spectroscopy (Philips XL30 ESEM-FEG/EDAX) was used to monitor pores, cracks, crystal structures, and morphological changes on the aggregate particles and aggregate-matrix interfaces (ITZs) of untreated and treated concrete mixtures. Elemental compositions were also examined by the findings of energy dispersive X-ray (EDAX) analyses. Since electrically conductive samples are required for microstructural analysis to have pure images, samples were coated by a thin layer of gold sprayed onto the sample surface. During SEM observation, different accelerating voltages (10, 15, 20 kV) were applied with the working distance in the range of 8.4-12.3 mm at various magnifications.

XRD analyses were performed with Rigaku D/MAX-Ultima+/PC X-ray diffraction equipment on powder samples taken from the aggregate-matrix interfaces in recycled aggregate concrete mixtures in order to evaluate mineralogical compositions and phase transformations after GGBFS treatment. The samples were taken with a needle, pounded, powdered, and then placed in the XRD device. The basic principle of XRD analysis is as follows. Electromagnetic waves coming from the X-ray tube go to the sample, and the waves reflected from the sample reach the detector [258], [259]. For the purpose of measuring the diffraction intensities for the 2 Theta values, the detector and tube move toward each other in an orbicular arc plane, while the sample is stationary, at a rate from extremely low angles to a high value in a certain period of time. Depending on the reflection rate and the properties of the atom, the 2 Theta angle-intensity graph is obtained. As it is known, phases have two different atomic arrangements, crystalline and amorphous. Although the arrangement of atoms and the angle they make with each other are systematic and definite in the crystal structures, those in amorphous structures are random. When electromagnetic waves enter a crystal phase at certain angles, most of the incoming wave is reflected to the detector,

enabling this phase to be determined. However, in amorphous structures, since the atoms are arranged at random angles, it does not give a clear peak on the graph and creates a cloudy background. For this reason, it is not appropriate to determine the amorphous phases by XRD method. Therefore, in order to analyze the crystal phases, XRD analysis was performed in this study.

First, the data obtained from the XRD (X-ray diffraction) was analyzed qualitatively, and the crystalline phases and their mineralogical compositions were found for each sample taken from the aggregate-matrix interfaces in recycled aggregate concrete mixtures. The percentages by mass of these phases were determined by the quantitative analysis carried out afterward. The Rietveld refinement method was applied to XRD findings by using Maud software for the quantification of crystalline phases [260]. The American Mineralogist Crystal Structure Database was utilized to obtain crystallographic information files. After the percentages by mass of the phases contained in the samples were found, the cellular parameters were also iterated to minimize the errors caused by the shift of the data, and the percent by mass of the phases was finalized with the emergence of these errors. Finally, the results were interpreted considering the phase transformations expected as a result of the pozzolanic reaction.

4. TEST RESULTS AND EVALUATION

In this chapter, the physical and mechanical properties of coarse aggregates are given, along with the results of tests conducted on fresh and hardened concrete mixtures as defined in the previous chapter.

4.1. Aggregate Properties

The physical and mechanical properties of the coarse aggregates used to produce the concrete mixtures in this study were determined according to the related tests as previously prescribed and results are presented in Table 4.1.

Table 4.1. Properties of coarse aggregates.

Properties	**FAA**		**RBA**		**RCA**		**CSt**	
	4-8	**8-16**	**4-8**	**8-16**	**4-8**	**8-16**	**4-8**	**8-16**
Unit Weight, (kg/m^3)	890	910	1030	1040	1370	1440	1650	1650
Specific Gravity (SSD)	1.65	1.67	2.08	2.10	2.40	2.43	2.70	2.70
Water Absorption, %	21.7	19.1	13.50	11.54	6.65	3.04	0.65	0.54
Flakiness Index (FI), %	0.1		6.08		11.68		16.38	
ACV, %	45.92		39.87		24.09		12.08	
AIV, %	50.86		45.14		24.12		11.25	

ACV: Aggregate Crushing Value. AIV: Aggregate Impact Value.

FAA is the least dense of all coarse aggregates, followed by RBA, RCA, and CSt. The water absorption capacitiy of CSt is significantly lower than that of FAA, RBA, and RCA. These trends are consistent with the literature [41], [112], [160], [161], [165] and can be explained by the presence of old adhered mortar on recycled concrete aggregates and the porous structure of recycled brick and fly ash aggregates. Besides, the water absorption values of recycled aggregates in the size range of 8-16 mm are lower than those of the recycled aggregates in the size of 4-8 mm, while the results of specific gravity are higher for the coarser recycled aggregates. Accordingly, it can be expressed that the specific gravity increases and the water absorption capacity decreases with an increase in the size of recycled aggregates. The coarser part of the RCA may be expected to be denser with the lower amount

of old adhered mortar on which open pores and cracks exist, resulting in decreased water absorption, as observed by Güneyisi et al. [41]. In addition to this, breaking the RCA into small pieces damages the aggregate itself, making it vulnerable to water absorption, as this also applies in the case of RBA. FAAs also became denser with fewer and mostly non-interconnected closed pores when the pellets increased in size during agglomeration, resulting in decreased water absorption and increased specific gravity, which was also detected by Kockal and Ozturan [125] for cold-bonded FAAs. On the other hand, the specific gravity and water absorption capacity of the recycled fly ash aggregates produced in this study fall within a similar range to those presented in the literature [117], [128], [129], [131], [261], [262].

In terms of flakiness index, it is quite possible to say that all coarse aggregates are suitable for concrete production in reference to BS 882 [214] because the FI values of coarse aggregates are much lower than 40%.

With respect to ACV and AIV, there is a big difference between aggregates in favor of CSt with the ACV of 12.08% and AIV of 11.25%, which means that FAA is the most disadvantageous one in terms of crushing strength and impact resistance because the higher the ACV and AIV value mechanically more flawed the material is. Besides, as expected, there is a positive correlation between aggregate crushing and impact values, as seen in Figure 4.1, and a negative correlation between each of these values and the unit weight of aggregates, as presented in Figures 4.2 and 4.3, respectively. These results are also consistent with the literature [66], [130], [167], [169], [171], [172], [263]. All the regression models constructed shown in these figures have high coefficient of determination (R^2) values that explain the level of significance of the linear relationship established between related variables. In other words, as a statistical measure, the coefficient of determination (R^2) shows the percentage of variance in the dependent variable that the regression equation can explain [264], [265].

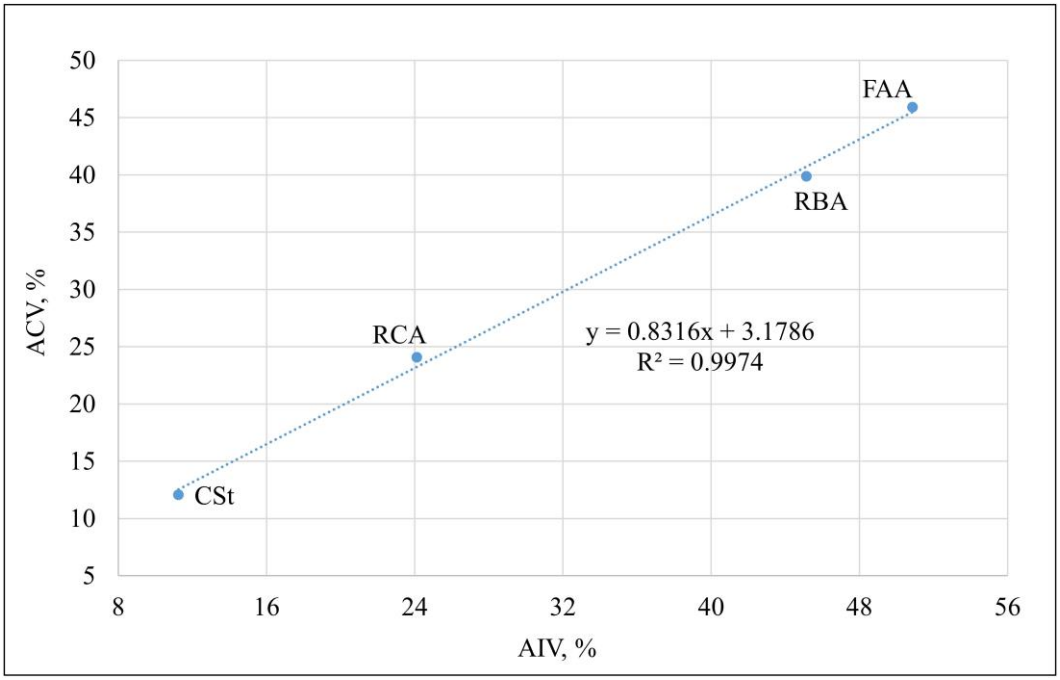

Figure 4.1. ACV vs AIV.

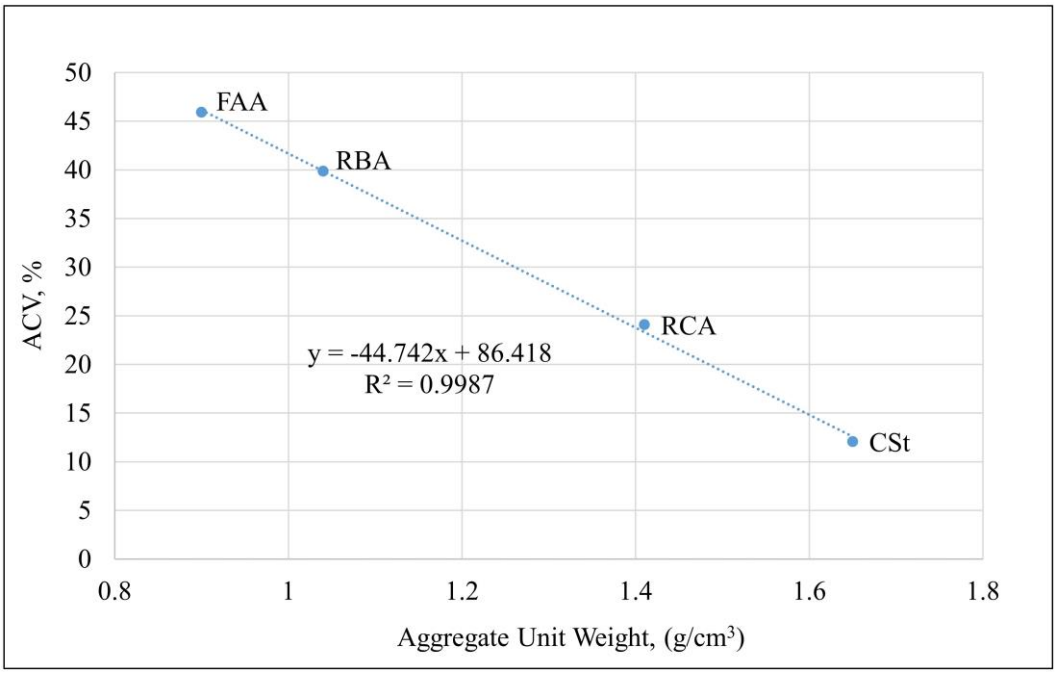

Figure 4.2. ACV vs aggregate unit weight.

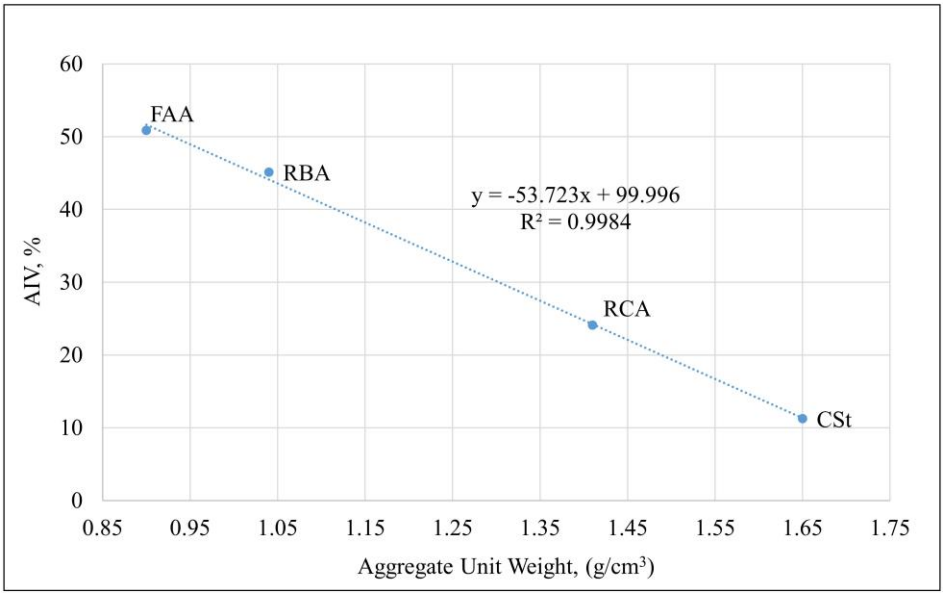

Figure 4.3. AIV vs aggregate unit weight.

4.2. Fresh Concrete Properties

Concrete mixes were cast by employing a superplasticizer (SP) at the required dosage for achieving the target workability. In order to minimize the slump loss due to the high water absorption of the recycled coarse aggregates, they were saturated in water for twenty-four hours and then surface dried on large-scale sieves for one hour before concrete mixing. It was observed that FAAC required the least amount of SP to maintain the specified slump value (18±2 cm) owing to the smoother surface texture and the greatest roundness of the fly ash aggregates (FAA) with the lowest flakiness index. On the other hand, the highest amount of SP, by weight of cementitious material, was used to get the target slump value for CStC (0.85%), followed by RCAC (0.75%) and RBAC (0.65%), which can be attributed to the fact that CSt has the lowest roundness with the highest flakiness index followed by RCA and RBA. The higher the flakiness index, the greater the surface area-to-volume ratio and so the water requirement to produce workable concrete. Fresh concrete mixes were workable and cohesive, and segregation was not observed. When RCA, RBA, and FAA totally replaced the CSt, the fresh unit weight of the concrete mixtures decreased from 2410 kg/m^3 to 2260, 2120, and 2000 kg/m^3, respectively. The use of coarse aggregates with different densities gave the opportunity to produce concrete mixtures with different unit weights. There was no change in the fresh unit weight of TRCAC, TRBAC, and TFAAC due to the change in the concrete production process. Replacing the crushed stone coarse aggregate fully with

recycled aggregates reduced the fresh density of the concrete by up to 17%, while the compressive strength values conformed to the limitation for structural use, which is 17 MPa for ACI 318-02 [255] and 21 MPa for ACI 213R-03 [266], a guide for structural lightweight-aggregate concrete.

4.3. Hardened Concrete Properties

In this study, the effects of using different recycled aggregates in full replacement, by volume, of natural crushed stone coarse aggregate (CSt) and treating the recycled aggregates by employing the GGBFS slurry during concrete mixing procedure on the mechanical properties of hardened concrete were investigated. For this purpose, three different recycled aggregates (RCA, RBA, FAA) were utilized in six different sustainable concrete mixtures as plain (RCAC, RBAC, FAAC) and surface treated (TRCAC, TRBAC, TFAAC) by the GGBFS slurry.

4.3.1. Compressive Strength and Modulus of Elasticity

The compressive strength of the concrete mixtures decreased from 45.51 MPa for the control concrete (CStC) and varied between 33.91 and 23.47 MPa for the recycled aggregate concrete mixtures due to the higher porosity and lower strength of the recycled aggregates, as shown in Table 4.2. Among the recycled aggregate concrete mixtures, a higher compressive strength was obtained with TRCAC followed by RCAC, TRBAC, RBAC, TFAAC, and FAAC, having a performance of 75, 69, 66, 61, 56, and 52% of CStC, respectively, as seen in Figure 4.4. Similarly, the modulus of elasticity of concrete mixtures decreased from 35.51 GPa for CStC and varied between 27.14 and 21.43 GPa for recycled aggregate concrete mixtures, as presented in Table 4.2. A higher modulus of elasticity was obtained with TRCAC followed by RCAC, TRBAC, RBAC, TFAAC, and FAAC, having the performance of 76, 74, 69, 66, 63, and 60% of CStC, respectively, as seen in Figure 4.5.

As a measure of statistical reliability, the coefficient of variation (CoV) is a meaningful index of variability because it accounts for both the mean and the standard deviation. In this respect, while the CoV values of the concrete mixtures RCAC, RBAC and FAAC were 10.10, 8.50 and 9.81% for compressive strength and 4.42, 3.36 and 3.51% for modulus of

elasticity, they decreased to 8.68, 6.47 and 8.53% for compressive strength and 3.03, 2.75 and 2.97% for modulus of elasticity for the concrete mixtures of TRCAC, TRBAC and TFAAC, respectively. It should be remembered that a lower CoV indicates higher statistical reliability [264], [265]. On the other hand, as it was expected, the correlation of the compressive strength (F_c) of the concrete mixtures with the crushing values of the coarse aggregates (ACV, %) was negative while it was positive with the unit weight of both untreated and treated concrete mixtures as presented in Figure 4.6 and Figures 4.7 and 4.8, respectively. All had sufficiently high coefficient of determination values (R^2). However, in the case of the relation between compressive strength and unit weight of concrete mixtures, the coefficient of determination for the set of concrete mixtures including CStC, TRCAC, TRBAC, and TFAAC (R^2=0.9445) was slightly higher than that for the set of concrete mixtures of CStC, RCAC, RBAC and FAAC (R^2=0.9132). Treating recycled aggregates by GGBFS slurry enhances the interface between these aggregates and the cement paste in concrete as a result of C-S-H gel being formed, from hydration and/or pozzolanic reactions, in the microcracks and voids on the surface of the aggregates, and thus improves the bonding ability and the strength on the interface. Similar improvements in the compressive strength and elastic modulus of concrete produced with recycled aggregates were also observed in the literature [62], [63], [67], [68], [191], [267] when recycled aggregates were coated with pozzolanic slurry during the mixing procedure.

Table 4.2. Compressive strength and modulus of elasticity of concrete mixtures.

Properties	**Statistical Parameters**	**CStC**	**TRCAC**	**RCAC**	**TRBAC**	**RBAC**	**TFAAC**	**FAAC**
Compressive Strength, Fc (MPa)	n	12	14	13	13	14	13	13
	Min	40.30	30.07	25.27	27.34	24.34	22.59	19.19
	Max	50.97	38.83	37.11	33.68	32.11	29.55	26.65
	Mean (x)	45.51	33.91	31.42	29.85	27.61	25.60	23.47
	SD (σ)	3.87	2.95	3.17	1.93	2.35	2.18	2.30
	SE (σ/√n)	1.12	0.79	0.88	0.54	0.63	0.61	0.64
	CoV (σ/x)%	8.49	8.68	10.10	6.47	8.50	8.53	9.81
Modulus of Elasticity, Ec (GPa)	n	12	14	13	13	14	13	13
	Min	34.20	25.92	23.71	23.53	22.27	21.31	19.95
	Max	36.58	28.43	28.48	25.58	24.73	23.43	22.48
	Mean (x)	35.51	27.14	26.20	24.41	23.44	22.24	21.43
	SD (σ)	0.90	0.82	1.16	0.67	0.79	0.66	0.75
	SE (σ/√n)	0.26	0.22	0.32	0.19	0.21	0.18	0.21
	CoV (σ/x)%	2.52	3.03	4.42	2.75	3.36	2.97	3.51

n= number of specimen tested; SD= Standard Deviation; SE= Standard Error; CoV= Coefficient of Variation

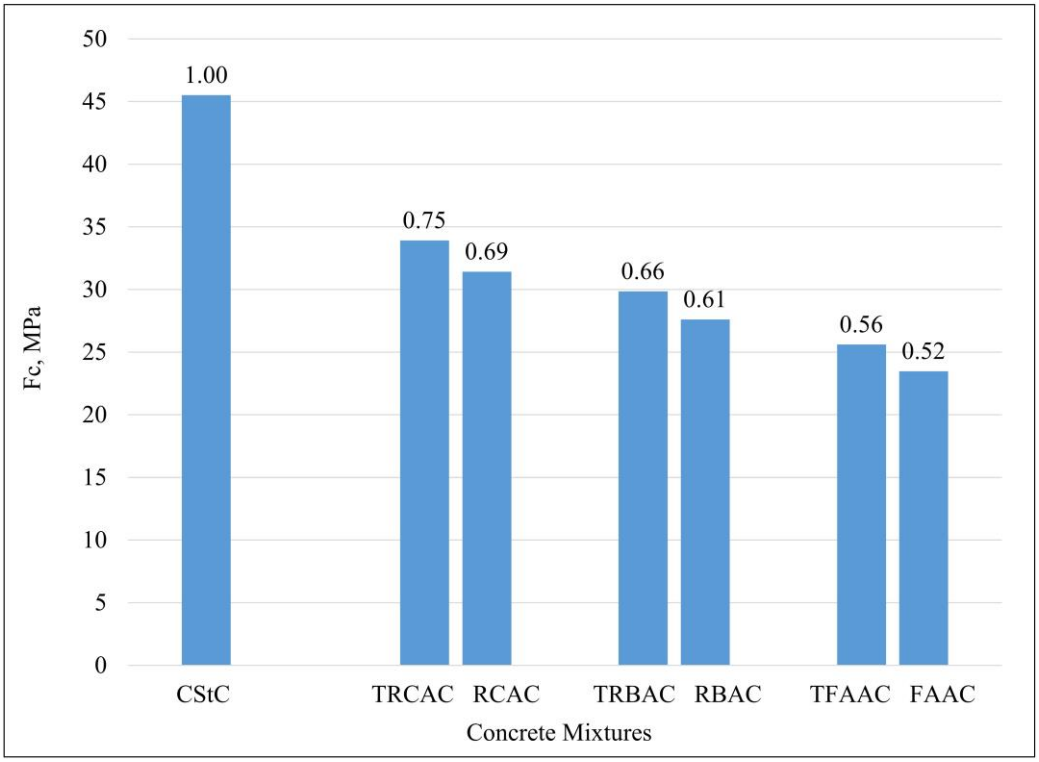

Figure 4.4. Compressive strength of concrete mixtures.

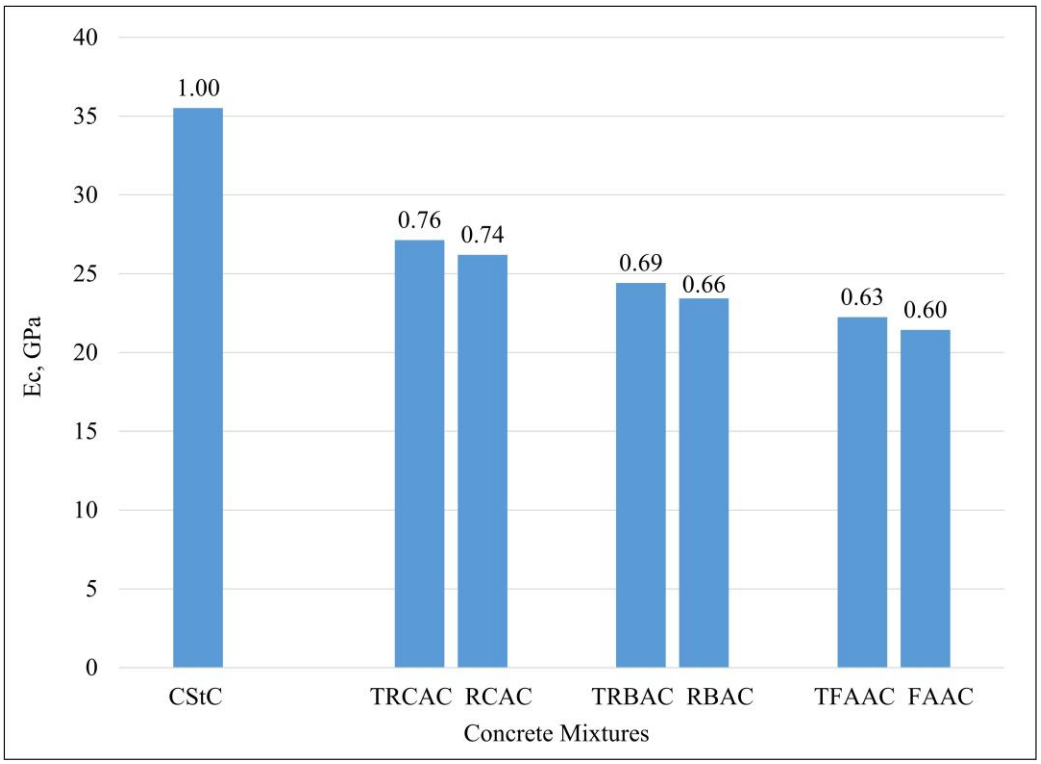

Figure 4.5. Elastic modulus of concrete mixtures.

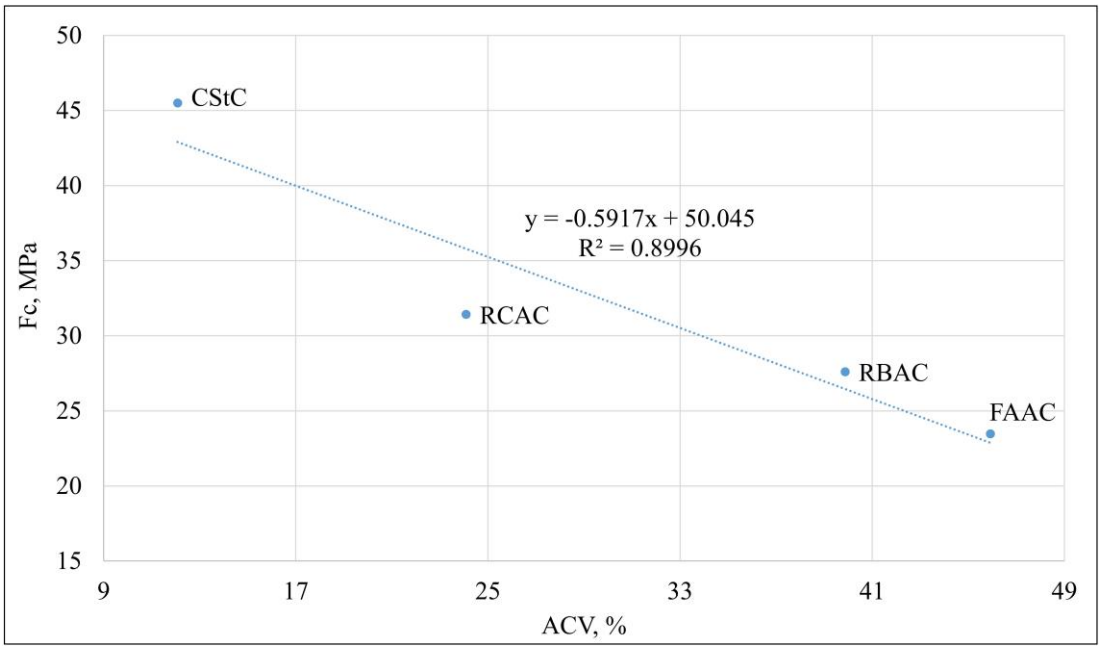

Figure 4.6. Fc of concrete mixtures vs ACV of related coarse aggregates.

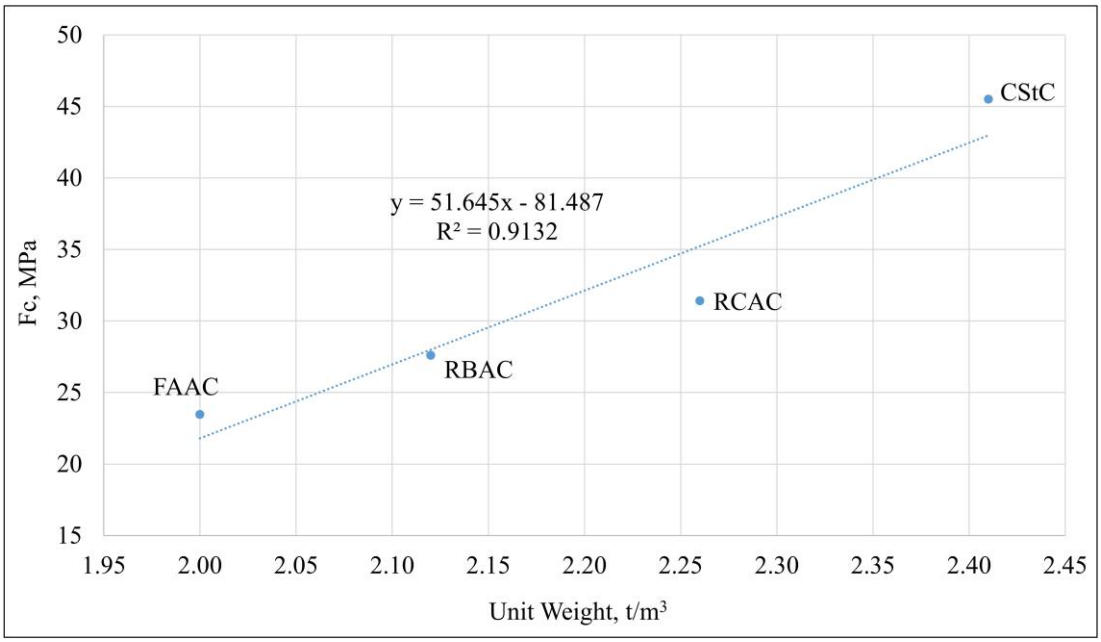

Figure 4.7. Relation between unit weight and Fc of untreated concrete mixtures.

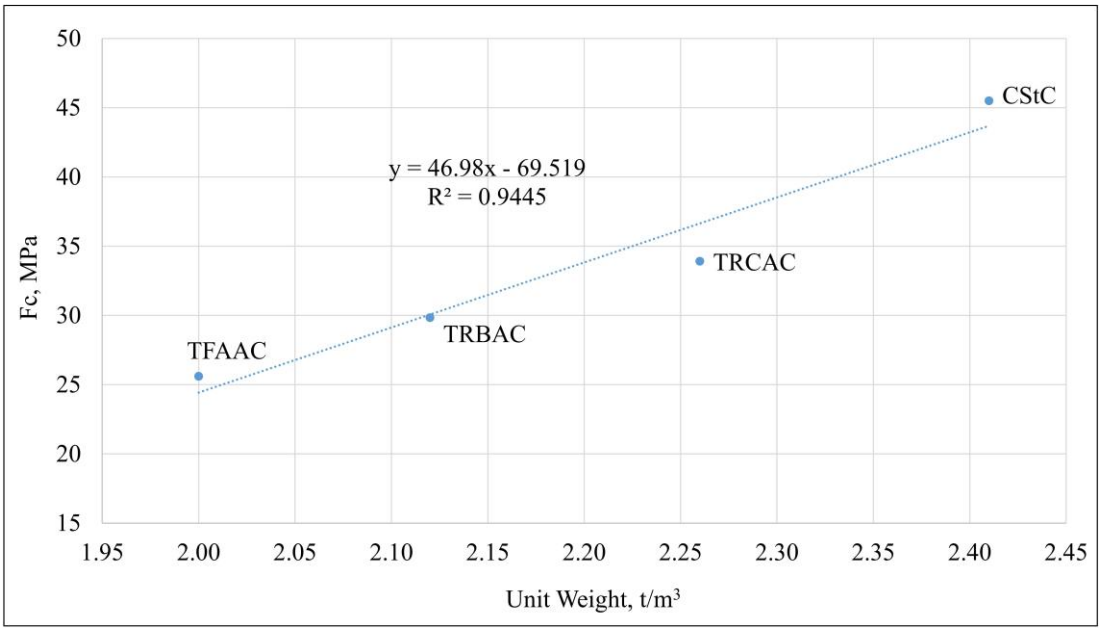

Figure 4.8. Relation between unit weight and Fc of treated concrete mixtures.

In the scope of this study, the relationship between the static modulus of elasticity and compressive strength of the concrete mixtures was also estimated, and the estimating equations obtained from the experimental results were compared with the prediction models given in different standards: TS500 [268], ACI 318M-05 [269], EN 1992-1-1 [270], CSA A23.3-04 [271] and NZS 3101-1 [272]. These were selected in a way to represent two worldwide standards (ACI and EN) together with additional standards (CSA and NZS) from different Anglo-Saxon countries and a national standard (TS500) of Turkey as the host country where this thesis was written. Different models are shown in Table 4.3 to predict the static modulus of elasticity of concrete based on the compressive strength recommended by the specified standards. The estimating equations constructed regarding the test results by using the simple regression analysis based on the least-squares method are given in Table 4.4. Because the coefficient of determination values (R^2) of estimating equations are sufficiently high, the statistical parameters of the measured modulus of elasticity values of the concrete mixtures shown in Table 4.5 can be used to represent the proposed models of the present work to compare with the models given by the specified standards. At this point, it should also be noted that the coefficient of determination values (R^2) of the estimating equations constructed for the concrete mixtures (TRCAC, TRBAC, and TFAAC) with treated recycled aggregates were slightly higher than those for the concrete mixtures (RCAC, RBAC, and FAAC) with untreated recycled aggregates. Besides, there is a positive

correlation between the compressive strength and the modulus of elasticity of all concrete mixtures regarding the estimating equations constructed with respect to the experimental results.

Table 4.3. Prediction models of the different codes for modulus of elasticity.

Codes	Prediction Models	Units
TS500	$\mathrm{Ec} = 3250\sqrt{f_{ck}} + 14000$	f_{ck}: (MPa) Ec: (MPa)
ACI 318M-05	$\mathrm{Ec} = 4700\sqrt{f_c'}$	f_c': (MPa) Ec: (MPa)
EN 1992-1-1	$\mathrm{Ec} = 22(f_{cm}/10)^{0.3}$	f_{cm}: (MPa) Ec: (GPa)
	$*\mathrm{Ec} = 22(f_{cm}/10)^{0.3}(2000/2200)^2$	f_{cm}: (MPa) Ec: (GPa)
CSA A23.3-04	$\mathrm{Ec} = 4500\sqrt{f_c'}$	f_c': (MPa) Ec: (MPa)
NZS 3101-1	$\mathrm{Ec} = 3320\sqrt{f_c'} + 6900$	f_c': (MPa) Ec: (MPa)

Ec: Modulus of elasticity at 28 days. f_c', f_{ck}: Characteristic compressive strength at 28 days.
f_{cm}: Mean compressive strength at 28 days.
*Stands for FAAC and TFAAC regarding the concrete unit weight.

Table 4.4. Estimating equations constructed for modulus of elasticity according to the test results.

Concrete Mixtures	Estimating Equations	Units
CStC	$\mathrm{Ec} = 3025.6\sqrt{f_{cm}} + 15121,\ \mathrm{R}^2 = 0.9447$	$f_{cm}: (MPa)\ Ec: (MPa)$
RCAC	$\mathrm{Ec} = 3854.6\sqrt{f_{cm}} + 4620.6,\ \mathrm{R}^2 = 0.8867$	
TRCAC	$\mathrm{Ec} = 3093.2\sqrt{f_{cm}} + 9139.3,\ \mathrm{R}^2 = 0.9012$	
RBAC	$\mathrm{Ec} = 3424.4\sqrt{f_{cm}} + 5457.1,\ \mathrm{R}^2 = 0.9155$	
TRBAC	$\mathrm{Ec} = 3788.0\sqrt{f_{cm}} + 3724.3,\ \mathrm{R}^2 = 0.9755$	
FAAC	$\mathrm{Ec} = 3007.6\sqrt{f_{cm}} + 6876.5,\ \mathrm{R}^2 = 0.9135$	
TFAAC	$\mathrm{Ec} = 3062.5\sqrt{f_{cm}} + 6758.3,\ \mathrm{R}^2 = 0.9912$	

Ec: Modulus of elasticity at 28 days. f_{cm}: Mean compressive strength at 28 days.

As seen in Table 4.5 and Figure 4.9, the mean modulus of elasticity values of TS500 and EN 1992-1-1 are very close to the experimental mean for the control concrete (CStC) with values of 35.91, 34.64, and 35.51 GPa, respectively. However, the models of ACI 318M-05, CSA A23.2-04, and NZS 3101-1 underestimate the modulus of elasticity with the values of 31.68, 30.33, and 29.28 GPa, respectively. Considering all the models, the CoV of the experimental values is lower than that of the calculated values, indicating that the proposed model is the most reliable one, which gives an opportunity to have a more precise

estimation around the mean in the case of control concrete. For the concrete mixtures produced with recycled concrete aggregates, the mean modulus of elasticity values of ACI 318M-05 are very close to the experimental means with slight overestimations of 0.43 and 0.77% for RCAC and TRCAC, respectively. However, for both RCAC and TRCAC, the CoV of the measured modulus of elasticity values is lower than that of ACI 318M-05, indicating that the proposed model is more reliable than the model of ACI 318M-05. On the other hand, the models of TS500 and EN 1992-1-1 overestimate the modulus of elasticity with an amount of 22.88 and 18.26% for RCAC and 21.28 and 16.86% for TRCAC, respectively. In comparison, CSA A23.2-04 and NZS 3101-1 underestimate the modulus of elasticity with an amount of 3.84 and 2.72% for RCAC and 3.51 and 3.39% for TRCAC, respectively.

For the concrete mixtures produced with recycled brick aggregates, on the other hand, the mean modulus of elasticity values of CSA A23.2-04 are very close to the experimental means with slight overestimations of 0.81 and 0.67% for RBAC and TRBAC, respectively. However, for both RBAC and TRBAC, the CoV of the measured modulus of elasticity values is lower than that of the CSA A23.2-04, indicating that the proposed model is more reliable than the model of CSA A23.2-04. The models of TS500, EN 1992-1-1, ACI 318M-05, and NZS 3101-1 highly overestimate the modulus of elasticity with an amount of 32.55, 27.22, 5.29, and 3.82% for RBAC and 30.06, 25.27, 5.15 and 2.54% for TRBAC, respectively.

For the concrete mixtures produced with recycled fly ash aggregates, the mean modulus of elasticity values of CSA A23.3-04 are very close to the experimental means with slight overestimations of 1.62 and 2.29% for FAAC and TFAAC, respectively. However, for both FAAC and TFAAC, the CoV of the measured modulus of elasticity values is lower than that of the CSA A23.3-04, indicating that the level of dispersion around the mean of the proposed model is lower than that of the related standard. In other words, the proposed model is statistically more reliable than the model of CSA A23.3-04. On the other hand, the models of TS500, ACI 318M-05, EN 1992-1-1, and NZS 3101-1 overestimate the modulus of elasticity with an amount of 38.71, 6.13, 9.48, and 7.17% for FAAC and 36.82, 6.84, 8.31, and 6.49% for TFAAC, respectively.

Table 4.5. Statistical parameters for assessing the measured and predicted results of modulus of elasticity.

Concrete Mixtures	Statistical Parameters	Modulus of Elasticity, Ec (GPa)					
		Measured	Calculated				
			TS500	ACI 318M-05	EN 1992-1-1	CSA A23.3-04	NZS 3101-1
CStC	n	12	12	12	12	12	12
	Min	34.20	34.63	29.84	33.42	28.57	27.98
	Max	36.58	37.20	33.55	35.86	32.13	30.60
	Mean (x)	35.51	35.91	31.68	34.64	30.33	29.28
	SD (σ)	0.90	0.94	1.35	0.89	1.29	0.96
	SE (σ/√n)	0.26	0.27	0.39	0.26	0.37	0.28
	CoV (σ/x)%	2.52	2.60	4.27	2.57	4.27	3.26
	$x_{calculated}$-$x_{measured}$	-	0.39	-3.84	-0.88	-5.18	-6.24
	% change	-	1.10	-10.80	-2.47	-14.59	-17.56
RCAC	n	13	13	13	13	13	13
	Min	23.71	30.34	23.63	29.06	22.62	23.59
	Max	28.48	33.80	28.63	32.61	27.41	27.13
	Mean (x)	26.20	32.20	26.31	30.99	25.20	25.49
	SD (σ)	1.16	0.92	1.33	0.94	1.27	0.94
	SE (σ/√n)	0.32	0.26	0.37	0.26	0.35	0.26
	CoV (σ/x)%	4.42	2.86	5.05	3.03	5.05	3.69
	$x_{calculated}$-$x_{measured}$	-	5.99	0.11	4.78	-1.01	-0.71
	% change	-	22.88	0.43	18.26	-3.84	-2.72
TRCAC	n	14	14	14	14	14	14
	Min	25.92	31.82	25.77	30.61	24.68	25.11
	Max	28.43	34.25	29.29	33.05	28.04	27.59
	Mean (x)	27.14	32.91	27.35	31.71	26.18	26.22
	SD (σ)	0.82	0.82	1.18	0.82	1.13	0.84
	SE (σ/√n)	0.22	0.22	0.32	0.22	0.30	0.22
	CoV (σ/x)%	3.03	2.49	4.33	2.60	4.33	3.19
	$x_{calculated}$-$x_{measured}$	-	5.77	0.21	4.57	-0.95	-0.92
	% change	-	21.28	0.77	16.86	-3.51	-3.39
RBAC	n	14	14	14	14	14	14
	Min	22.27	30.04	23.19	28.73	22.20	23.28
	Max	24.73	32.42	26.63	31.22	25.50	25.71
	Mean (x)	23.44	31.06	24.67	29.81	23.62	24.33
	SD (σ)	0.79	0.72	1.03	0.75	0.99	0.73
	SE (σ/√n)	0.21	0.19	0.28	0.20	0.26	0.20
	CoV (σ/x)%	3.36	2.30	4.19	2.50	4.19	3.00
	$x_{calculated}$-$x_{measured}$	-	7.63	1.24	6.38	0.19	0.89
	% change	-	32.55	5.29	27.22	0.81	3.82
TRBAC	n	13	13	13	13	13	13
	Min	23.53	30.99	24.57	29.75	23.53	24.26
	Max	25.58	32.86	27.28	31.67	26.11	26.17
	Mean (x)	24.41	31.75	25.67	30.53	24.57	25.03
	SD (σ)	0.67	0.57	0.82	0.58	0.79	0.58
	SE (σ/√n)	0.19	0.16	0.23	0.16	0.22	0.16
	CoV (σ/x)%	2.75	1.79	3.20	1.92	3.20	2.32
	$x_{calculated}$-$x_{measured}$	-	7.34	1.26	6.12	0.16	0.62
	% change	-	30.06	5.15	25.07	0.67	2.54

n= number of specimen tested; SD= Standard Deviation; SE= Standard Error; CoV= Coefficient of Variation

Table 4.5. Statistical parameters for assessing the measured and predicted results of modulus of elasticity (cont.).

Concrete Mixtures	Statistical Parameters	Modulus of Elasticity, Ec (GPa)					
		Measured	Calculated				
			TS500	ACI 318M-05	EN 1992-1-1	CSA A23.3-04	NZS 3101-1
FAAC	n	13	13	13	13	13	13
	Min	19.95	28.24	20.59	22.11	19.71	21.44
	Max	22.48	30.78	24.26	24.40	23.23	24.04
	Mean (x)	21.43	29.73	22.75	23.46	21.78	22.97
	SD (σ)	0.75	0.78	1.12	0.70	1.08	0.79
	SE (σ/√n)	0.21	0.22	0.31	0.19	0.30	0.22
	CoV (σ/x)%	3.51	2.62	4.94	2.98	4.94	3.46
	$x_{calculated}$-$x_{measured}$	-	8.30	1.31	2.03	0.35	1.54
	% change	-	38.71	6.13	9.48	1.62	7.17
TFAAC	n	13	13	13	13	13	13
	Min	21.31	29.45	22.34	23.22	21.39	22.68
	Max	23.43	31.67	25.55	25.17	24.46	24.95
	Mean (x)	22.24	30.43	23.76	24.09	22.75	23.69
	SD (σ)	0.66	0.70	1.01	0.61	0.97	0.71
	SE (σ/√n)	0.18	0.19	0.28	0.17	0.27	0.20
	CoV (σ/x)%	2.97	2.29	4.25	2.55	4.25	3.01
	$x_{calculated}$-$x_{measured}$	-	8.19	1.52	1.85	0.51	1.44
	% change	-	36.82	6.84	8.31	2.29	6.49

n= number of specimen tested; SD= Standard Deviation; SE= Standard Error; CoV= Coefficient of Variation

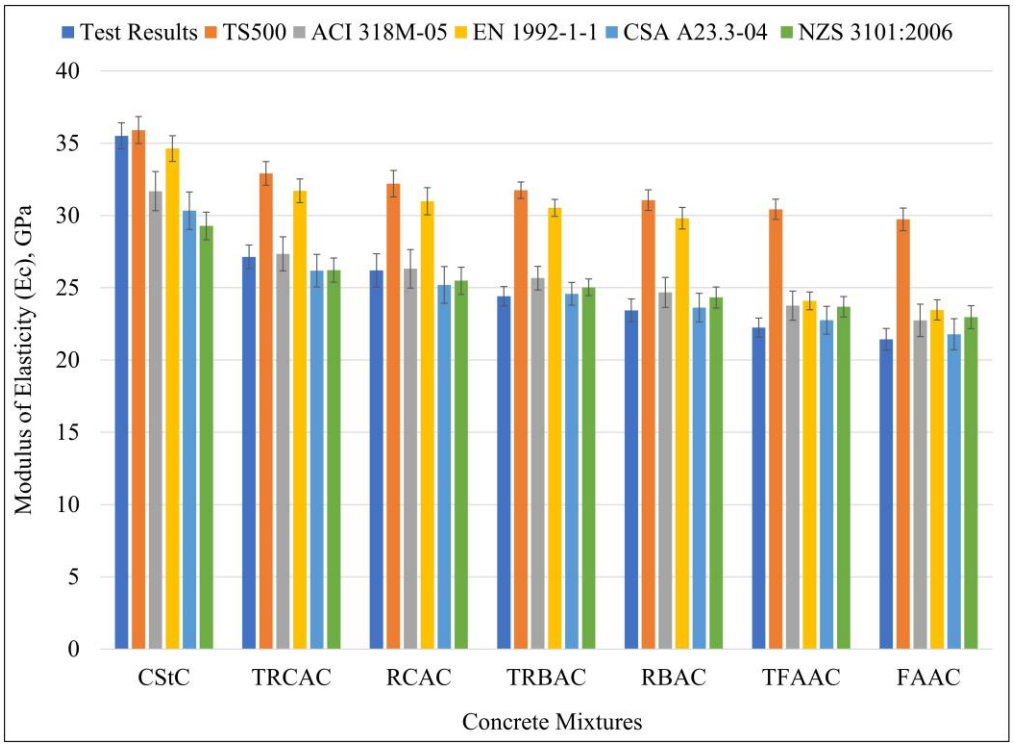

Figure 4.9. The measured and predicted results of the modulus of elasticity.

4.3.2. Splitting Tensile Strength

The splitting tensile strength of the concrete mixtures decreased from 3.85 MPa for control concrete (CStC) and varied between 3.11 and 2.28 MPa when the crushed stone was replaced by recycled coarse aggregates. The reduction in the splitting tensile strength of concrete can be attributed to the higher porosity and lower strength of the recycled aggregates. Among the recycled aggregate concrete mixtures, a higher splitting tensile strength was obtained with TRCAC followed by RCAC, TRBAC, RBAC, TFAAC, and FAAC, which had a performance of 81, 78, 72, 67, 63, and 59% of CStC, respectively, as seen in Figure 4.10. Treatment of recycled aggregates with GGBFS slurry during concrete mixing increased the splitting tensile strength of recycled aggregate concrete mixtures. According to the previous studies conducted by Tam and Tam [60], Güneyisi et al. [41], and Kisku et al. [267], the splitting tensile strength of recycled aggregate concrete also increased when recycled aggregates were treated with pozzolanic admixtures during the multi-step concrete mixing procedure.

On the other hand, as a statistical measure, the CoV values of the concrete mixtures RCAC, RBAC, and FAAC produced with untreated recycled coarse aggregates decreased from 10.36, 8.24, and 9.00% for the splitting tensile strength to 7.24, 7.32, and 7.41% for the concrete mixtures of TRCAC, TRBAC, and TFAAC with treated recycled coarse aggregates, respectively. The lower the CoV, the higher the statistical reliability.

Within the scope of this thesis, the relationship between the splitting tensile strength and compressive strength of the concrete mixtures was also estimated. The estimating equations obtained from the experimental results were compared with the prediction models given in different codes: TS500 [268], ACI 363R-92 [273], EN 1992-1-1[270], CSA A23.3-04 [271], and NZS 3101-1 [272]. Different models for predicting the splitting tensile strength of concrete based on the compressive strength recommended by the specified codes are shown in Table 4.6. The estimating equations constructed regarding the test results by using the simple regression analysis based on the least-squares method are given in Table 4.7. Since the coefficient of determination values (R^2) of estimating equations are sufficiently high, statistical parameters of measured splitting tensile strength values of concrete mixtures shown in Table 4.8 can be used to represent the proposed models of this study to compare

with the models given by the specified codes. The coefficient of determination values (R^2) of the estimating equations constructed for the concrete mixtures (TRCAC, TRBAC, and TFAAC) with treated recycled aggregates were slightly higher than those for the concrete mixtures (RCAC, RBAC, and FAAC) with untreated recycled aggregates. The higher the coefficient of determination (R^2), the higher the percentage of variance in the dependent variable that can be explained by the regression equation. On the other hand, there is a positive correlation between the splitting tensile strength and compressive strength of all concrete mixtures in regard to the estimating equations constructed with reference to the experimental results.

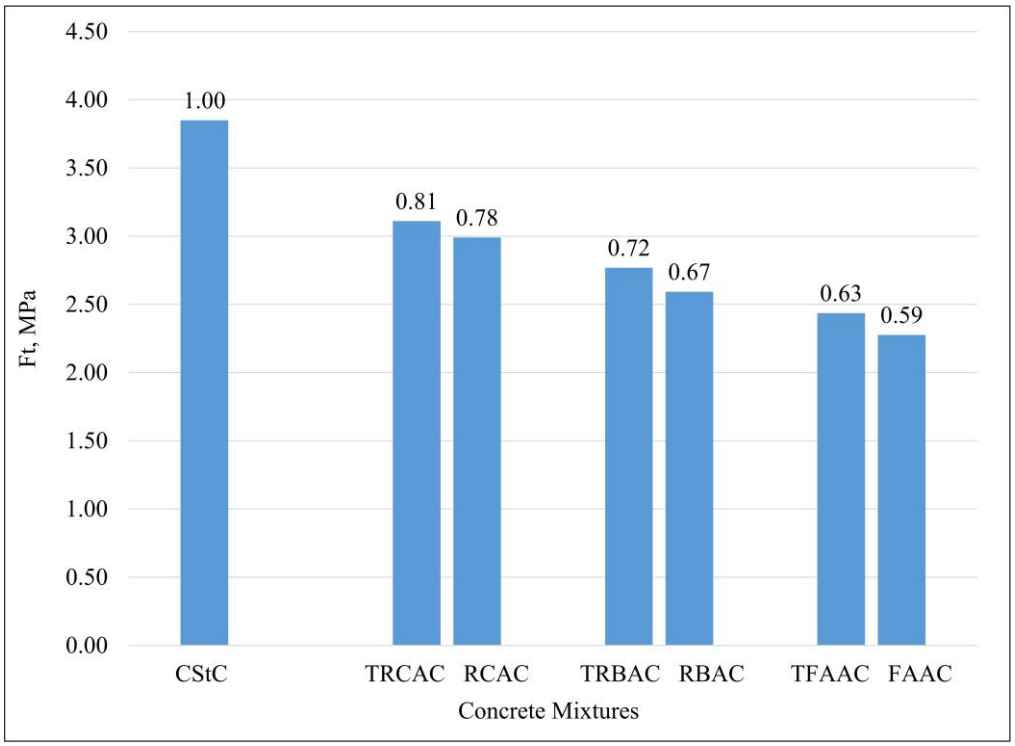

Figure 4.10. Splitting tensile strength of concrete mixtures.

As seen in Table 4.8 and Figure 4.11, the mean splitting tensile strength values of ACI 363R-92 and EN 1992-1-1 are close to the experimental mean for the control concrete (CStC) with the values of 3.98, 3.73, and 3.85 MPa, respectively. However, the CoV of ACI 363R-92 is lower than that of EN 1992-1-1 and the proposed model of this study constructed regarding the experimental results of the splitting tensile strength test, indicating that the level of dispersion around the mean for the model recommended by ACI 363R-92 is the lowest in the case of control concrete. In other words, the lower the CoV, the more accurate

the prediction. The models of TS500 and NZS 3101-1, on the other hand, underestimate the splitting tensile strength with the values of 3.54 and 3.64 MPa, respectively, while CSA A23.3-04 overestimates it with the splitting tensile strength of 4.52 MPa.

For the concrete mixtures produced with recycled concrete aggregates, the mean splitting tensile strength values of NZS 3101-1 are very close to the experimental means with slight overestimations of 1.10 and 0.45% for RCAC and TRCAC, respectively. However, for both RCAC and TRCAC, the CoV of NZS 3101-1 is lower than that of the measured splitting tensile strength values, indicating that it is more likely to get a precise estimation around the mean by the model of NZS 3101-1 compared to the proposed model of this study. On the other hand, the models of ACI 363R-92 and CSA A23.3-04 highly overestimate the splitting tensile strength with an amount of 10.47 and 25.44% for RCAC and 9.75 and 24.63% for TRCAC, respectively, while TS500 and EN 1992-1-1 underestimate the splitting tensile strength with an amount of 1.70 and 8.92% for RCAC and 2.34 and 7.19% for TRCAC.

Table 4.6. Prediction models of the different codes for splitting tensile strength.

Codes	**Prediction Models**	**Units**
TS500	$f_{ct,sp} = 0.525\sqrt{f_{ck}}$	$f_{ct,sp}$: (MPa) f_{ck}: (MPa)
ACI 363R-92	$f_{ct,sp} = 0.59\sqrt{f_{cm}}$	$f_{ct,sp}$: (MPa) f_{cm}: (MPa)
EN 1992-1-1	$f_{ct,sp} = 1/3(f_{cm} - 8)^{2/3}$	$f_{ct,sp}$: (MPa) f_{cm}: (MPa)
	$*f_{ct,sp} = 1/3(f_{cm} - 8)^{\frac{2}{3}}(0.4 + 0.6 * 2000/2200)$	$f_{ct,sp}$: (MPa) f_{cm}: (MPa)
CSA A23.3-04	$f_{ct,sp} = 0.67\sqrt{f_c'}$	$f_{ct,sp}$: (MPa) f_c': (MPa)
NZS 3101-1	$f_{ct,sp} = 0.54\sqrt{f_c'}$	$f_{ct,sp}$: (MPa) f_c': (MPa)

f_c', f_{ck}: Characteristic compressive strength at 28 days. f_{cm}: Mean compressive strength at 28 days.
$f_{ct,sp}$: Indirect tensile strength of concrete at 28 days.
*Stands for FAAC and TFAAC regarding the concrete unit weight.

For the concrete mixtures produced with recycled brick aggregates, the mean splitting tensile strength values of TS500 are close to the experimental means with slight overestimations of 5.59 and 2.99% for RBAC and TRBAC, respectively. However, for both RBAC and TRBAC, the CoV of TS 500 is lower than that of the measured splitting tensile strength values, indicating that the model of TS500 allows for a more precise estimation around the mean compared to the model proposed in this study. On the other hand, the

models of ACI 363R-92, CSA A23.3-04, and NZS 3101-1 highly overestimate the splitting tensile strength with an amount of 18.66, 34.75, and 8.61% for RBAC and 15.75, 31.44, and 5.94% for TRBAC, respectively, while EN 1992-1-1 underestimates the splitting tensile strength with an amount of 7.78% for RBAC and 6.89% for TRBAC.

Table 4.7. Estimating equations constructed for splitting tensile strength according to the test results.

Concrete Mixtures	**Estimating Equations**	**Units**
CStC	$f_{ct,sp} = 0.5579\sqrt{f_{cm}} + 0.0889,\ R^2 = 0.8697$	$f_{ct,sp}$: (MPa) f_{cm}: (MPa)
RCAC	$f_{ct,sp} = 1.0153\sqrt{f_{cm}} - 2.6940,\ R^2 = 0.8601$	
TRCAC	$f_{ct,sp} = 0.9558\sqrt{f_{cm}} - 2.4203,\ R^2 = 0.9626$	
RBAC	$f_{ct,sp} = 0.9974\sqrt{f_{cm}} - 2.6102,\ R^2 = 0.8035$	
TRBAC	$f_{ct,sp} = 1.2676\sqrt{f_{cm}} - 4.1172,\ R^2 = 0.8547$	
FAAC	$f_{ct,sp} = 0.8340\sqrt{f_{cm}} - 1.7599,\ R^2 = 0.9483$	
TFAAC	$f_{ct,sp} = 0.8379\sqrt{f_{cm}} - 1.800,\ R^2 = 0.9954$	

$f_{ct,sp}$: Indirect tensile strength of concrete at 28 days. f_{cm}: Mean compressive strength at 28 days.

For the concrete mixtures produced with recycled fly ash aggregates, the mean splitting tensile strength values of TS500 are close to the experimental means with relatively moderate overestimations of 11.63 and 8.96% for FAAC and TFAAC, respectively. However, for both FAAC and TFAAC, the CoV of TS500 is lower than that of the measured splitting tensile strength values, indicating that the level of dispersion around the mean for the model recommended by TS500 is lower than that of the proposed model of this study. In other words, the proposed model is statistically less reliable than the model of TS500. On the other hand, the models of ACI 363R-92, CSA A23.3-04, and NZS 3101-1 highly overestimate the splitting tensile strength with an amount of 25.45, 42.46, and 14.82% for FAAC and 22.45, 39.05, and 12.07% for TFAAC, respectively, while EN 1992-1-1 underestimates the splitting tensile strength with an amount of 14.22% for FAAC and 12.59% for TFAAC.

Table 4.8. Statistical parameters for assessing the measured and predicted results of splitting tensile strength.

Concrete Mixtures	Statistical Parameters	Splitting Tensile Strength, Ft (MPa)					
		Measured	Calculated				
			TS500	ACI 363R-92	EN 1992-1-1	CSA A23.3-04	NZS 3101-1
CStC	n	12	12	12	12	12	12
	Min	3.61	3.33	3.75	3.38	4.25	3.43
	Max	4.15	3.75	4.21	4.09	4.78	3.86
	Mean (x)	3.85	3.54	3.98	3.73	4.52	3.64
	SD (σ)	0.17	0.15	0.17	0.26	0.19	0.16
	SE (σ/√n)	0.05	0.04	0.05	0.07	0.06	0.04
	CoV (σ/x)%	4.47	4.27	4.27	6.90	4.27	4.27
	$x_{calculated}$-$x_{measured}$	-	-0.31	0.13	-0.12	0.67	-0.21
	% change	-	-8.07	3.31	-3.08	17.32	-5.45
RCAC	n	13	13	13	13	13	13
	Min	2.54	2.64	2.97	2.23	3.37	2.71
	Max	3.61	3.20	3.59	3.15	4.08	3.29
	Mean (x)	2.99	2.94	3.30	2.72	3.75	3.02
	SD (σ)	0.31	0.15	0.17	0.25	0.19	0.15
	SE (σ/√n)	0.09	0.04	0.05	0.07	0.05	0.04
	CoV (σ/x)%	10.36	5.05	5.05	9.05	5.05	5.05
	$x_{calculated}$-$x_{measured}$	-	-0.05	0.31	-0.27	0.76	0.03
	% change	-	-1.70	10.47	-8.92	25.44	1.10
TRCAC	n	13	13	13	13	13	13
	Min	2.76	2.88	3.24	2.62	3.67	2.96
	Max	3.51	3.23	3.63	3.22	4.13	3.33
	Mean (x)	3.11	3.04	3.41	2.89	3.88	3.12
	SD (σ)	0.23	0.12	0.14	0.20	0.15	0.12
	SE (σ/√n)	0.06	0.03	0.04	0.06	0.04	0.03
	CoV (σ/x)%	7.24	4.00	4.00	7.00	4.00	4.00
	$x_{calculated}$-$x_{measured}$	-	-0.07	0.30	-0.22	0.77	0.01
	% change	-	-2.34	9.75	-7.19	24.63	0.45
RBAC	n	13	13	13	13	13	13
	Min	2.15	2.59	2.91	2.15	3.31	2.66
	Max	2.91	2.96	3.33	2.76	3.78	3.04
	Mean (x)	2.59	2.74	3.08	2.39	3.50	2.82
	SD (σ)	0.21	0.10	0.11	0.17	0.13	0.10
	SE (σ/√n)	0.06	0.03	0.03	0.05	0.04	0.03
	CoV (σ/x)%	8.24	3.68	3.68	6.96	3.68	3.68
	$x_{calculated}$-$x_{measured}$	-	0.15	0.48	-0.20	0.90	0.22
	% change	-	5.59	18.66	-7.78	34.75	8.61
TRBAC	n	12	12	12	12	12	12
	Min	2.39	2.74	3.08	2.40	3.50	2.82
	Max	3.02	3.00	3.37	2.82	3.83	3.08
	Mean (x)	2.77	2.85	3.21	2.58	3.64	2.93
	SD (σ)	0.20	0.08	0.09	0.13	0.10	0.08
	SE (σ/√n)	0.06	0.02	0.03	0.04	0.03	0.02
	CoV (σ/x)%	7.32	2.72	2.72	4.98	2.72	2.72
	$x_{calculated}$-$x_{measured}$	-	0.08	0.44	-0.19	0.87	0.16
	% change	-	2.99	15.75	-6.89	31.44	5.94

n= number of specimen tested; SD= Standard Deviation; SE= Standard Error; CoV= Coefficient of Variation

Table 4.8. Statistical parameters for assessing the measured and predicted results of splitting tensile strength (cont.).

Concrete Mixtures	Statistical Parameters	Splitting Tensile Strength, Ft (MPa)					
		Measured	Calculated				
			TS500	ACI 363R-92	EN 1992-1-1	CSA A23.3-04	NZS 3101-1
FAAC	n	13	13	13	13	13	13
	Min	1.95	2.30	2.58	1.58	2.94	2.37
	Max	2.59	2.71	3.05	2.22	3.46	2.79
	Mean (x)	2.28	2.54	2.86	1.95	3.24	2.61
	SD (σ)	0.20	0.13	0.14	0.20	0.16	0.13
	SE (σ/√n)	0.06	0.03	0.04	0.05	0.04	0.04
	CoV (σ/x)%	9.00	4.94	4.94	10.02	4.94	4.94
	$x_{calculated}$-$x_{measured}$	-	0.26	0.58	-0.32	0.97	0.34
	% change	-	11.63	25.45	-14.22	42.46	14.82
TFAAC	n	13	13	13	13	13	13
	Min	2.19	2.50	2.80	1.88	3.18	2.57
	Max	2.76	2.85	3.21	2.44	3.64	2.94
	Mean (x)	2.44	2.65	2.98	2.13	3.39	2.73
	SD (σ)	0.18	0.11	0.13	0.18	0.14	0.12
	SE (σ/√n)	0.05	0.03	0.04	0.05	0.04	0.03
	CoV (σ/x)%	7.41	4.25	4.25	8.25	4.25	4.25
	$x_{calculated}$-$x_{measured}$	-	0.22	0.55	-0.31	0.95	0.29
	% change	-	8.96	22.45	-12.59	39.05	12.07

n= number of specimen tested; SD= Standard Deviation; SE= Standard Error; CoV= Coefficient of Variation

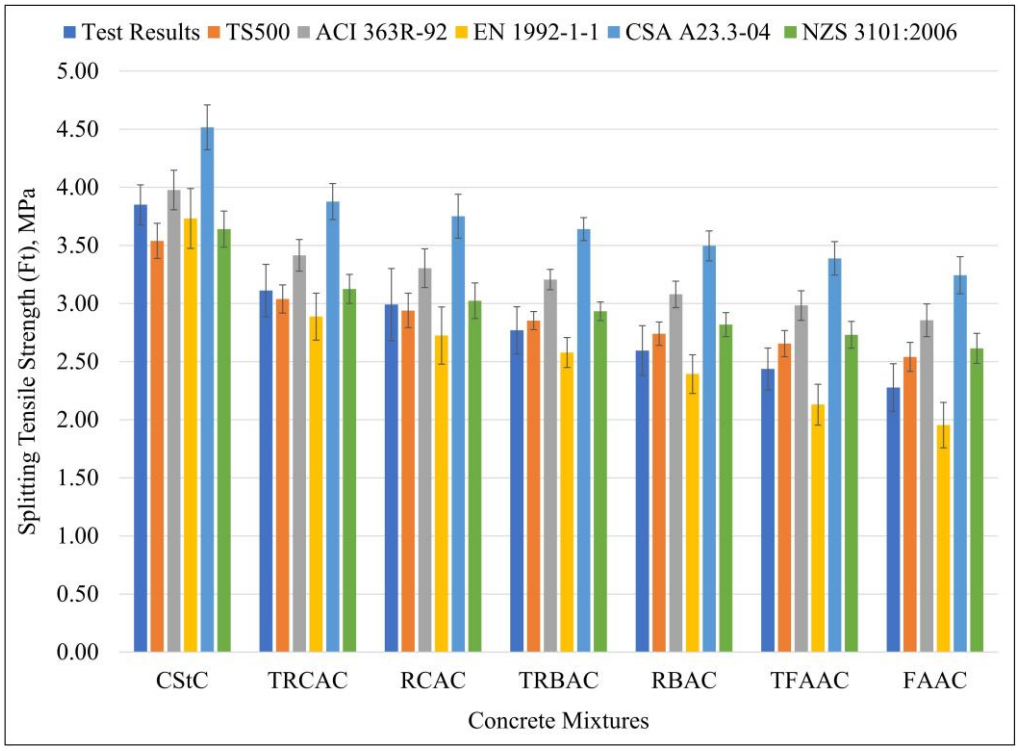

Figure 4.11. The measured and predicted results of the splitting tensile strength.

4.3.3. Flexural Strength

The flexural strength of concrete mixtures decreased from 6.93 MPa for control concrete (CStC) and varied between 4.70 and 2.65 MPa with the full replacement of crushed stone by recycled coarse aggregates. The reduction in the flexural strength of concrete can be accounted for by the higher porosity and lower strength of the recycled aggregates. Among the recycled aggregate concrete mixtures, a higher flexural strength was obtained with TRCAC followed by RCAC, TRBAC, RBAC, TFAAC, and FAAC, which had a performance of 68, 65, 61, 57, 41, and 38% of CStC, respectively, as seen in Figure 4.12. The flexural strength of the recycled aggregate concrete mixtures increased by treating the recycled aggregates with GGBFS slurry during concrete production. It was also observed in the literature [60], [68], [191], [274] that the flexural strength capacity of the concrete produced with recycled aggregates increased when the recycled aggregates were coated with pozzolanic slurry during the concrete mixing procedure.

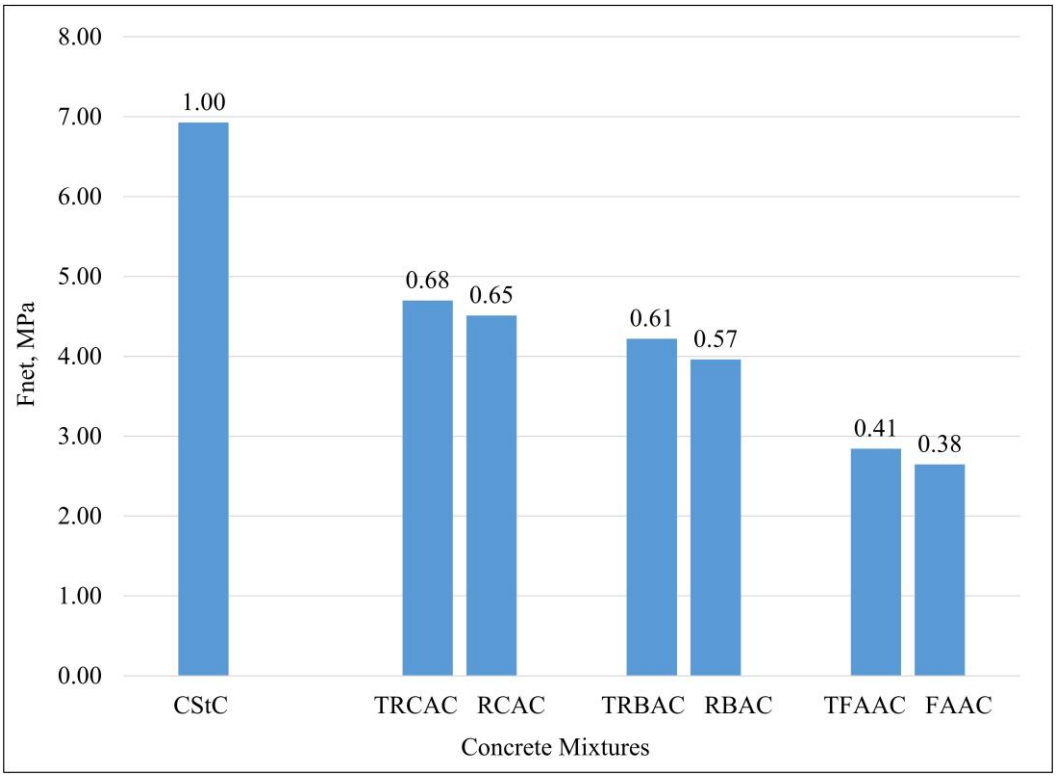

Figure 4.12. Flexural strength of concrete mixtures.

On the other hand, the CoV values of the concrete mixtures RCAC, RBAC, and FAAC produced with untreated recycled coarse aggregates decreased from 7.53, 5.17, and 8.71% for flexural strength to 5.84, 5.00, and 6.86% for the concrete mixtures of TRCAC, TRBAC, and TFAAC with treated recycled coarse aggregates, respectively. Treating the recycled aggregates decreased the CoV values, and thus increased the accuracy of the estimate.

The load-CMOD curves of concrete mixtures constructed under a three-point bending test performed on beam specimens with a notch at mid-span are presented in Figure 4.13. The curves constructed for untreated concrete mixtures produced with recycled aggregates are illustrated with dotted lines, whereas the corresponding curves for treated concrete mixtures are shown with solid lines in the same colors. These representative curves of the related concrete mixtures are chosen regarding the average peak load and $CMOD_c$ (critical crack mouth opening displacement at peak load) values of twelve specimens tested for each concrete mixture.

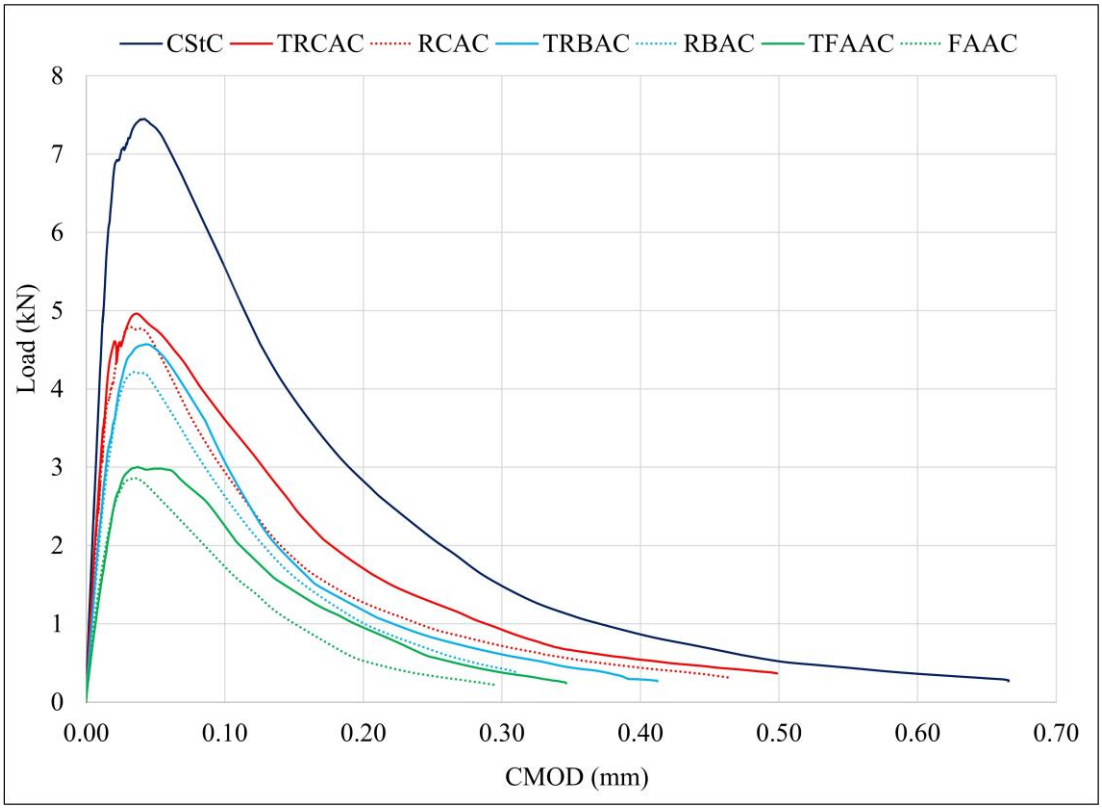

Figure 4.13. Load-CMOD curves of concrete mixtures.

As seen in Figure 4.13, treating the recycled aggregates increased the load carrying capacity of recycled aggregate concrete mixtures with increased peak load and $CMOD_c$ values. All concrete mixtures display a straight pre-peak line, however, treated recycled aggregate concrete mixtures show relatively more gradual post-peak softening curves compared to the untreated recycled aggregate concrete mixtures. In light of the above findings, one may address that treating the recycled aggregates with slag slurry can increase the fracture energy of concrete, which is calculated as the area under the load-CMOD curve.

The relationship between the flexural and compressive strength of the concrete mixtures was also estimated with the equations constructed regarding the test results by using the simple regression analysis based on the least-squares method. The estimating equations, shown in Table 4.9, were compared with the prediction models given in different codes: TS500 [268], ACI 363R-92 [273], EN 1992-1-1 [270], CSA A23.3-04 [271], and NZS 3101-1 [272]. Different models are presented in Table 4.10 to predict the flexural strength of concrete based on the compressive strength recommended by the specified codes. Since the coefficient of determination values (R^2) of estimating equations are sufficiently high, statistical parameters of measured flexural strength values of concrete mixtures shown in Table 4.11 were used to represent the proposed models of this study to compare with the models given by the specified codes. It should be noted that there is a positive correlation between the flexural and compressive strength of all the concrete mixtures according to the estimating equations constructed with reference to the experimental results.

Table 4.9. Estimating equations constructed for flexural strength according to the test results.

Concrete Mixtures	**Estimating Equations**	**Units**
CStC	$f_{ct,f} = 2.0625\sqrt{f_{cm}} - 6.9762,\ R^2 = 0.8891$	$f_{ct,f}$: (MPa) f_{cm}: (MPa)
RCAC	$f_{ct,f} = 1.1300\sqrt{f_{cm}} - 1.8377,\ R^2 = 0.9102$	
TRCAC	$f_{ct,f} = 1.1992\sqrt{f_{cm}} - 2.2713,\ R^2 = 0.9413$	
RBAC	$f_{ct,f} = 1.3383\sqrt{f_{cm}} - 2.9762,\ R^2 = 0.9818$	
TRBAC	$f_{ct,f} = 1.0626\sqrt{f_{cm}} - 1.5908,\ R^2 = 0.8261$	
FAAC	$f_{ct,f} = 0.8674\sqrt{f_{cm}} - 1.5602,\ R^2 = 0.8678$	
TFAAC	$f_{ct,f} = 1.0195\sqrt{f_{cm}} - 2.2801,\ R^2 = 0.9869$	

$f_{ct,f}$: Flexural strength at 28 days. f_{cm}: Mean compressive strength at 28 days.

Table 4.10. Prediction models of the different codes for flexural strength.

Codes	Prediction Models	Units
TS500	$f_{ct,f} = 0.7\sqrt{f_{ck}}$	$f_{ct,f}$: (MPa) f_{ck}: (MPa)
ACI 363R-92	$f_{ct,f} = 0.94\sqrt{f_{cm}}$	$f_{ct,f}$: (MPa) f_{cm}: (MPa)
EN 1992-1-1	$f_{ct,f} = 0.45(f_{cm} - 8\ \text{MPa})^{2/3}$	$f_{ct,f}$: (MPa) f_{cm}: (MPa)
	$*f_{ct,f} = 0.45(f_{cm} - 8\ \text{MPa})^{2/3}(0.4 + 0.6 * 2000/2200)$	$f_{ct,f}$: (MPa) f_{cm}: (MPa)
CSA A23.3-04	$f_{ct,f} = 0.6\sqrt{f_{cm}}$	$f_{ct,f}$: (MPa) f_{cm}: (MPa)
	$**f_{ct,f} = 0.6 \times 0.85 \times \sqrt{f_{cm}}$	$f_{ct,f}$: (MPa) f_{cm}: (MPa)
NZS 3101-1	$f_{ct,f} = 0.8\sqrt{f_{cm}}$	$f_{ct,f}$: (MPa) f_{cm}: (MPa)

f_{ck}: Characteristic compressive strength at 28 days. f_{cm}: Mean compressive strength at 28 days.
$f_{ct,f}$: Flexural strength at 28 days.
*Stands for FAAC and TFAAC regarding the concrete unit weight.
**Stands for the concrete mixtures having unit weight between 1850 and 2150 kg/m^3 regarding the related standard.

As seen in Table 4.11 and Figure 4.14, the mean flexural strength of ACI 363R-92 is close to the experimental mean for the control concrete (CStC) with the values of 6.34 MPa and 6.93 MPa, respectively. However, the CoV of ACI 363R-92 is lower than that of the measured flexural strength, indicating that the level of dispersion around the mean is lower for the model recommended by ACI 363R-92 in the case of control concrete. On the other hand, the models of TS500, EN 1992-1-1, CSA A23.3-04, and NZS 3101-1, highly underestimate the flexural strength with the values of 4.72, 5.04, 4.04, and 5.39 MPa, respectively.

For the concrete mixtures produced with recycled concrete aggregates, the mean flexural strength values of NZS 3101-1 are very close to the experimental means with slight underestimations of 0.36 and 1.04% for RCAC and TRCAC, respectively. However, for both RCAC and TRCAC, the CoV of NZS 3101-1 is lower than that of the measured flexural strength values, indicating that it is more likely to obtain a precise estimation around the mean by the model of NZS 3101-1 compared to the model proposed in this study. On the other hand, the model of ACI 363R-92 highly overestimates the flexural strength with an amount of 17.07% for RCAC and 16.28% for TRCAC, while TS500, EN 1992-1-1, and CSA A23.3-04 highly underestimate the flexural strength with an amount of 12.82, 17.99 and 25.27% for RCAC and 13.41, 16.41 and 25.78% for TRCAC, respectively.

Table 4.11. Statistical parameters for assessing the measured and predicted results of flexural strength.

Concrete Mixtures	Statistical Parameters	Flexural Strength, Fnet (MPa)					
		Measured	Calculated				
			TS500	ACI 363R-92	EN.1992-1-1	CSA A23.3-04	NZS 3101-1
CStC	n	12	12	12	12	12	12
	Min	5.97	4.44	5.97	4.56	3.81	5.08
	Max	7.95	5.00	6.71	5.52	4.28	5.71
	Mean (x)	6.93	4.72	6.34	5.04	4.04	5.39
	SD (σ)	0.63	0.20	0.27	0.35	0.17	0.23
	SE (σ/√n)	0.18	0.06	0.08	0.10	0.05	0.07
	CoV (σ/x)%	9.09	4.27	4.27	6.90	4.27	4.27
	$x_{calculated}$-$x_{measured}$	-	-2.21	-0.59	-1.89	-2.88	-1.53
	% change	-	-31.87	-8.52	-27.27	-41.61	-22.14
RCAC	n	12	12	12	12	12	12
	Min	3.65	3.52	4.73	3.01	3.02	4.02
	Max	5.07	4.26	5.73	4.26	3.66	4.87
	Mean (x)	4.51	3.93	5.28	3.70	3.37	4.49
	SD (σ)	0.34	0.20	0.27	0.34	0.17	0.23
	SE (σ/√n)	0.10	0.06	0.08	0.10	0.05	0.07
	CoV (σ/x)%	7.53	5.10	5.10	9.11	5.10	5.10
	$x_{calculated}$-$x_{measured}$	-	-0.58	0.77	-0.81	-1.14	-0.02
	% change	-	-12.82	17.07	-17.99	-25.27	-0.36
TRCAC	n	12	12	12	12	12	12
	Min	4.24	3.86	5.18	3.57	3.31	4.41
	Max	5.07	4.31	5.79	4.34	3.70	4.93
	Mean (x)	4.70	4.07	5.46	3.93	3.49	4.65
	SD (σ)	0.27	0.16	0.21	0.26	0.13	0.18
	SE (σ/√n)	0.08	0.04	0.06	0.08	0.04	0.05
	CoV (σ/x)%	5.84	3.82	3.82	6.68	3.82	3.82
	$x_{calculated}$-$x_{measured}$	-	-0.63	0.77	-0.77	-1.21	-0.05
	% change	-	-13.41	16.28	-16.41	-25.78	-1.04
RBAC	n	12	12	12	12	12	12
	Min	3.63	3.45	4.64	2.90	2.52	3.95
	Max	4.40	3.86	5.19	3.58	2.82	4.42
	Mean (x)	3.96	3.63	4.87	3.19	2.64	4.15
	SD (σ)	0.20	0.11	0.14	0.18	0.08	0.12
	SE (σ/√n)	0.06	0.03	0.04	0.05	0.02	0.04
	CoV (σ/x)%	5.17	2.93	2.93	5.56	2.93	2.93
	$x_{calculated}$-$x_{measured}$	-	-0.33	0.91	-0.77	-1.32	0.19
	% change	-	-8.39	23.02	-19.48	-33.26	4.70
TRBAC	n	12	12	12	12	12	12
	Min	3.79	3.66	4.91	3.24	2.67	4.18
	Max	4.48	4.06	5.46	3.92	2.96	4.64
	Mean (x)	4.22	3.83	5.14	3.52	2.79	4.38
	SD (σ)	0.21	0.13	0.17	0.21	0.09	0.14
	SE (σ/√n)	0.06	0.04	0.05	0.06	0.03	0.04
	CoV (σ/x)%	5.00	3.30	3.30	6.01	3.30	3.30
	$x_{calculated}$-$x_{measured}$	-	-0.39	0.92	-0.70	-1.43	0.15
	% change	-	-9.29	21.81	-16.51	-33.91	3.66

n= number of specimen tested; SD= Standard Deviation; SE= Standard Error; CoV= Coefficient of Variation

For the concrete mixtures produced with recycled brick aggregates, the mean flexural strength values of NZS 3101-1 are close to the experimental means with slight overestimations of 4.70 and 3.66% for RBAC and TRBAC, respectively. However, for both RBAC and TRBAC, the CoV of NZS 3101-1 is lower than that of the measured flexural strength values, indicating that the model of NZS 3101-1 gives an opportunity to have a more precise estimation around the mean compared to the proposed model of this study. On the other hand, the model of ACI 363R-92 highly overestimates the flexural strength with an amount of 23.02% for RBAC and 21.81% for TRBAC, while TS500, EN 1992-1-1, and CSA A23.3-04 highly underestimate the flexural strength with an amount of 8.39, 19.48 and 33.26% for RBAC and 9.29, 16.51 and 33.91% for TRBAC, respectively.

Table 4.11. Statistical parameters for assessing the measured and predicted results of flexural strength (cont.).

Concrete Mixtures	**Statistical Parameters**	**Flexural Strength, Fnet (MPa)**					
		Measured	**Calculated**				
			TS500	**ACI 363R-92**	**EN.1992-1-1**	**CSA A23.3-04**	**NZS 3101-1**
FAAC	n	12	12	12	12	12	12
	Min	2.37	3.07	4.12	2.13	2.23	3.50
	Max	3.11	3.61	4.85	2.99	2.63	4.13
	Mean (x)	2.65	3.39	4.56	2.65	2.47	3.88
	SD (σ)	0.23	0.17	0.23	0.27	0.13	0.20
	SE (σ/√n)	0.07	0.05	0.07	0.08	0.04	0.06
	CoV (σ/x)%	8.71	5.10	5.10	10.32	5.10	5.10
	$x_{calculated}$-$x_{measured}$	-	0.75	1.91	0.0002	-0.17	1.23
	% change	-	28.28	72.26	0.01	-6.54	46.60
TFAAC	n	12	12	12	12	12	12
	Min	2.60	3.33	4.47	2.54	2.42	3.80
	Max	3.18	3.73	5.01	3.18	2.72	4.26
	Mean (x)	2.84	3.52	4.72	2.84	2.56	4.02
	SD (σ)	0.20	0.13	0.18	0.21	0.10	0.15
	SE (σ/√n)	0.06	0.04	0.05	0.06	0.03	0.04
	CoV (σ/x)%	6.86	3.78	3.78	7.39	3.78	3.78
	$x_{calculated}$-$x_{measured}$	-	0.68	1.88	0.002	-0.28	1.18
	% change	-	23.75	66.18	-0.08	-9.84	41.43

n= number of specimen tested; SD= Standard Deviation; SE= Standard Error; CoV= Coefficient of Variation

For the concrete mixtures produced with recycled fly ash aggregates, the mean flexural strength values of EN 1992-1-1 are super close to the experimental means with a slight overestimation of 0.01% for FAAC and a slight underestimation of 0.08% for TFAAC. However, for both FAAC and TFAAC, the CoV of the measured flexural strength values is lower than that of EN 1992-1-1, indicating that the level of dispersion around the mean for

the proposed model is lower than that of the model recommended by EN 1992-1-1. In other words, the proposed model of this study is statistically more reliable than the model of EN 1992-1-1. On the other hand, the models of TS500, ACI 363R-92, and NZS 3101-1 highly overestimate the flexural strength with an amount of 28.28, 72.26, and 46.60% for FAAC and 23.75, 66.18, and 41.43% for TFAAC, respectively. In comparison, CSA A23.3-04 underestimates the flexural strength with an amount of 6.54% for FAAC and 9.84% for TFAAC.

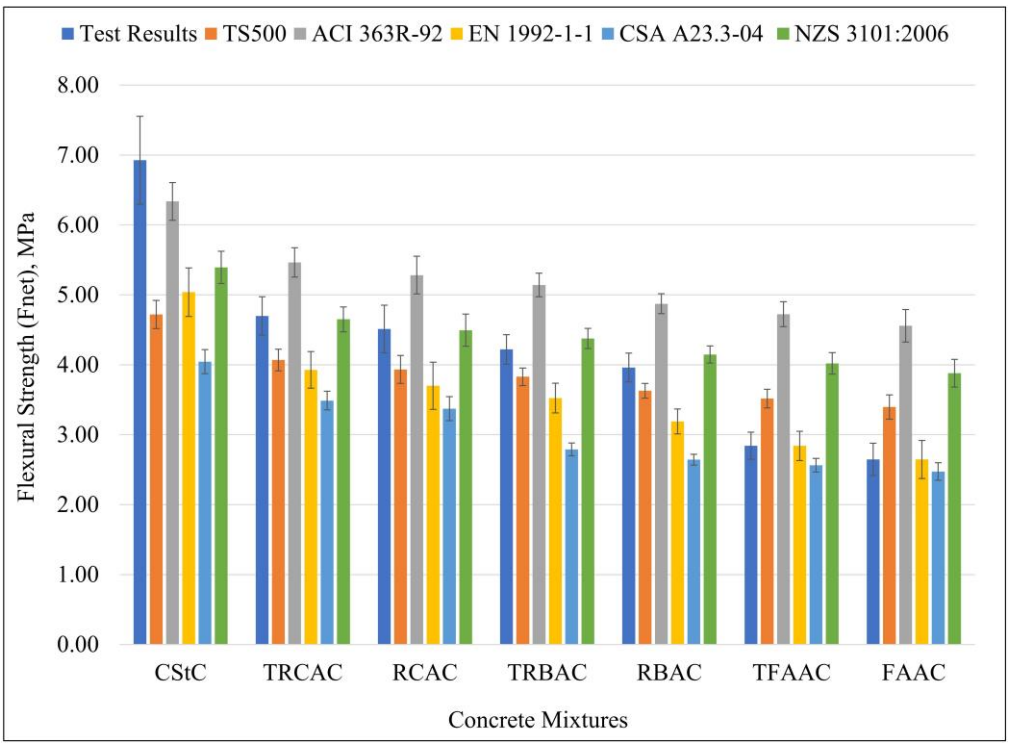

Figure 4.14. The measured and predicted results of the flexural strength.

In summary, in the scope of this study, the relationship between the static modulus of elasticity, the splitting tensile strength and the flexural strength with the compressive strength of the concrete mixtures produced was estimated with the equations constructed regarding the test results by using the simple regression analysis based on the least-squares method. And, the estimating equations obtained from the experimental findings were compared with the prediction models given in different codes. The results discussed in detail above are summarized in Table 4.12 for the sake of simplicity. It shows different codes proposing prediction models for the corresponding mechanical properties that are in good agreement with the experimental results.

Table 4.12. The codes whose prediction models were observed to be in good agreement with the experimental results.

Concrete Mixtures	Modulus of Elasticity, Ec	Splitting Tensile Strength, Ft	Flexural Strength, Fnet
CStC	TS500	EN 1992-1-1	ACI 363R-92
		ACI 363R-92	
TRCAC	ACI 318M-05	NZS 3101:2006	NZS 3101:2006
		TS500	
RCAC	ACI 318M-05	NZS 3101:2006	NZS 3101:2006
		TS500	
TRBAC	CSA A23.3-04	TS500	NZS 3101:2006
RBAC	CSA A23.3-04	TS500	NZS 3101:2006
TFAAC	CSA A23.3-04	TS500	EN 1992-1-1
FAAC	CSA A23.3-04	TS500	EN 1992-1-1

4.3.4. Impact Resistance

In order to determine the impact resistance of concrete mixtures, a drop-weight impact test was performed on 50mm thick notched disks sliced from 150x300mm notched cylinder specimens. A manually operated compaction hammer was dropped repeatedly on the impact piston to apply impact load to the disk specimens. In the meantime, the number of blows required to cause the first visible crack through the line of triangular notches located at the ends of the diameter of disk specimens and to end up with failure (ultimate resistance) was recorded.

The average failure impact energy of the concrete mixtures decreased from 97.38 Nm for control concrete (CStC) and varied between 77.06 and 65.20 Nm with the full replacement of crushed stone by recycled coarse aggregates, as shown in Table 4.13. The reduction in the impact resistance of concrete can be attributed to the higher porosity and lower strength of the recycled aggregates. Among the recycled aggregate concrete mixtures, TRCAC, TRBAC, and TFAAC had higher impact energy values at 79, 74, and 69% of CStC compared to RCAC, RBAC, and FAAC at 77, 70, and 67% of CStC, respectively, as seen in Figure 4.15. Besides, the CoV values of the concrete mixtures RCAC, RBAC, and FAAC

produced with untreated recycled coarse aggregates decreased from 27.47, 22.84, and 25.96% for the impact energy at failure to 24.57, 22.00, and 22.80% for the concrete mixtures of TRCAC, TRBAC, and TFAAC with treated recycled coarse aggregates, respectively. Treating the recycled aggregates decreased the CoV values and thus increased the statistical reliability. On the other hand, as shown in Figure 4.16, treating the recycled aggregates did not increase the post-cracking impact resistance of concrete specimens because the treated specimens failed with only an additional drop of hammer following the first crack as the untreated concrete specimens.

The correlation between the number of blows required to first crack for the concrete mixtures and the impact values of the corresponding coarse aggregates (AIV, %) was also investigated, as presented in Figure 4.17. It was observed as expected that there was a negative correlation with a sufficiently high coefficient of determination (R^2).

The cumulative percent in the number of specimens tested with the corresponding number of blows at failure for concrete mixtures was exhibited in Figures 4.18 to 4.21. While the specimens of control concrete (CStC) failed within seven blows, it was a maximum of five blows for the recycled aggregate concrete specimens. Similarly, half of the CStC specimens failed within four blows, while half of the recycled aggregate concrete specimens failed within a maximum of three blows. As seen in Figure 4.19, roughly 5 and 20% of the specimens of TRCAC and RCAC failed within two blows, respectively. Besides, roundly 20 and 30% of the specimens of RCAC and TRCAC, respectively, required five blows to fail. The specimens of RBAC failed within four blows, whereas 10% of the TRBAC specimens required five blows to fail, as demonstrated in Figure 4.20. Approximately 10 and 20% of the specimens of TRBAC and RBAC, respectively, failed within two blows. In other words, it was determined that there is a nearly 10 and 20% probability that a TRBAC and RBAC specimen will fail within two blows, respectively. For recycled fly ash aggregate concrete mixtures, it was observed that almost 10 and 20% of the specimens of TFAAC and FAAC failed within two blows, respectively, as shown in Figure 4.21. Considering these findings, it is quite possible to claim that treating the recycled aggregates increases the number of blows to failure and thus the impact resistance of concrete.

Table 4.13. Drop-Weight impact test results.

Concrete Mixtures	Statistical Parameters	Number of Blows		First Crack Impact Energy (Nm)	Failure Impact Energy (Nm)
		First Crack	Failure		
CStC	n	24	24	24	24
	Min	2	3	40.65	60.97
	Max	6	7	121.94	142.26
	Mean (x)	3.79	4.79	77.06	97.38
	SD (σ)	1.38	1.38	28.10	28.10
	SE (σ/√n)	0.28	0.28	5.74	5.74
	CoV (σ/x)%	36.46	28.85	36.46	28.85
RCAC	n	24	24	24	24
	Min	1	2	20.32	40.65
	Max	4	5	81.29	101.62
	Mean (x)	2.67	3.67	54.19	74.52
	SD (σ)	1.01	1.01	20.47	20.47
	SE (σ/√n)	0.21	0.21	4.18	4.18
	CoV (σ/x)%	37.77	27.47	37.77	27.47
TRCAC	n	24	24	24	24
	Min	1	2	20.32	40.65
	Max	4	5	81.29	101.62
	Mean (x)	2.79	3.79	56.74	77.06
	SD (σ)	0.93	0.93	18.93	18.93
	SE (σ/√n)	0.19	0.19	3.86	3.86
	CoV (σ/x)%	33.37	24.57	33.37	24.568
RBAC	n	24	24	24	24
	Min	1	2	20.32	40.65
	Max	3	4	60.97	81.29
	Mean (x)	2.33	3.33	47.42	67.74
	SD (σ)	0.76	0.76	15.47	15.47
	SE (σ/√n)	0.16	0.16	3.16	3.16
	CoV (σ/x)%	32.63	22.84	32.63	22.84
TRBAC	n	24	24	24	24
	Min	1	2	20.32	40.65
	Max	4	5	81.29	101.62
	Mean (x)	2.54	3.54	51.65	71.98
	SD (σ)	0.78	0.78	15.83	15.83
	SE (σ/√n)	0.16	0.16	3.23	3.23
	CoV (σ/x)%	30.65	22.00	30.65	22.00

n= number of specimen tested; SD= Standard Deviation; SE= Standard Error; CoV= Coefficient of Variation

Table 4.13. Drop-Weight impact test results (cont.).

Concrete Mixtures	Statistical Parameters	Number of Blows		First Crack Impact Energy (Nm)	Failure Impact Energy (Nm)
		First Crack	Failure		
FAAC	n	24	24	24	24
	Min	1	2	20.32	40.65
	Max	4	5	81.29	101.62
	Mean (x)	2.21	3.21	44.88	65.20
	SD (σ)	0.83	0.83	16.93	16.93
	SE (σ/√n)	0.17	0.17	3.46	3.46
	CoV (σ/x)%	37.72	25.96	37.72	25.96
TFAAC	n	24	24	24	24
	Min	1	2	20.32	40.65
	Max	4	5	81.29	101.62
	Mean (x)	2.29	3.29	46.57	66.90
	SD (σ)	0.75	0.75	15.25	15.25
	SE (σ/√n)	0.15	0.15	3.11	3.11
	CoV (σ/x)%	32.75	22.80	32.75	22.80

n= number of specimen tested; SD= Standard Deviation; SE= Standard Error; CoV= Coefficient of Variation

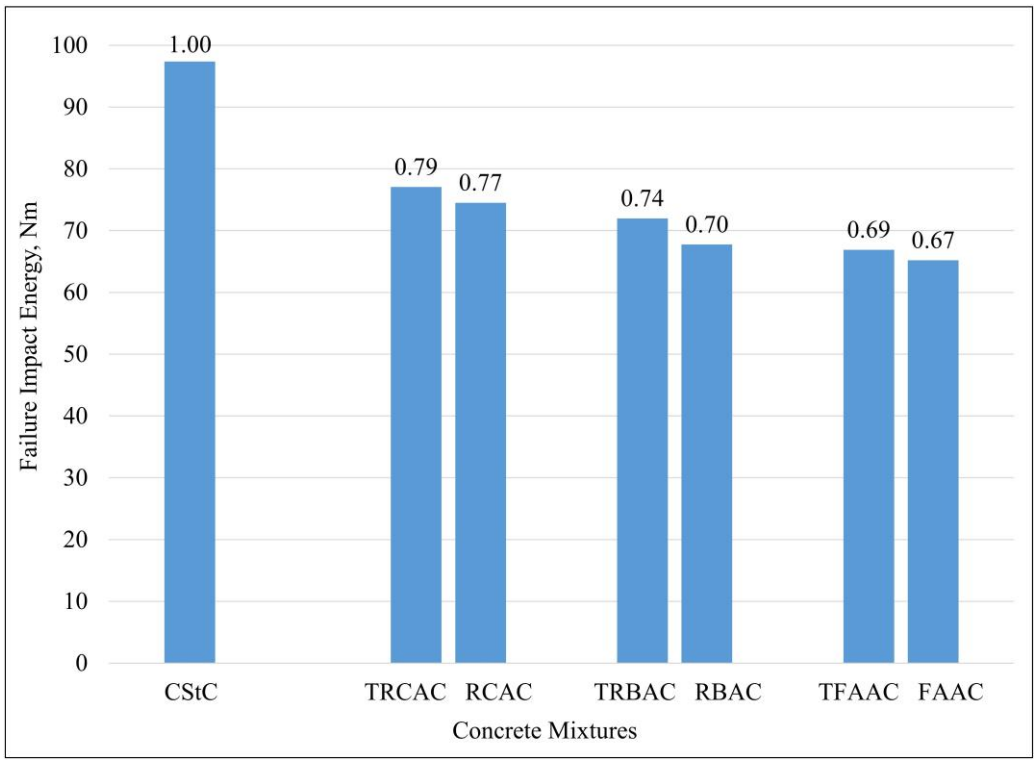

Figure 4.15. Failure impact energy of concrete mixtures.

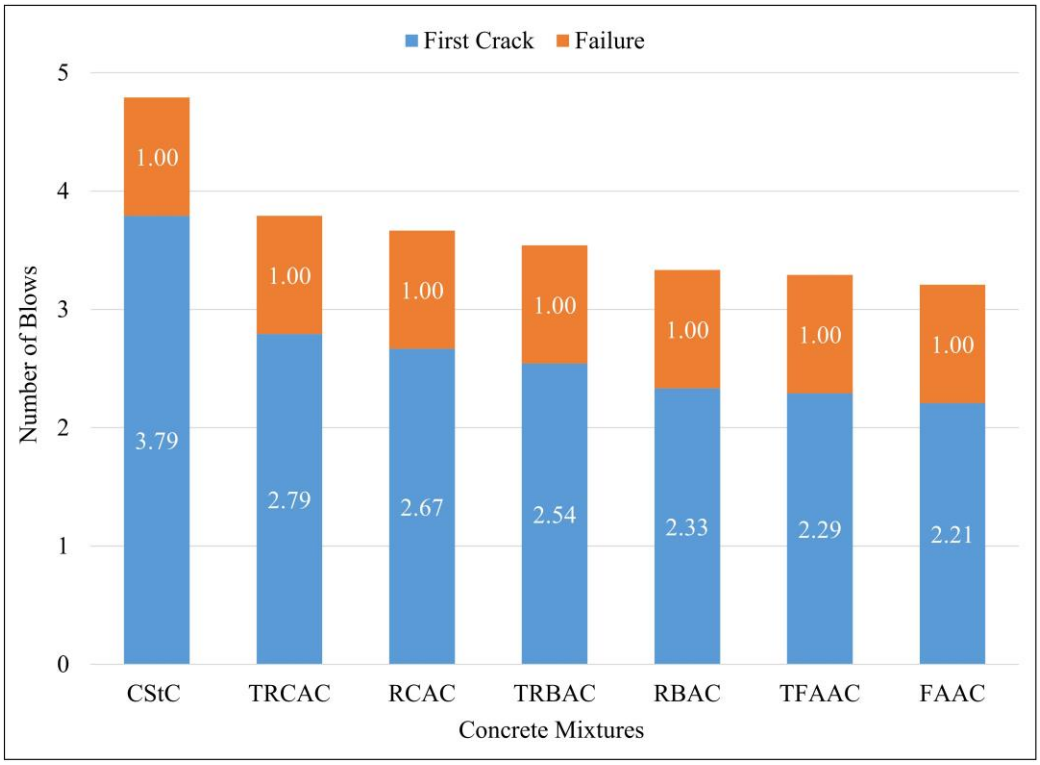

Figure 4.16. Number of blows for concrete mixtures.

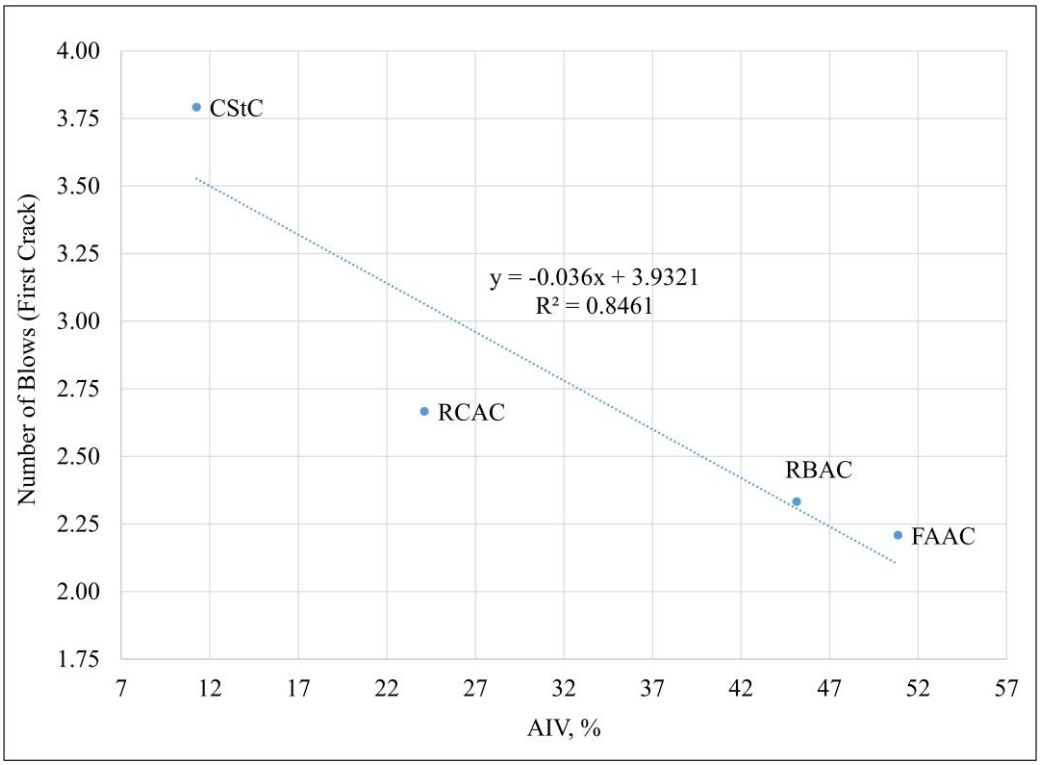

Figure 4.17. Number of blows to first crack vs AIV.

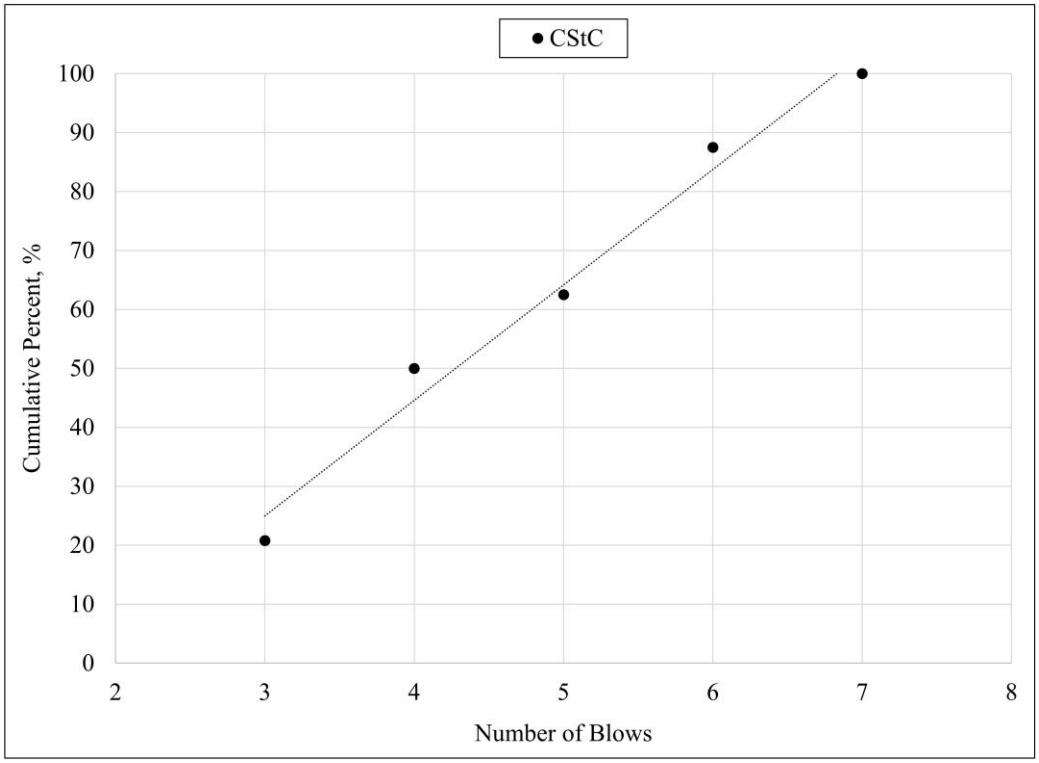

Figure 4.18. Impact resistance of control concrete in blows at failure.

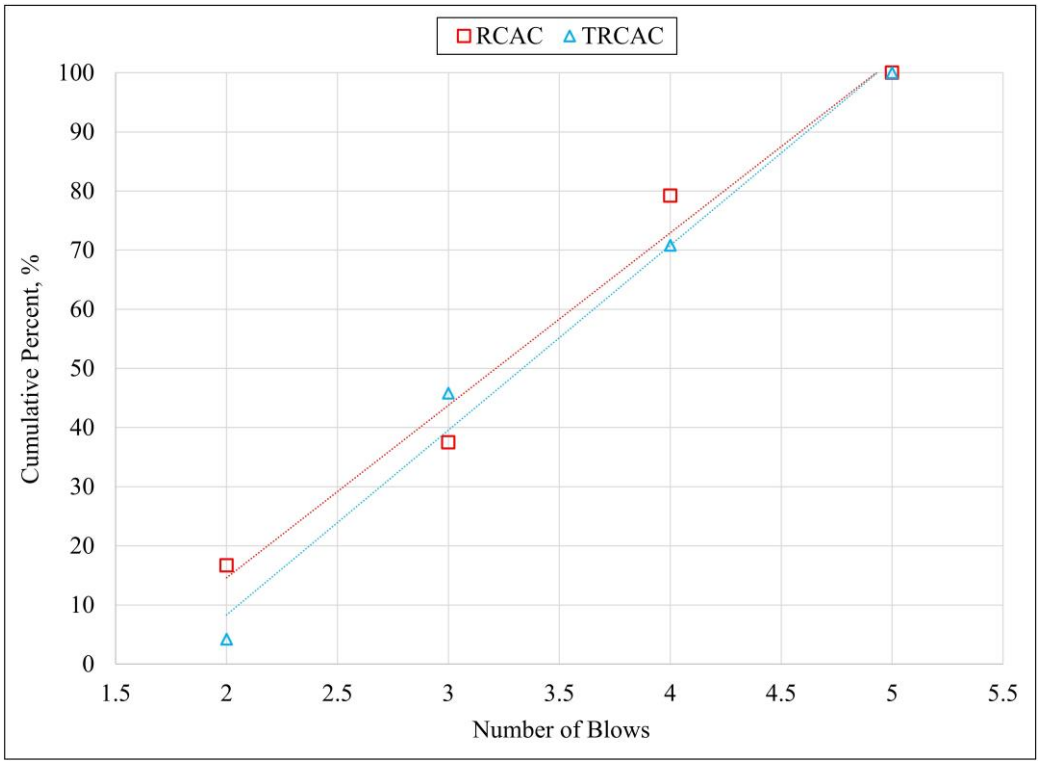

Figure 4.19. Impact resistance of RCAC and TRCAC in blows at failure.

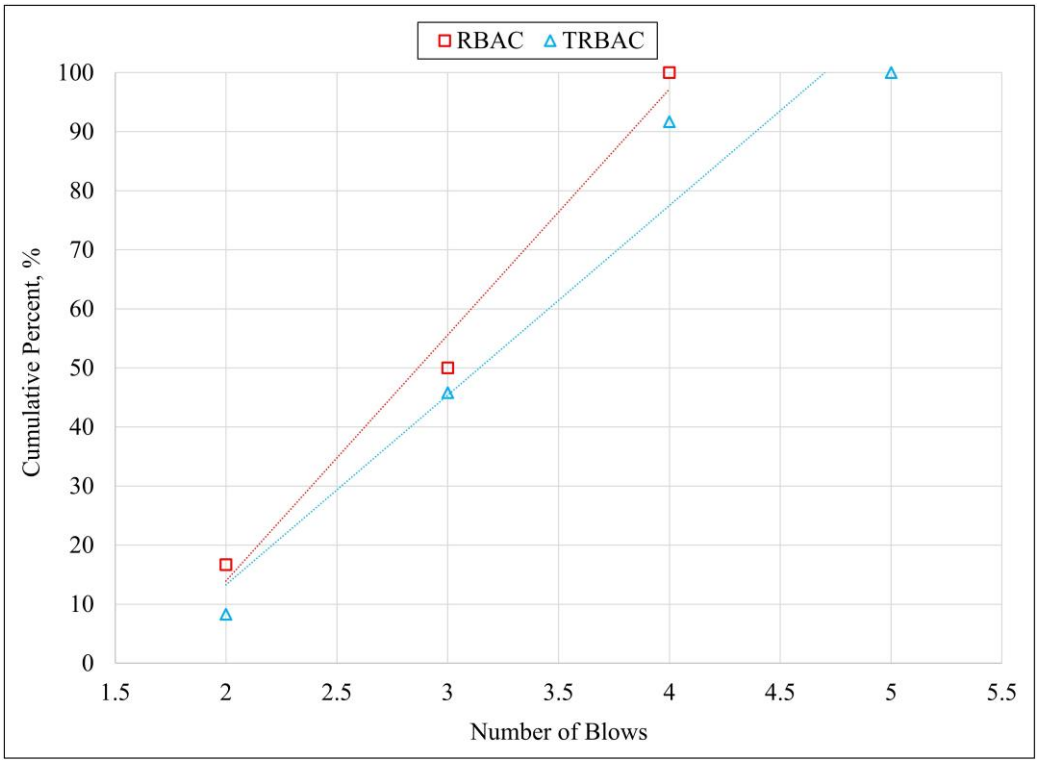

Figure 4.20. Impact resistance of RBAC and TRBAC in blows at failure.

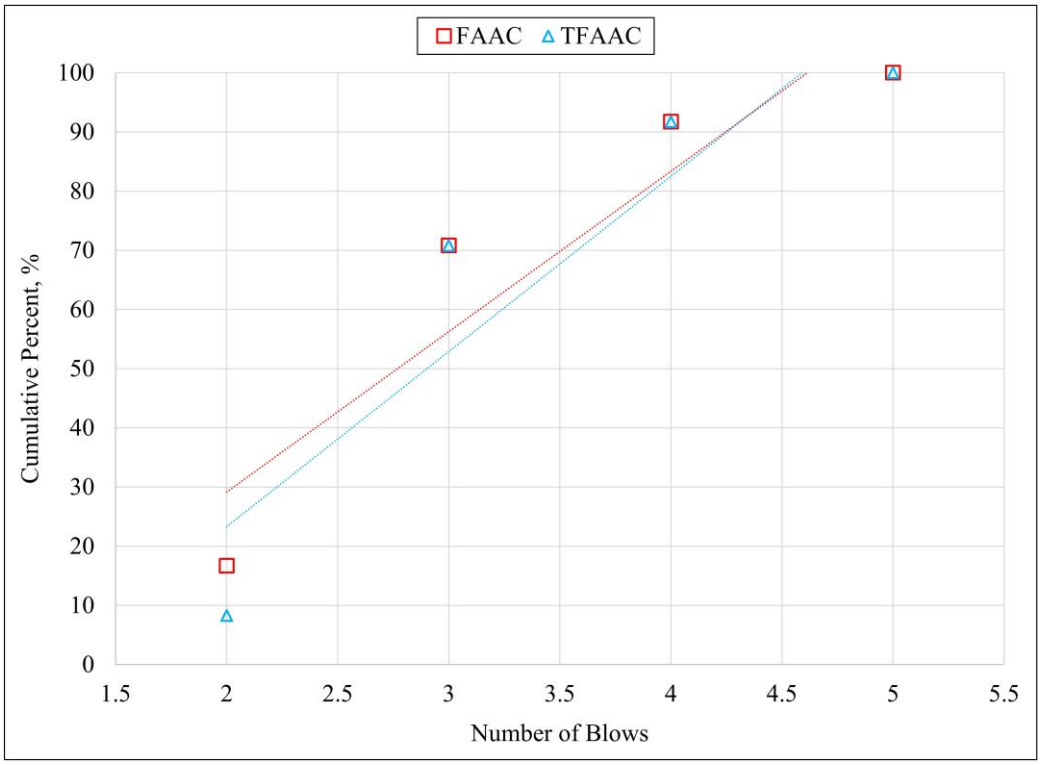

Figure 4.21. Impact resistance of FAAC and TFAAC in blows at failure.

In this study, the minimum number of tests, *n*, required to be performed to maintain the percentage error in the average number of blows measured to the first crack and the ultimate impact resistance of the concrete mixtures under a certain limit, *e*, at a specified level of confidence was also determined by the following expression [235], [275]–[279]:

$$n = t^2 v^2 / e^2 \tag{4.1}$$

where *v* stands for the coefficient of variation, and *t* refers to the value of the Student's t-distribution depending on the level of confidence and the degrees of freedom, which is associated with the number of disk specimens tested.

Table 4.14 presents the minimum number of tests that need to be carried out to keep the error in the average number of blows to the first crack and ultimate impact resistance of the concrete mixtures under certain limits of 5, 10, 20, and 30%, at the confidence levels of 90 and 95%. As expected, for both FC and UR, the number of specimens required to be tested increased with an increase in confidence level, whereas it decreased with an increase in the percentage error for all concrete mixtures. For instance, the number of specimens required to be tested to maintain the error under 5% in the case of UR for CStC was 143 and 99, while it was 4 and 3 for a 30% error at 95 and 90% confidence levels, respectively, as seen in Figure 4.22. On the other hand, a higher number of specimens is required for the concrete mixtures produced with untreated recycled aggregates compared to the corresponding treated concrete mixtures regardless of the confidence level and percentage error in the measured average number of blows to FC and UR. For example, the minimum number of specimens needed to maintain the error under 10% at a confidence level of 90% for UR is roundly 22 and 18 for RCAC and TRCAC, respectively, as illustrated in Figure 4.23. It increases to 89 and 71 when the error decreases to 5% at a 90% confidence level for RCAC and TRCAC at UR, respectively. If the error in the average measured number of blows to FC is kept under 20%, the number of specimens required to be tested should be at least 15 and 12 at a confidence level of 95% for RCAC and TRCAC, respectively. However, it increases to 61 and 48 when the error decreases to 10% at a 95% confidence level for RCAC and TRCAC at FC, respectively. In the case of concrete mixtures produced with recycled brick aggregates, the minimum number of tests that need to be performed to maintain the error under 5% at a confidence level of 95% is nearly 89 and 83 for RBAC and

TRBAC at UR, respectively, as exhibited in Figure 4.24. It decreases to 6 and 5 when the error increases to 20% at a 95% confidence level for RBAC and TRBAC at UR, respectively. If the error in the average measured number of blows to FC is kept under 10%, the number of tests required to be carried out should be at least 31 and 28 at a confidence level of 90% for RBAC and TRBAC, respectively. However, it decreases to 4 and 3 when the error increases to 30% at a 90% confidence level for RBAC and TRBAC at FC, respectively. Similarly, for concrete mixtures produced with recycled fly ash aggregates, the minimum number of specimens required to be examined to maintain the error, for instance, under 10% at a 90% confidence level is approximately 42 and 32 for FAAC and TFAAC at FC, respectively, as shown in Figure 4.25. It decreases to 5 and 4 when the error increases to 30% at a confidence level of 90% for FAAC and TFAAC at FC, respectively.

In this study, the minimum number of specimens that need to be tested to maintain the percent error in the average number of blows to FC and UR of the concrete mixtures under a certain limit at a specific level of confidence decreased with a decrease in the variation of impact resistance. As mentioned above, treating the recycled aggregates decreased the CoV values and thus decreased the minimum number of specimens required to be tested.

However, considering that 24 specimens were tested for each concrete mixture within the scope of this study, the error in the average measured number of blows to FC and UR appears only to be below 20 and 10% at a confidence level of 95 and 90%, respectively, for recycled aggregate concrete mixtures. If it is desired to reduce the margin of error and increase the confidence level, it should be noted that the number of experiments conducted in this study should be increased for all concrete mixtures, as shown in Table 4.14.

Table 4.14. Number of repetition required to keep the error under a specified limit at a certain level of confidence.

Concrete Mixtures	Percentage Error in Average, *e*															
	<5				<10				<20				<30			
	Level of Confidence															
	95%		90%		95%		90%		95%		90%		95%		90%	
	Number of Tests, *n*															
	FC	UR	FC	UR	FC	UR	FC	UR	FC	UR	FC	UR	FC	UR	FC	UR
CStC	227.6	142.5	156.2	97.8	56.9	35.6	39.1	24.5	14.2	8.9	9.8	6.1	6.3	4.0	4.3	2.7
RCAC	244.3	129.2	167.6	88.7	61.1	32.3	41.9	22.2	15.3	8.1	10.5	5.5	6.8	3.6	4.7	2.5
TRCAC	190.7	103.4	130.8	70.9	47.7	25.8	32.7	17.7	11.9	6.5	8.2	4.4	5.3	2.9	3.6	2.0
RBAC	182.3	89.3	125.1	61.3	45.6	22.3	31.3	15.3	11.4	5.6	7.8	3.8	5.1	2.5	3.5	1.7
TRBAC	160.9	82.8	110.4	56.9	40.2	20.7	27.6	14.2	10.1	5.2	6.9	3.6	4.5	2.3	3.1	1.6
FAAC	243.6	115.4	167.2	79.2	60.9	28.9	41.8	19.8	15.2	7.2	10.4	5.0	6.8	3.2	4.6	2.2
TFAAC	183.7	89.0	126.1	61.1	45.9	22.3	31.5	15.3	11.5	5.6	7.9	3.8	5.1	2.5	3.5	1.7

FC= First Crack; UR= Ultimate Resistance

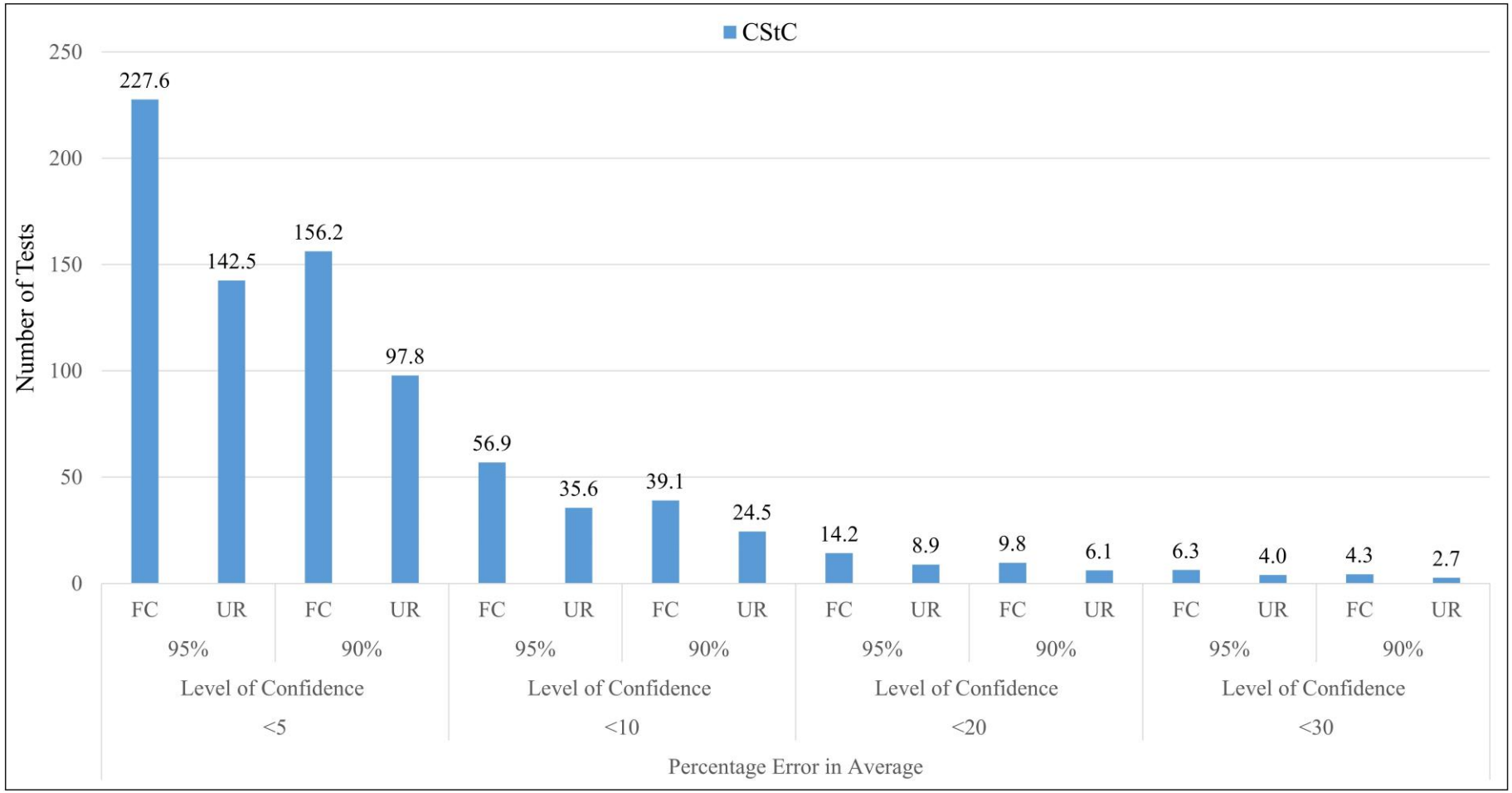

Figure 4.22. Number of tests required to keep the error under a specified limit at a certain level of confidence in the case of CStC.

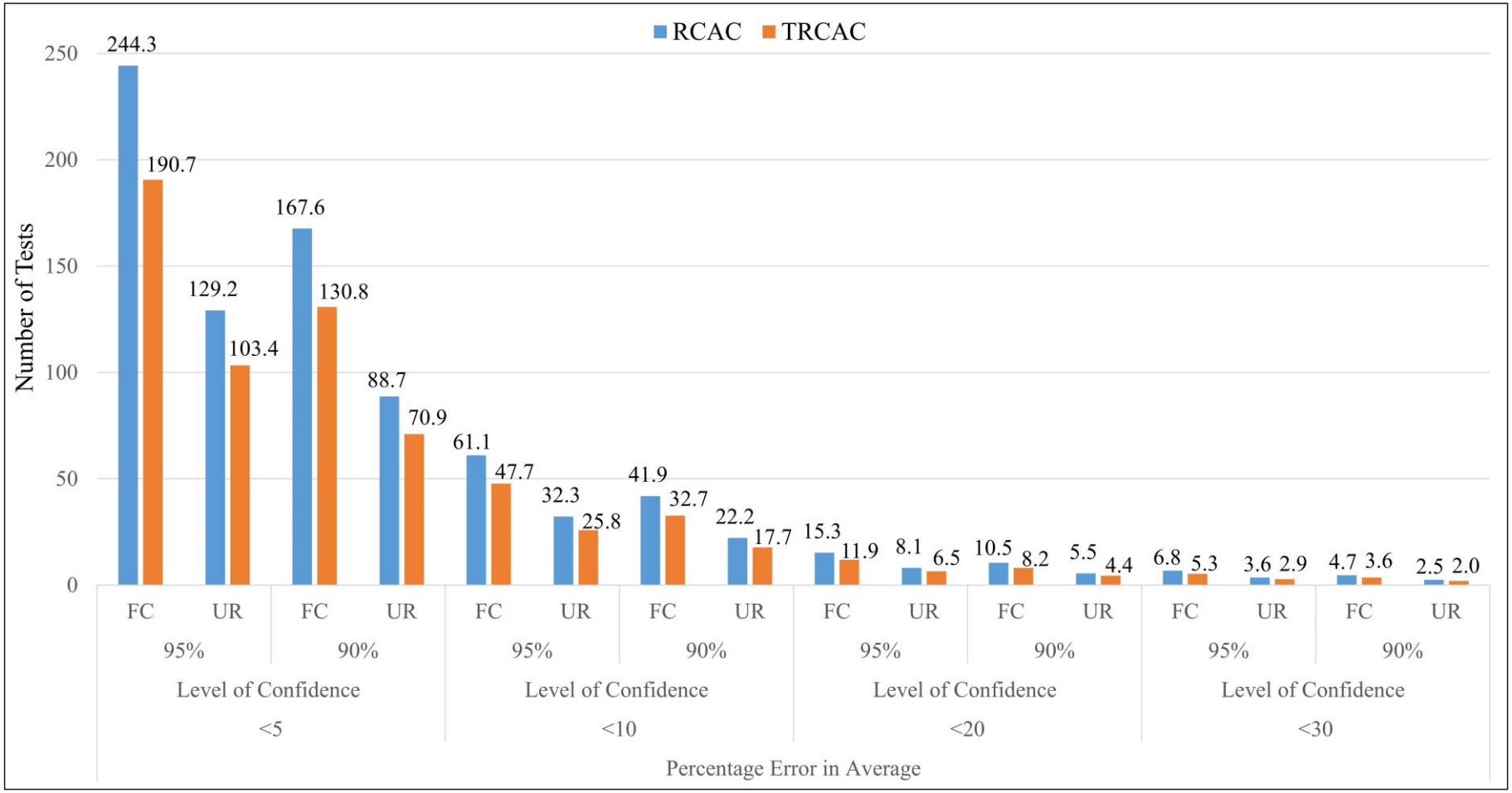

Figure 4.23. Number of tests required to keep the error under a specified limit at a certain level of confidence in the case of RCAC and TRCAC.

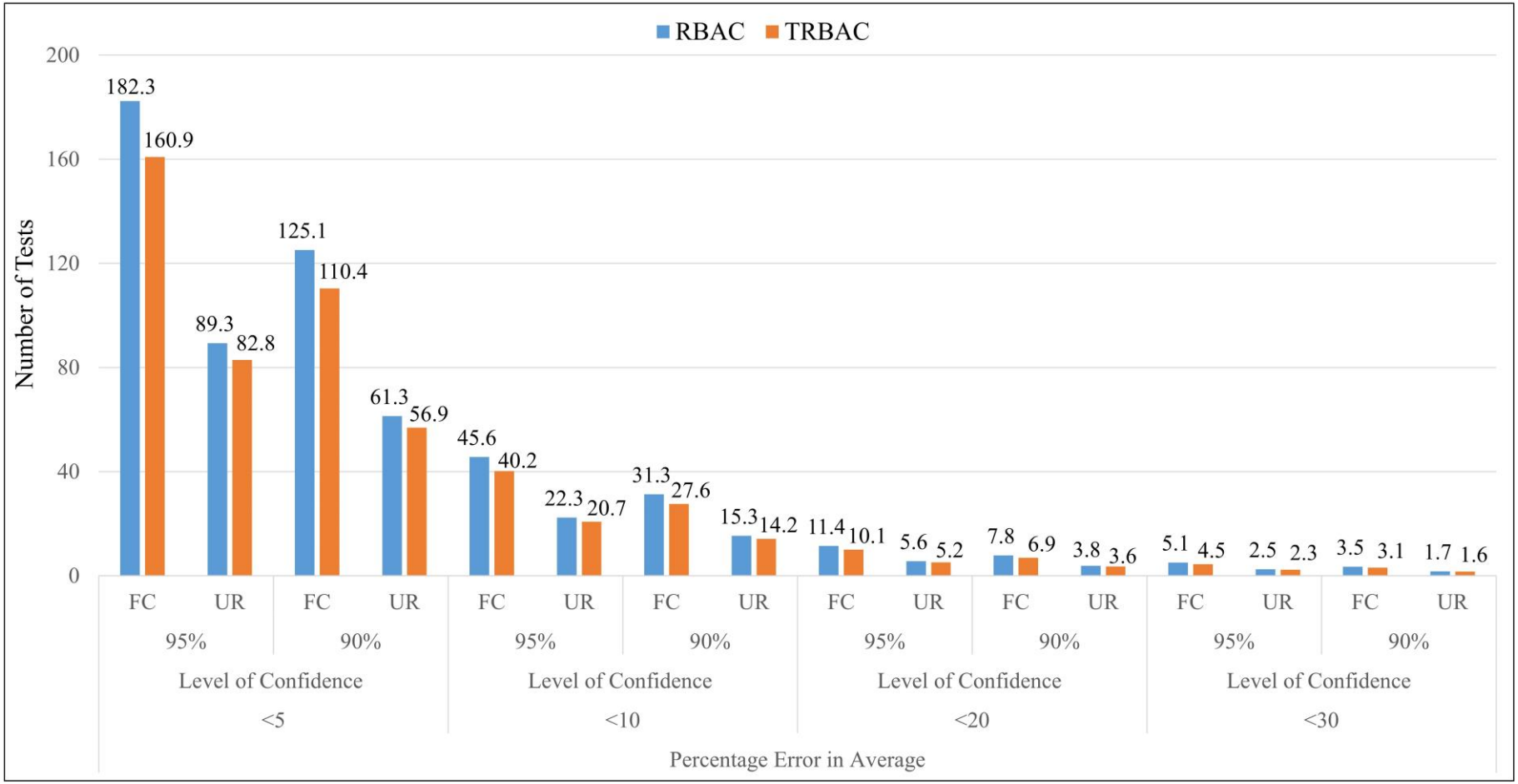

Figure 4.24. Number of tests required to keep the error under a specified limit at a certain level of confidence in the case of RBAC and TRBAC.

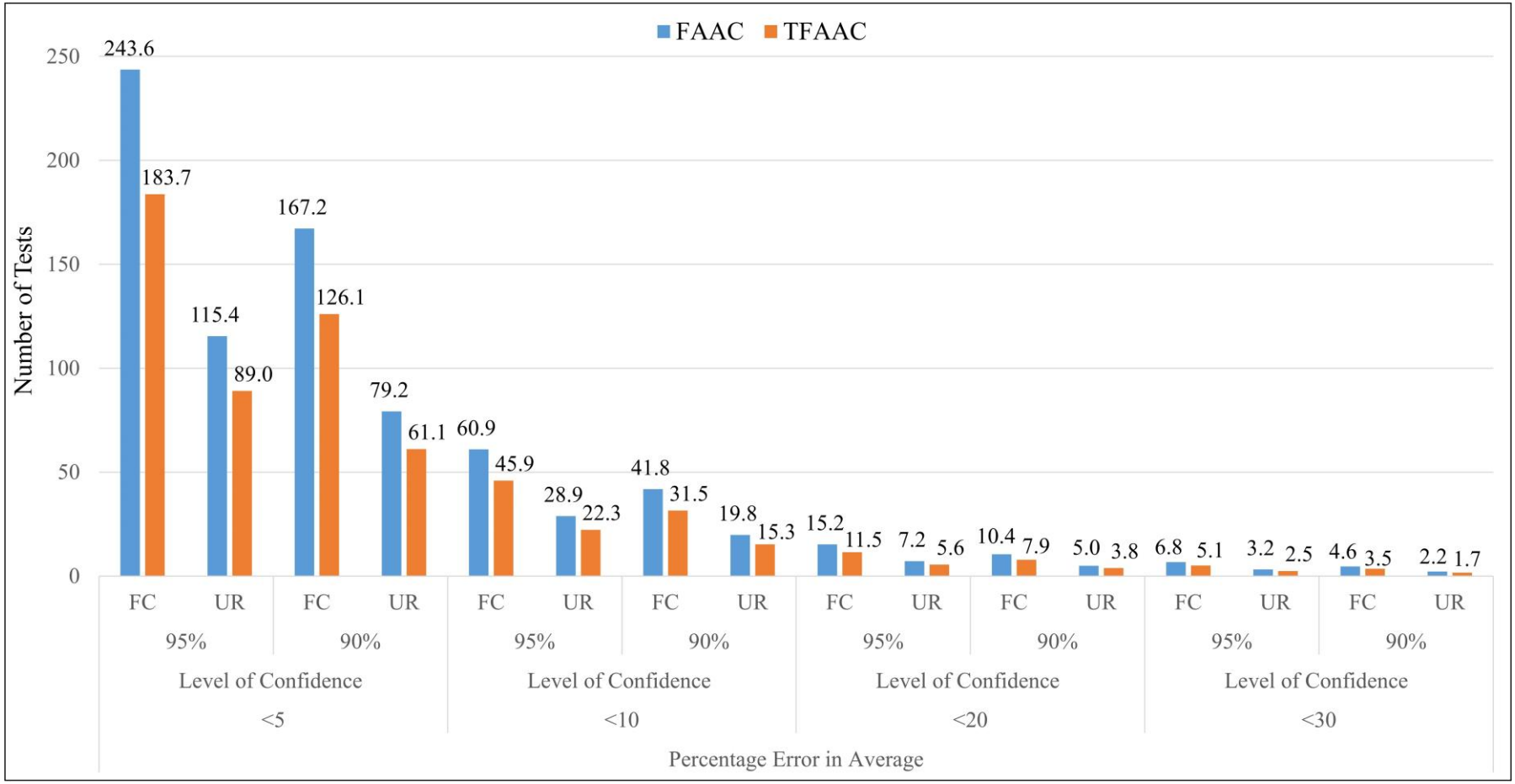

Figure 4.25. Number of tests required to keep the error under a specified limit at a certain level of confidence in the case of FAAC and TFAAC.

4.3.5. Fracture Properties of Concrete under Three Point Bending

The Fracture parameters of the concrete mixtures produced in this study were calculated according to the findings of the three-point bending test conducted on the beam specimens with a notch at mid-span.

The fracture toughness (K_{IC}^{S}), which indicates the ability of the concrete to withstand crack extension or, more specifically, the resistance against brittle fracture, of the concrete mixtures decreased from 1.36 MPa.m$^{1/2}$ for control concrete (CStC) and varied between 0.91 and 0.47 MPa.m$^{1/2}$ for the recycled aggregate concrete mixtures, as presented in Table 4.15. Among the recycled aggregate concrete mixtures, higher fracture toughness was obtained with TRCAC followed by RCAC, TRBAC, RBAC, TFAAC, and FAAC, showing 67, 63, 58, 52, 38, and 34% performance of CStC, respectively, as seen in Figure 4.26.

The critical crack-tip opening displacement ($CTOD_c$) is another parameter to measure the fracture performance of concrete, showing the limit beyond which crack propagation becomes unsteady. In other words, the $CTOD_c$ is reached when the beam specimen is exposed to the maximum load that it can carry under the bending test. At this point, unstable crack propagation begins, and the crack continues to propagate even if the load remains constant or decreases. Besides, the more brittle the concrete, the smaller the $CTOD_c$, so the brittle concrete reaches the $CTOD_c$ more quickly under loading. When the concrete mixtures are compared in terms of $CTOD_c$, it is seen in Table 4.15 that CStC, which has the highest resistance to brittle fracture(K_{IC}^{S}), has the highest $CTOD_c$ as well. The average $CTOD_c$ of the concrete mixtures decreased from 0.0118 mm for the control concrete (CStC) and varied between 0.0100 and 0.0068 mm with the full replacement of crushed stone by recycled coarse aggregates, as shown in Table 4.15. Among the recycled aggregate concrete mixtures, TRCAC, TRBAC, and TFAAC had higher $CTOD_c$ values at 85, 76, and 63% of CStC compared to RCAC, RBAC, and FAAC at 79, 66, and 57% of CStC, respectively, as shown in Figure 4.27.

The fracture energy or the energy absorption capacity of the concrete mixtures, G_F, was also determined in the scope of this study. The average fracture energy of the concrete mixtures given in Table 4.15 decreased from 157.31 N/m for the control concrete (CStC)

and varied between 98.77 and 63.15 N/m when recycled aggregates were utilized in place of crushed stone coarse aggregate (CSt) that can be attributed to the higher porosity and lower strength of the recycled aggregates. Among the recycled aggregate concrete mixtures, TRCAC had the highest fracture energy followed by RCAC, TRBAC, RBAC, TFAAC and FAAC with a performance of 63, 58, 52, 50, 42, and 40% of CStC, respectively, as illustrated in Figure 4.28.

In addition, as a measure of brittleness, the characteristic length (l_{ch}) of the concrete mixtures was calculated by Equation 3.15. As demonstrated in Table 4.15, the overall characteristic length reduced from 383.93 mm for the control concrete (CStC) and varied between 278.22 and 180.27 mm with the use of recycled aggregates as a substitute for crushed stone coarse aggregate (CSt). Among the recycled aggregate concrete mixtures, TRCAC, TRBAC, and TFAAC had higher l_{ch} values at 72, 63, and 48% of CStC compared to RCAC, RBAC, and FAAC at 70, 60, and 47% of CStC, respectively, as presented in Figure 4.29. It should be noted that there is an inverse relationship between the characteristic length and the brittleness of concrete. As the magnitude of the characteristic length decreases, the brittleness of the concrete increases [280]. In this respect, it is seen that the FAAC with the lowest characteristic length is the most brittle concrete mixture, while the CStC with the highest characteristic length is the least brittle one in the production plan. Besides, treating the recycled aggregates with slag slurry during concrete mixing increased the characteristic length and so decreased the brittleness of recycled aggregate concrete mixtures.

Treating the recycled aggregates by the direct slurry method not only improved the fracture properties of recycled aggregate concrete mixtures, but also increased the statistical reliability of the findings in terms of fracture parameters. As given in Table 4.15, the CoV values for all the fracture parameters of the recycled aggregate concrete mixtures decreased when the recycled aggregates were treated with slag slurry. For instance, the CoV values of RCAC, RBAC, and FAAC produced with untreated recycled coarse aggregates decreased from 13.69, 4.24, and 7.12% for fracture toughness to 5.76, 4.11, and 6.39% for TRCAC, TRBAC, and TFAAC produced with treated recycled coarse aggregates, respectively. The lower the CoV, the higher the statistical reliability.

Table 4.15. Fracture parameters of concrete mixtures.

Concrete Mixtures	Statistical Parameters	K_{IC}^{S} (MPa $m^{1/2}$)	$CTOD_c$ (mm)	G_F (N/m)	l_{ch} (mm)
CStC	n	12	12	12	12
	Min	1.1271	0.0097	104.8926	272.0291
	Max	1.5526	0.0145	199.3620	489.0597
	Mean (x)	1.3596	0.0118	157.3092	383.9332
	SD (σ)	0.1254	0.0012	27.5806	74.9822
	SE (σ/√n)	0.0362	0.0004	7.9618	21.6455
	CoV (σ/x)%	9.2232	10.5563	17.5327	19.5300
RCAC	n	12	12	12	12
	Min	0.6260	0.0037	77.9481	178.4734
	Max	1.0357	0.0157	116.1845	318.1242
	Mean (x)	0.8589	0.0093	91.8057	267.6622
	SD (σ)	0.1175	0.0044	11.5475	38.3990
	SE (σ/√n)	0.0339	0.0013	3.3335	11.0848
	CoV (σ/x)%	13.6860	46.9538	12.5782	14.3461
TRCAC	n	12	12	12	12
	Min	0.8192	0.0070	86.7730	243.9689
	Max	0.9975	0.0131	113.2206	318.8438
	Mean (x)	0.9091	0.0100	98.7658	278.2173
	SD (σ)	0.0524	0.0021	7.3839	25.3665
	SE (σ/√n)	0.0151	0.0006	2.1315	7.3227
	CoV (σ/x)%	5.7617	20.8936	7.4761	9.1175
RBAC	n	12	12	12	12
	Min	0.6679	0.0048	66.3592	196.5775
	Max	0.7566	0.0102	97.6371	280.4237
	Mean (x)	0.7022	0.0078	79.3235	231.4516
	SD (σ)	0.0298	0.0016	7.9420	26.1359
	SE (σ/√n)	0.0086	0.0005	2.2926	7.5448
	CoV (σ/x)%	4.2377	20.7972	10.0121	11.2922
TRBAC	n	12	12	12	12
	Min	0.7331	0.0065	68.5599	211.4480
	Max	0.8280	0.0113	91.8894	283.5457
	Mean (x)	0.7842	0.0090	81.5934	241.6065
	SD (σ)	0.0323	0.0014	7.8248	18.4479
	SE (σ/√n)	0.0093	0.0004	2.2588	5.3254
	CoV (σ/x)%	4.1133	15.8240	9.5900	7.6355

n= number of specimen tested; SD= Standard Deviation; SE= Standard Error; CoV= Coefficient of Variation

Table 4.15. Fracture parameters of concrete mixtures (cont.).

Concrete Mixtures	Statistical Parameters	K_{IC}^{S} (MPa $m^{1/2}$)	$CTOD_c$ (mm)	G_F (N/m)	l_{ch} (mm)
FAAC	n	12	12	12	12
	Min	0.4382	0.0041	45.4532	138.3584
	Max	0.5454	0.0090	90.3251	284.3535
	Mean (x)	0.4709	0.0068	63.1463	180.2678
	SD (σ)	0.0335	0.0014	14.6179	45.2455
	SE (σ/√n)	0.0097	0.0004	4.2198	13.0612
	CoV (σ/x)%	7.1179	20.9411	23.1492	25.0990
TFAAC	n	12	12	12	12
	Min	0.4702	0.0051	51.2527	142.7962
	Max	0.5749	0.0097	90.3841	281.3840
	Mean (x)	0.5172	0.0075	66.3153	184.8060
	SD (σ)	0.0331	0.0011	12.9870	41.8497
	SE (σ/√n)	0.0095	0.0003	3.7490	12.0810
	CoV (σ/x)%	6.3933	15.1450	19.5837	22.6452

n= number of specimen tested; SD= Standard Deviation; SE= Standard Error; CoV= Coefficient of Variation

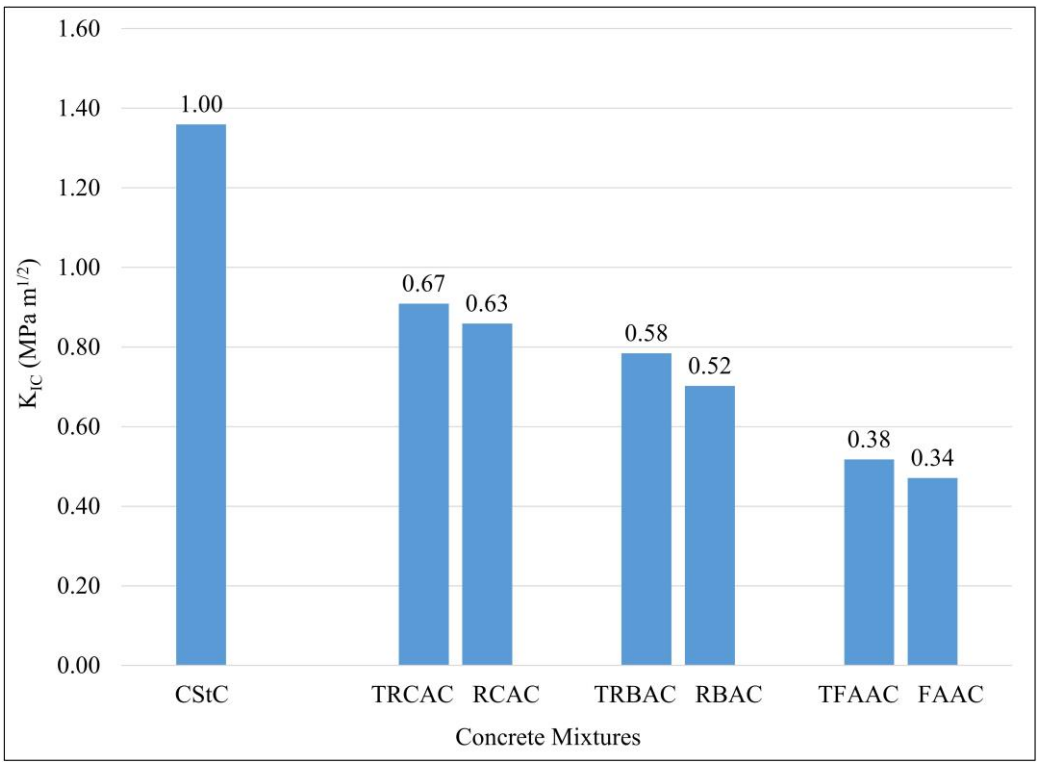

Figure 4.26. Fracture toughness of concrete mixtures.

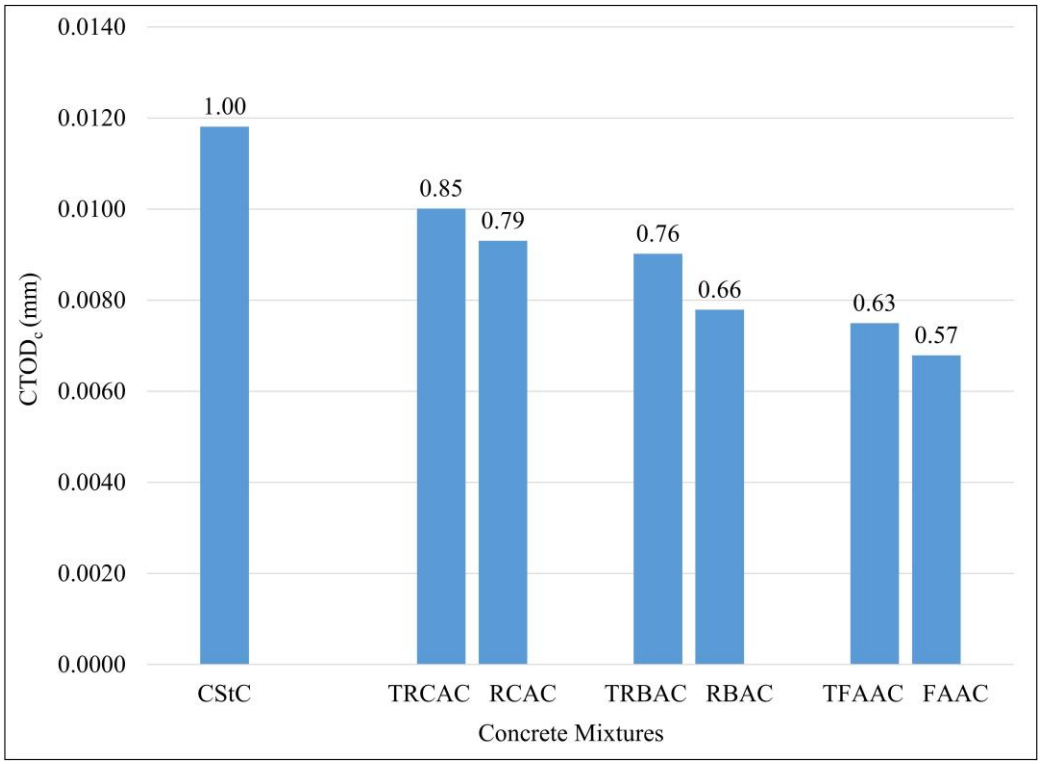

Figure 4.27. Critical crack tip opening displacement of concrete mixtures.

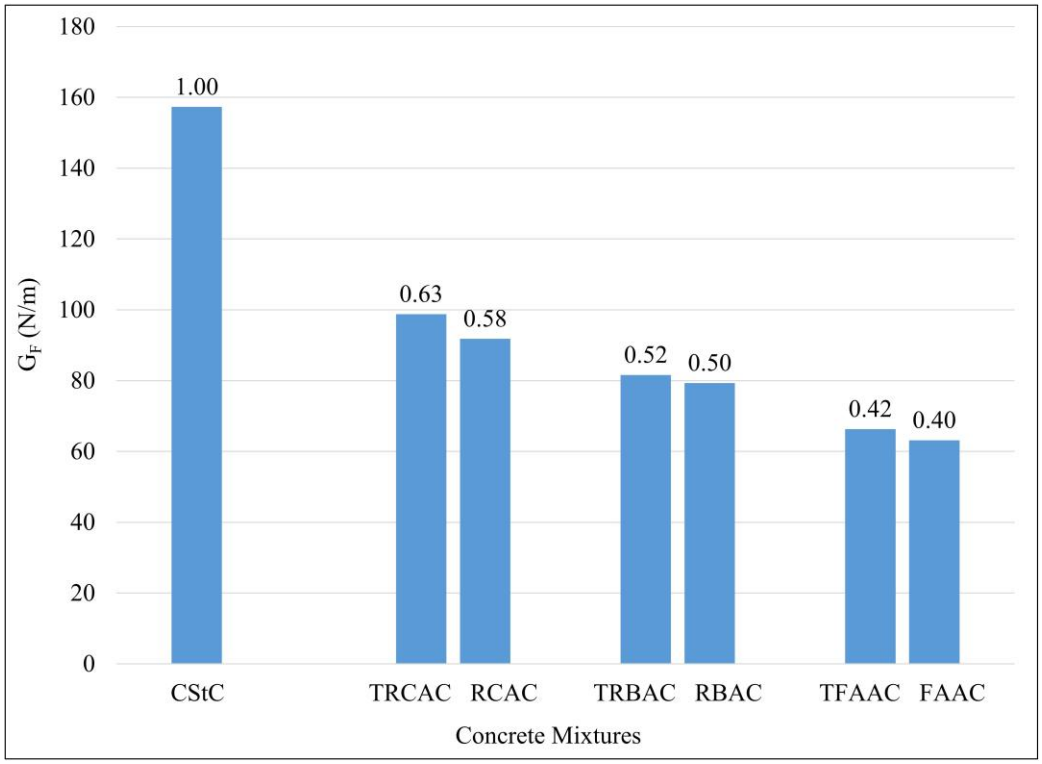

Figure 4.28. Fracture energy of concrete mixtures.

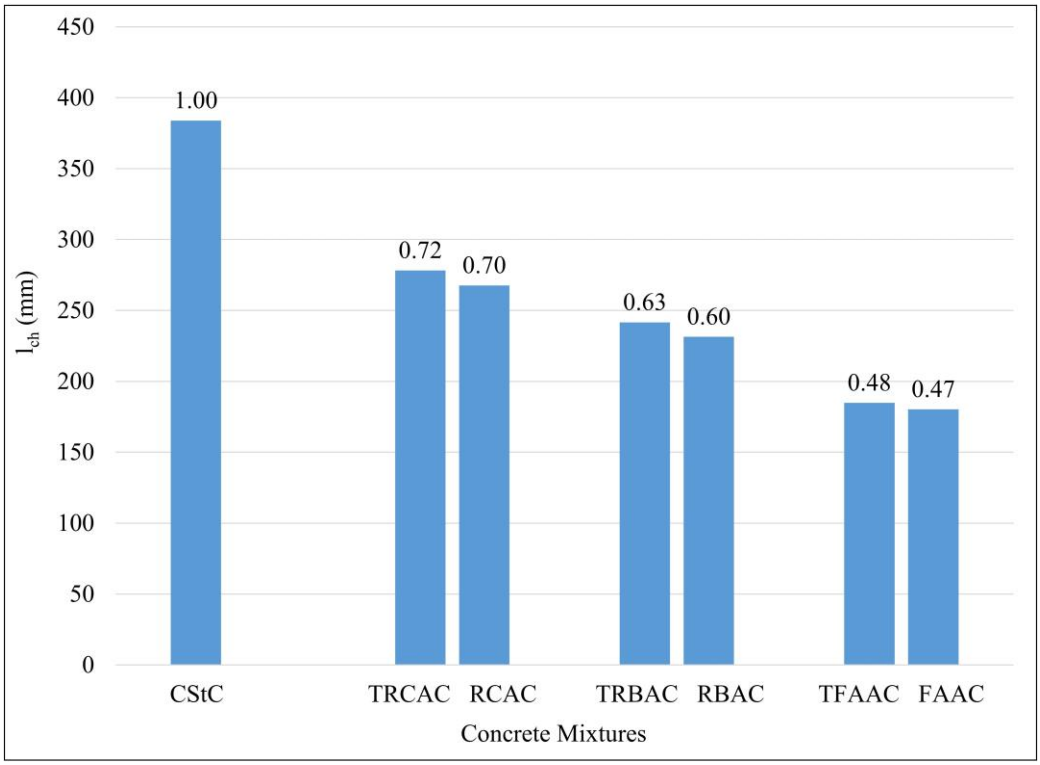

Figure 4.29. Characteristic length of concrete mixtures.

4.3.6. Bond Strength between Rebar and Concrete

In order to investigate the bond strength between the reinforcing bars and the concrete mixtures, the pull-out test was conducted by applying an axial tensile load on the reinforcing bars embedded in the cubic specimens. The variation in bond strength with height over concrete was also examined by comparing the bond strength developed between the concrete mixtures and the reinforcing bars located at the top, middle, and bottom in column specimens. Additionally, the effect of the overlying and underlying concrete layers was analyzed by comparing the bond strength values of the bars in cubic specimens with those of the bottom (τ_{bot}) and the top (τ_{top}) bars in column specimens, respectively. The bond strength values obtained from the experiments were normalized (τ_{nz}) with respect to the Equation 3.17 to carry out a fair comparison between different concrete mixtures with varied strength capacity.

On the other hand, the bond strength values obtained as a result of the experiments (τ_{exp}) and those calculated according to the relevant standard (τ_{ACI}) were compared to

determine whether the anchorage length (5d) in cubic and column specimens is sufficient to ensure the minimum bond strength required for the reinforcement to carry the load.

The average bond strength values obtained in cubic and column specimens for the concrete mixtures are shown in Table 4.16. When concrete mixtures are compared in terms of bond strength, it is seen that CStC has the highest values both for the bars in cubic specimens and for those embedded in different locations in column specimens. For concrete mixtures produced with recycled aggregates, higher bond strength values were achieved by treating the recycled aggregates with slag slurry in cubic and column specimens, as demonstrated in Figures 4.30 and 4.32, respectively. Similar results were observed when the bond strength values obtained in the cubic and column specimens were normalized considering the compressive strength of the concrete mixtures, as presented in Figures 4.31 and 4.33, respectively. When the results obtained for the bottom and top bars in the column specimens produced with the same concrete mixtures were compared to examine the effect of the location of the bars on the bond strength, it was observed that the bond strength of the bottom bars was significantly higher than that of the top bars for all concrete mixtures. This can be attributed to the bleeding (water gain especially under top reinforcing bar), static segregation (accumulation of aggregates at the bottom of column specimens owing to gravity) and cracks and/or voids that may occur especially adjacent to the top bar when it restrains the plastic concrete that has a tendency to consolidate even after initial placement and following finishing procedures. In connection with this, the bottom reinforcing bars pulled from the column specimens, regardless of whether they are produced with treated or untreated recycled aggregates, tend to have more mortar adhered on the surface between the ribs through the anchorage length compared to the top bars, as can be seen in Figures 4.34 to 4.37. On the other hand, the amount of mortar adhered on the surface of the reinforcing bars especially that on the top bars pulled from the column specimens produced with treated recycled aggregates was higher than that on the equivalent bars pulled from the column specimens produced with untreated recycled aggregates. Treating recycled aggregates with slag slurry not only increased the bond strength values but also decreased the difference between the bond strength of the top and bottom bars as a general trend, as shown in Figure 4.38. Coating recycled aggregates with slag slurry during concrete mixing could have increased cohesion and reduced bleeding and segregation in fresh concrete.

In addition, the effect of the overlying and underlying concrete layers was investigated by comparing the bond strength values of the reinforcing bars in cubic specimens, τ_{cube}, with the bond strength values of the bottom and the top bars in column specimens, τ_{bot} and τ_{top}, respectively. As shown in Figure 4.39, for all concrete mixtures, the underlying concrete layer has a negative effect on the bond strength with the ratio of τ_{top}/τ_{cube} less than 1.0 while it is contrary for the overlying concrete layer with the ratio of τ_{bot}/τ_{cube} bigger than 1.0 referring to higher homogeneity and better compaction of the material. The positive effect of the overlying concrete layer on the bond strength developed between the reinforcing bar and the concrete increased slightly as a general trend when the recycled aggregates were treated with slag slurry during concrete mixing.

On the other hand, as mentioned above, for cubic and column specimens it was examined separately whether the preferred anchorage length (5d) in this study was sufficient to ensure the minimum bond strength required for the reinforcement to carry the load with reference to the specified design code. As seen in Figure 4.40, the ratio τ_{exp}/τ_{ACI} higher than 1.0 refers to the fact that the anchorage length for the cubic specimens was sufficient for all concrete mixtures; however, the required anchorage length decreased with increasing τ_{exp}/τ_{ACI} ratio when the recycled aggregates were treated with slag slurry. In terms of column specimens, it was seen that the anchorage length was sufficient for the bottom bars for all concrete mixtures, while it was generally not sufficient, especially for the top bars for recycled aggregate concrete mixtures (Figure 4.41). However, the treatment of the recycled aggregates decreased the minimum required anchorage length with respect to the specified design code for all bars in different locations in the column specimens.

Table 4.16. Average bond strength values.

Concrete Mixtures	**Specimens**		**τ_{exp} (MPa)**	**τ_{nz} (MPa$^{0.5}$)**	**τ_{ACI} (MPa)**
CStC	Column	Top	6.60	0.98	4.49
		Mid	9.76	1.45	5.84
		Bot	26.58	3.94	5.84
	Cubic		19.24	2.85	5.84
RCAC	Column	Top	3.44	0.61	3.73
		Mid	5.28	0.94	4.85
		Bot	18.99	3.39	4.85
	Cubic		12.42	2.22	4.85
TRCAC	Column	Top	4.20	0.72	3.87
		Mid	6.87	1.18	5.04
		Bot	20.39	3.50	5.04
	Cubic		13.59	2.33	5.04
RBAC	Column	Top	2.88	0.55	3.50
		Mid	4.84	0.92	4.54
		Bot	16.45	3.13	4.54
	Cubic		11.42	2.17	4.54
TRBAC	Column	Top	3.14	0.58	3.64
		Mid	5.07	0.93	4.73
		Bot	18.38	3.36	4.73
	Cubic		12.00	2.20	4.73
FAAC	Column	Top	1.93	0.40	3.22
		Mid	3.77	0.78	4.19
		Bot	13.02	2.69	4.19
	Cubic		9.93	2.05	4.19
TFAAC	Column	Top	2.33	0.46	3.37
		Mid	4.10	0.81	4.38
		Bot	15.07	2.98	4.38
	Cubic		10.86	2.15	4.38

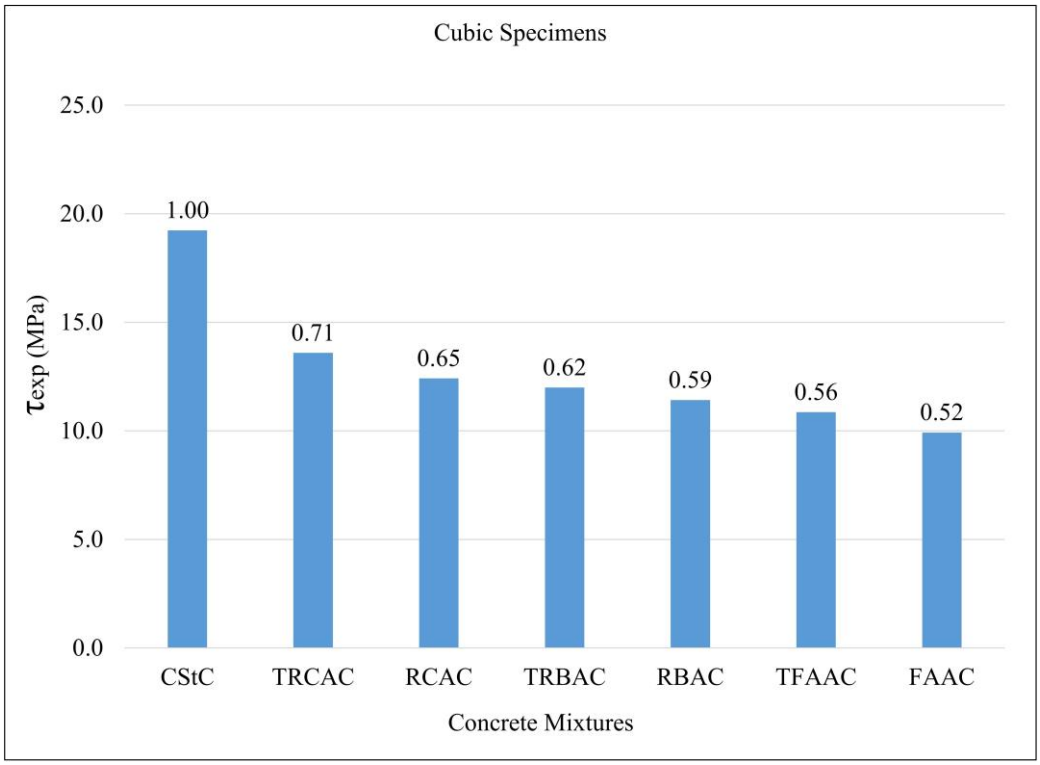

Figure 4.30. Bond strength values for rebars in cubic specimens.

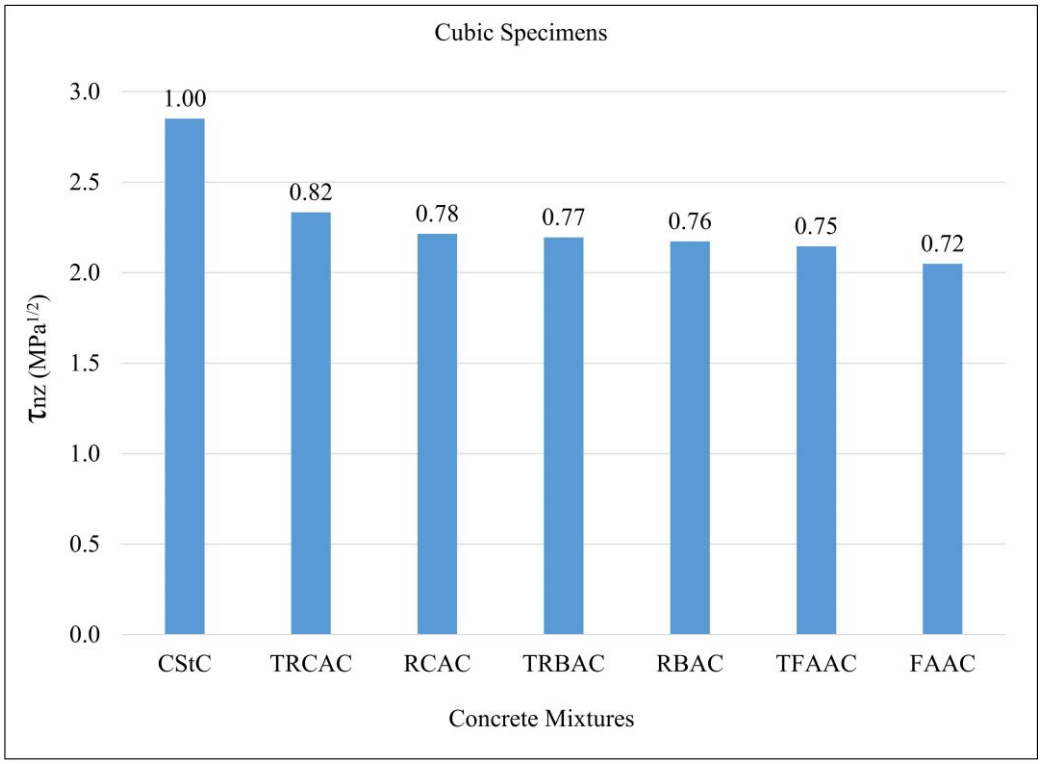

Figure 4.31. Normalized bond strength values for rebars in cubic specimens.

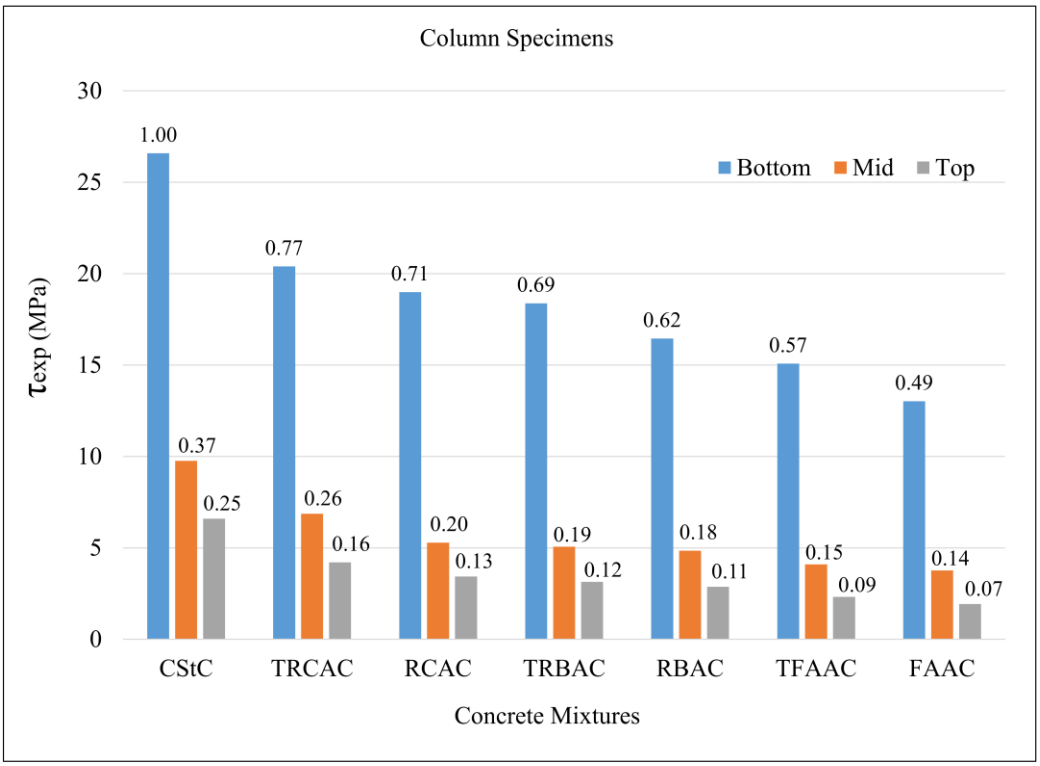

Figure 4.32. Bond strength values for rebars in column specimens.

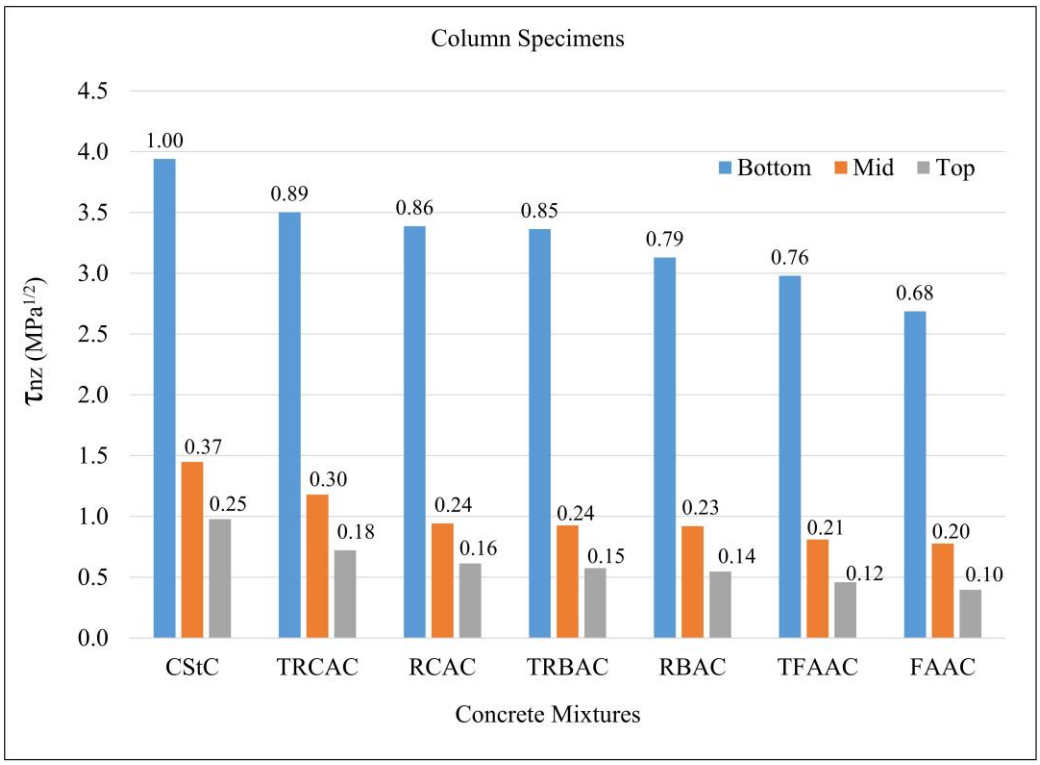

Figure 4.33. Normalized bond strength values for rebars in column specimens.

Figure 4.34. Mortar adhered on bars in a column specimen of FAAC.

Figure 4.35. Mortar adhered on bars in a column specimen of TFAAC.

Figure 4.36. Mortar adhered on bars in a column specimen of RCAC.

Figure 4.37. Mortar adhered on bars in a column specimen of TRCAC.

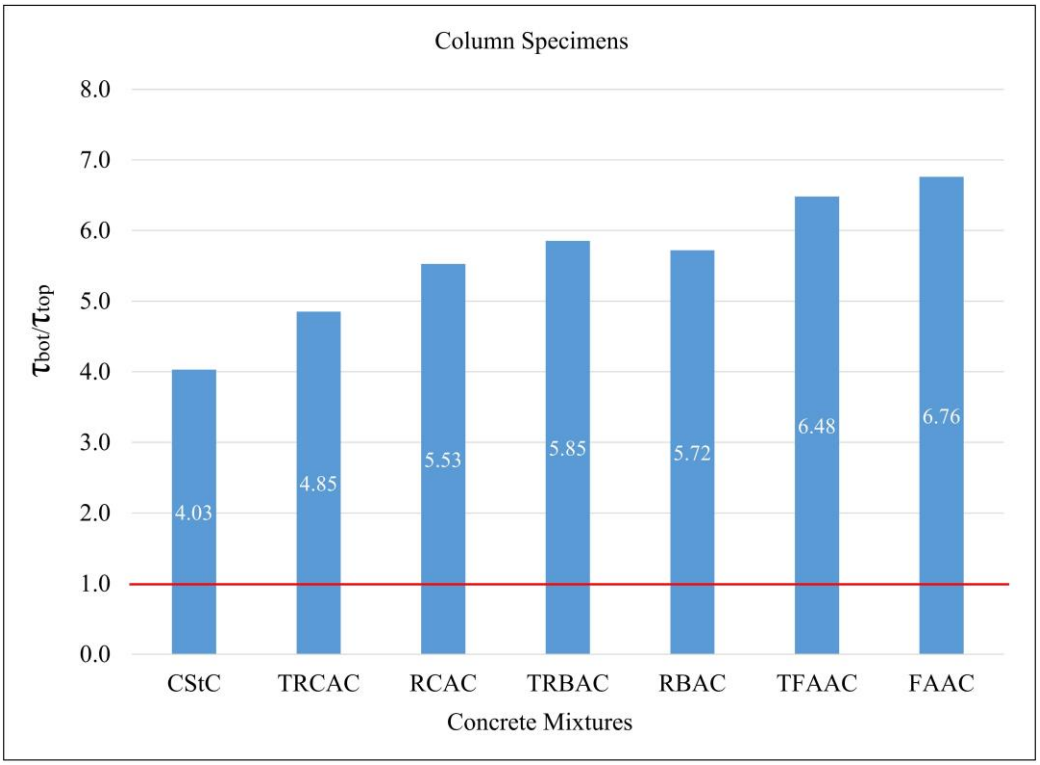

Figure 4.38. Bond strength variation over height in column specimens.

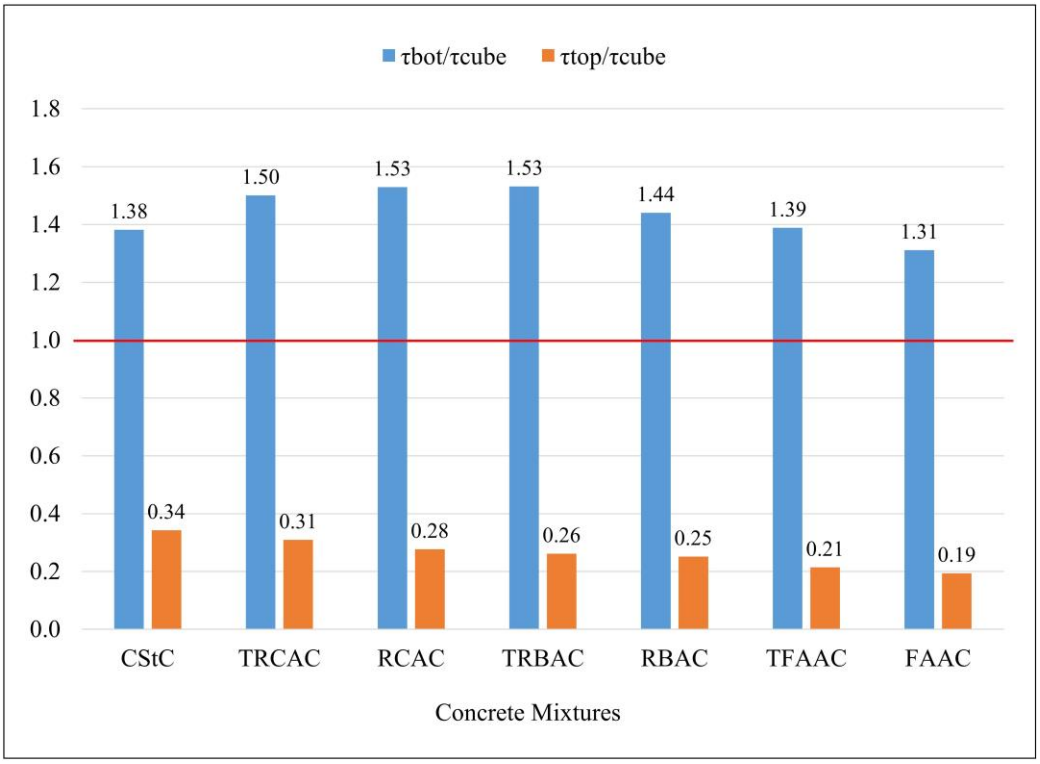

Figure 4.39. Effect of underlying and overlying concrete layers on bond strength.

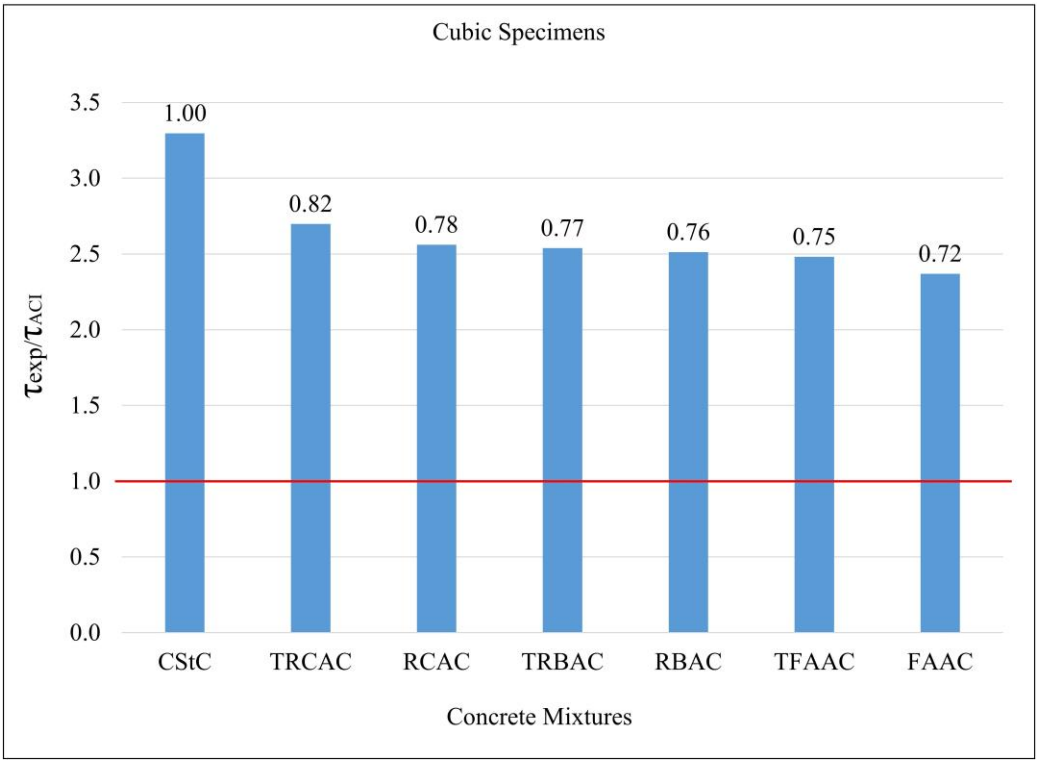

Figure 4.40. Bond length sufficiency for the rebars in cubic specimens.

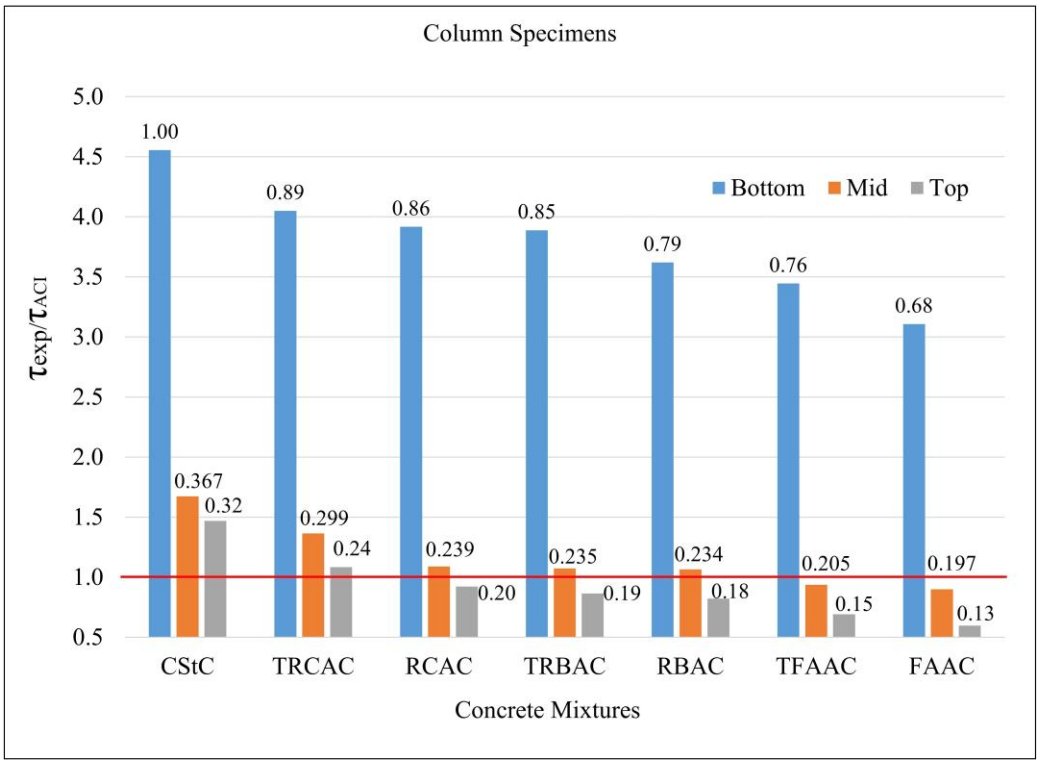

Figure 4.41. Bond length sufficiency for the rebars in column specimens.

4.3.7. Microstructural Investigations

Microstructural investigations were performed on samples taken from recycled aggregates and hardened concrete specimens to examine the effect of recycled aggregate treatment during the concrete mixing procedure with slag slurry on the mechanical properties of the recycled aggregate concrete.

4.3.7.1. ESEM/EDAX Observations. First, the crystal morphologies of the recycled fly ash aggregates (FAAs) produced in the laboratory were examined, and the presence of microstructural formations that would cause them to gain strength was investigated with reference to the findings of energy dispersive X-ray spectroscopy (EDAX) analyses and by using environmental scanning electron microscope (ESEM) pictures. As indicated in the previous studies [281]–[286], C-S-H gel formations from hydration and/or pozzolanic reaction emerged in regions having atomic ratios of Ca/Si in the range between 0.8 and 2.5. The regions of the matrix investigated in the scope of this study had a Ca/Si ratio in the range specified in the literature. Therefore, it can be declared that the C-S-H gels, which provide cement binding and strengthening properties, appeared to be in a form that surrounded the fly ash grains and joined them together, as seen in Figure 4.42. It was also observed that CH (calcium hydroxide) crystals were formed as thin hexagonal plates as reported by Neville [287] and Taylor [286] in the voids of the matrix and in the interface between C-S-H gels and fly ash grains. Furthermore, the ettringite needles (calcium sulfoaluminate) arose from the reaction between calcium aluminate in cement and sulfate compounds such as gypsum and pozzolanic admixture, as noticed by Mehta and Monteiro [288].

In addition, the effect of the surface treatment applied to the recycled aggregates was examined based on the microscopic observations shown in Figures 4.43 to 4.49. Accordingly, it can be said that slag grains (with a high Blaine fineness, 5253 cm^2/g) fill the voids and cracks on the surface of the aggregates and in the interfaces between the aggregates and the concrete matrix and also provide the formation of C-S-H that will increase the strength as a result of the pozzolanic reaction, thus ensuring that the interfaces, voids, and cracks take a more dense structural form.

4.3.7.2. XRD Analysis. Powder samples taken from the aggregate-matrix interfaces were

subjected to XRD analysis in order to determine the change in the microstructure of ITZs as a result of the aggregate surface treatment process. For this purpose, qualitative analysis was performed on the XRD data obtained to determine the crystalline phases and their mineralogical compositions in the samples. Then, quantitative analysis was carried out to find the percentages by mass of these crystalline phases on XRD patterns with the Rietveld refinement method using Maud software [260]. The refinement of the diffraction data was limited in an angular interval of 5-40° (in 2θ) since the most resolved peaks with the highest intensities existed in this range.

As a result of XRD analysis, the crystallographic phases contained in the samples and their compositions with the database codes are given in Table 4.17. These phases, their angles, and sample matching were given in Figures 4.50 to 4.52. As an example, the compatibility of the Maud model with XRD data for TFAAC was shown in Figure 4.53. The black dots and the red line represented the XRD data of TFAAC and the created model between 0 and 40°, respectively. The cloudy background was due to the amorphous phases (mostly C-S-H) in the matrix [289]. Considering the fact that the cement matrix has a complex microstructure and consists of many phases, it is seen that the model fits very well with the data. It has been observed that the compatibility of the relevant models and XRD data for all concrete mixtures is at an acceptable level.

Table 4.17. Crystallographic phases and compositions contained in the samples.

Phases	**Abbreviations**	**Compositions**	**Database Codes***
Quartz (1)	Q1	SiO_2	0006212
Quartz (2)	Q2	SiO_2	0015465
Calcite	C	$CaCO_3$	0000984
Clinochlore	C1	$Mg_6Al_4O_{10}(OH)_8$	0002740
Albite	A	$NaAlSi_3O_8$	0001285
Margarite	M	$CaAl_2Si_2Al_2O_{10}(OH)_2$	9000604
Portlandite	P	$Ca(OH)_2$	0000117
Ettringite	E	$Ca_6(Al(OH)_6)_2(SO_4)_3(H_2O)_{26}$	0017886
Belite	C2	Ca_2SiO_4	0020214
Alite	C3	Ca_3SiO_5	1540704

***** The American Mineralogist Crystal Structure Database.

The percentages by mass of the crystal phases contained in the samples are given in Table 4.18. Powder samples taken from the interfaces consist of fine aggregates used in the concrete production and cement matrix. However, most of the phases contained in the samples originated from the aggregate. Considering this fact, the change in the matrix should be taken into account in order to understand the effect of the treatment process on the microstructure. For this reason, the matrix was considered as a whole and Table 4.19 was obtained by keeping the ratios between the phases (portlandite, ettringite and others) constituting the matrix constant.

The amount of portlandite and ettringite from the matrix phases of the powder samples taken from the interfaces decreased in the concrete mixtures produced with recycled aggregates treated with slag slurry, as shown in Table 4.19. This can be explained by the formation of secondary hydration products by depleting the portlandite as a result of the pozzolanic activity of the slag. Similarly, considering that ettringite formation is dependent on the presence of portlandite, consumption of portlandite by a pozzolanic reaction explains the decrease in the amount of ettringite. These results confirm the findings obtained in the ESEM analysis.

Table 4.18. Phases (mass %) in the samples determined by the Rietveld refinement method.

Concrete Mixtures	**Aggregate**						**Matrix**		
	Quartz-1	**Quartz-2**	**Calcite**	**Clinochlore**	**Albite**	**Margarite**	**Portlandite**	**Ettringite**	**Others***
FAAC	29.7	0.5	19.3	15.0	20.2	3.1	2.2	1.6	8.3
TFAAC	13.7	1.1	36.6	5.9	24.3	4.5	1.2	0.1	12.7
RBAC	31.6	5.8	19.6	13.2	15.3	3.6	2.4	0.6	7.9
TRBAC	31.6	0.3	24.9	7.3	19.0	5.2	0.3	0.1	11.3
RCAC	25.4	1.5	32.3	9.1	17.1	3.3	2.5	1.0	8.0
TRCAC	17.5	2.4	28.3	7.5	16.0	5.1	3.1	0.8	19.5

*C_2S and C_3S

Table 4.19. Relative weight percentage by mass calculated for portlandite and ettringite in matrix.

Concrete Mixtures	**Matrix**		
	Portlandite	**Ettringite**	**Others**
FAAC	18.28	12.82	68.90
TFAAC	8.29	0.71	91.00
RBAC	21.91	5.59	72.50
TRBAC	2.57	0.86	96.57
RCAC	21.47	8.55	69.98
TRCAC	13.20	3.26	83.55

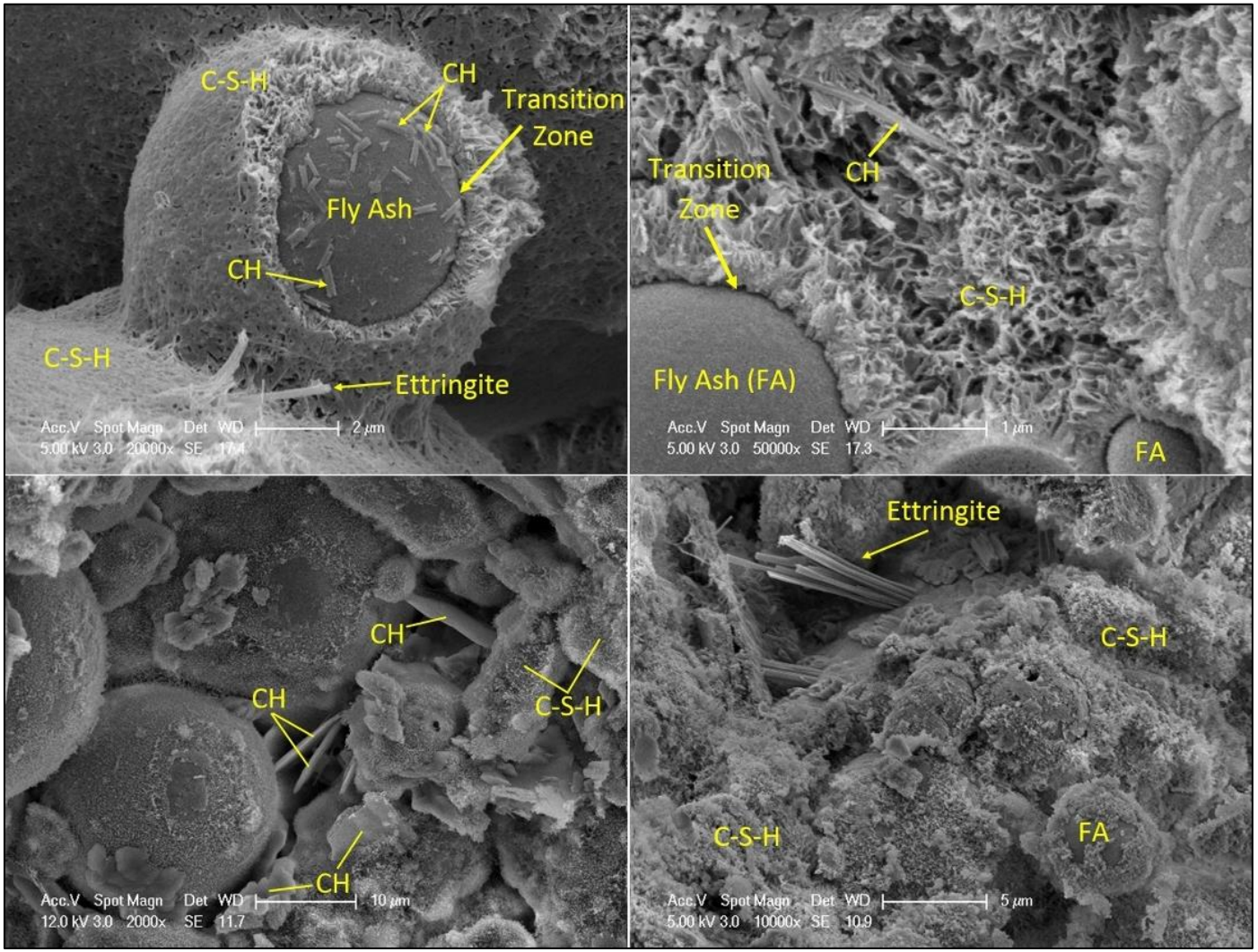

Figure 4.42. SEM observations showing the crystal morphology of FAA at different magnifications.

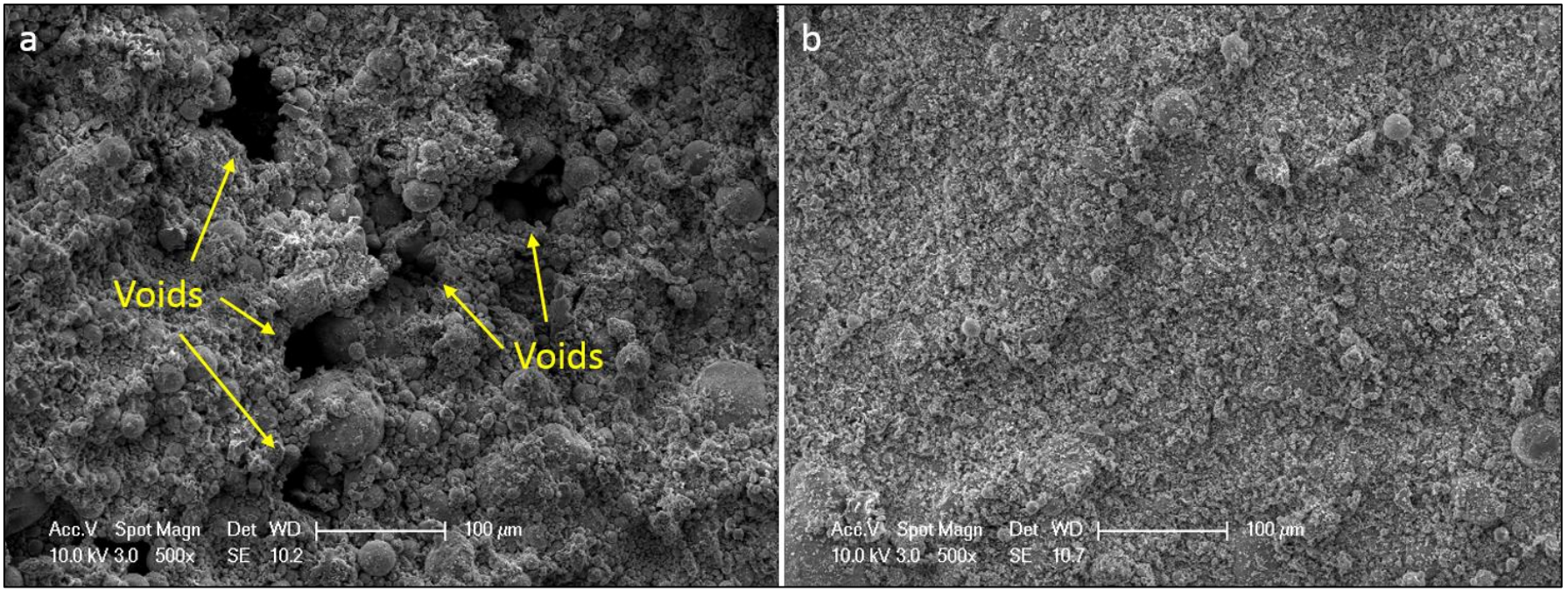

Figure 4.43. SEM observations; (a) FAAC, (b) TFAAC.

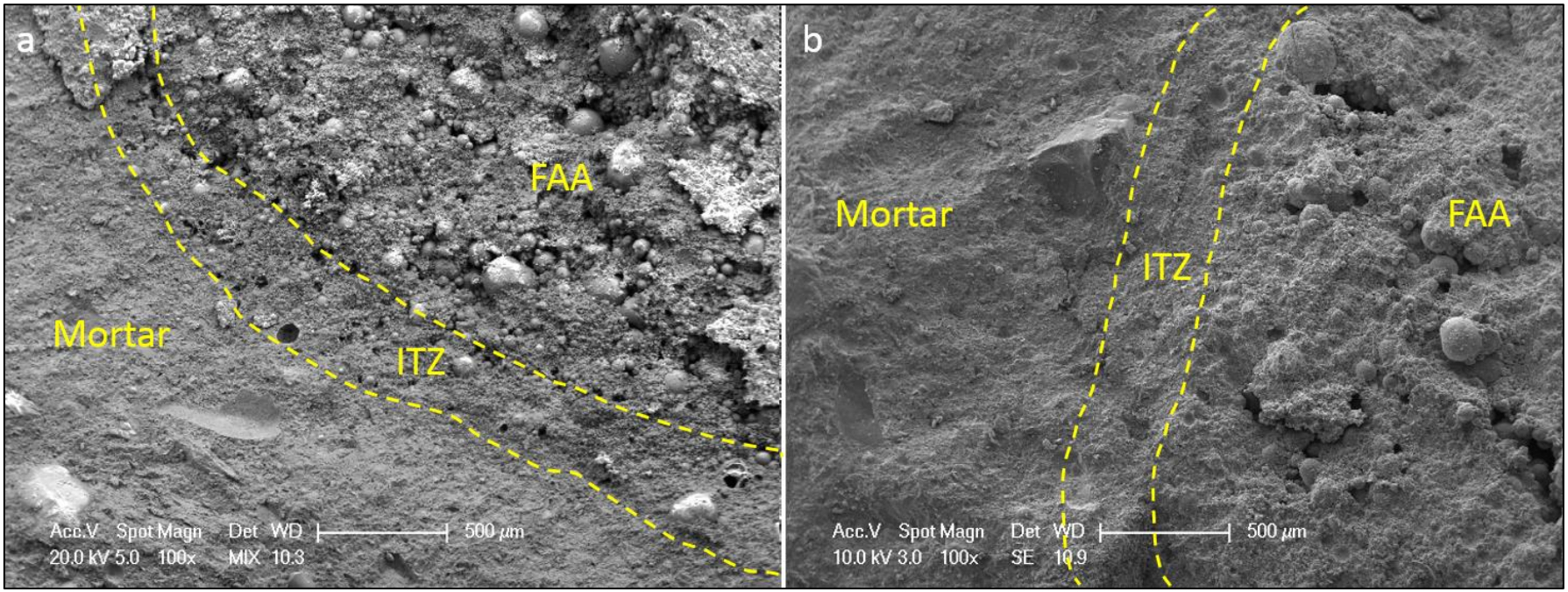

Figure 4.44. SEM observations; (a) FAAC, (b) TFAAC.

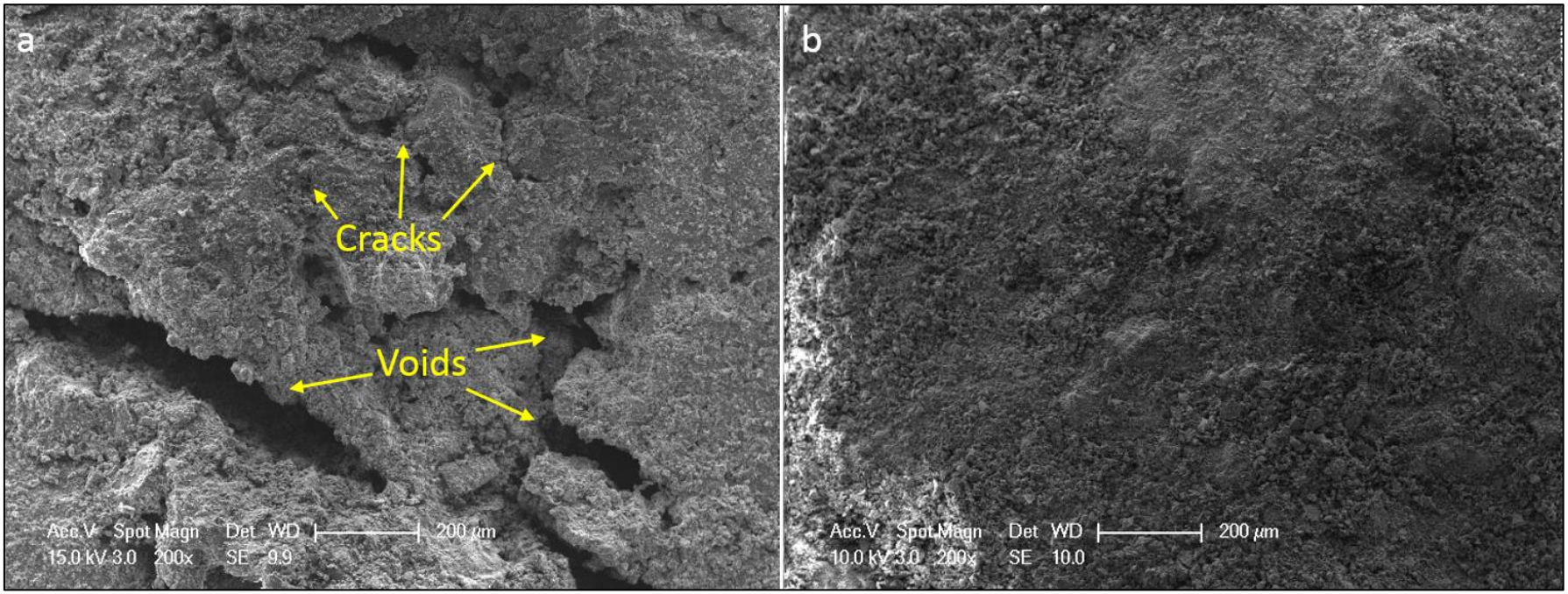

Figure 4.45. SEM observations; (a) RBAC, (b) TRBAC.

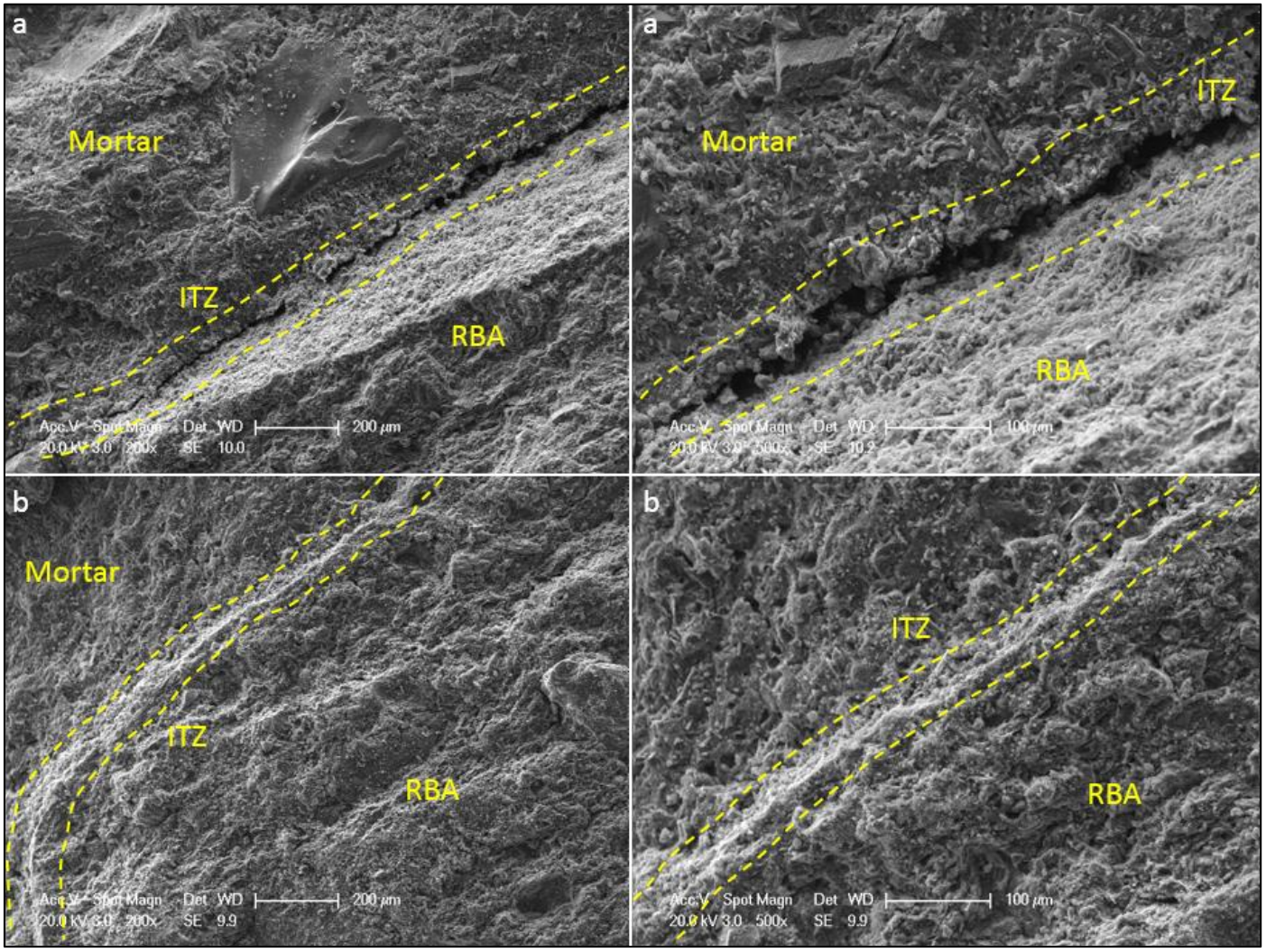

Figure 4.46. SEM observations; (a) RBAC, (b) TRBAC.

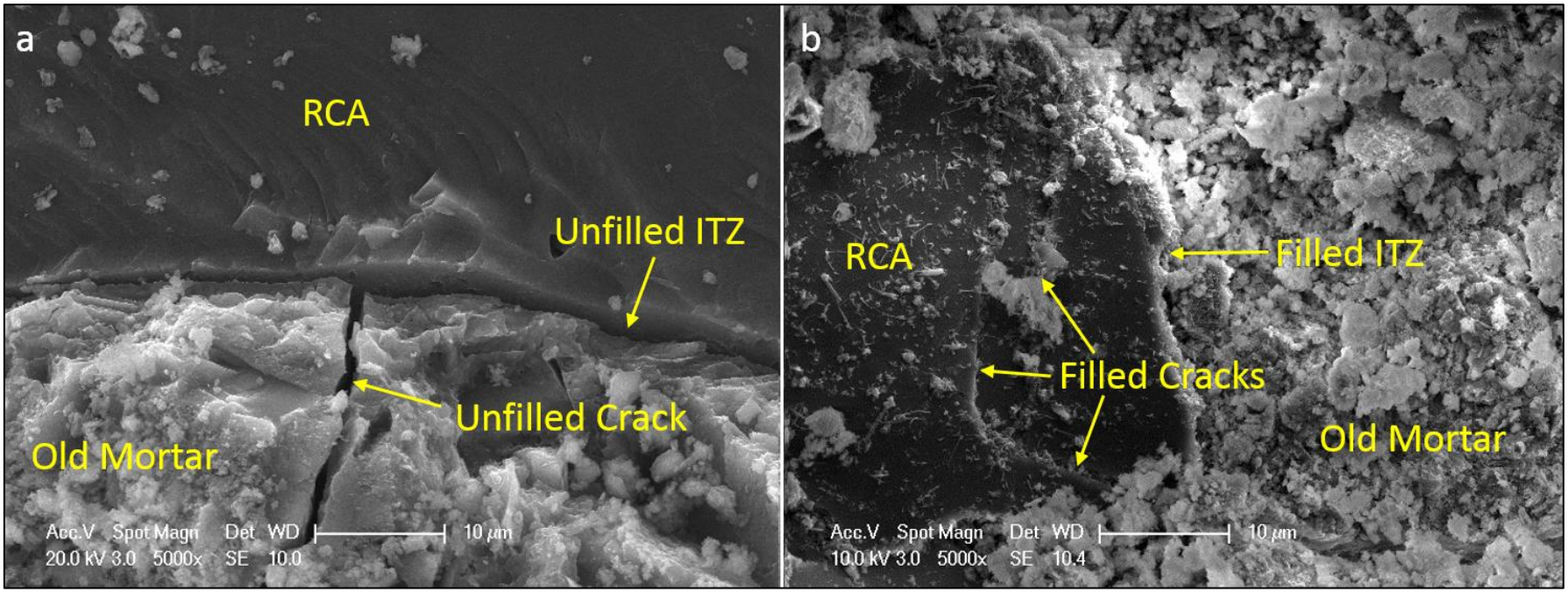

Figure 4.47. SEM observations; (a) RCAC, (b) TRCAC.

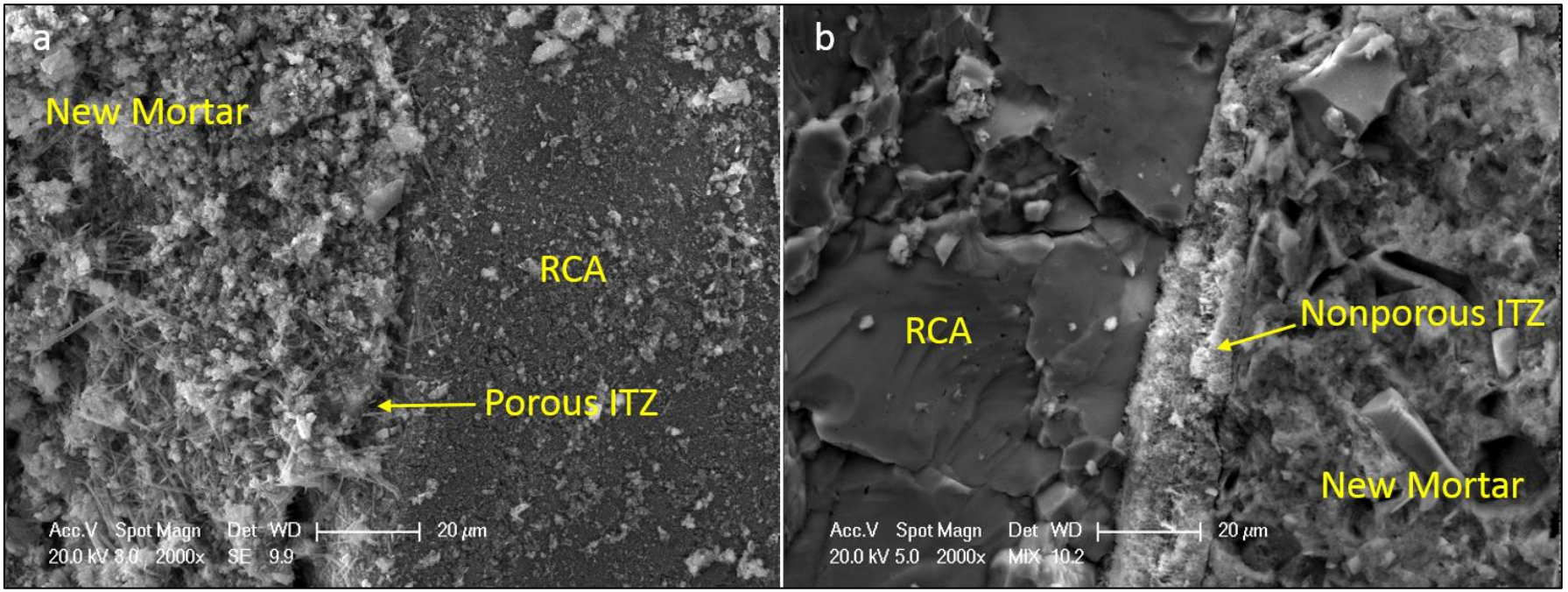

Figure 4.48. SEM observations; (a) RCAC, (b) TRCAC.

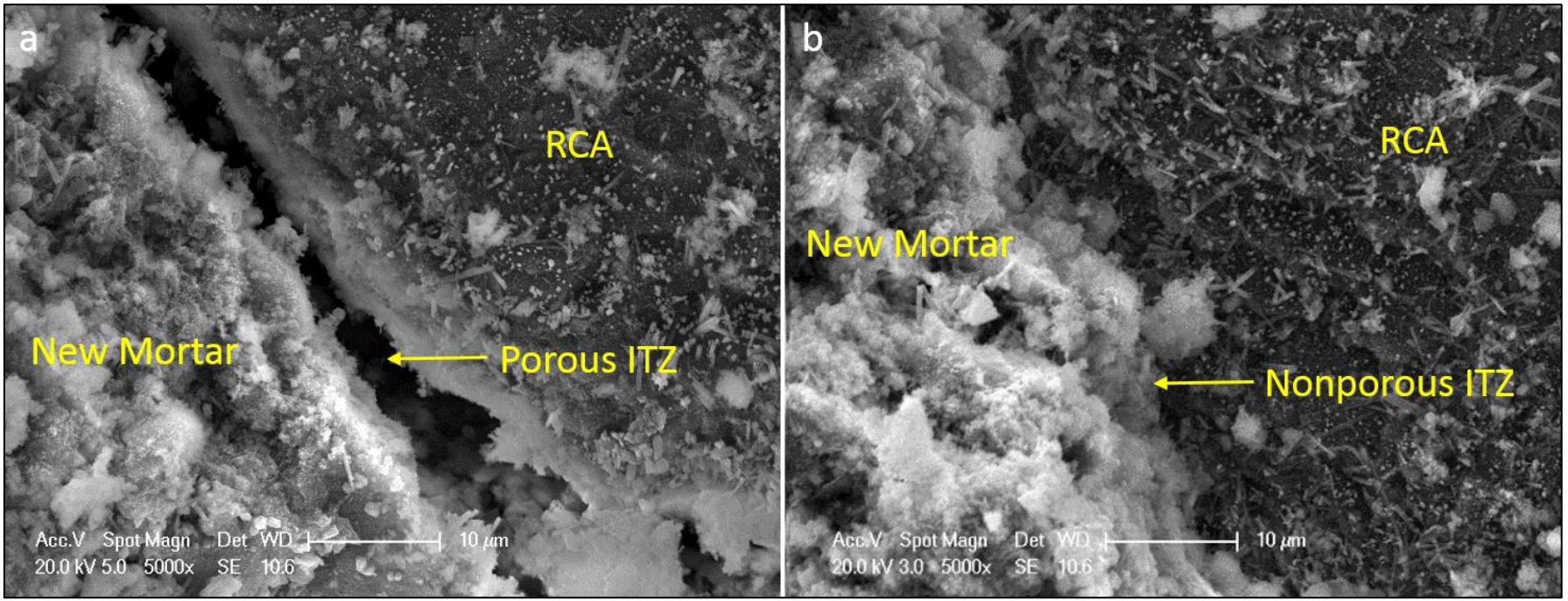

Figure 4.49. SEM observations; (a) RCAC, (b) TRCAC.

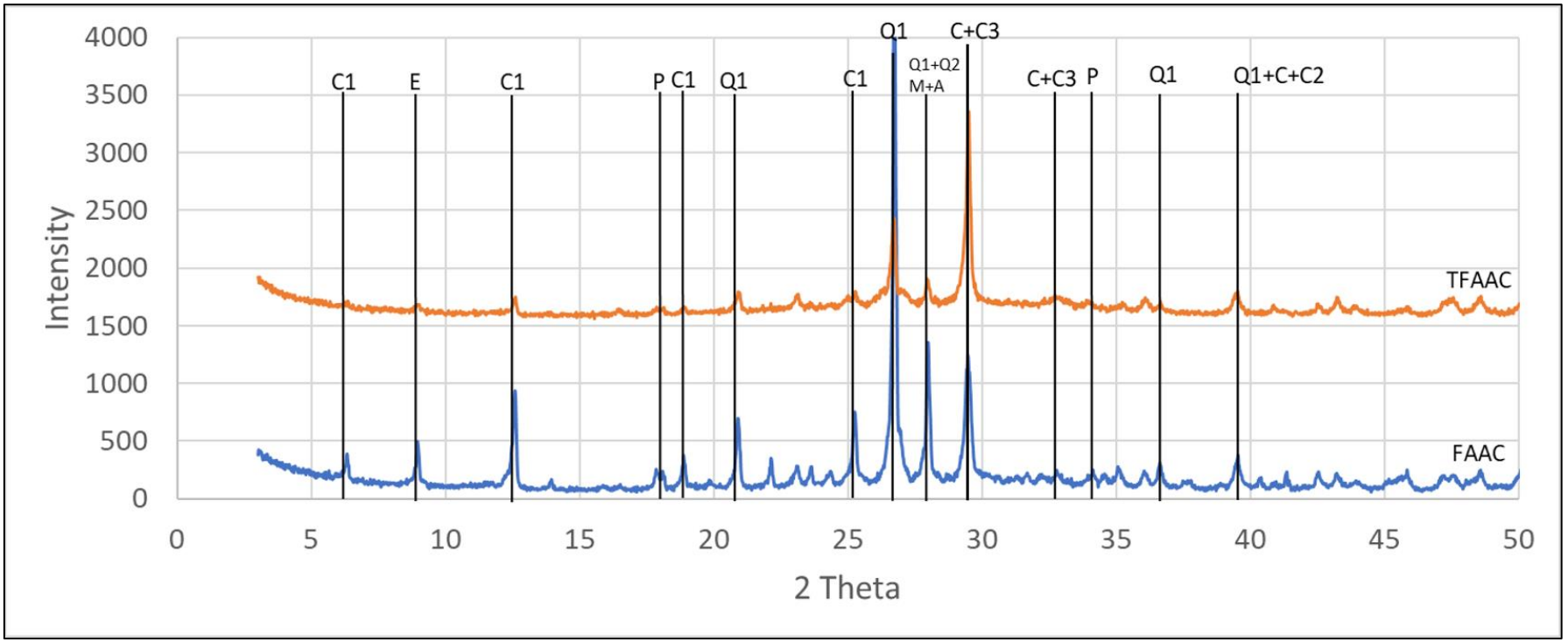

Figure 4.50. XRD patterns of samples taken from FAAC and TFAAC.

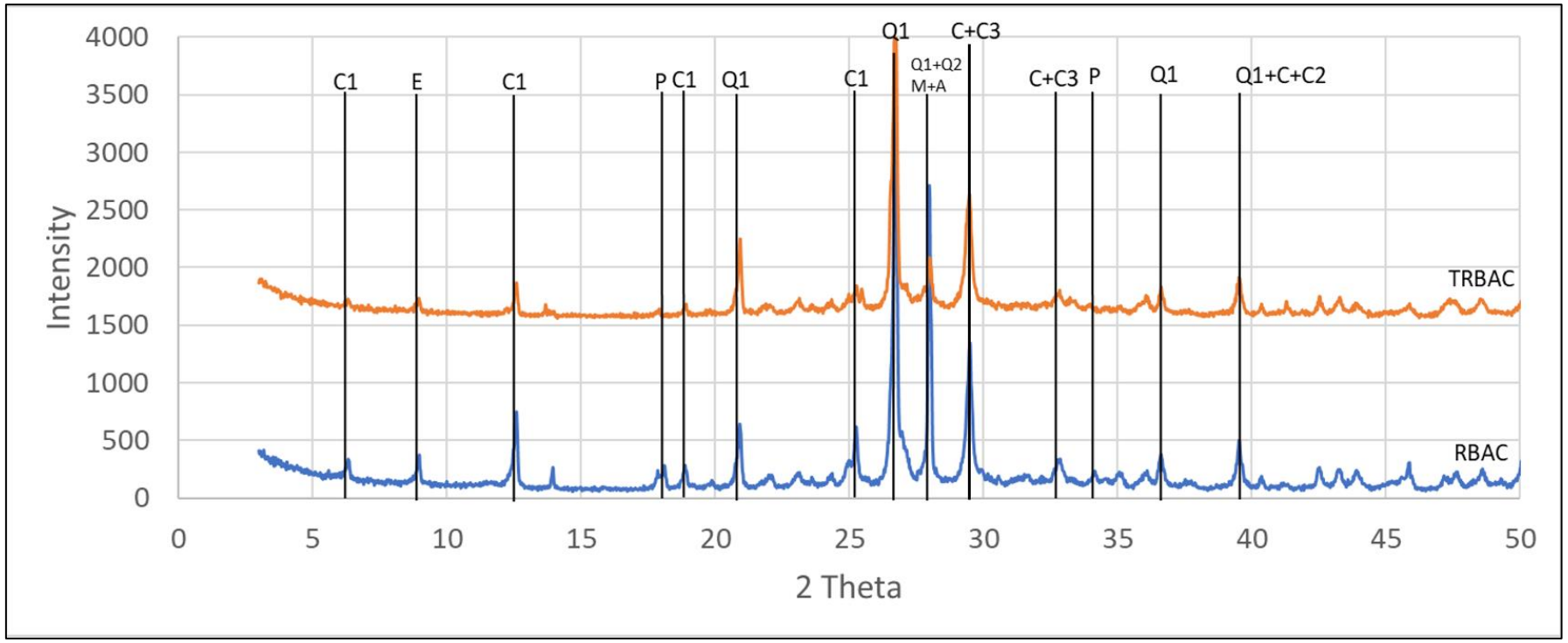

Figure 4.51. XRD patterns of samples taken from RBAC and TRBAC.

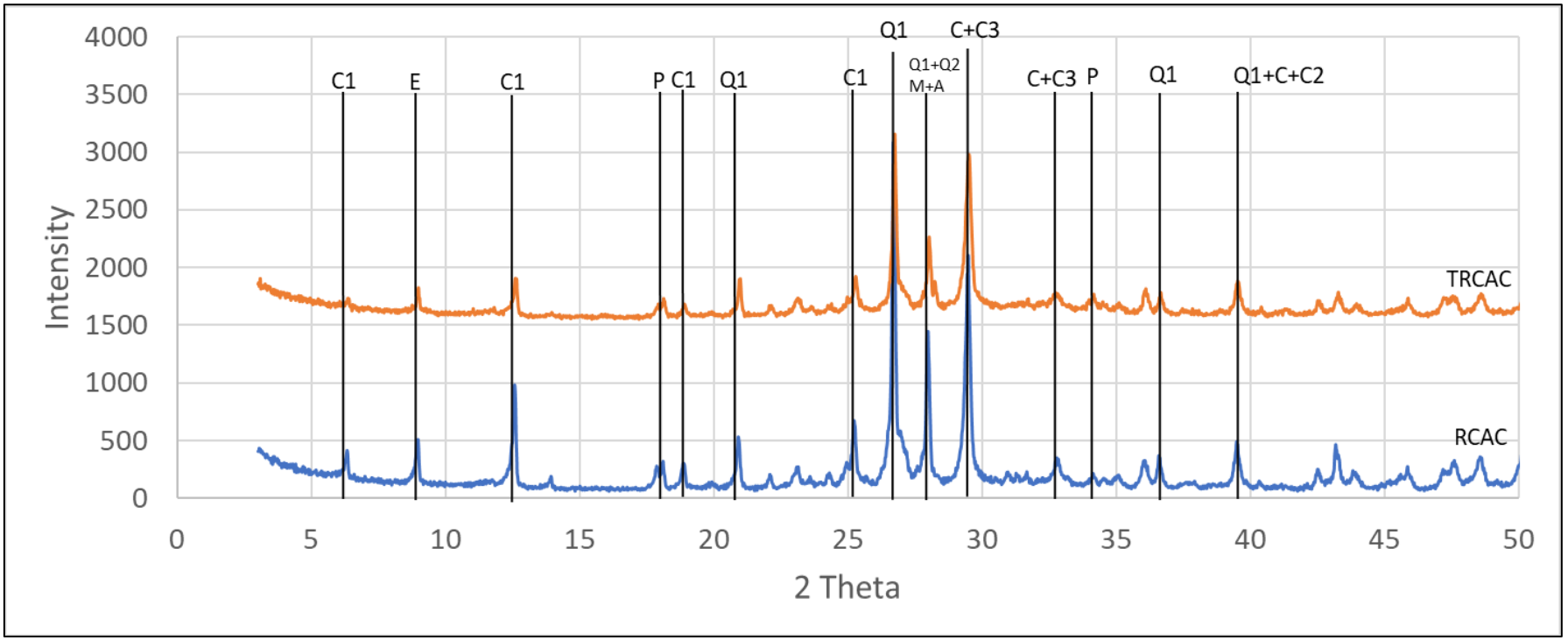

Figure 4.52. XRD patterns of samples taken from RCAC and TRCAC.

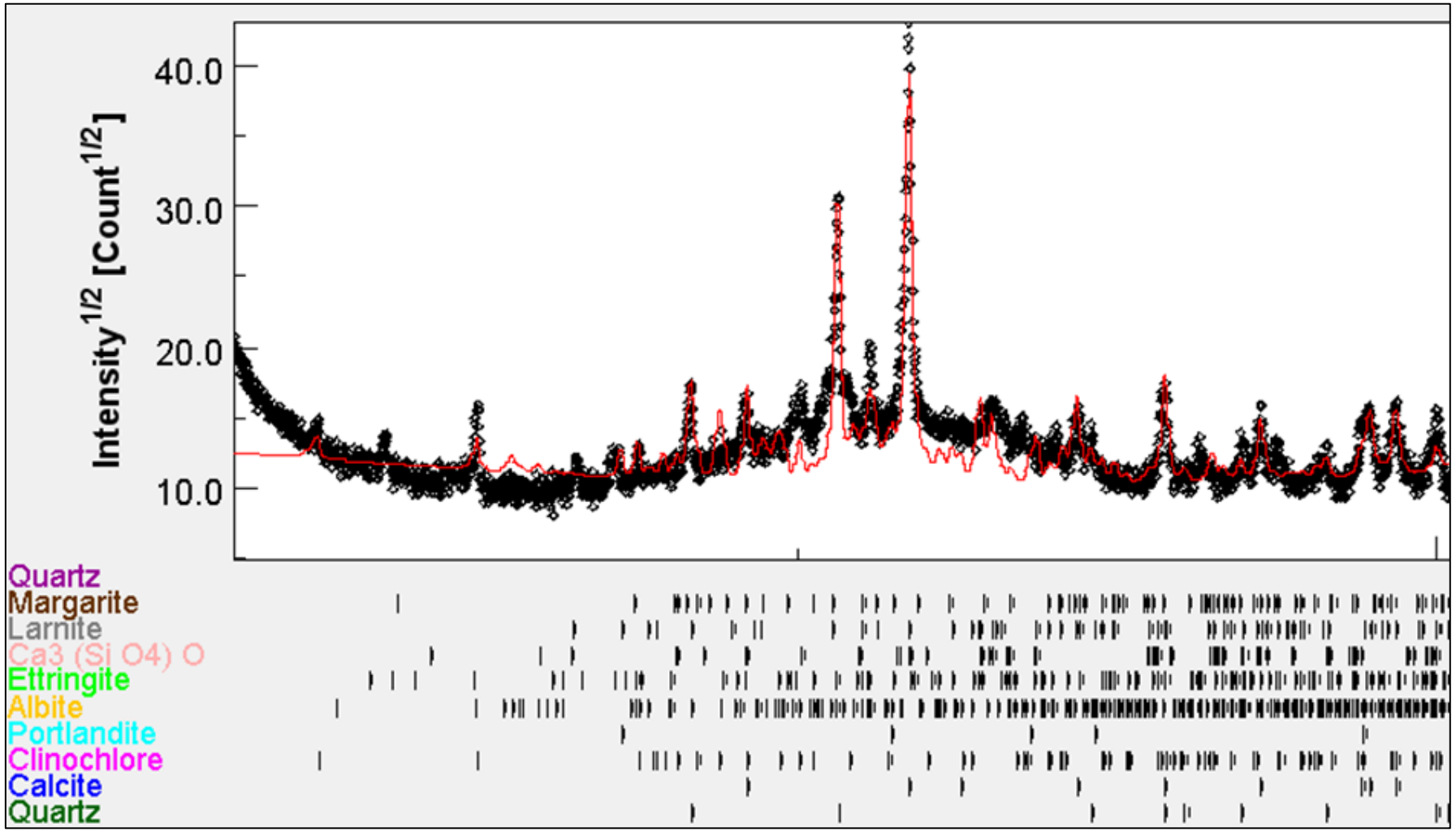

Figure 4.53. The compatibility of the MAUD model with XRD data for TFAAC (black dots=XRD data, red line=model).

5. SUMMARY AND CONCLUSIONS

In this study, the mechanical properties of sustainable concrete mixtures produced with different recycled aggregates were investigated. To produce sustainable concrete mixtures, three different recycled aggregates were used as coarse aggregates in total replacement, by volume, of crushed limestone. The crushed recycled brick aggregates (RBA) and recycled concrete aggregates (RCA) were obtained from an aggregate recycling plant of İSTAÇ (The İstanbul Environmental Protection and Waste Processing Corporation). Recycled fly ash aggregates (FAA) were produced through the cold-bonding agglomeration process under laboratory conditions. The physical properties of the coarse aggregates, such as unit weight, specific gravity, water absorption capacity, and flakiness index, were determined along with mechanical properties such as aggregate crushing and impact values. Six recycled aggregate concrete mixtures were produced by replacing both the No-I and No-II crushed stone coarse aggregates (CSt) in size fractions of 4-8mm and 8-16mm in diameter, respectively, in the control concrete with recycled aggregates, which were utilized as plain (RBA, RCA, FAA) and surface treated (TRBA, TRCA, TFAA) by the direct slurry method with GGBFS. The mechanical properties of concrete mixtures such as compressive strength (F_c), splitting tensile strength (F_t), modulus of elasticity (E_c), flexural strength (F_{net}), impact resistance, bond strength between the reinforcing bar and the concrete were identified according to the test instructions stipulated by the relevant standards, as well as fracture parameters such as fracture toughness (K_{IC}^{S}), critical crack-tip opening displacement ($CTOD_c$), fracture energy (GF) and the characteristic length (l_{ch}) of concrete mixtures. The correlation of aggregate crushing and impact values with the compressive strength and impact resistance of concrete mixtures produced with related coarse aggregates was also investigated. In addition, the relationship between the splitting tensile strength, static modulus of elasticity, and flexural strength with the compressive strength of the concrete mixtures was estimated with the equations constructed regarding the test results by using the simple regression analysis based on the least-squares method. And, the estimating equations obtained from the experimental results were compared with the prediction models given in different codes: TS500 [268], ACI 318M-05 [269], EN 1992-1-1 [270], CSA A23.3-04 [271], NZS 3101-1 [272], and ACI 363R-92 [273].

On the other hand, microstructural investigations were performed on samples taken from recycled aggregates and hardened concrete specimens to analyze the effect of recycled aggregate treatment during the concrete mixing procedure with slag slurry on the mechanical properties of the recycled aggregate concrete. For this purpose, pores, cracks, crystal structures, and morphological changes in aggregate particles and aggregate-matrix interfaces (ITZs) of untreated and treated concrete mixtures were monitored. Besides, the crystal morphologies of the recycled fly ash aggregates (FAAs) produced in the laboratory were examined, and the presence of microstructural formations that would cause them to gain strength was investigated with reference to the findings of energy dispersive X-ray spectroscopy (EDAX) analyses and by using environmental scanning electron microscope (ESEM) pictures.

XRD analyses were also performed on powder samples taken from aggregate-matrix interfaces in recycled aggregate concrete mixtures to examine the change in the microstructure of ITZs as a result of the aggregate surface treatment process. To do so, qualitative analysis was conducted on the XRD data obtained to determine the crystalline phases and their mineralogical compositions in the samples. Then, quantitative analysis was carried out to find the percentages by mass of these crystalline phases on XRD patterns with the Rietveld refinement method using Maud software. Finally, the results were interpreted considering the phase transformations expected as a result of the pozzolanic reaction.

Based on the results of experiments presented above, the following conclusions can be drawn:

- When the crystal morphologies of the recycled fly ash aggregates (FAAs) produced in the laboratory were examined, it was observed that products of hydration and/or pozzolanic reaction such as C-S-H gels, portlandite (calcium hydroxide) and ettringite (calcium sulfoaluminate) were formed.
- CSt had lower water absorption capacity and higher specific gravity compared to recycled aggregates that can be explained by the presence of old adhered mortar in RCA and the porous structure of RBA and FAA. However, with an increase in the size of recycled aggregates, the water absorption capacity of the recycled aggregates

decreased with fewer cracks and mostly non-interconnected closed pores, and they became denser.

- In terms of the flakiness index, the use of coarse aggregates (CSt, RCA, RBA, FAA) in concrete production has been found not to cause a problem with reference to the specified standard.
- Among the coarse aggregates, FAA had the highest ACV and AIV followed by RBA, RCA, and CSt. Since the increase in ACV and AIV indicates that the material is mechanically more defective, CSt is the most advantageous aggregate, while FAA is the most disadvantageous one in terms of ACV and AIV. In addition, each of these values has a negative correlation with the unit weight of the aggregates.
- Fresh concrete mixes were workable and cohesive, and segregation was not observed. When RCA, RBA, and FAA totally replaced CSt, the fresh unit weight of the concrete mixtures decreased in proportion to the unit weight of the recycled aggregates. However, there was no change in the fresh unit weight of TRCAC, TRBAC, and TFAAC due to the change in the concrete production process. Replacing the crushed stone coarse aggregate completely with recycled aggregates reduced the fresh density of the concrete by up to 17%, while compressive strength values conformed to the limitation for structural use.
- It has been observed that the correlation between the compressive strength of the concrete mixtures and the crushing values of the corresponding coarse aggregates (ACV, %) was negative. There was a similar relationship between the impact resistance of the concrete mixtures and the impact values of the coarse aggregates (AIV, %), both with a sufficiently high coefficient of determination (R^2).
- As expected, the relationship between compressive strength and fresh unit weight of concrete mixtures was positive. However, the significance level of the linear relationship established between compressive strength and unit weight was slightly higher for concrete mixtures produced with recycled aggregates treated with slag slurry.
- In terms of the mechanical properties and fracture parameters of the concrete mixtures investigated in the scope of this study, CStC is the most favourable one followed by TRCAC, RCAC, TRBAC, RBAC, TFAAC and FAAC. Treating the recycled aggregates by the direct slurry method improved the mechanical properties and fracture parameters of recycled aggregate concrete mixtures with increased statistical

reliability. For example, treating recycled aggregates with slag slurry not only increased the bond strength between the reinforcement bars and the concrete mixtures, but also decreased the minimum required anchorage length for the reinforcement to carry the load. Even if the improvement in the mechanical properties and fracture parameters of the recycled concrete mixtures is not at significant levels, it can be said that the gains achieved are remarkable considering that the recycled aggregates are treated only by changing the concrete mixing method.

- ESEM and EDAX investigations have shown that secondary hydration products were formed as a result of the pozzolanic activity of fine slag grains, which penetrated and filled the voids and cracks on the surface of the treated recycled aggregates and in the interfaces between these aggregates and the concrete matrix, improving the mechanical properties and fracture parameters of the recycled concrete mixtures.
- With respect to the XRD analyses, it can also be said that treatment of recycled aggregates with slag slurry improved the mechanical properties and fracture parameters of the recycled concrete mixtures due to the formation of secondary hydration products at the interface between the treated recycled aggregates and the concrete matrix as a result of the pozzolanic activity of the slag. The findings obtained from the XRD analyses confirm the results of the ESEM and EDAX investigations.
- The results for the relationship between the static modulus of elasticity and compressive strength of the concrete mixtures demonstrated that the models proposed by TS 500 and EN 1992-1-1 were in good agreement with the relationship obtained from the experimental results for control concrete (CStC), while there were underestimations for the models of ACI 318M-05, CSA A23.3-04 and NZS 3101-1. For RCAC and TRCAC concrete mixtures, the ACI 318M-05 estimation for the static modulus of elasticity was close to the actual test result with slight overestimations. However, the expressions of TS 500 and EN 1992-1-1 gave considerable overestimations, while relatively lower underestimations obtained by the models of CSA A23.3-04 and NZS 3101-1. For RBAC and TRBAC, the expression recommended by CSA A23.3-04 was in good agreement with the relationship obtained from the experimental results. However, there was a considerable overestimation for the models of TS 500 and EN 1992-1-1, while the expressions of ACI 318M-05 and NZS 3101-1 gave relatively lower overestimations for the static modulus of elasticity. For FAAC and TFAAC, the mean modulus of elasticity values of CSA A23.3-04 are

very close to the experimental means with slight overestimations. However, the prediction model of TS 500 gave a considerable overestimation while relatively lower overestimations obtained by the models of ACI 318M-05, EN 1992-1-1 and NZS 3101-1.

- The results for the relationship between the splitting tensile strength and compressive strength of the concrete mixtures showed that the models proposed by ACI 363R-92 and EN 1992-1-1 were in good agreement with the relationship obtained from the experimental results for control concrete (CStC), while there was an underestimation for both the models of TS 500 and NZS 3101-1 and an overestimation for the model of CSA A23.3-04. For RCAC and TRCAC, the estimation of NZS 3101-1 for the splitting tensile strength was close to the actual test results with slight overestimations. However, the expressions of ACI 363R-92 and CSA A23.3-04 gave considerable overestimations while relatively lower underestimations were obtained by the models of TS 500 and EN 1992-1-1. For RBA and TRBA, the mean splitting tensile strength values of TS500 were close to the experimental means with slight overestimations. However, there was a considerable overestimation for the prediction models of ACI 363R-92 and CSA A23.3-04 and a relatively lower overestimation for NZS 3101-1, while the expression of EN 1992-1-1 gave an underestimation for the splitting tensile strength. For FAAC and TFAAC, the expression recommended by TS 500 was in good agreement with the relationship obtained from the experimental results with relatively moderate overestimations. However, the models of ACI 363R-92, CSA A23.3-04, and NZS 3101-1 gave considerable overestimations, while relatively lower underestimations obtained by the expression of EN 1992-1-1.
- The results for the relation between the flexural strength and compressive strength of the concrete mixtures indicated that the model proposed by ACI 363R-92 was in good agreement with the relationship obtained from the experimental results for CStC with relatively lower underestimation, while there were serious underestimations for the models of TS500, EN 1992-1-1, CSA A23.3-04, and NZS 3101-1. On the other hand, the expression recommended by NZS 3101-1 had the compliance with the relationship obtained from the experimental results for RBAC, TRBAC, RCAC, and TRCAC, however, the expressions of TS 500, EN 1992-1-1 and CSA A23.3-04 gave considerable underestimations, while a significant overestimation obtained by the model of ACI 363R-92. For FAAC and TFAAC, the mean flexural strength values of

EN 1992-1-1 were super close to the experimental means. However, there was a considerable overestimation for the prediction models of ACI 363R-92 and NZS 3101-1 and a relatively lower overestimation for TS500, while the expression of CSA A23.3-04 gave a relatively lower underestimation for flexural strength.

After briefly describing the findings of this study, the following recommendations can be provided for future work.

- Although the impact resistance of recycled aggregate concrete mixtures increased with the treatment of recycled aggregates, it was seen that increasing the number of specimens tested would be beneficial, since the statistical variation in the results obtained by the drop-weight impact test was higher compared to other mechanical properties.
- To increase the improvement in the mechanical properties and fracture parameters of recycled aggregate concrete mixtures, a combination of different treatment methods investigated in the literature [5], [9], [45], [49], [59], [63], [67], [69], [71], [117], [128], [131], [132], [290]–[292] can be employed on recycled aggregates. In terms of RCA, for instance, mechanical grinding and/or pre-soaking in acid solution for removing of adhered old mortar can be utilized before a multi-stage mixing method with a puzzolanic slurry. However, it should be considered that methods to remove old mortar attached to recycled concrete aggregates are generally cost-intensive and time-consuming, with secondary environmental impacts. For FAA, on the other hand, a multi-stage mixing method with a puzzolanic slurry can be applied following the addition of polypropylene fibers and/or tire chips into recycled fly ash pellets during agglomeration, which has been introduced as an alternative treatment method for recycled fly ash aggregates in the literature [132].

REFERENCES

1. Akhtar, A., and A. K. Sarmah, "Construction and Demolition Waste Generation and Properties of Recycled Aggregate Concrete: A Global Perspective", *Journal of Cleaner Production*, Vol. 186, pp. 262-281, 2018.

2. Poon, C. S., Z. H. Shui, and L. Lam, "Effect of Microstructure of ITZ on Compressive Strength of Concrete Prepared with Recycled Aggregates", *Construction and Building Materials*, Vol. 18, No. 6, pp. 461-468, 2004.

3. Debieb, F., and S. Kenai, "The Use of Coarse and Fine Crushed Bricks as Aggregate in Concrete", *Construction and Building Materials*, Vol. 22, No. 5, pp. 886-893, 2008.

4. Marinković, S., V. Radonjanin, M. Malešev, and I. Ignjatović, "Comparative Environmental Assessment of Natural and Recycled Aggregate Concrete", *Waste Management*, Vol. 30, No. 11, pp. 2255-2264, 2010.

5. Xuan, D., B. Zhan, and C. S. Poon, "Assessment of Mechanical Properties of Concrete Incorporating Carbonated Recycled Concrete Aggregates", *Cement and Concrete Composites*, Vol. 65, pp. 67-74, 2016.

6. Kisku, N., H. Joshi, M. Ansari, S. K. Panda, S. Nayak, and S. C. Dutta, "A Critical Review and Assessment for Usage of Recycled Aggregate as Sustainable Construction Material", *Construction and Building Materials*, Vol. 131, pp. 721-740, 2017.

7. Xiao, J., C. Wang, T. Ding, and A. Akbarnezhad, "A Recycled Aggregate Concrete High-Rise Building: Structural Performance and Embodied Carbon Footprint", *Journal of Cleaner Production*, Vol. 199, pp. 868-881, 2018.

8. Zhang, L.W., A. O. Sojobi, V. K. R. Kodur, and K. M. Liew, "Effective Utilization and Recycling of Mixed Recycled Aggregates for a Greener Environment", *Journal of Cleaner Production*, Vol. 236, p. 117600, 2019.

9. Shi, C., Y. Li, J. Zhang, W. Li, L. Chong, and Z. Xie, "Performance Enhancement of Recycled Concrete Aggregate - A Review", *Journal of Cleaner Production*, Vol. 112, pp. 466-472, 2016.

10. Ozturk, O., H. Yildirim, N. Ozyurt, and T. Ozturan, "Evaluation of Mechanical Properties and Structural Behaviour of Concrete Pavements Produced with Virgin and Recycled Aggregates: An Experimental and Numerical Study", *International Journal of Pavement Engineering*, Vol. 23, No. 14, pp. 5239-5253, 2022.

11. Shi, X., M. M. Mirsayar, A. Mukhopadhyay, and D. Zollinger, "Characterization of Two-Parameter Fracture Properties of Portland Cement Concrete Containing Reclaimed Asphalt Pavement Aggregates by Semicircular Bending Specimens", *Cement and Concrete Composites*, Vol. 95, pp. 56-69, 2019.

12. Rao, A., K. N. Jha, and S. Misra, "Use of Aggregates from Recycled Construction and Demolition Waste in Concrete", *Resources, Conservation and Recycling*, Vol. 50, No. 1, pp. 71-81, 2007.

13. Zheng, C., C. Lou, G. Du, X. Li, Z. Liu, and L. Li, "Mechanical Properties of Recycled Concrete with Demolished Waste Concrete Aggregate and Clay Brick Aggregate", *Results in Physics*, Vol. 9, pp. 1317-1322, 2018.

14. Mi, R., G. Pan, K. M. Liew, and T. Kuang, "Utilizing Recycled Aggregate Concrete in Sustainable Construction for a Required Compressive Strength Ratio", *Journal of Cleaner Production*, Vol. 276, 2020.

15. Zhang, J., Y. Yan, Z. Hu, X. Fan, and Y. Zheng, "Utilization of Low-Grade Pyrite Cinder for Synthesis of Microwave Heating Ceramics and Their Microwave Deicing Performance in Dense-Graded Asphalt Mixtures", *Journal of Cleaner Production*, Vol. 170, pp. 486-495, 2018.

16. Nagataki, S., A. Gokce, T. Saeki, and M. Hisada, "Assessment of Recycling Process Induced Damage Sensitivity of Recycled Concrete Aggregates", *Cement and Concrete*

Research, Vol. 34, No. 6, pp. 965-971, 2004.

17. Ann, K. Y., H. Y. Moon, Y. B. Kim, and J. Ryou, "Durability of Recycled Aggregate Concrete Using Pozzolanic Materials", *Waste Management*, Vol. 28, No. 6, pp. 993-999, 2008.

18. Hu, J., Z. Wang, and Y. Kim, "Feasibility Study of Using Fine Recycled Concrete Aggregate in Producing Self-Consolidation Concrete", *Journal of Sustainable Cement-Based Materials*, Vol. 2, No. 1, pp. 20-34, 2013.

19. Munir, M. J., S. M. S. Kazmi, Y. F. Wu, A. Hanif, and M. U. A. Khan, "Thermally Efficient Fired Clay Bricks Incorporating Waste Marble Sludge: An Industrial-Scale Study", *Journal of Cleaner Production*, Vol. 174, pp. 1122-1135, 2018.

20. Tam, V. W. Y., A. Butera, and K. N. Le, "Carbon-Conditioned Recycled Aggregate in Concrete Production", *Journal of Cleaner Production*, Vol. 133, pp. 672-680, 2016.

21. Ryu, J. S., "Improvement on Strength and Impermeability of Recycled Concrete Made from Crushed Concrete Coarse Aggregate", *Journal of Materials Science Letters*, Vol. 21, pp. 1565-1567, 2002.

22. Martínez-Lage, I., P. Vázquez-Burgo, and M. Velay-Lizancos, "Sustainability Evaluation of Concretes with Mixed Recycled Aggregate Based on Holistic Approach: Technical, Economic and Environmental Analysis", *Waste Management*, Vol. 104, pp. 9-19, 2020.

23. Wong, C. L., K. H. Mo, S. P. Yap, U. J. Alengaram, and T. C. Ling, "Potential Use of Brick Waste as Alternate Concrete-Making Materials: A Review", *Journal of Cleaner Production*, Vol. 195, pp. 226-239, 2018.

24. Wang, B., L. Yan, Q. Fu, and B. Kasal, "A Comprehensive Review on Recycled Aggregate and Recycled Aggregate Concrete", *Resources, Conservation and Recycling*, Vol. 171, p. 105565, 2021.

25. Mueller, A., S. N. Sokolova, and V. I. Vereshagin, “Characteristics of Lightweight Aggregates from Primary and Recycled Raw Materials”, *Construction and Building Materials*, Vol. 22, No. 4, pp. 703-712, 2008.

26. Zhang, S., P. He, and L. Niu, “Mechanical Properties and Permeability of Fiber-Reinforced Concrete with Recycled Aggregate Made from Waste Clay Brick”, *Journal of Cleaner Production*, Vol. 268, p.121690, 2020.

27. Rashid, K., M. U. Rehman, J. de Brito, and H. Ghafoor, “Multi-Criteria Optimization of Recycled Aggregate Concrete Mixes”, *Journal of Cleaner Production*, Vol. 276, p.124316, 2020.

28. Tam, V. W. Y., C. M. Tam, and K. N. Le, “Removal of Cement Mortar Remains from Recycled Aggregate Using Pre-Soaking Approaches”, *Resources, Conservation and Recycling*, Vol. 50, No. 1, pp. 82-101, 2007.

29. Ismail, S., and M. Ramli, “Engineering Properties of Treated Recycled Concrete Aggregate (RCA) for Structural Applications”, *Construction and Building Materials*, Vol. 44, pp. 464-476, 2013.

30. Kim, Y., A. Hanif, S. M. S. Kazmi, M. J. Munir, and C. Park, “Properties Enhancement of Recycled Aggregate Concrete Through Pretreatment of Coarse Aggregates – Comparative Assessment of Assorted Techniques”, *Journal of Cleaner Production*, Vol. 191, pp. 339-349, 2018.

31. Pawluczuk, E., K. Kalinowska-Wichrowska, M. Bołtryk, J. R. Jiménez, and J. M. Fernández, “The Influence of Heat and Mechanical Treatment of Concrete Rubble on the Properties of Recycled Aggregate Concrete”, *Materials*, Vol. 12, No. 3, p. 367, 2019.

32. Purushothaman, R., R. R. Amirthavalli, and L. Karan, “Influence of Treatment Methods on the Strength and Performance Characteristics of Recycled Aggregate Concrete”, *Journal of Materials in Civil Engineering*, Vol. 27, No. 5, p. 04014168,

2014.

33. Babu, V. S., A. K. Mullick, K. K. Jain, and P. K. Singh, "Strength and Durability Characteristics of High-Strength Concrete with Recycled Aggregate-Influence of Processing", *Journal of Sustainable Cement-Based Materials*, Vol. 4, No. 1, pp. 54-71, 2014.

34. Katz, A., "Treatments for the Improvement of Recycled Aggregate", *Journal of Materials in Civil Engineering*, Vol. 16, No. 6, pp. 597-603, 2004.

35. Pandurangan, K., A. Dayanithy, and S. Om Prakash, "Influence of Treatment Methods on the Bond Strength of Recycled Aggregate Concrete", *Construction and Building Materials*, Vol. 120, pp. 212-221, 2016.

36. Saravanakumar, P., K. Abhiram, and B. Manoj, "Properties of Treated Recycled Aggregates and Its Influence on Concrete Strength Characteristics", *Construction and Building Materials*, Vol. 111, pp. 611-617, 2016.

37. Dilbas, H., Ö. Çakır, and H. Yıldırım, "An Experimental Investigation on Fracture Parameters of Recycled Aggregate Concrete with Optimized Ball Milling Method", *Construction and Building Materials*, Vol. 252, p. 119118, 2020.

38. Kazemian, F., H. Rooholamini, and A. Hassani, "Mechanical and Fracture Properties of Concrete Containing Treated and Untreated Recycled Concrete Aggregates", *Construction and Building Materials*, Vol. 209, pp. 690-700, 2019.

39. Çakır, Ö., and H. Dilbas, "Durability Properties of Treated Recycled Aggregate Concrete: Effect of Optimized Ball Mill Method", *Construction and Building Materials*, Vol. 268, p.121776, 2021.

40. Ismail, S., and M. Ramli, "Mechanical Strength and Drying Shrinkage Properties of Concrete Containing Treated Coarse Recycled Concrete Aggregates", *Construction and Building Materials*, Vol. 68, pp. 726-739, 2014.

41. Güneyisi, E., M. Gesoğlu, Z. Algin, and H. Yazici, "Effect of Surface Treatment Methods on the Properties of Self-Compacting Concrete with Recycled Aggregates", *Construction and Building Materials*, Vol. 64, pp. 172-183, 2014.

42. Verma, A., V. S. Babu, and S. Arunachalam, "Influence of Modified Two-Stage Mixing Approaches on Recycled Aggregate Treated with A Hybrid Method of Treatment", *Australian Journal of Structural Engineering*, Vol. 23, No. 3, pp. 230-253, 2022.

43. Tsujino, M., T. Noguchi, M. Tamura, M. Kanematsu, and I. Maruyama, "Application of Conventionally Recycled Coarse Aggregate to Concrete Structure by Surface Modification Treatment", *Journal of Advanced Concrete Technology*, Vol. 5, No. 1, pp. 13-25, 2007.

44. Kou, S. C., and C. S. Poon, "Properties of Concrete Prepared with PVA-Impregnated Recycled Concrete Aggregates", *Cement and Concrete Composites*, Vol. 32, No. 8, pp. 649-654, 2010.

45. Shi, C., Z. Wu, Z. Cao, T. C. Ling, and J. Zheng, "Performance of Mortar Prepared with Recycled Concrete Aggregate Enhanced by CO_2 and Pozzolan Slurry", *Cement and Concrete Composites*, Vol. 86, pp. 130-138, 2018.

46. Yang, J., W. M. Shaban, K. Elbaz, B. S. Thomas, J. Xie, and L. Li, "Properties of Concrete Containing Strengthened Crushed Brick Aggregate by Pozzolan Slurry", *Construction and Building Materials*, Vol. 247, p. 118612, 2020.

47. Kazemian, F., H. Rooholamini, and A. Hassani, "Mechanical and Fracture Properties of Concrete Containing Treated and Untreated Recycled Concrete Aggregates", *Construction and Building Materials*, Vol. 209, pp. 690-700, 2019.

48. Spaeth, V., and A. D. Tegguer, "Improvement of Recycled Concrete Aggregate Properties by Polymer Treatments", *International Journal of Sustainable Built Environment*, Vol. 2, No. 2, pp. 143-152, 2013.

49. Shaban, W. M., K. Elbaz, J. Yang, B. S. Thomas, X. Shen, L. Li, Y. Du, J. Xie, and L. Li, "Effect of Pozzolan Slurries on Recycled Aggregate Concrete: Mechanical and Durability Performance", *Construction and Building Materials*, Vol. 276, p.121940, 2021.

50. Shaban, W. M., J. Yang, H. Su, Q. Liu, D. C.W. Tsang, L. Wang, J. Xie, and L. Li, "Properties of Recycled Concrete Aggregates Strengthened by Different Types of Pozzolan Slurry", *Construction and Building Materials*, Vol. 216, pp. 632-647, 2019.

51. Velardo, P., I. F. Sáez del Bosque, A. Matías, M. I. Sánchez de Rojas, and C. Medina, "Properties of Concretes Bearing Mixed Recycled Aggregate with Polymer-Modified Surfaces", *Journal of Building Engineering*, Vol. 38, p.102211, 2021.

52. Liang, Y., Z. Ye, F. Vernerey, and Y. Xi, "Development of Processing Methods to Improve Strength of Concrete with 100% Recycled Coarse Aggregate", *Journal of Materials in Civil Engineering*, Vol. 27, No. 5, pp. 1-9, 2015.

53. Wang, J., J. Zhang, D. Cao, H. Dang, and B. Ding, "Comparison of Recycled Aggregate Treatment Methods on the Performance for Recycled Concrete", *Construction and Building Materials*, Vol. 234, p.117366, 2020.

54. Katz, A., "Treatments for the Improvement of Recycled Aggregate", *Journal of Materials in Civil Engineering*, Vol. 16, No. 6, pp. 597-603, 2004.

55. Sasanipour, H., F. Aslani, and J. Taherinezhad, "Chloride Ion Permeability Improvement of Recycled Aggregate Concrete Using Pretreated Recycled Aggregates by Silica Fume Slurry", *Construction and Building Materials*, Vol. 270, p. 121498, 2021.

56. Kisku, N., P. Rajhans, S. K. Panda, V. Pandey, and S. Nayak, "Microstructural Investigation of Recycled Aggregate Concrete Produced by Adopting Equal Mortar Volume Method along with Two Stage Mixing Approach", *Structures*, Vol. 24, No. January, pp. 742-753, 2020.

57. Gao, C., L. Huang, L. Yan, R. Jin, and H. Chen, “Mechanical Properties of Recycled Aggregate Concrete Modified by Nano-Particles”, *Construction and Building Materials*, Vol. 241, p. 118030, 2020.

58. Bui, N. K., T. Satomi, and H. Takahashi, “Influence of Industrial By-Products and Waste Paper Sludge Ash on Properties of Recycled Aggregate Concrete”, *Journal of Cleaner Production*, Vol. 214, pp. 403-418, 2019.

59. Yue, Y., Y. Zhou, F. Xing, G. Gong, B. Hu, and M. Guo, “An Industrial Applicable Method to Improve the Properties of Recycled Aggregate Concrete by Incorporating Nano-Silica and Micro-$CaCO_3$”, *Journal of Cleaner Production*, Vol. 259, p.120920, 2020.

60. Tam, V. W. Y., and C. M. Tam, “Diversifying Two-Stage Mixing Approach (TSMA) for Recycled Aggregate Concrete: TSMAs and TSMAsc”, *Construction and Building Materials*, Vol. 22, No.10, pp. 2068-2077, 2008.

61. Tam, V. W. Y., and C. M. Tam, “Assessment of Durability of Recycled Aggregate Concrete Produced by Two-Stage Mixing Approach”, *Journal of Materials Science*, Vol. 42, pp. 3592-3602, 2007.

62. Tam, V. W. Y., X. F. Gao, and C. M. Tam, “Microstructural Analysis of Recycled Aggregate Concrete Produced from Two-Stage Mixing Approach”, *Cement and Concrete Research*, Vol. 35, No. 6, pp. 1195-1203, 2005.

63. Babu, V. S., A. K. Mullick, K. K. Jain, and P. K. Singh, “Strength and Durability Characteristics of High-Strength Concrete with Recycled Aggregate - Influence of Mixing Techniques”, *Journal of Sustainable Cement-Based Materials*, Vol. 3, No. 2, pp. 88-110, 2014.

64. Kisku, N., P. Rajhans, S. K. Panda, S. Nayak, and V. Pandey, “Development of Durable Concrete from C&D Waste by Adopting Identical Mortar Volume Method in Conjunction with Two-Stage Mixing Procedure”, *Construction and Building*

Materials, Vol. 256, p. 119361, 2020.

65. Zhang, W., S. Wang, P. Zhao, L. Lu, and X. Cheng, "Effect of the Optimized Triple Mixing Method on the ITZ Microstructure and Performance of Recycled Aggregate Concrete", *Construction and Building Materials*, Vol. 203, pp. 601-607, 2019.

66. Pradhan, S., S. Kumar, and S. V. Barai, "Recycled Aggregate Concrete: Particle Packing Method (PPM) of Mix Design Approach", *Construction and Building Materials*, Vol. 152, pp. 269-284, 2017.

67. Kong, D., T. Lei, J. Zheng, C. Ma, J. Jiang, and J. Jiang, "Effect and Mechanism of Surface-Coating Pozzalanics Materials Around Aggregate on Properties and ITZ Microstructure of Recycled Aggregate Concrete", *Construction and Building Materials*, Vol. 24, No. 5, pp. 701-708, 2010.

68. Li, J., H. Xiao, and Y. Zhou, "Influence of Coating Recycled Aggregate Surface with Pozzolanic Powder on Properties of Recycled Aggregate Concrete", *Construction and Building Materials*, Vol. 23, No. 3, pp. 1287-1291, 2009.

69. Ding, Y., J. Wu, P. Xu, X. Zhang, and Y. Fan, "Treatment Methods for the Quality Improvement of Recycled Concrete Aggregate (RCA) - A Review", *Journal of Wuhan University of Technology-Mater. Sci. Ed.*, Vol. 36, No. 1, pp. 77-92, 2021.

70. Tam, V. W. Y., M. Soomro, and A. C. J. Evangelista, "Quality Improvement of Recycled Concrete Aggregate by Removal of Residual Mortar: A Comprehensive Review of Approaches Adopted", *Construction and Building Materials*, Vol. 288, p. 123066, 2021.

71. Shaban, W. M., J. Yang, H. Su, K. H. Mo, L. Li, and J. Xie, "Quality Improvement Techniques for Recycled Concrete Aggregate: A Review", *Journal of Advanced Concrete Technology*, Vol. 17, No. 4, pp. 151-167, 2019.

72. Li, Y., S. Zhang, R. Wang, Y. Zhao, and C. Men, "Effects of Carbonation Treatment

on the Crushing Characteristics of Recycled Coarse Aggregates", *Construction and Building Materials*, Vol. 201, pp. 408-420, 2019.

73. Makul, N., "A Review on Methods to Improve the Quality of Recycled Concrete Aggregates", *Journal of Sustainable Cement-Based Materials*, Vol. 10, No. 2, pp. 65-91, 2021.

74. Tang, P., M. V. A. Florea, and H. J. H. Brouwers, "Employing Cold Bonded Pelletization to Produce Lightweight Aggregates from Incineration Fine Bottom Ash", *Journal of Cleaner Production*, Vol. 165, pp. 1371-1384, 2017.

75. Bhattacharjee, U., and T. C. Kandpal, "Potential of Fly Ash Utilisation in India", *Energy*, Vol. 27, No. 2, pp. 151-166, 2002.

76. Das, B., S. Prakash, P. S. R. Reddy, and V. N. Misra, "An Overview of Utilization of Slag and Sludge from Steel Industries", *Resources, Conservation and Recycling*, Vol. 50, No. 1, pp. 40-57, 2007.

77. Zhang, X., J. Chen, J. J. Jiang, J. Li, R. D. Tyagi, and R. Y. Surampalli, "The Potential Utilization of Slag Generated from Iron- and Steelmaking Industries: A Review", *Environmental Geochemistry and Health*, Vol. 42, pp. 1321-1334, 2020.

78. Xu, G., and X. Shi, "Characteristics and Applications of Fly Ash as a Sustainable Construction Material: A State-of-the-Art Review", *Resources, Conservation and Recycling*, Vol. 136, pp. 95-109, 2018.

79. Amran, M., G. Murali, N. H. A. Khalid, R. Fediuk, T. Ozbakkaloglu, Y. H. Lee, S. Haruna, and Y. Y. Lee, "Slag Uses in Making an Ecofriendly and Sustainable Concrete: A Review", *Construction and Building Materials*, Vol. 272, p. 121942, 2021.

80. Wang, X., X. Li, X. Yan, C. Tu, and Z. Yu, "Environmental Risks for Application of Iron and Steel Slags in Soils in China: A Review", *Pedosphere*, Vol. 31, No. 1, pp. 28-

42, 2021.

81. Chen, J., B. Yan, H. Li, P. Li, and H. Guo, “Vitrification of Blast Furnace Slag and Fluorite Tailings for Giving Diopside-Fluorapatite Glass-Ceramics”, *Materials Letters*, Vol. 218, pp. 309-312, 2018.

82. Ahmad, J., K. J. Kontoleon, A. Majdi, M. T. Naqash, A. F. Deifalla, N. B. Kahla, H. F. Isleem, and S. M. A. Qaidi, “A Comprehensive Review on the Ground Granulated Blast Furnace Slag (GGBS) in Concrete Production”, *Sustainability*, Vol. 14, No.14, p.8783, 2022.

83. Buddhdev, B. G., and K. L. Timani, “Critical Review for Utilization of Blast Furnace Slag in Geotechnical Application”, *Problematic Soils and Geoenvironmental Concerns*, edited by Gali, M. L., and P. R. Rao, P., Vol. 88, Springer, Singapore, pp. 87-98, 2021.

84. Giergiczny, Z., “Fly Ash and Slag”, *Cement and Concrete Research*, Vol. 124, p.105826, 2019.

85. Ibrahim, M., M. K. Rahman, S. K. Najamuddin, Z. S. Alhelal, and C. E. Acero, “A Review on Utilization of Industrial By-Products in the Production of Controlled Low Strength Materials and Factors Influencing the Properties”, *Construction and Building Materials*, Vol. 325, p. 126704, 2022.

86. Tang, P., and H. J. H. Brouwers, “The Durability and Environmental Properties of Self-Compacting Concrete Incorporating Cold Bonded Lightweight Aggregates Produced from Combined Industrial Solid Wastes”, *Construction and Building Materials*, Vol. 167, pp. 271-285, 2018.

87. Li, L., T. C. Ling, and S. Y. Pan, “Environmental Benefit Assessment of Steel Slag Utilization and Carbonation: A Systematic Review”, *Science of The Total Environment*, Vol. 806, p. 150280, 2022.

88. Gesoğlu, M., E. Güneyisi, S. F. Mahmood, H. Ö. Öz, and K. Mermerdaş, "Recycling Ground Granulated Blast Furnace Slag as Cold Bonded Artificial Aggregate Partially Used in Self-Compacting Concrete", *Journal of Hazardous Materials*, Vol. 235-236, pp. 352-358, 2012.

89. Zhao, J., Z. Li, D. Wang, P. Yan, L. Luo, H. Zhang, H. Zhang, and X. Gu, "Hydration Superposition Effect and Mechanism of Steel Slag Powder and Granulated Blast Furnace Slag Powder", *Construction and Building Materials*, Vol. 366, p. 130101, 2023.

90. Huang, D., P. Chen, H. Peng, Q. Yuan, and X. Tian, "Drying Shrinkage Performance of Medium-Ca Alkali-Activated Fly Ash and Slag Pastes", *Cement and Concrete Composites*, Vol. 130, p. 104536, 2022.

91. Özbay, E., M. Erdemir, and H. İ. Durmuş, "Utilization and Efficiency of Ground Granulated Blast Furnace Slag on Concrete Properties - A review", *Construction and Building Materials*, Vol. 105, pp. 423-434, 2016.

92. Zakira, U., K. Zheng, N. Xie, and B. Birgisson, "Development of High-Strength Geopolymers from Red Mud and Blast Furnace Slag", *Journal of Cleaner Production*, Vol. 383, p. 135439, 2023.

93. Ozkan, H., and N. Kabay, "Manufacture of Sintered Aggregate Using Washing Aggregate Sludge and Ground Granulated Blast Furnace Slag: Characterization of the Aggregate and Effects on Concrete Properties", *Construction and Building Materials*, Vol. 342, p. 128025, 2022.

94. Jeong, Y., W. S. Yum, D. Jeon, and J. E. Oh, "Strength Development and Microstructural Characteristics of Barium Hydroxide-Activated Ground Granulated Blast Furnace Slag", *Cement and Concrete Composites*, Vol. 79, pp. 34-44, 2017.

95. Behera, S. K., D.P. Mishra, P. Singh, K. Mishra, S. K. Mandal, C. N. Ghosh, R. Kumar, and P. K. Mandal, "Utilization of Mill Tailings, Fly Ash and Slag as Mine Paste

Backfill Material: Review and Future Perspective", *Construction and Building Materials*, Vol. 309, p. 125120, 2021.

96. Oge, M., D. Ozkan, M. B. Celik, M. Sabri Gok, and A. Cahit Karaoglanli, "An Overview of Utilization of Blast Furnace and Steelmaking Slag in Various Applications", *Materials Today: Proceedings*, Vol. 11, pp. 516-525, 2019.

97. Baykal, G., and A. G. Döven, "Utilization of Fly Ash by Pelletization Process; Theory, Application Areas and Research Results", *Resources, Conservation and Recycling*, Vol. 30, No. 1, pp. 59-77, 2000.

98. Siddique, R., and P. Cachim, *Waste and Supplementary Cementitious Materials in Concrete: Characterisation, Properties and Applications*, Woodhead Publishing, Chennai, India, 2018.

99. Matthes, W., A. Vollpracht, Y. Villagrán, S. Kamali-Bernard, D. Hooton, E. Gruyaert, M. Soutsos, and N. D. Belie, "Ground Granulated Blast-Furnace Slag", in *Properties of Fresh and Hardened Concrete Containing Supplementary Cementitious Materials*, N. D. Belie, M. Soutsos, and E. Gruyaert, Eds., Cham, Switzerland: Springer International Publishing, 2018, pp. 1-53.

100. Sideris, K., H. Justnes, M. Soutsos, and T. Sui, "Fly Ash", in *Properties of Fresh and Hardened Concrete Containing Supplementary Cementitious Materials*, N. D. Belie, M. Soutsos, and E. Gruyaert, Eds., Cham, Switzerland: Springer International Publishing, 2018, pp. 55-98.

101. Sobolev, K., M. Kozhukhova, K. Sideris, E. Menéndez, and M. Santhanam, "Alternative Supplementary Cementitious Materials", in *Properties of Fresh and Hardened Concrete Containing Supplementary Cementitious Materials*, N. D. Belie, M. Soutsos, and E. Gruyaert, Eds., Cham, Switzerland: Springer International Publishing, 2018, pp. 233-282.

102. Kalra, N., M. C. Jain, H. C. Joshi, R. Choudhary, R. C. Harit, B. K. Vatsa, S. K.

Sharma, and V. Kumar, "Flyash as A Soil Conditioner and Fertilizer", *Bioresource Technology*, Vol. 64, No. 3, pp. 163-167, 1998.

103. Yoo, J. G., and Y. M. Jo, "Finding the Optimum Binder for Fly Ash Pelletization", *Fuel Processing Technology*, Vol. 81, No. 3, pp. 173-186, 2003.

104. Colangelo, F., and R. Cioffi, "Use of Cement Kiln Dust, Blast Furnace Slag and Marble Sludge in the Manufacture of Sustainable Artificial Aggregates by Means of Cold Bonding Pelletization", *Materials*, Vol. 6, No. 8, pp. 3139-3159, 2013.

105. Zuo, Y., M. Nedeljković, and G. Ye, "Pore Solution Composition of Alkali-Activated Slag/Fly Ash Pastes", *Cement and Concrete Research*, Vol. 115, pp. 230-250, 2019.

106. Gesoğlu, M., E. Güneyisi, and H. Ö. Öz, "Properties of Lightweight Aggregates Produced with Cold-Bonding Pelletization of Fly Ash and Ground Granulated Blast Furnace Slag", *Materials and Structures*, Vol. 45, pp. 1535-1546, 2012.

107. Das, S. K., A. K. Tripathi, S. K. Kandi, S. M. Mustakim, B. Bhoi, and P. Rajput, "Ferrochrome Slag: A Critical Review of Its Properties, Environmental Issues and Sustainable Utilization", *Journal of Environmental Management*, Vol. 326, p. 116674, 2023.

108. Verma, C. L., S. K. Handa, S. K. Jain, and R. K. Yadav, "Techno-Commercial Perspective Study for Sintered Fly Ash Light-Weight Aggregates in India", *Construction and Building Materials*, Vol. 12, No. 6-7, pp. 341-346, 1998.

109. Kayali, O., M. N. Haque, and B. Zhu, "Some Characteristics of High Strength Fiber Reinforced Lightweight Aggregate Concrete", *Cement and Concrete Composites*, Vol. 25, No. 2, pp. 207-213, 2003.

110. Zhang, M. H., and O. E. Gjorv, "Characteristics of Lightweight Aggregates for High-Strength Concrete", *ACI Materials Journal*, Vol. 88, No. 2, pp. 150-158, 1991.

111. Kayali, O., "Fly Ash Lightweight Aggregates in High Performance Concrete", *Construction and Building Materials*, Vol. 22, No. 12, pp. 2393-2399, 2008.

112. Kockal, N. U., and T. Ozturan, "Effects of Lightweight Fly Ash Aggregate Properties on the Behavior of Lightweight Concretes", *Journal of Hazardous Materials*, Vol. 179, No. 1-3, pp. 954-965, 2010.

113. Rasheed, R., H. Javed, A. Rizwan, F. Sharif, A. Yasar, A. B. Tabinda, S. R. Ahmad, Y. Wang, and Y. Su, "Life Cycle Assessment of A Cleaner Supercritical Coal-Fired Power Plant", *Journal of Cleaner Production*, Vol. 279, p. 123869, 2021.

114. Babbitt, C. W., and A. S. Lindner, "A Life Cycle Inventory of Coal Used for Electricity Production in Florida", *Journal of Cleaner Production*, Vol. 13, No. 9, pp. 903-912, 2005.

115. Manikandan, R., and K. Ramamurthy, "Influence of Fineness of Fly Ash on the Aggregate Pelletization Process", *Cement and Concrete Composites*, Vol. 29, No. 6, pp. 456-464, 2007.

116. Harikrishnan, K. I., and K. Ramamurthy, "Influence of Pelletization Process on the Properties of Fly Ash Aggregates", *Waste Management*, Vol. 26, No. 8, pp. 846-852, 2006.

117. Gesoğlu, M., T. Özturan, and E. Güneyisi, "Effects of Fly Ash Properties on Characteristics of Cold-Bonded Fly Ash Lightweight Aggregates", *Construction and Building Materials*, Vol. 21, No. 9, pp. 1869-1878, 2007.

118. Rivera, F., P. Martínez, J. Castro, and M. López, "Massive Volume Fly-Ash Concrete: A More Sustainable Material with Fly Ash Replacing Cement and Aggregates", *Cement and Concrete Composites*, Vol. 63, pp. 104-112, 2015.

119. Kockal, N. U., and T. Ozturan, "Microstructural and Mineralogical Characterization of Artificially Produced Pellets for Civil Engineering Applications", *Journal of*

Materials in Civil Engineering, Vol. 29, No. 2, pp. 04016214, 2016.

120. Nadesan, M. S., and P. Dinakar, "Mix Design and Properties of Fly Ash Waste Lightweight Aggregates in Structural Lightweight Concrete", *Case Studies in Construction Materials*, Vol. 7, pp. 336-347, 2017.

121. Narattha, C., and A. Chaipanich, "Phase Characterizations, Physical Properties and Strength of Environment-Friendly Cold-Bonded Fly Ash Lightweight Aggregates", *Journal of Cleaner Production*, Vol. 171, pp. 1094-1100, 2018.

122. Colangelo, F., F. Messina, and R. Cioffi, "Recycling of MSWI Fly Ash by Means of Cementitious Double Step Cold Bonding Pelletization: Technological Assessment for the Production of Lightweight Artificial Aggregates", *Journal of Hazardous Materials*, Vol. 299, pp. 181-191, 2015.

123. Lu, C. H., J. C. Chen, K. H. Chuang, and M. Y. Wey, "The Different Properties of Lightweight Aggregates with the Fly Ashes of Fluidized-Bed and Mechanical Incinerators", *Construction and Building Materials*, Vol. 101, pp. 380-388, 2015.

124. Kockal, N. U., and T. Ozturan, "Characteristics of Lightweight Fly Ash Aggregates Produced with Different Binders and Heat Treatments", *Cement and Concrete Composites*, Vol. 33, No. 1, pp. 61-67, 2011.

125. Kockal, N. U., and T. Ozturan, "Durability of Lightweight Concretes with Lightweight Fly Ash Aggregates", *Construction and Building Materials*, Vol. 25, No. 3, pp. 1430-1438, 2011.

126. Colangelo, F., F. Messina, L. D. Palma, and R. Cioffi, "Recycling of Non-Metallic Automotive Shredder Residues and Coal Fly-Ash in Cold-Bonded Aggregates for Sustainable Concrete", *Composites Part B: Engineering*, Vol. 116, pp. 46-52, 2017.

127. Gomathi, P., and A. Sivakumar, "Accelerated Curing Effects on the Mechanical Performance of Cold Bonded and Sintered Fly Ash Aggregate Concrete",

Construction and Building Materials, Vol. 77, pp. 276-287, 2015.

128. Gesoğlu, M., T. Özturan, and E. Güneyisi, "Effects of Cold-Bonded Fly Ash Aggregate Properties on the Shrinkage Cracking of Lightweight Concretes", *Cement and Concrete Composites*, Vol. 28, No. 7, pp. 598-605, 2006.

129. Gesoğlu, M., T. Özturan, and E. Güneyisi, "Shrinkage Cracking of Lightweight Concrete Made with Cold-Bonded Fly Ash Aggregates", *Cement and Concrete Research*, Vol. 34, No. 7, pp. 1121-1130, 2004.

130. Kockal, N. U., and T. Ozturan, "Strength and Elastic Properties of Structural Lightweight Concretes", *Materials & Design*, Vol. 32, No. 4, pp. 2396-2403, 2011.

131. Güneyisi, E., M. Gesoglu, O. A. Azez, and H. Ö. Öz, "Effect of Nano Silica on the Workability of Self-Compacting Concretes Having Untreated and Surface Treated Lightweight Aggregates", *Construction and Building Materials*, Vol. 115, pp. 371-380, 2016.

132. Yıldırım, H., and T. Özturan, "Impact Resistance of Concrete Produced with Plain and Reinforced Cold-Bonded Fly Ash Aggregates", *Journal of Building Engineering*, Vol. 42, p.102875, 2021.

133. Ibrahim, M., W. Alimi, R. Assaggaf, B. A. Salami, and E. A. Oladapo, "An Overview of Factors Influencing the Properties of Concrete Incorporating Construction and Demolition Wastes", *Construction and Building Materials*, Vol. 367, p. 130307, 2023.

134. Aslam, M. S., B. Huang, and L. Cui, "Review Of Construction and Demolition Waste Management in China and USA", *Journal of Environmental Management*, Vol. 264, p. 110445, 2020.

135. Coelho, A., and J. de Brito, "Environmental Analysis of A Construction and Demolition Waste Recycling Plant in Portugal - Part I: Energy Consumption and CO_2 Emissions", *Waste Management*, Vol. 33, No. 5, pp. 1258-1267, 2013.

136. Brito, J. D., and N. Saikia, *Recycled Aggregate in Concrete: Use of Industrial, Construction and Demolition Waste*, Springer, London, 2013.

137. Lu, W., B. Chi, Z. Bao, and A. Zetkulic, "Evaluating the Effects of Green Building on Construction Waste Management: A Comparative Study of Three Green Building Rating Systems", *Building and Environment*, Vol. 155, pp. 247-256, 2019.

138. Devi, S. V., R. Gausikan, S. Chithambaranathan, and J. W. Jeffrey, "Utilization of Recycled Aggregate of Construction and Demolition Waste as A Sustainable Material", *Materials Today: Proceedings*, Vol. 45, pp. 6649-6654, 2020.

139. Dos Reis, G. S., M. Quattrone, W. M. Ambrós, B. G. Cazacliu, and C. H. Sampaio, "Current Applications of Recycled Aggregates from Construction and Demolition: A Review", *Materials*, Vol. 14, No. 7, pp. 1-21, 2021.

140. Pacheco-Torgal, F., V. W. Y. Tam, J. A. Labrincha, Y. Ding, and J. de Brito, *Handbook of Recycled Concrete and Demolition Waste*, Woodhead Publishing Limited, Cambridge 2013.

141. Salgado, F. de A., and F. de A. Silva, "Recycled Aggregates from Construction and Demolition Waste Towards An Application on Structural Concrete: A Review", *Journal of Building Engineering*, Vol. 52, p. 104452, 2022.

142. Tam, V. W. Y., M. Soomro, and A. C. J. Evangelista, "A Review of Recycled Aggregate in Concrete Applications (2000–2017)", *Construction and Building Materials*, Vol. 172, pp. 272-292, 2018.

143. Rao, M. C., S. K. Bhattacharyya, and S. V. Barai, *Systematic Approach of Characterisation and Behaviour of Recycled Aggregate Concrete*, Springer, Singapore, 2019.

144. Pacheco, J. and J. de Brito, "Recycled Aggregates Produced from Construction and Demolition Waste for Structural Concrete: Constituents, Properties and Production",

Materials, Vol. 14, No. 19, p. 5748, 2021.

145. Xiao, J., *Recycled Aggregate Concrete Structures*, Springer-Verlag, Berlin, 2018.

146. Ramamurthy, K., and K. I. Harikrishnan, "Influence of Binders on Properties of Sintered Fly Ash Aggregate", *Cement and Concrete Composites*, Vol. 28, No. 1, pp. 33-38, 2006.

147. Güneyisi, E., M. Gesoğlu, Ö. Pürsünlü, and K. Mermerdaş, "Durability Aspect of Concretes Composed of Cold Bonded and Sintered Fly Ash Lightweight Aggregates", *Composites Part B: Engineering*, Vol. 53, pp. 258-266, 2013.

148. Gesoğlu, M., E. Güneyisi, T. Özturan, H. Ö. Öz, and D. S. Asaad, "Permeation Characteristics of Self Compacting Concrete Made with Partially Substitution of Natural Aggregates with Rounded Lightweight Aggregates", *Construction and Building Materials*, Vol. 59, pp. 1-9, 2014.

149. Kumar, P., D. Pasla, and T. J. Saravanan, "Self-Compacting Lightweight Aggregate Concrete and Its Properties: A Review", *Construction and Building Materials*, Vol. 375, p. 130861, 2023.

150. Nadesan, M. S., and P. Dinakar, "Structural Concrete Using Sintered Flyash Lightweight Aggregate: A Review", *Construction and Building Materials*, Vol. 154, pp. 928-944, 2017.

151. Chandra, S., and L. Berntsson, *Lightweight Aggregate Concrete: Science, Technology and Applications*, William Andrew Publishing, New York, 2002.

152. Wang, B., L. Yan, Q. Fu, and B. Kasal, "A Comprehensive Review on Recycled Aggregate and Recycled Aggregate Concrete", *Resources, Conservation and Recycling*, Vol. 171, p. 105565, 2021.

153. Bai, G., C. Zhu, C. Liu, and B. Liu, "An Evaluation of the Recycled Aggregate

Characteristics and the Recycled Aggregate Concrete Mechanical Properties", *Construction and Building Materials*, Vol. 240, p. 117978, 2020.

154. Berredjem, L., N. Arabi, and L. Molez, "Mechanical and Durability Properties of Concrete Based on Recycled Coarse and Fine Aggregates Produced from Demolished Concrete", *Construction and Building Materials*, Vol. 246, p. 118421, 2020.

155. Poon, C. S., and D. Chan, "Feasible Use of Recycled Concrete Aggregates and Crushed Clay Brick As Unbound Road Sub-Base", *Construction and Building Materials*, Vol. 20, No. 8, pp. 578-585, 2006.

156. Topçu, İ. B., and S. Şengel, "Properties of Concretes Produced with Waste Concrete Aggregate", *Cement and Concrete Research*, Vol. 34, No. 8, pp. 1307-1312, 2004.

157. Etxeberria, M., E. Vázquez, A. Marí, and M. Barra, "Influence of Amount of Recycled Coarse Aggregates and Production Process on Properties of Recycled Aggregate Concrete", *Cement and Concrete Research*, Vol. 37, No. 5, pp. 735-742, 2007.

158. Gómez-Soberón, J. M. V., "Porosity of Recycled Concrete with Substitution of Recycled Concrete Aggregate: An Experimental Study", *Cement and Concrete Research*, Vol. 32, No. 8, pp. 1301-1311, 2002.

159. Juan, M. S. D., and P. A. Gutiérrez, "Study on the Influence of Attached Mortar Content on the Properties of Recycled Concrete Aggregate", *Construction and Building Materials*, Vol. 23, No. 2, pp. 872-877, 2009.

160. Butler, L., J. S. West, and S. L. Tighe, "Effect of Recycled Concrete Coarse Aggregate from Multiple Sources on the Hardened Properties of Concrete with Equivalent Compressive Strength", *Construction and Building Materials*, Vol. 47, pp. 1292-1301, 2013.

161. Yang, J., Q. Du, and Y. Bao, "Concrete with Recycled Concrete Aggregate and Crushed Clay Bricks", *Construction and Building Materials*, Vol. 25, No. 4, pp. 1935-

1945, 2011.

162. Mazhoud, B., T. Sedran, B. Cazacliu, A. Cothenet, and J. M. Torrenti, “Influence of Residual Mortar Volume on the Properties of Recycled Concrete Aggregates”, *Journal of Building Engineering*, Vol. 57, p. 104945, 2022.

163. Duan, Z. H., and C. S. Poon, “Properties of Recycled Aggregate Concrete Made with Recycled Aggregates with Different Amounts wf Old Adhered Mortars”, *Materials & Design*, Vol. 58, pp. 19-29, 2014.

164. Younis, K. H., and K. Pilakoutas, “Strength Prediction Model and Methods for Improving Recycled Aggregate Concrete”, *Construction and Building Materials*, Vol. 49, pp. 688-701, 2013.

165. Gesoglu, M., E. Güneyisi, H. Ö. Öz, I. Taha, and M. T. Yasemin, “Failure Characteristics of Self-Compacting Concretes Made with Recycled Aggregates”, *Construction and Building Materials*, Vol. 98, pp. 334-344, 2015.

166. Chi, J. M., R. Huang, C. C. Yang, and J. J. Chang, “Effect of Aggregate Properties on the Strength and Stiffness of Lightweight Concrete”, *Cement and Concrete Composites*, Vol. 25, No. 2, pp. 197-205, 2003.

167. Abdulla, N. A., “Effect of Recycled Coarse Aggregate Type on Concrete”, *Journal of Materials in Civil Engineering*, Vol. 27, No. 10, p. 04014273, 2015.

168. Wu, K., S. Luo, J. Zheng, J. Yan, and J. Xiao, “Influence of Carbonation Treatment on the Properties of Multiple Interface Transition Zones and Recycled Aggregate Concrete”, *Cement and Concrete Composites*, Vol. 127, p. 104402, 2022.

169. Rao, M. C., S. K. Bhattacharyya, and S. V. Barai, “Behaviour of Recycled Aggregate Concrete Under Drop Weight Impact Load”, *Construction and Building Materials*, Vol. 25, No. 1, pp. 69-80, 2011.

170. Kavussi, A., A. Hassani, F. Kazemian, and M. Taghipoor, "Laboratory Evaluation of Treated Recycled Concrete Aggregate in Asphalt Mixtures", *International Journal of Pavement Research and Technology*, Vol. 12, pp. 26-32, 2019.

171. Prasad, C. V. S. R., "Light Weight Concrete Using FlyAsh Aggregate", *International Journal of Innovative Technologies*, Vol. 5, No. 3, pp. 460-463, 2017.

172. Ravichandra, R., J. K. Dattatreya, and S. M. Maheshwarappa, "An Experimental Study on Properties of Fly ash Aggregate Comparing with Natural Aggregate", *Journal of Civil Engineering and Environmental Technology*, Vol. 2, No. 11, pp. 64-68, 2015.

173. Kisku, N., P. Rajhans, S. K. Panda, V. Pandey, and S. Nayak, "Microstructural Investigation of Recycled Aggregate Concrete Produced by Adopting Equal Mortar Volume Method Along With Two Stage Mixing Approach", *Structures*, Vol. 24, pp. 742-753, 2020.

174. Kou, S. C., C. S. Poon, and M. Etxeberria, "Influence of Recycled Aggregates on Long Term Mechanical Properties and Pore Size Distribution of Concrete", *Cement and Concrete Composites*, Vol. 33, No. 2, pp. 286-291, 2011.

175. Lorrain, M. S., M. P. Barbosa, and L. C. P. Silva Fº, "Estimation of Compressive Strength Based on Pull-Out Bond Test Results for On-Site Concrete Quality Control", *IBRACON Structures and Materials Journal*, Vol. 4, No. 4, pp. 582-591, 2011.

176. Vu, C. C., O. Plé, J. Weiss, and D. Amitrano, "Revisiting the Concept of Characteristic Compressive Strength of Concrete", *Construction and Building Materials*, Vol. 263, p. 120126, 2020.

177. ACI Committee 318, *Building Code Requirements for Structural Concrete (ACI 318-19) and Commentary (ACI 318R-19)*, American Concrete Institute, Farmington Hills, 2019.

178. Turkish Building Seismic Code, *Principles for the Design of Buildings Under*

Earthquake Effect, Disaster and Emergency Management Presidency, Ankara, 2018.

179. Viso, J. R. D., J. R. Carmona, and G. Ruiz, "Shape and Size Effects on the Compressive Strength of High-Strength Concrete", *Cement and Concrete Research*, Vol. 38, No. 3, pp. 386-395, 2008.

180. Yazıcı, H., "The Effect of Curing Conditions on Compressive Strength of Ultra High Strength Concrete with High Volume Mineral Admixtures", *Building and Environment*, Vol. 42, No. 5, pp. 2083-2089, 2007.

181. Gyurkó, Z., and R. Nemes, "Specimen Size and Shape Effect on the Compressive Strength of Normal Strength Concrete", *Periodica Polytechnica Civil Engineering*, Vol. 64, No. 1, pp. 276-286, 2020.

182. Chen, H. J., T. Yen, and K. H. Chen, "Use of Building Rubbles as Recycled Aggregates", *Cement and Concrete Research*, Vol. 33, No. 1, pp. 125-132, 2003.

183. Khatib, J. M., "Properties of Concrete Incorporating Fine Recycled Aggregate", *Cement and Concrete Research*, Vol. 35, No. 4, pp. 763-769, 2005.

184. Tayeh, B. A., D. M. A. Saffar, and R. Alyousef, "The Utilization of Recycled Aggregate in High Performance Concrete: A Review", *Journal of Materials Research and Technology*, Vol. 9, No. 4, pp. 8469-8481, 2020.

185. Poon, C. S., and D. Chan, "Effects of Contaminants on the Properties of Concrete Paving Blocks Prepared with Recycled Concrete Aggregates", *Construction and Building Materials*, Vol. 21, No. 1, pp. 164-175, 2007.

186. Poon, C. S., and C. S. Lam, "The Effect of Aggregate-to-Cement Ratio and Types of Aggregates on the Properties of Pre-Cast Concrete Blocks", *Cement and Concrete Composites*, Vol. 30, No. 4, pp. 283-289, 2008.

187. Xiao, J. Z., J. B. Li, and C. Zhang, "On Relationships Between the Mechanical

Properties of Recycled Aggregate Concrete: An Overview", *Materials and Structures*, Vol. 39, pp. 655-664, 2006.

188. Li, W., J. Xiao, Z. Sun, S. Kawashima, and S. P. Shah, "Interfacial Transition Zones in Recycled Aggregate Concrete with Different Mixing Approaches", *Construction and Building Materials*, Vol. 35, pp. 1045-1055, 2012.

189. López-Gayarre, F., P. Serna, A. Domingo-Cabo, M. A. Serrano-López, and C. López-Colina, "Influence of Recycled Aggregate Quality and Proportioning Criteria on Recycled Concrete Properties", *Waste Management*, Vol. 29, No. 12, pp. 3022-3028, 2009.

190. Padmini, A. K., K. Ramamurthy, and M. S. Mathews, "Influence of Parent Concrete on the Properties of Recycled Aggregate Concrete", *Construction and Building Materials*, Vol. 23, No. 2, pp. 829-836, 2009.

191. Tam, V. W. Y., C. M. Tam, and Y. Wang, "Optimization on Proportion for Recycled Aggregate in Concrete Using Two-Stage Mixing Approach", *Construction and Building Materials*, Vol. 21, No. 10, pp. 1928-1939, 2007.

192. Dilbas, H., Ö. Çakır, and C. D. Atiş, "Experimental Investigation on Properties of Recycled Aggregate Concrete with Optimized Ball Milling Method", *Construction and Building Materials*, Vol. 212, pp. 716-726, 2019.

193. Silva, R. V., J. De Brito, and R. K. Dhir, "Establishing a Relationship Between Modulus of Elasticity and Compressive Strength of Recycled Aggregate Concrete", *Journal of Cleaner Production*, Vol. 112, pp. 2171-2186, 2016.

194. Etxeberria, M., A. R. Marí, and E. Vázquez, "Recycled Aggregate Concrete As Structural Material", *Materials and Structures*, Vol. 40, pp. 529-541, 2007.

195. Kou, S. C., C. S. Poon, and D. Chan, "Influence of fly ash as a cement addition on the hardened properties of recycled aggregate concrete", *Materials and Structures*, Vol.

41, pp. 1191-1201, 2008.

196. Alnahhal, M. F., U. J. Alengaram, M. Z. Jumaat, M. A. Alqedra, K. H. Mo, and M. Sumesh, "Evaluation of Industrial By-Products As Sustainable Pozzolanic Materials in Recycled Aggregate Concrete", *Sustainability*, Vol. 9, No. 5, p. 767, 2017.

197. Katkhuda, H., and N. Shatarat, "Improving the Mechanical Properties of Recycled Concrete Aggregate Using Chopped Basalt Fibers and Acid Treatment", *Construction and Building Materials*, Vol. 140, pp. 328-335, 2017.

198. Silva, R. V., J. De Brito, and R. K. Dhir, "Tensile Strength Behaviour of Recycled Aggregate Concrete", *Construction and Building Materials*, Vol. 83, pp. 108-118, 2015.

199. Afroughsabet, V., L. Biolzi, and T. Ozbakkaloglu, "Influence of Double Hooked-End Steel Fibers and Slag on Mechanical and Durability Properties of High Performance Recycled Aggregate Concrete", *Composite Structures*, Vol. 181, pp. 273-284, 2017.

200. Yaba, H. K., H. S. Naji, K. H. Younis, and T. K. Ibrahim, "Compressive and Flexural Strengths of Recycled Aggregate Concrete: Effect of Different Contents of Metakaolin", *Materials Today: Proceedings*, Vol. 45, pp. 4719-4723, 2021.

201. ACI Committee 544, *Measurement of Properties of Fiber Reinforced Concrete (ACI 544.2R-89)*, American Concrete Institute, Farmington Hills, 1989.

202. Xiao, J., L. Li, L. Shen, and C. S. Poon, "Compressive Behaviour of Recycled Aggregate Concrete Under Impact Loading", *Cement and Concrete Research*, Vol. 71, pp. 46-55, 2015.

203. Xia, D. T., S. J. Xie, M. Fu, and F. Zhu, "Effects of Maximum Particle Size of Coarse Aggregates and Steel Fiber Contents on the Mechanical Properties and Impact Resistance of Recycled Aggregate Concrete", *Advances in Structural Engineering*, Vol. 24, No. 13, pp. 3085-3098, 2021.

204. Lemaitre, J., *A Course on Damage Mechanics*, Second Edition, Springer, Berlin, 1996.

205. Chakraborty, S., and K. V. L. Subramaniam, "Influences of Matrix Strength and Weak Planes on Fracture Response of Recycled Aggregate Concrete", *Theoretical and Applied Fracture Mechanics*, Vol. 124, p. 103801, 2023.

206. Li, T., J. Xiao, Y. Zhang, and B. Chen, "Fracture Behavior of Recycled Aggregate Concrete Under Three-Point Bending", *Cement and Concrete Composites*, Vol. 104, p. 103353, 2019.

207. Gesoglu, M., E. Güneyisi, H. Ö. Öz, I. Taha, and M. T. Yasemin, "Failure Characteristics of Self-Compacting Concretes Made with Recycled Aggregates", *Construction and Building Materials*, Vol. 98, pp. 334-344, 2015.

208. Breccolotti, M., and A. L. Materazzi, "Structural Reliability of Bonding Between Steel Rebars and Recycled Aggregate Concrete", *Construction and Building Materials*, Vol. 47, pp. 927-934, 2013.

209. Namarak, C., W. Tangchirapat, and C. Jaturapitakkul, "Bar-Concrete Bond in Mixes Containing Calcium Carbide Residue, Fly Ash and Recycled Concrete Aggregate", *Cement and Concrete Composites*, Vol. 89, pp. 31-40, 2018.

210. ASTM Standard C618, *Standard Specification for Coal Fly Ash and Raw or Calcined Natural Pozzolan for Use in Concrete*, ASTM International, West Conshohocken, 2019.

211. ASTM Standard C29/C29M, *Standard Test Method for Bulk Density ("Unit Weight") and Voids in Aggregate*, ASTM International, West Conshohocken, 2017.

212. ASTM Standard C127, *Standard Test Method for Relative Density (Specific Gravity) and Absorption of Coarse*, ASTM International, West Conshohocken, 2015.

213. British Standard (BS EN 933-3), *Tests for Geometrical Properties of Aggregates-Part*

3: Determination of Particle Shape - Flakiness Index, British Standards Institution, London, 2012.

214. British Standard (BS 882), *Specification for Aggregates from Natural Sources for Concrete*, British Standards Institution, London, 1992.

215. British Standard (BS 812-110), *Testing Aggregates - Part 110: Methods of Determination of Aggregate Crushing Value (ACV)*, British Standards Institution, London, 1990.

216. British Standard (BS 812-112), *Testing Aggregates - Part 112: Methods for Determination of Aggregate Impact Value (AIV)*, British Standards Institution, London, 1990.

217. Turkish Standard (TS 802), *Design of Concrete Mixes*, Turkish Standards Institution, Ankara, 2009.

218. ASTM Standard C494/C494M, *Standard Specification for Chemical Admixtures for Concrete*, ASTM International, West Conshohocken, 2019.

219. British Standard (BS EN 480-10), *Admixtures for Concrete, Mortar and Grout - Test Methods - Part 10: Determination of Water Soluble Chloride Content*, British Standards Institution, London, 2009.

220. British Standard (BS EN 480-12), *Admixtures for Concrete, Mortar and Grout - Test Methods - Part 12: Determination of the Alkali Content of Admixtures*, British Standards Institution, London, 2005.

221. Lee, H. S., X. Y. Wang, L. N. Zhang, and K. T. Koh, "Analysis of the Optimum Usage of Slag for the Compressive Strength of Concrete", *Materials*, Vol. 8, No. 3, pp. 1213-1229, 2015.

222. Turkish Standard (TS 13515), *Complementary Turkish Standard to TS EN 206-1*,

Turkish Standards Institution, Ankara, 2012.

223. Turkish Standard (TS EN 206-1), *Concrete-Part 1: Specification, Performance, Production and Conformity*, Turkish Standards Institution, Ankara, 2000.

224. ASTM Standard C192/C192M, *Standard Practice for Making and Curing Concrete Test Specimens in the Laboratory*, ASTM International, West Conshohocken, 2019.

225. Shayan, A., and A. M. Xu, "Performance and Properties of Structural Concrete Made with Recycled Concrete Aggregate", *ACI Materials Journal*, Vol. 100, No. 5, pp. 371-380, 2003.

226. ASTM Standard C143/C143M, *Standard Test Method for Slump of Hydraulic-Cement Concrete*, ASTM International, West Conshohocken, 2020.

227. ASTM Standard C138/C138M, *Standard Test Method for Density (Unit Weight), Yield, and Air Content (Gravimetric) of Concrete*, ASTM International, West Conshohocken, 2017.

228. ASTM Standard C39/C39M, *Standard Test Method for Compressive Strength of Cylindrical Concrete Specimens*, ASTM International, West Conshohocken, 2020.

229. ASTM Standard C42/C42M, *Standard Test Method for Obtaining and Testing Drilled Cores and Sawed Beams of Concrete*, ASTM International, West Conshohocken, 2020.

230. ASTM Standard C617/C617M, *Standard Practice for Capping Cylindrical Concrete Specimens*, ASTM International, West Conshohocken, 2015.

231. ASTM Standard C469/C469M, *Standard Test Method for Static Modulus of Elasticity and Poisson's Ratio of Concrete in Compression*, ASTM International, West Conshohocken, 2014.

232. ASTM Standard C496/C496M, *Standard Test Method for Splitting Tensile Strength of Cylindrical Concrete Specimens*, ASTM International, West Conshohocken, 2017.

233. Japan Concrete Institute Standard (JCI-S-001), *Method of Test for Fracture Energy of Concrete by use of Notched Beam*, Japan Concrete Institute, Tokyo, 2003.

234. ASTM Standard D7264/D7264M, *Standard Test Method for Flexural Properties of Polymer Matrix Composite Materials*, ASTM International, West Conshohocken, 2015.

235. Badr, A., and A. F. Ashour, "Modified ACI Drop-Weight Impact Test for Concrete", *ACI Materials Journal*, Vol. 102, No. 4, pp. 249-255, 2005.

236. ASTM Standard D1557, *Standard Test Methods for Laboratory Compaction Characteristics of Soil Using Modified Effort*, ASTM International, West Conshohocken, 2012.

237. Gopalaratnam, V. S., and S. P. Shah, "Properties of Steel Fiber Reinforced Concrete Subjected to Impact Loading", *ACI Materials Journal*, Vol. 83, No. 1, pp. 117-126, 1986.

238. Mohammadi, Y., R. Carkon-Azad, S. P. Singh, and S. K. Kaushik, "Impact Resistance of Steel Fibrous Concrete Containing Fibres of Mixed Aspect Ratio", *Construction and Building Materials*, Vol. 23, No. 1, pp. 183-189, 2009.

239. Jenq, Y., and S. P. Shah, "Two Parameter Fracture Model for Concrete", *Journal of Engineering Mechanics*, Vol. 111, No. 10, pp. 1227-1241, 1985.

240. Shah, S. P., S. E. Swartz, and C. Ouyang, *Fracture Mechanics of Concrete: Applications of Fracture Mechanics to Concrete, Rock and Other Quasi-Brittle Materials*, John Wiley & Sons Inc., New York, 1995.

241. Kumar, S., and S. V. Barai, *Concrete Fracture Models and Applications*, Springer,

New York, 2011.

242. Das, S., M. Aguayo, V. Dey, R. Kachala, B. Mobasher, G. Sant, N. Neithalath, "The Fracture Response of Blended Formulations Containing Limestone Powder: Evaluations Using Two-Parameter Fracture Model and Digital Image Correlation", *Cement and Concrete Composites*, Vol. 53, pp. 316-326, 2014.

243. Guo, Y. C., J. H. Zhang, G. Chen, G. M. Chen, and Z. H. Xie, "Fracture Behaviors of A New Steel Fiber Reinforced Recycled Aggregate Concrete with Crumb Rubber", *Construction and Building Materials*, Vol. 53, pp. 32-39, 2014.

244. Shah, S.P., "Determination of Fracture Parameters (K_{IC}^{S} and $CTOD_c$) of Plain Concrete Using Three-Point Bend Tests", *Materials and Structures*, Vol. 23, pp. 457-460, 1990.

245. Xu, S., and H. W. Reinhardt, "Crack Extension Resistance and Fracture Properties of Quasi-Brittle Softening Materials Like Concrete Based on the Complete Process of Fracture", *International Journal of Fracture*, Vol. 92, pp. 71-99, 1998.

246. Xu, S., and H. W. Reinhardt, "A Simplified Method for Determining Double-K Fracture Parameters for Three-Point Bending Tests", *International Journal of Fracture*, Vol. 104, pp. 181-209, 2000.

247. Kizilkanat, A. B., N. Kabay, V. Akyüncü, S. Chowdhury, and A. H. Akça, "Mechanical Properties and Fracture Behavior of Basalt and Glass Fiber Reinforced Concrete: An Experimental Study", *Construction and Building Materials*, Vol. 100, pp. 218-224, 2015.

248. RILEM 50-FMC, "Determination of the Fracture Energy of Mortar and Concrete by Means of Three-Point Bend Tests on Notched Beams", *Materials and Structures*, Vol. 18, No. 106, pp. 287-290, 1985.

249. Hillerborg, A., "The Theoretical Basis of A Method to Determine the Fracture Energy G_F of Concrete", *Materials and Structures*, Vol. 18, No. 106, pp. 291-296, 1985.

250. British Standard (BS EN 10080), *Steel for the Reinforcement of Concrete-Weldable Reinforcing Steel-General*, British Standards Institution, London, 2005.

251. Trezos, K. G., I. P. Sfikas, and C. G. Pasios, "Influence of Water-to-Binder Ratio on Top-Bar Effect and on Bond Variation Across Length In Self-Compacting Concrete Specimens", *Cement and Concrete Composites*, Vol. 48, pp. 127-139, 2014.

252. ASTM Standard C234, *Standard Test Method for Comparing Concretes on the Basis of the Bond Developed with Reinforcing Steel*, ASTM International, West Conshohocken, 1991.

253. Al-Shannag, M. J., and A. Charif, "Bond Behavior of Steel Bars Embedded in Concretes Made with Natural Lightweight Aggregates", *Journal of King Saud University - Engineering Sciences.*, Vol. 29, No. 4, pp. 365-372, 2017.

254. Hoque, M. M., M. N. Islam, M. Islam, and M. A. Kader, "Bond Behavior of Reinforcing Bars Embedded in Concrete Made With Crushed Clay Bricks As Coarse Aggregates", *Construction and Building Materials*, Vol. 244, p.118364, 2020.

255. ACI Committee 318, *Building Code Requirements for Structural Concrete (ACI 318-02) and Commentary (ACI 318R-02)*, American Concrete Institute, Farmington Hills 2002.

256. ASTM Standard A615/A615M, *Standard Specification for Deformed and Plain Carbon-Steel Bars for Concrete*, ASTM International, West Conshohocken, 2020.

257. ACI Committee 408, *Bond and Development of Straight Reinforcing Bars in Tension*, American Concrete Institute, Farmington Hills, 2003.

258. Perkins, D., *Mineralogy*, Third Edition, Pearson Education Limited, Harlow, 2014.

259. Elena, J., and M. D. Lucia, "Application of X-Ray Diffraction (XRD) and Scanning Electron Microscopy (SEM) Methods to the Portland Cement Hydration Processes",

Journal of Applied Engineering Sciences, Vol. 2(15), No. 1, pp. 35-42, 2012.

260. Lutterotti, L., "Total Pattern Fitting for the Combined Size-Strain-Stress-Texture Determination in Thin Film Diffraction", *Nuclear Instruments and Methods in Physics Research Section B: Beam Interactions with Materials and Atoms*, Vol. 268, No. 3-4, pp. 334-340, 2010.

261. Güneyisi, E., M. Gesoglu, T. Özturan, and S. Ipek, "Fracture Behavior and Mechanical Properties of Concrete with Artificial Lightweight Aggregate and Steel Fiber", *Construction and Building Materials*, Vol. 84, pp. 156-168, 2015.

262. Güneyisi, E., M. Gesoglu, H. Ghanim, S. Ipek, and I. Taha, "Influence of the Artificial Lightweight Aggregate on Fresh Properties and Compressive Strength of the Self-Compacting Mortars", *Construction and Building Materials*, Vol. 116, pp. 151-158, 2016.

263. Eguchi, K., K. Teranishi, A. Nakagome, H. Kishimoto, K. Shinozaki, and M. Narikawa, "Application of Recycled Coarse Aggregate by Mixture to Concrete Construction", *Construction and Building Materials*, Vol. 21, No. 7, pp. 1542-1551, 2007.

264. Walpole, R. E., R. H. Myers, S. L. Myers, and K. Ye, *Probability & Statistics for Engineers & Scientists*, Ninth Edition, Pearson Education Limited, Harlow, 2017.

265. Moore, D. S., G. P. McCabe, and B. A. Craig, *Introduction to the Practice of Statistics*, Eighth Edition W. H. Freeman and Company, New York, 2014.

266. ACI Committee 213, *Guide for Structural Lightweight-Aggregate Concrete (ACI 213R-03)*, American Concrete Institute, Farmington Hills, 2003.

267. Kisku, N., P. Rajhans, S. K. Panda, S. Nayak, and V. Pandey, "Development of Durable Concrete from C&D Waste by Adopting Identical Mortar Volume Method in Conjunction with Two-Stage Mixing Procedure", *Construction and Building*

Materials, Vol. 256, p.119361, 2020.

268. Turkish Standard (TS 500), *Requirements for Design and Construction of Reinforced Concrete Structures*, Turkish Standards Institution, Ankara, 2000.

269. ACI Committee 318, *Building Code Requirements for Structural Concrete and Commentary (ACI 318M-05)*, American Concrete Institute, Farmington Hills, 2005.

270. European Standard (EN 1992-1-1), *Eurocode 2: Design of Concrete Structures - Part 1-1 : General Rules and Rules for Buildings*, European Committee for Standardization, Brussels, 2004.

271. Canadian Standard (CSA-A23.3-04), *Design of Concrete Structures*, Canadian Standards Association (CSA), Mississauga, Ontario, 2004.

272. New Zeland Standard (NZS 3101-1), *Concrete Structures Standard-Part 1: The Design of Concrete Ctructures*, Standards Council of New Zeland, Wellington 2006.

273. ACI Committee 363, *State-of-the-Art Report on High-Strength Concrete (ACI 363R-92)*, American Concrete Institute, Farmington Hills, 1992.

274. Kisku, N., P. Rajhans, S. K. Panda, V. Pandey, and S. Nayak, "Microstructural Investigation of Recycled Aggregate Concrete Produced by Adopting Equal Mortar Volume Method Along With Two Stage Mixing Approach", *Structures*, Vol. 24, pp. 742-753, 2020.

275. Swamy, R. N., and H. Stavrides, "Some Statistical Considerations of Steel Fiber Composites", *Cement and Concrete Research*, Vol. 6, No. 2, pp. 201-206, 1976.

276. Soroushian, P., M. Nagi, and A. Alhozaimy, "Statistical Variations in the Mechanical Properties of Carbon Fiber Reinforced Cement Composites", *ACI Materials Journal*, Vol. 89, No. 2, pp. 131-138, 1992.

277. Nataraja, M. C., N. Dhang, and A. P. Gupta, "Statistical Variations in Impact Resistance of Steel Fiber-Reinforced Concrete Subjected to Drop Weight Test", *Cement and Concrete Research*, Vol. 29, No. 7, pp. 989-995, 1999.

278. Badr, A., A. F. Ashour, and A. K. Platten, "Statistical Variations in Impact Resistance of Polypropylene Fibre-Reinforced Concrete", *International Journal of Impact Engineering*, Vol. 32, No. 11, pp. 1907-1920, 2006.

279. Myers, J. J., and M. Tinsley, "Impact Resistance of Blast Mitigation Material Using Modified ACI Drop-Weight Impact Test", *ACI Materials Journal*, Vol. 110, No. 3, pp. 339-348, 2013.

280. Akcay, B., and M. A. Tasdemir, "Optimisation of Using Lightweight Aggregates in Mitigating Autogenous Deformation of Concrete", *Construction and Building Materials*, Vol. 23, No. 1, pp. 353-363, 2009.

281. Djaknoun, S., E. Ouedraogo, and A. Ahmed Benyahia, "Characterisation of the Behaviour of High Performance Mortar Subjected to High Temperatures", *Construction and Building Materials*, Vol. 28, No. 1, pp. 176-186, 2012.

282. Lee, S. F., and S. Jacobsen, "Study of Interfacial Microstructure, Fracture Energy, Compressive Energy and Debonding Load of Steel Fiber-Reinforced Mortar", *Materials and Structures*, Vol. 44, pp. 1451-1465, 2011.

283. Erdem, S., A. R. Dawson, and N. H. Thom, "Impact Load-Induced Micro-Structural Damage and Micro-Structure Associated Mechanical Response of Concrete Made with Different Surface Roughness and Porosity Aggregates", *Cement and Concrete Research*, Vol. 42, No. 2, pp. 291-305, 2012.

284. Akca, A. H., and N. Ö. Zihnioğlu, "High Performance Concrete Under Elevated Temperatures", *Construction and Building Materials*, Vol. 44, pp. 317-328, 2013.

285. Gartner, E. M., K. E. Kurtis, and P. J. M. Monteiro, "Proposed Mechanism of C-S-H

Growth Tested by Soft X-Ray Microscopy", *Cement and Concrete Research*, Vol. 30, No. 5, pp. 817-822, 2000.

286. Taylor, H. F. W., *Cement Chemistry*, Third Edition, Academic Press, London, 1992.

287. Neville, A. M., *Properties of Concrete*, Fifth Edition, Pearson Education Limited, Harlow, 2011.

288. Mehta, P. K., and P. J. M. Monteiro, *Concrete: Microstructure, Properties, And Materials*, Fourth Edition, McGraw-Hill Education, New York, 2014.

289. Hoshino, S., K. Yamada, and H. Hirao, "XRD/Rietveld Analysis of the Hydration and Strength Development of Slag and Limestone Blended Cement", *Journal of Advanced Concrete Technology*, Vol. 4, No. 3, pp. 357-367, 2006.

290. Tam, V. W. Y., H. Wattage, K. N. Le, A. Buteraa, and M. Soomro, "Methods to Improve Microstructural Properties of Recycled Concrete Aggregate: A Critical Review", *Construction and Building Materials*, Vol. 270, p. 121490, 2021.

291. Kazmi, S. M. S., M. J. Munir, Y. F. Wu, I. Patnaikuni, Y. Zhou, and F. Xing, "Influence of Different Treatment Methods on the Mechanical Behavior of Recycled Aggregate Concrete: A Comparative Study", *Cement and Concrete Composites*, Vol. 104, p. 103398, 2019.

292. Ouyang, K., C. Shi, H. Chu, H. Guo, B. Song, Y. Ding, X. Guan, J. Zhu, H. Zhang, Y. Wang, and J. Zheng, "An Overview on the Efficiency of Different Pretreatment Techniques for Recycled Concrete Aggregate", *Journal of Cleaner Production*, Vol. 263, p.121264, 2020.

APPENDIX A: COPYRIGHTS OF FIGURES

ELSEVIER LICENSE
TERMS AND CONDITIONS

Jun 15, 2023

This Agreement between HASAN YILDIRIM ("You") and Elsevier ("Elsevier") consists of your license details and the terms and conditions provided by Elsevier and Copyright Clearance Center.

License Number	5570420858686
License date	Jun 15, 2023
Licensed Content Publisher	Elsevier
Licensed Content Publication	Construction and Building Materials
Licensed Content Title	Techno-commercial perspective study for sintered fly ash light-weight aggregates in India
Licensed Content Author	C.L Verma,S.K Handa,S.K Jain,R.K Yadav
Licensed Content Date	Sep 1, 1998
Licensed Content Volume	12
Licensed Content Issue	6-7
Licensed Content Pages	6
Start Page	341
End Page	346
Type of Use	reuse in a thesis/dissertation

Figure A.1. Copyrights of Figure 2.1 page 1.

Portion	figures/tables/illustrations
Number of figures/tables/illustrations	1
Format	both print and electronic
Are you the author of this Elsevier article?	No
Will you be translating?	No
Title	MECHANICAL PROPERTIES AND FRACTURE PARAMETERS OF SUSTAINABLE CONCRETE PRODUCED WITH RECYCLED AGGREGATES
Institution name	Boğaziçi University
Expected presentation date	Jun 2023
Portions	Figure 2.1

Figure A.2. Copyrights of Figure 2.1 page 2.

ELSEVIER LICENSE
TERMS AND CONDITIONS

Jun 15, 2023

This Agreement between HASAN YILDIRIM ("You") and Elsevier ("Elsevier") consists of your license details and the terms and conditions provided by Elsevier and Copyright Clearance Center.

License Number	5570421378441
License date	Jun 15, 2023
Licensed Content Publisher	Elsevier
Licensed Content Publication	Resources, Conservation and Recycling
Licensed Content Title	Utilization of fly ash by pelletization process; theory, application areas and research results
Licensed Content Author	Gökhan Baykal,Ata Gürhan Döven
Licensed Content Date	Jul 1, 2000
Licensed Content Volume	30
Licensed Content Issue	1
Licensed Content Pages	19
Start Page	59
End Page	77
Type of Use	reuse in a thesis/dissertation

Figure A.3. Copyrights of Figure 2.2, 2.3, 2.4, and 2.5 page 1.

Portion	figures/tables/illustrations
Number of figures/tables/illustrations	4
Format	both print and electronic
Are you the author of this Elsevier article?	No
Will you be translating?	No
Title	MECHANICAL PROPERTIES AND FRACTURE PARAMETERS OF SUSTAINABLE CONCRETE PRODUCED WITH RECYCLED AGGREGATES
Institution name	Boğaziçi University
Expected presentation date	Jun 2023
Portions	Figure 2.2, Figure 2.3, Figure 2.4, Figure 2.5,

Figure A.4. Copyrights of Figure 2.2, 2.3, 2.4, and 2.5 page 2.

ELSEVIER LICENSE
TERMS AND CONDITIONS

Jun 15, 2023

This Agreement between HASAN YILDIRIM ("You") and Elsevier ("Elsevier") consists of your license details and the terms and conditions provided by Elsevier and Copyright Clearance Center.

License Number	5570421147679
License date	Jun 15, 2023
Licensed Content Publisher	Elsevier
Licensed Content Publication	Cement and Concrete Research
Licensed Content Title	Compressive behaviour of recycled aggregate concrete under impact loading
Licensed Content Author	Jianzhuang Xiao,Long Li,Luming Shen,Chi Sun Poon
Licensed Content Date	May 1, 2015
Licensed Content Volume	71
Licensed Content Issue	n/a
Licensed Content Pages	10
Start Page	46
End Page	55
Type of Use	reuse in a thesis/dissertation

Figure A.5. Copyrights of Figure 2.6 page 1.

Portion	figures/tables/illustrations
Number of figures/tables/illustrations	1
Format	both print and electronic
Are you the author of this Elsevier article?	No
Will you be translating?	No
Title	MECHANICAL PROPERTIES AND FRACTURE PARAMETERS OF SUSTAINABLE CONCRETE PRODUCED WITH RECYCLED AGGREGATES
Institution name	Boğaziçi University
Expected presentation date	Jun 2023
Portions	Figure 2.6

Figure A.6. Copyrights of Figure 2.6 page 2.

ELSEVIER LICENSE
TERMS AND CONDITIONS

Jun 15, 2023

This Agreement between HASAN YILDIRIM ("You") and Elsevier ("Elsevier") consists of your license details and the terms and conditions provided by Elsevier and Copyright Clearance Center.

License Number	5570420586874
License date	Jun 15, 2023
Licensed Content Publisher	Elsevier
Licensed Content Publication	Construction and Building Materials
Licensed Content Title	Structural reliability of bonding between steel rebars and recycled aggregate concrete
Licensed Content Author	Marco Breccolotti,Annibale Luigi Materazzi
Licensed Content Date	Oct 1, 2013
Licensed Content Volume	47
Licensed Content Issue	n/a
Licensed Content Pages	8
Start Page	927
End Page	934
Type of Use	reuse in a thesis/dissertation

Figure A.7. Copyrights of Figure 2.7 page 1.

Portion	figures/tables/illustrations
Number of figures/tables/illustrations	1
Format	both print and electronic
Are you the author of this Elsevier article?	No
Will you be translating?	No
Title	MECHANICAL PROPERTIES AND FRACTURE PARAMETERS OF SUSTAINABLE CONCRETE PRODUCED WITH RECYCLED AGGREGATES
Institution name	Boğaziçi University
Expected presentation date	Jun 2023
Portions	Figure 2.7

Figure A.8. Copyrights of Figure 2.7 page 2.

APPENDIX B: COPYRIGHTS OF TABLES

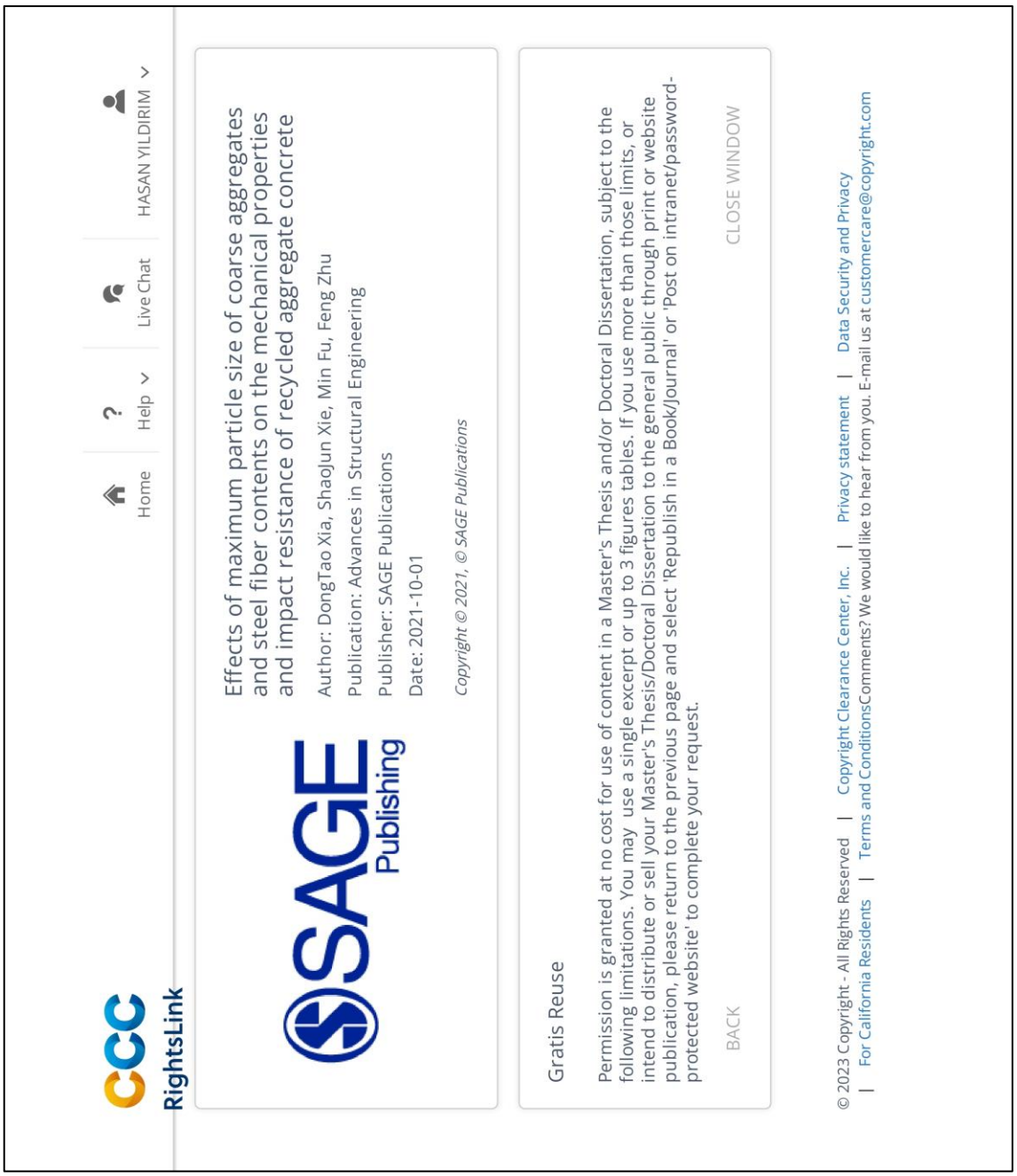

Figure B.1. Copyrights of Table 2.1.